ENHANCING PERFORMANCE OF RADIANT COOLING SYSTEM THROUGH DECOUPLING OF LATENT-SENSIBLE LOAD

Ph.D. Thesis

Prateek Srivastava
ID No. 2014REN9047

CENTER FOR ENERGY AND ENVIRONMENT

MALAVIYA NATIONAL INSTITUTE OF TECHNOLOGY JAIPUR, INDIA

March 2019

Dedicated to my family

ENHANCING PERFORMANCE OF RADIANT COOLING SYSTEM THROUGH DECOUPLING OF LATENT-SENSIBLE LOAD

Submitted in

fulfillment of the requirements for the degree of

Doctor of Philosophy

by

Prateek Srivastava

ID: 2014REN9047

Under the Supervision of

Prof. Jyotirmay Mathur

Dr. Mahabir Bhandari

CENTRE FOR ENERGY AND ENVIRONMENT

MALAVIYA NATIONAL INSTITUTE OF TECHNOLOGY JAIPUR, INDIA

March 2019

DECLARATION

I, **Prateek Srivastava**, declare that this thesis titled, " **ENHANCING PERFORMANCE OF RADIANT COOLING SYSTEM THROUGH DECOUPLING OF LATENT-SENSIBLE LOAD**" and the work presented in it, are my own. I confirm that:

- This work was done wholly or mainly while in candidature for a research degree at this university.

- Where any part of this thesis has previously been submitted for a degree or any other qualification at this university or any other institution, this has been clearly stated.

- Where I have consulted the published work of others, this is always clearly attributed.

- Where I have quoted from the work of others, the source is always given. With the exception of such quotations, this thesis is entirely my own work.

- I have acknowledged all main sources of help.

- Where the thesis is based on work done by myself, jointly with others, I have made clear exactly what was done by others and what I have contributed myself.

Date: 27/03/2019

Prateek Srivastava
(2014REN9047)

CERTIFICATE

This is to certify that the thesis entitled **"ENHANCING PERFORMANCE OF RADIANT COOLING SYSTEM THROUGH DECOUPLING OF LATENT-SENSIBLE LOAD"** being submitted by **Prateek Srivastava (2014REN9047)** is a bonafide research work carried out under my supervision and guidance in fulfillment of the requirement for the award of the degree of **Doctor of Philosophy** in the Centre for Energy and Environment, Malaviya National Institute of Technology, Jaipur, India. The matter embodied in this thesis is original and has not been submitted to any other University or Institute for the award of any other degree.

Place: Jaipur
Date: 27/03/2019

Jyotirmay Mathur
Professor
Center for Energy and Environment
MNIT Jaipur

Dr. Mahabir Bhandari
Scientist,
Oak Ridge National Laboratory,
USA

ACKNOWLEDGEMENT

I would also like to thank **Shashank Vyas, Anuj, Vivek, Robin, Gaurav, Chanderashekar Pratap, Santosh, Prateek**, all fellow students, all faculty, technical, non-technical staff of Centre for Energy and Environment MNIT, Jaipur for supporting and helping me throughout the research work.

Last but not the least, I would like to thank my family for their inspiration and motivation throughout my work, I owe everything to them. Besides this, several people have knowingly and unknowingly helped me in the successful completion of this project.

ABSTRACT

Indian building stock is going to increase fivefold uptil 2030, energy demand is increasing at a very rapid rate. Improving energy efficiency in the Heating Ventilation and Air-Conditioning (HVAC) systems is the foundation to improve the energy efficiency of the buildings. Radiant Cooling System (RCS) has a reputation for increasing the thermal comfort and reducing the energy consumption of buildings. Main advantages of the radiant cooling system are low operational noise and reduced fan energy, which usually accounts for more than 30-40% of the total energy consumption of HVAC energy for commercial buildings. RCS can only cater to the sensible load of the space hence requires a parallel system to meet the latent load. In conventional HVAC systems the total load of the building is met by single HVAC system, in RCS sensible and the latent load is decoupled. Two different HVAC systems i.e. RCS and DOAS are used to meet the decoupled (sensible and latent) load.

Dedicated Outdoor Air Systems (DOAS) can parallely work with RCS to meet the latent load and are beneficial in meeting the ventilation requirements. However, all dedicated outdoor air systems configurations do not provide the same benefits in different climates. This study presents an experimental and simulation-based analysis of various configurations of radiant cooling system and dedicated outdoor air systems among diverse climate zones of India through analysis of energy saving opportunity with each with respect to conventional non-radiant all-air system.

There are different strategies to decouple sensible and latent load in HVAC systems using cooling coil and sensible/energy recovery/desiccant wheels of different types in DOAS. Six different decoupling strategies are identified and then simulated on the EnergyPlus platform using a calibrated building model having RCS for the different climatic condition. The six DOAS strategies are noted below:

Strategy-1: Low temperature cooling coil

Strategy-2: Energy recovery wheel with low temperature cooling coil

Strategy-3: Energy recovery wheel, sensible wheel with low temperature cooling coil

Strategy-4: Desiccant wheel with high-temperature cooling coil

Strategy-5: Desiccant wheel, sensible wheel with high-temperature cooling coil

Strategy-6: Desiccant wheel, indirect evaporative cooling system with high-temperature cooling coil

After simulations, a psychrometric chamber based experimental setup is developed to test the different decoupling strategies to evaluate actual energy deployment and thermal performance as per the design of experiment for the different climatic condition. Based on the simulation and experimental results for cooling coil based strategies, Strategy-2 [comprise of energy recovery wheel (cater both sensible & latent load) and low-temperature cooling coil] offers maximum energy savings potential for Hot and Dry, Warm and Humid, and Composite climate over conventional all-air system. Strategy-1 (comprise of low-temperature cooling coil with no use of wheel) offers maximum energy savings potential for the Temperate climate.

Strategy-5 (comprise of desiccant wheel, sensible wheel and high-temperature cooling coil) offers maximum energy savings potential for Hot and Dry, Warm and Humid, and Composite climate. For Temperate climate in case of active heater regeneration Strategy-5 (comprise of desiccant wheel, sensible wheel and high-temperature cooling coil) offers maximum energy savings potential and while using waste heat for regeneration Strategy-6 (comprise of desiccant wheel, indirect evaporative cooling system and high-temperature cooling coil) offers maximum energy savings potential.

After analyzing the different decoupling strategies the recommended strategy for composite climate i.e. Strategy-2 (comprise of energy recovery wheel and low-temperature cooling coil) is used with RCS in an experimental setup was developed at MNIT Jaipur (Jaipur falls in composite climate). RCS is fed through a chiller and cooling tower (used as a water side economizer) for supplying chilled water in RCS. A separate chiller is used to supply water in cooling coil of DOAS. Experiments were conducted for chiller and cooling tower based RCS in MNIT Jaipur. Based on the architectural data of the building and HVAC plant specifications, models are developed and calibrated using the experimental data.

Based on the simulation results using calibrated models of the annual simulation cooling tower based RCS was found to save 7% energy in Hot and Dry climate, 11% in Composite climate and 22% in Temperate climate.

Different types of RCS [radiant panel cooling (RCP), embedded surface cooling system (ESCS) and thermal activated building system (TABS)] were also analyzed and compared for energy savings opportunity

It has been found through this study that radiant cooling system has a significant potential of providing energy savings in all the climatic conditions found in India. Proper selection of type of radiant cooling system, chiller operating temperature and utilizing free cooling opportunity (where exists), radiant cooling system can offer upto 7%, 11%, 22% energy savings in Hot and Dry, Composite climate, and Temperate climate respectively, provided the DOAS working in conjunction is optimized in configuration and operating condition.

Table of Contents

List of Figures

List of Table

Nomenclature

HVAC	-	Heating Ventilation & Air Conditioning
DX	-	Direct expansion
VRF	-	Variable refrigerant flow
VRV	-	Variable refrigerant volume
RCS	-	Radiant cooling system
RPM	-	Rotation per minute
RCP	-	Radiant cooling panel
ESCS	-	Embedded surface cooling system
TABS	-	Thermally activated building system
DOAS	-	Dedicated outdoor air system
DBT	-	Dry Bulb Temperature
WBT	-	Wet Bulb Temperature
MRT	-	Mean Radiant Temperature
OT	-	Operative Temperature
RH	-	Relative humidity
BTU	-	British thermal unit
REHVA	-	Federation of European Heating, Ventilation and Air Conditioning Associations
PLC	-	Programmable logic control
XPS	-	Extruded polystyrene
NMBE	-	Normalized Mean Bias Error
CV-RMSE	-	Coefficient of Variation of Root Mean Square Error
SHGC	-	Solar heat gain coefficient
WWR	-	Window wall ratio
TMY	-	Typical meteorological year
RTD	-	Resistance temperature detector
MNIT	-	Malaviya National Institute of Technology
ISO	-	International Organization for Standardization
ERW	-	Energy recovery wheel
SW	-	Sensible wheel
DW	-	Desiccant wheel
AUST	-	Area-weighted average temperature

1.1   Background

India's economy and the population are rapidly expanding; meeting the nation's energy demand requires future planning, better policies, and implementation of energy efficient system. Total constructed area (building stock) in 2005 was around 2,100 million square meters and is predicted to grow five-fold to reach around 10,400 million square meters in 2030 in India (Figure 1-1). India's forecast towards growth in the building sector is a large expansion; therefore new buildings need to be made more efficient and existing buildings energy consumption needs to be optimized. Building energy includes all the energy consumption associated with building such as Heating Ventilation and Air-conditioning (HVAC), lighting (interior and exterior), water heating, elevators, and escalators, as well as the operation of electric and electronic equipment. India's forecast towards growth in the building sector is huge, and the heating ventilation and air conditioning (HVAC) system application for the building space would require a significant energy use. In such a scenario it is high on priority to optimize the energy consumption towards the HVAC system and come up with more energy efficient HVAC system. Within the commercial building, HVAC systems are the most energy consuming components. HVAC systems consume about 31% of the energy used by commercial buildings in India (Figure 1-2). Striving for energy efficient buildings does not mean to overlook thermal comfort as people stay most of the time indoors.
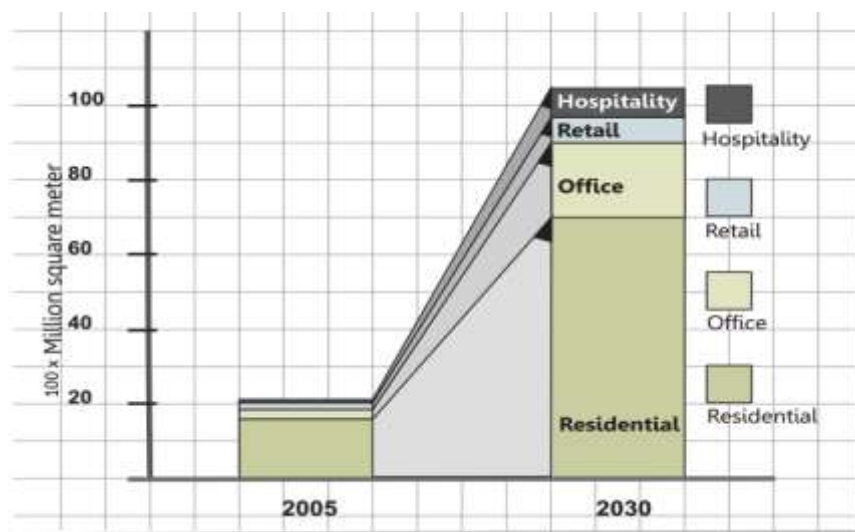
Figure 1-1: Building Stock in India – 2005 to 2030 [1]
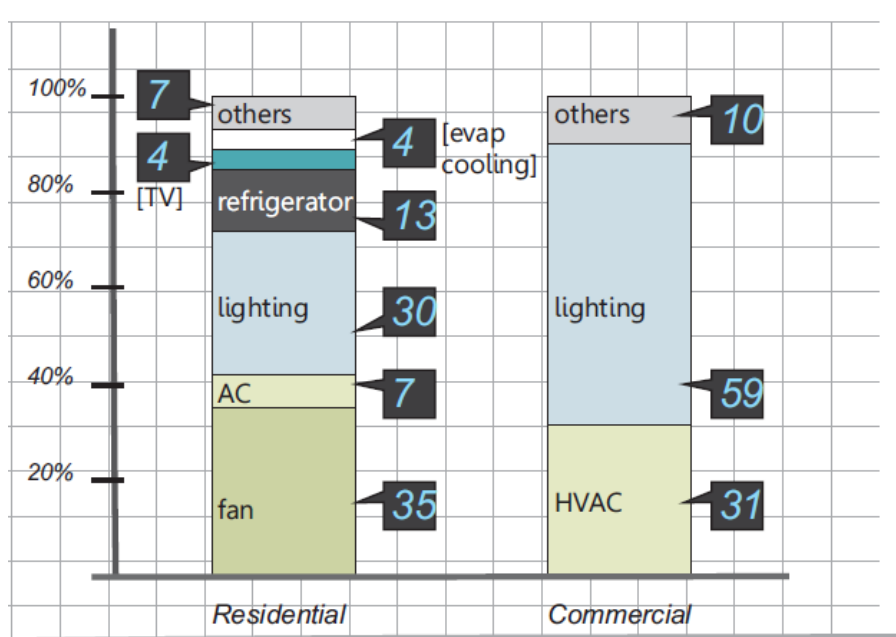
Figure 1-2: Energy Consumption details of a commercial building [1]

In present scenario vapour compression based HVAC system is largely used in the country. An air-based system such as DX system and central system are popular in India. Improving energy efficiency in the HVAC systems is the key to make the commercial building sector efficient.

Transportation of heat transfer medium to extract heat from the buildings contributes to major share of HVAC energy consumption. Energy consumption can be reduced by minimizing the volumetric flow of the heat transfer fluid by changing it form air to water. Air is having low density and specific heat, thus require a large volumetric flow rate to extract the same amount of heat energy compared to water, which has high density (832 times higher than air) and specific heat (4000 times higher than air).

In conventional air based HVAC system, the surface area of heat exchangers for cooling application is usually small. Thus the central plant needs to cool the chilled water to lower temperature to provide sufficient cooling. In conventional system air at low temperature enters the building to cater the building load; low temperature air creates stratification of air which leads to lower thermal comfort.

Cooling capacity, space area to be cooled, desired indoor thermal conditions determine the type of system used. There are different types of air and water-based systems being used in the residential, healthcare, education and commercial buildings. Table 1-1 shows the application of different HVAC Systems by Building Type in India.

2

Table 1-1: Application of HVAC Systems by Building Type [1]

Segments	Types of Chillers/HVAC Used
Residential	Predominantly window and un-ducted split systems. High-end residential buildings have also started using VRF/VRV systems.
Infrastructure (Airports/Metros)	Demand for water-cooled chillers (centrifugal and screw chillers especially) is more because of higher tonnage requirements and greater efficiency. VRF systems are installed in smaller facilities and in buildings with specific space conditioning needs within large infrastructure projects.
Healthcare	Centrifugal, screw and water-cooled chillers are common.
Education	VRF systems are preferred in smaller establishments and centrifugal systems are more in demand in large projects.

Energy Audit studies carried out in several office buildings, hotels and hospitals in India indicate energy saving potential of 23% to 46% by the installation of efficient lighting, efficient HVAC, etc. (IEB 2012). According to the ECBC Tip sheet for HVAC, USAID ECO – III Project (June 2009), there is an enormous potential of saving energy by an HVAC design to well optimized HVAC system design [2]. Most of buildings are currently using conventional air conditioning systems in the sense that they use air not only for ventilation but also as a heat transfer medium (sensible cooling). For improving the energy efficiency and thermal comfort of the HVAC system radiant cooling system is a good alternative. In the radiant cooling system, sensible cooling of the building is taken care by a temperature controlled surface in which chilled water flows and for meeting latent load and providing ventilation a dedicated outdoor air system is used. Radiant cooling systems (RCS) separate the cooling and ventilation tasks of a building, provide energy savings and provide better thermal comfort compared to conventional air conditioning systems.

1.2 Radiant cooling system

The radiant cooling system (RCS) is a temperature controlled surface system to provide sensible cooling in the space. The temperature of the building structure (ceiling, floor, wall etc.) is reduced by the means of chilled water which flows through a network of pipes embedded in the structural surfaces or in the panels act as a ceiling. Lower structure temperature triggers the radiative heat exchange from the human body to cold surfaces and provides sensible cooling inside the building. A separate air system (dedicated outdoor air system) is used for the ventilation requirements and handling the latent load. Thus, RCS separates the task of ventilation and thermal conditioning and more than 50% heat transfer takes place through radiation along with convection to provide better thermal comfort in

the space. Since in radiant cooling system most of the sensible heat gain is removed by radiant heat transfer, it has been observed that occupant feels the same comfort at higher indoor air temperature (setpoint) compared to the conventional all-air system. Separating thermal conditioning and ventilation task, radiant cooling system eliminates the need for recirculated air and thus reduces the energy consumption as well as heat generation of the fan. The available information on the performance of radiant cooling systems establishes the fact that these systems not only reduce the energy consumption and peak power demand but also provide draft-free and noise-free cooling with reduced building space cooling requirements [3], [4].

1.2.1 Types of radiant cooling system

There is no exact categorization of the radiant cooling system (RCS). Based on the REHVA guidebook [5] it has been classified primarily of three types. 1) Radiant ceiling panel (RCP): It is a metal suspended ceiling on the back of it has a copper piping and then overall insulated from the back. It can be used in new construction as well as retrofit. 2) Embedded surface cooling system (ESCS): PEX, or small, closely spaced plastic tubing "mats" are embedded in the wall, ceiling or floor insulated from the building. It can be used for the retrofit or new construction. 3) Thermally activated building system (TABS): PEX pipe are generally embedded in the slab while casting, it can be used for new construction. Table 1-2 shows the schematic of the three types of radiant cooling systems as per the REHVA classification. Table 1-3 shows a comparison of different types of RCS.

Based on ISO-11855, Embedded Surface System has been further classified into seven types (A to G) depending on pipe location (Table 2 in part 2 of ISO 11855 [6]).

- Type A-D: radiant piping layers are insulated from building the structure, and tubing is embedded in either the surface thermal diffusion layer (screed or concrete) (Type A and C), or in the insulation layer (Type B), or between the insulation and surface diffusion layers (Type D),
- Type E: Thermally activated building system (TABS), as the radiant piping, is placed in the concrete, it as a thermal mass.
- Type F: the Capillary tube is used in place of PEX pipe embedded in radiant layers which are insulated from the building structure.
- Type G: Used for floor application, wooden constructions, and pipes in or under the subfloor.

1.2.2 Advantages

The radiant cooling system has various advantages over conventional air system as follow:

- Energy efficient
- Improved indoor air quality
- Improved thermal comfort
- Integration with low-grade energy sources
- Reduced noise and ductwork
- Building load is decoupled

Table 1-2: Schematic of the three types of radiant cooling systems (REHVA classification [5])
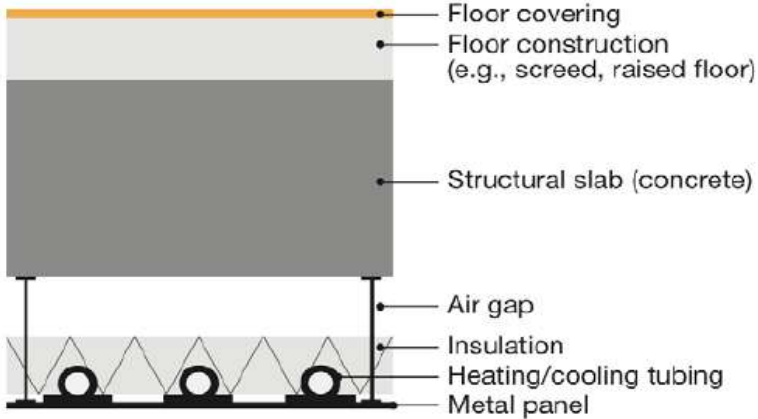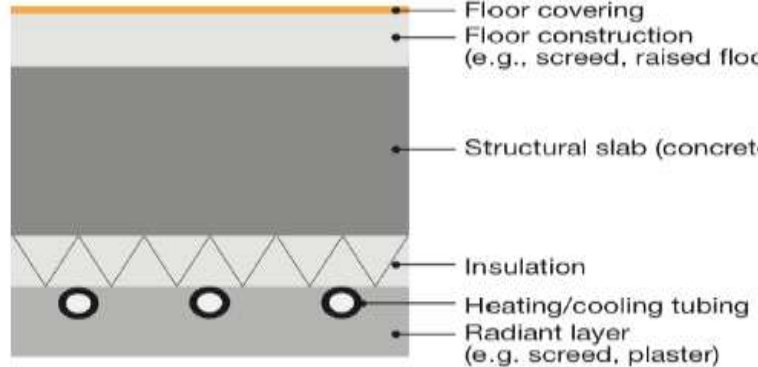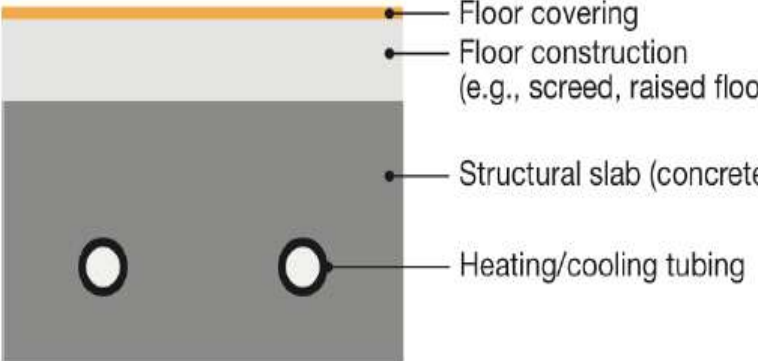
System types	Schematics
Radiant Cooling Panel (RCP)	Floor covering — Floor construction (e.g., screed, raised floor) — Structural slab (concrete) — Air gap — Insulation — Heating/cooling tubing — Metal panel
Embedded surface cooling system (ESCS)	Floor covering — Floor construction (e.g., screed, raised floor) — Structural slab (concrete) — Insulation — Heating/cooling tubing — Radiant layer (e.g. screed, plaster)
Thermally active building system (TABS)	Floor covering — Floor construction (e.g., screed, raised floor) — Structural slab (concrete) — Heating/cooling tubing

Table 1-3: Comparison of different types of RCS

Parameters	RCP	ESCS	TABS
Design	Pipes are attached to a thin Aluminium or steel extruded surfaces called panels.	Pipes are integrated into floors, walls or ceiling concrete.	Pipes are isolated from the building structure by insulation on floors, walls, and ceilings.
Thermal Inertia	Low	High	Medium
Thermal Mass	Low	High	Medium
Typical Surface Area	50-70% of the ceiling area.	Up to 100% of Ceiling/Floor Area	Up to 100 % of wall area
Best Application	- Buildings with greater variation in skin loads - Buildings with spaces with highly variable internal loads - Mixed-mode buildings with zoned or seasonal operation.	- Buildings with high-performance envelopes - Moderate Climates - Use with natural ventilation with low-energy cooling / heating sources.	- Buildings with high solar load or peak load. - Suitable for hot climates with less load variation. - Can be used for new construction / retrofitting both.
Additional Opportunities	Good for retrofit applications. Some designs integrate with acoustic solutions.	Use to remove solar loads from structural elements, or to create a "constant-temperature" slab or pre-cooled building.	Have benefits of both the panel system and the TABS system.
Cost	Highest cost per unit active surface area.	Lowest cost/unit active surface area.	Cost is higher than the ESCS system and lower than the panel system.

1.2.1 Limitations

Radiant cooling system is useful where the sensible load is higher and has humidity control, but there are several areas like restaurant, lobby, and kitchen etc. where humidity control is very difficult, hence its application can fetch a problem of condensation. The radiant cooling system can only meet sensible load, the total load is decoupled into primary (humidity control) and secondary (sensible load) load, also known as decoupling of the load. For controlling the humidity a dedicated outdoor air system needs to be coupled with RCS. As per ASHRAE 62.1 [7], outdoor air needs to be provided in the space which can be done by adding dedicated outdoor air with the radiant cooling system. The radiant cooling system also has a limitation of cooling capacity, in order to counter the condensation problem surface temperature need to be maintained higher than dew point temperature (DPT). Figure 1-3 shows different components of the radiant cooling system. There is a chiller to supply chilled water to the pipes embedded in the structure of the building chilled water pipelines. The radiant cooling system can cater

to the sensible load of the space but to meet the latent load and provide ventilation in the space a separate parallel dedicated outdoor air system (DOAS) is required.
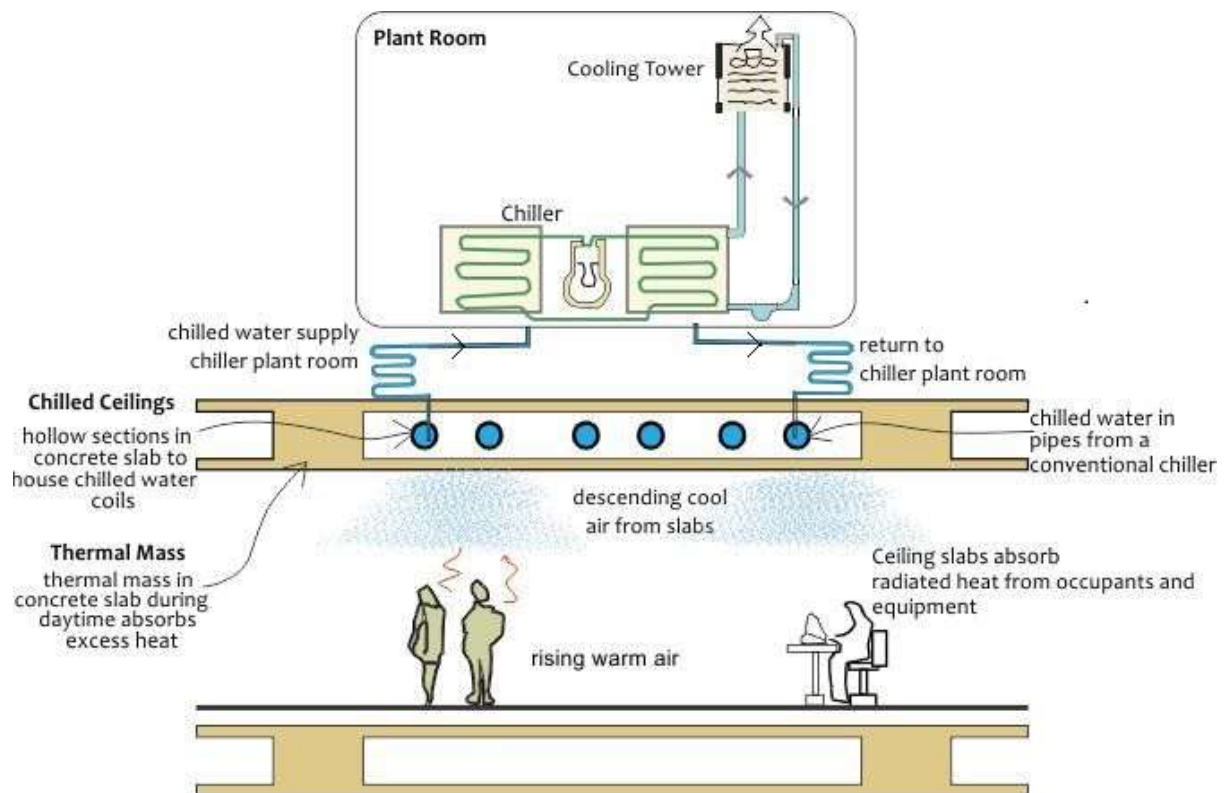
Figure 1-3: Components of the radiant cooling system (https://www.energywarden.net)

1.3 Dedicated outdoor air system

The radiant cooling system caters only sensible load of the space however for latent load and ventilation, dedicated outdoor air system is designed and incorporated. The concept of DOAS fulfils ASHRAE Standard 62.1 ventilation requirements. The concept of DOAS was introduced several decades ago and it is capable of delivering the requirement of 100% outdoor air (OA) in the space. This system is also recognized for the first time for decoupling of the building load which helps in energy saving in HVAC system. For decoupling the load, system is divided into two parts i.e. the primary system and the secondary system. The primary system is used for humidity control and delivering ventilation air requirement and secondary system is used for sensible cooling. By decoupling the load overall size of the system can be minimized. DOAS coupled with radiant cooling system, provides better indoor air quality. Different dehumidification techniques (i.e. cooling coil, desiccant wheel and membrane-based heat exchanger) are available to be integrated into DOAS. Figure 1-4 shows different combinations of RCS and DOAS. The largest amount of moisture load on the HVAC system is due to the incorporation of ventilation air [8] as shown in Figure 1-5.
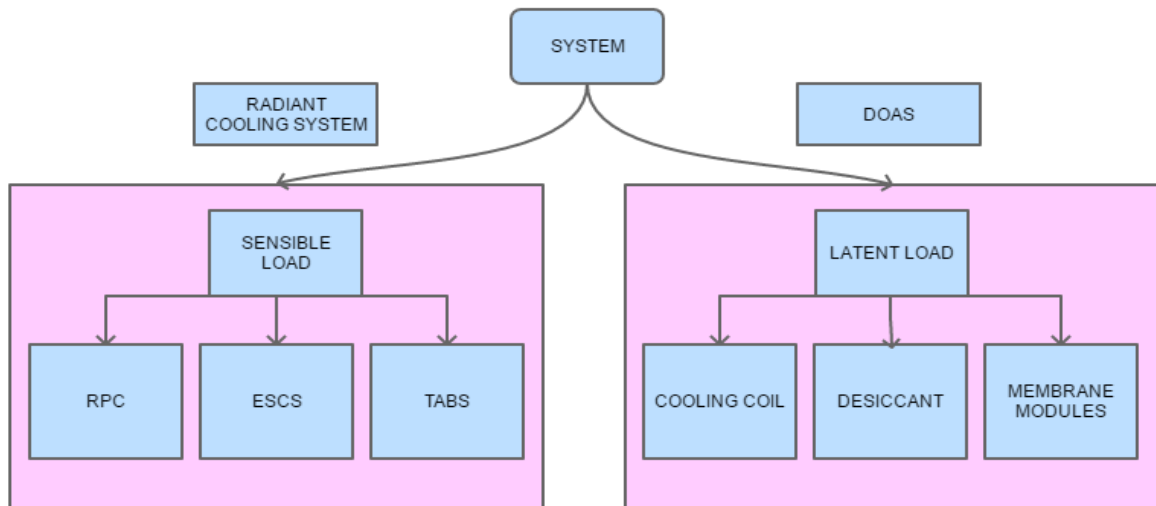
Figure 1-4: Combinations of RCS with DOAS
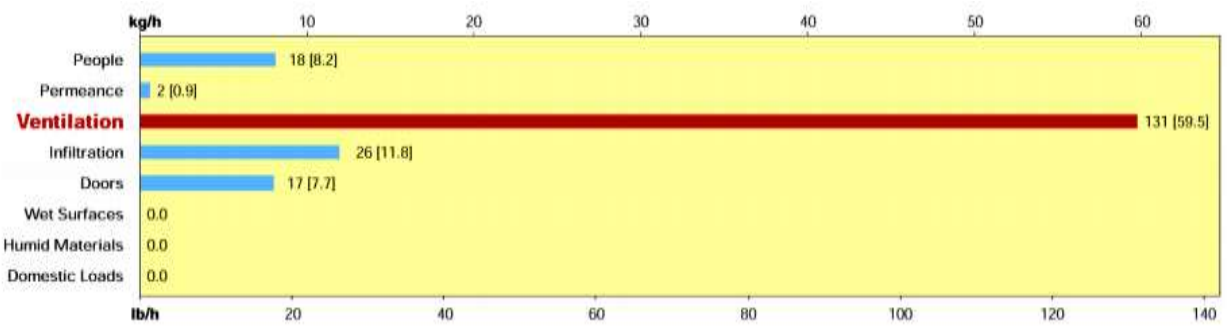
Figure 1-5: The largest moisture load in most commercial buildings comes from the ventilation air [8]

For industrial and commercial building outdoor air requirements can typically be calculated by using local building code or ANSI/ASHRAE standard 62.1. While calculating the outdoor air requirement for the space one should consider the following three factors: a) codes/standard- outdoor air delivered in the space is based on minimum required by the code/standard, b) exhaust: some buildings need higher exhaust air than outdoor air (laboratories, facilities with any bathrooms) and c) load: in some cases secondary system may require increased outdoor airflow typically involve humidification or dehumidification (chilled ceiling or passive chilled beams) [9].

Minimum ventilation requirement in the breathing zone

ANSI/ASHRAE standard 62.1-2016 prescribes the ventilation requirement in two ways. First, is based on the number of occupants and second is based on the floor area of space. V_{bz} is outdoor airflow required for breathing, R_p (people-related ventilation rate) is quantified in terms of cfm/person, R_a (building-related ventilation rate) is quantified in terms of cfm/ft^2, P_z is a number of people expected to occupy space and A_z is space area.

8

$$V_{bz} = (R_p \times P_z) + (R_a \times A_z) \qquad\qquad (1)$$

$$V_{oz} = \frac{V_{bz}}{E_z} \qquad\qquad (2)$$

Under some circumstances, ventilation air can increase humidity level in the zone if the DOAS is not properly sized and designed. When zone humidity increases, occupants tend to start adjusting the thermostat to lower temperature to achieve thermal comfort which deteriorates building energy efficiency. Increased zone humidity level can create health issues such as respiratory diseases and mold growth [10]. For proper functioning of the radiant cooling system with a dedicated outdoor air system, proper control is required.

1.4   Controls for Radiant Cooling System

To enhance the performance of a building and improve energy efficiency a good control strategy is required. Any high-efficiency building system cannot perform as desired without implementing the controls properly. Improper control strategies may lead to poor performance, high response time, energy intensive system, inappropriate thermal comfort in the zone and condensation on the chilled surface. Over the years, there have been many different control solutions developed by researchers, implemented on the radiant cooling system. The performance of the system mostly governs by the proper implementation of the control and data acquisition system. The objective of applying controls in the building is to provide comfortable and cheap operating cost for the occupants, without implementation of proper control it is impossible. Optimal performance of the building can only be achieved by minimizing losses i.e. by supplying a desired flow of chilled water, chilled water temperature to compensate the cooling load based on hourly variation in the building. Achieving proper operation and maximum energy savings from the buildings precision electronic or direct digital controls need to be used.

Controls are generally applied in RCS for varying pressure (flow) and temperature. (Applications Handbook, chapter 54 Radiant Heating, and Cooling)

- Two port control valve is used to control chilled water flow rate
- Injection circuit is used to control chilled water temperature

In order to stabilize the thermal environment of the space, the control system is required to balance the heat load under the transient condition of the HVAC system under different outdoor climate conditions. If the HVAC system performance varies according to fluctuating load under the transient condition, only then the system can become energy efficient. In radiant cooling system, capacity of the radiant cooling system is fixed based on the chilled surface area for the sensible load. During fluctuating load, proper controls are required to vary the volumetric flow of air (CFM) from the dedicated outdoor air system.

The control of the radiant cooling system can be classified as (ISO 18566 [11]):

- Central control (modulates the control at the plant level)
- Zone control (modulates the control at the zone level)
- Individual room control (modulates the control at the room level)

Central control: The central control modulates the supply chilled water temperature of the radiant cooling system based on the space cooling requirement. Based on the space cooling requirement as per the settings of thermostat chilled water flow rate and chilled water temperature is controlled accordingly. [12] Has suggested for achieving better control in the chilled water system, it is recommended to control the average water temperature i.e. mean value of supply and return chilled water temperature, with respect to ambient and/or indoor zone temperatures, rather than controlling supply water temperature.

Condensation prevention is also a major aspect of the proper functioning of the radiant cooling system. Condensation can be controlled by a central control system by keeping the chilled water temperature at an offset of 1-2 °C from dew point temperature at that instant. Air must be properly dehumidified below the dew point temperature to enhance the performance of the radiant cooling system. Dedicated outdoor air system should also be properly controlled with the variation of load in order to provide energy savings and proper thermal comfort in the space. Bigger buildings must be divided into multiple thermal zones to enhance the system performance. Every zone should be provided with a thermostat to control the radiant cooling system and a dedicated outdoor air system accordingly.

Zone control: For enhancing the performance and thermal comfort of the system with improving energy efficiency it is recommended to control each zone using a separate thermostat in the zone, individual zone control valve can be modulated accordingly. For achieving better thermal comfort in the zone it is advisable to operate the thermostat on operative temperature rather than dry bulb temperature.

"Self-regulating" control has lot of impact on the radiant cooling system. This "self-regulating" depends on two parameters i.e. difference in room and radiant cooled surface temperature, and secondly temperature difference between room and the average water temperature in the radiant pipes of the structure. This control helps in providing stable and uniform temperature throughout the space with providing better thermal comfort to the occupant.

Individual room control: It is recommended for improving comfort and energy savings. Besides energy benefits, adjustment of the room temperature set-point individually from room provide flexibility to improve comfort. The valve on the manifold in a chilled water pipe is controlled by a room sensor. The sensor and control wiring mostly installed altogether with the main power wiring; as a result room sensors are installed near the switch of the main power, which otherwise would have been more beneficial if position in the occupied zone. To solve this problem, individual room temperature control systems, using a link based on wireless transmission between the room sensors and the control valves, can improve the quality of the control.

1.5   Research motivation and objective

A smart building is a mirror of low energy consumption and low carbon emission. It can only work smartly by proper integration and optimization of various emerging technologies. Striving for energy efficiency by compromising thermal comfort is not recommended. Radiant cooling technology along with DOAS with appropriate controls can reduce the energy consumption of buildings and improve the thermal comfort of the building. The radiant cooling system offers a prospective alternative to the currently overwhelming use of all-air systems. The performance of the radiant cooling system coupled with DOAS is variable and it is dependent on the climate. The concept of the radiant cooling system is new in real buildings and experimental investigation for India, hence energy benefits from this system needs to be investigated for the different climatic

condition. Various DOAS strategies were found in literature but appropriate strategies for different climatic condition needs to be identified.

The objective of this thesis is to identify the most energy efficient combinations, behaviour and advantage of RCS coupled with DOAS in different Indian climatic conditions. Dedicated outdoor air system performs differently in different Indian climatic conditions in conjunction with the radiant cooling system. In order to enhance the performance of the radiant cooling system with a dedicated outdoor air system, the right combination of the two is required to install. This dissertation also aims to enhance the understanding of the operation of the radiant cooling system with chiller and cooling tower for chilled water application. Comparison of different types of radiant cooling system for energy consumption and heat transfer phenomenon was studied for different types of RCS. The objective statements of this research are:

- Examining the applicability of different latent-sensible decoupling technique for DOAS in various climatic zones.

- Performance evaluation of various types of Radiant cooling system.

1.6 Organization of the thesis

The entire thesis is summed up in six chapters. Presented below are the highlights of the chapters.

Chapter 1 presents an overview of the problem statement and outlines the tasks performed in the present research.

Chapter 2 literature review discusses different studies available for the radiant cooling system and dedicated outdoor system in the area of experiment, theoretical, simulation etc. Literature for different parameters like energy benefits, thermal comfort/indoor air quality, and heat transfer model/cooling capacity are discussed. It also discusses benefits, needs of decoupling and ventilation with humidity control for DOAS.

Chapter 3 showcases the methodology of the entire thesis.

Chapter 4 provides information about decoupling strategies and their component. It includes initial simulation details and results, provides the groundwork for the development of an experimental setup for the testing of DOAS strategies.

Chapter 5 includes the development of experimental setup for testing decoupling strategies. The chapter discusses the design of indoor-outdoor chamber, sensors and instrumentation, controls of the chambers and the experimental results to evaluate the performance of decoupling strategies for different climatic conditions.

Chapter 6 Based on the results of chapter 4, we integrated the decoupling strategy into the real-time radiant cooling system to identify the energy saving potential. An experimental setup is designed and developed to integrate DOAS with the radiant cooling system. The system is integrated with parallel chiller and cooling tower for a chilled water source. Analyzed the performance of the radiant cooling system with DOAS for chiller and cooling tower as a source of chilled water for the different climatic condition. Different types of radiant cooling system have been compared.

Chapter 6 This chapter provides the conclusion of the work done in the thesis and provides a recommendation for the implementation of the radiant cooling system with a dedicated outdoor air system combination. The scope of further research is also outlined in the chapter.

This chapter has been focused on the literature review related to Radiant Cooling System (RCS) and Dedicated Outdoor Air System (DOAS), their behaviour and performance trend. However, there are numerous studies on the radiant heating and cooling system to evaluate the thermal performance of the system and to implement the system for practical applications. This chapter outlines the literature review on the basic and applied research in RCS and DOAS systems for the built environment and various studies of DOAS energy performance have been reviewed in details.

2.1 Historical Background & research trends in radiant cooling system

The radiant heating system began thousands of years ago, credit is given to the ancient Romans for giving life to these systems, but archaeology and research of the ancient texts show Asia to be the earliest known developer of such systems, preceding the Romans by thousands of years [13]. People have utilized a mixture of architectural techniques to adapt dwelling design and cultural practice to local climate conditions like thermal mass, shading, strategically-placed vents, atria, and so forth. The Roman hypocaust system contained raised floors made of concrete and covered in mosaic tiles. Circumstantial information suggests that, at the same time, the Turks were cooling their dwellings by tapping cold river water and circulating it through gaps in walls or floors [14]. Figure 2-1 shows the Hypocaust flues from the Roman bath.

Figure 2-1: Hypocaust flues from a Roman bath [14]

[15] History of Roman hypocaust has been reviewed, which supplies hot combustion gases through cavity walls and floors, and carried out numerical analysis to

evaluate the parameters of hypocaust: cavity width and storage capacity of a hypocaust. They also suggested the combination of a hypocaust and modern HVAC systems, such as solar air collectors, solar chimney, and hydronic heating system for the heating purpose. [16], [17], [18] Korean Ondol is another type of traditional radiant heating system that utilizes the hot combustion gas to warm floor stones for heating. It has been used in Korea since 400 B.C., however, since the 1970s, the floor heating system has been transformed into a water-based floor heating system in order to improve fuel efficiency as well as indoor. [19] Initially, radiant system was more popular for heating application in cold climate, especially in East Asia compared to cooling but slowly radiant cooling system gained interest among researchers and engineers and have been extended to cooling applications in a mild climate such as Europe and North America, even in hot and humid climate such as Southeast Asia and China. In India, it is slowly picking up the market share in HVAC industry.

[3] For thousands of years, people have utilized a mixture of architectural techniques to adapt dwelling design and cultural practice to local climate conditions like thermal mass, shading, strategically-placed vents, atria, and so forth. The implementation of the radiant cooling system can also be a viable option since it is more energy efficient along with energy and peak power saving potential in comparison to all-air conventional air conditioning.

[20] After the industrial revolution, mechanical heating and cooling of indoor spaces have gained interest. A computer-based model was developed for radiant cooling systems for the RADCOOL software that works under the SPARK environment, where the two-dimensional cooling ceiling and cooling panels can be analyzed based on the heat balance of each component.

The radiant cooling system has slowly gained interest in recent years, the floor heating system is almost installed in all residential buildings in Korea. In Germany, Austria and Denmark almost 30-50% of new residential buildings are coming up with radiant heating-cooling systems [15]. Figure 2-2 shows the numbers of Building and Environment publications, published on the radianr heating and cooling system, which demonstrates growing interests in recent years. Radiant panel cooling systems were initially tested in the laboratories in European countries in the early 1990s [21]. Radiant cooling has been increasingly applied in western European countries after successful

verification of the system, it was found it has enough potential to increase energy efficiency and improve thermal comfort [22]. Application of the radiant cooling system in hot and humid climate, it is a critical issue to avoid condensation on radiant surfaces, because in tropical climates dew-point temperature typically exceeds the surface temperature of radiant surface.
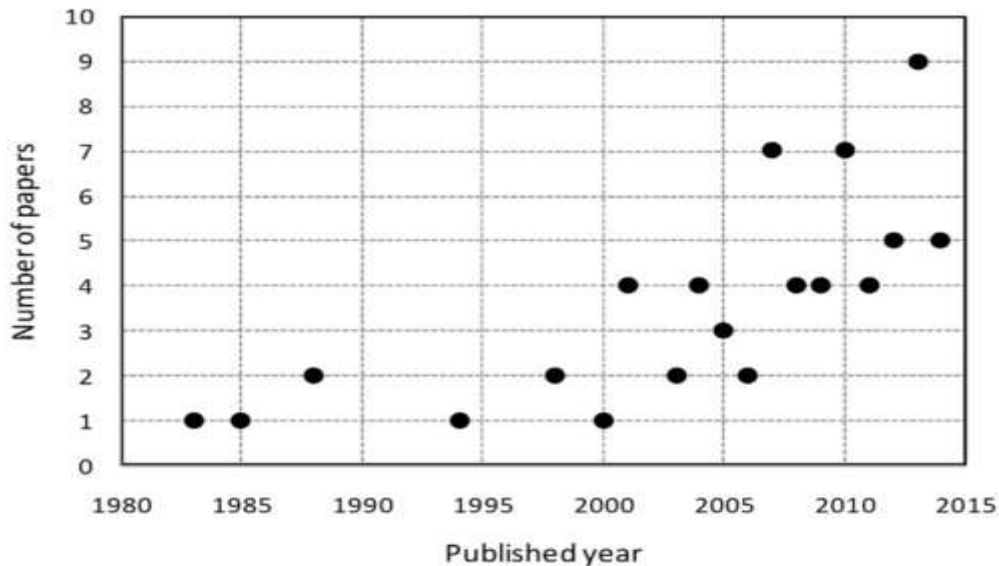
Figure 2-2: Annual number of published articles on the RHC system [17]

From the Roman era to present date, application of RCS is widely used in different parts of the world. The technology of the RCS has become reliable and people are taking advantage of it for both cooling as well as heating. In the subsequent subheadings, different aspects of RCS such as heat transfer model, testing standards, experimental and simulation analysis, thermal comfort analysis has been discussed in details below.

2.2   Heat transfer model & cooling capacity estimation in RCS

Heat transfer and cooling capacity are some of the most important parameters for the system design and operation. [23] Introduced heat transfer coefficients for radiant cooling ceiling system.

[24] Stated that the heat transfer coefficient of the radiant floor heating is 9-11 W/m^2 K, and more than half of the total heat transfer is due to radiation (~5.5 W/m^2 K). In case of the radiant floor cooling, the total heat transfer exchange is 7 W/m^2 K, while the radiant heat transfer coefficient is also approximately 5.5 W/m^2 K, which is applied to all cases of radiant heating and cooling system using the floor, ceiling, and wall surfaces.

[25] Thermal performance of a hollow core concrete floor system for passive cooling was studied using numerical techniques to solve the one & two-dimensional models of the transient heat transfer through the building components. Computer simulations for a warm and sunny day in Montrbal show that, during occupancy, the hollow core floor system provides thermal comfort without mechanical cooling.

[26] Heat transfer dynamics of a space cooled by RCS is much different from all-air system has been discussed through an experimental study. How such differences affect the cooling load calculation methods and sensible cooling load for radiant systems and energy modelling methods. While maintaining similar thermal comfort conditions, cooling rates for radiant cooling system vary from air systems. The instantaneous cooling rate for the radiant cooling system was approx. varies from 18–21% higher than the air system for the tested conditions. The radiant system removed 75–82% of total heat gains while the air system removed 61–63% due to the amount of energy stored in the non-active thermal mass. Proposed the use of the new definition for the RCS load (different from air system cooling load). Simplified cooling load calculation methods, such as radiant time series or weighting factor methods, may lead to incorrect results while calculating the load for radiant cooling systems.

[27] Presented total heat transfer coefficient for cooled ceiling based RCS is $13.2 W/m^2$ K, and $5.8 W/m^2$ K for a heated radiant ceiling. It was stated that the radiative heat transfer coefficient can be considered constant, approximately 5.6 W/m^2 K for radiant heated and cooling ceiling system, while convective heat transfer coefficient varies significantly depending on the radiant surface temperature. The cooled ceiling has higher convective heat transfer (up to 4.4 W/m2 K) than the heated ceiling (up to 0.3 W/m^2 K), concludes that the ceiling is more appropriate for cooling purpose.

[28] Describes a parametric study to calculate the energy saving and peak power reduction potential of radiant cooling systems in a building in the US. They made a numerical modelling of the RCS and conventional all-air system at different locations of U.S. they shows that radiant cooling can be used in the U.S with low risk of condensation. The energy savings potential is climate-dependent and is large in retrofitted buildings than in new construction. The potential savings of the simulated radiant cooling system are lower in cold, moist climates and higher in hot, dry climates. At the locations studied, the achievable energy savings of the system vary between 17% and 42% compared to base-case. The achievable peak power savings vary between 22% and 37%.

Many studies have suggested that some system configuration and control strategies for the practical applications of the RCS. In particular, a parallel system such as DV (Displacement ventilation) and DOAS (Dedicated Outdoor Air System) was suggested and investigated, in order to provide outdoor air and/or to remove latent load from the space equipped with the RCS.

[29] the designing parameters of the radiant panel system, used stainless steel panels made out of two corrugated stainless-steel foils and seam welded on the periphery and spot welded at many places for proper water distribution. They found that at a given volume flow rate, water is about 4000 times more efficient for heat transport than air. Most of the cooling ceiling panels are usually built from elements, which consist of a plate to which a water-cooled tube is attached. This configuration adds a thermal resistance between the tube and the plate surface, due to imperfect contact, thus limiting the heat transfer from the water tubes to the panel surface and environment. The panels are made from 0.6-mm thick and 860 mm wide, stainless steel sheet. The panels are similar to a thin cushion, where the water is in direct contact with more than 98% of the area. They also present the steps in panel manufacturing and the sustainability of panel. After manufacturing these panels, custom coated with a transparent, white, or colour paint or electroplated with black chrome selective layer.

[26] Presents an experimental study to identify the difference in cooling load calculation methods and sensible cooling load for radiant systems and air system. Demonstrated the difference in the heat transfer dynamics in the space conditioned by radiant cooling systems differs from the conventional air systems. How such differences impact design cooling load calculation and energy modelling methods. Cooling rates are different in the radiant cooling system compared to air system even when similar thermal comfort condition is maintained. The instantaneous cooling rate for the radiant system was on average 18–21% higher than the air system for the tested conditions. The radiant cooling system removed 75–82% of total heat gains during the period when the heater was on while the air system removed 61–63%. Energy stored in the non-active thermal mass is one of the major reasons for the difference. General cooling load calculation methods like RTS or weighting factor methods can lead to incorrect results for radiant systems. A new definition and calculation for the radiant system cooling load must be used.

[30] Experimental and simulation studied of the various characteristics of panel-based RCS and practical application of an office building was discussed. RCS is compared with the conventional air system on the parameters i.e. energy consumption, cost and thermal comfort. A radiant ceiling panel creates less vertical variation of air temperature while heating, than a conventional system. The radiant cooling system has an advantage over conventional all air HVAC system and provides less noise, less draft, more comfortable atmosphere. RCS is only responsible for handling the sensible load of the zone, whereas parallel air system is used for latent load and ventilation, less amount of air will be required to meet the load, which consumes less fan power. The estimated ROI time was 1 to 17 years depending on the first cost of the radiant panels. [23] The hydronic radiant cooling system reduces the air transportation due to the separation of ventilation and cooling task hence suggested for residential and commercial air conditioning where the major part of the energy is consumed by fans only to drawn the air into the room. This single improvement reduces the energy consumption and peak power requirements. In the hydronic cooling system, large surfaces are available for the heat transfer between the human and surface, very small temperature difference will be required between the surfaces and surrounding air. This makes the system efficient, reduce electricity requirements and furthermore space requirement for ducting work and the ventilation system is reduced by 20%. RCS has an advantage of less space requirement, draft-free, reduce energy consumption with enhanced air quality and if the specific cooling load is above 55 W/m^2 it may be lower in the first cost of the system.

[31] The benefits achieved by separating the task of cooling and ventilation were discussed. The study is precisely focused on the latent load treatment with the independent air dehumidification with energy recovery. Moisture load in ventilation air contributed about 68% for the most commercial buildings. Total ventilation load comprises of moisture load form outdoor air, and moisture load from human activities. Four independent dehumidification systems i.e. mechanical dehumidification is compared with different energy recovery means of the heat pump, sensible heat exchanger, membrane-based heat exchanger, and desiccant wheel with an evaporative cooler. Membrane-based heat exchanger with mechanical dehumidification is the most energy efficient. This study shows heat recovery with independent air dehumidification can save up to 29-42% of primary energy. Thermal comfort & Indoor air quality with the RCS

In RCS, higher air temperature also can provide adequate thermal comfort for cooling and that is why it is also known as high-temperature cooling system[32], this article is focused on the thermal comfort model, mean radiant temperature is more significant parameter compared to air temperature for occupant comfort, especially for radiant environment that means either the room has radiant ceiling cooling system or the room with radiant floor heating. There are different studies which have developed thermal comfort models and some have also developed tools to analyze thermal comfort based on the survey data.

In RCS heat transfer takes place majorly through radiation along with convection mode. It becomes important to understand different testing standards available to test RCS.

2.3   Testing standards for Radiant Cooling system

Panel based radiant cooling systems are more popular because they are easy to install and can be installed down the roof as fall ceiling during the renovation. The designing of the RCS is complex as compared to conventional air system because the performance of the RCS depends on several parameters like supply water temperature which cannot go below the zone air dew point temperature and the capacity of the system depends on flow rate and availability of radiant surface. Due to the large variation in performance of the system with little change in input parameters different manufacturer claim different load handling capacity so panel capacity testing standards are developed. Some of them are described below.

Standard ASHRAE 138, 2009

ASHRAE Standard 138, [33] establishes uniform methods for laboratory testing for rating the thermal performance of ceiling panels manufactured for radiant panel heating and cooling of indoor spaces. This standard covers steady-state testing of ceiling panels at panel surface temperatures from 24°C to 65°C (75°F to 149°F) for nonmetal heat transfer elements in the ceiling panel or from 24°C to 150°C (75°F to 302°F) for metal heat transfer elements in the ceiling panel. Sensible cooling ceiling panels are tested from 14°C to 24°C (57°F to 75°F). This standard provides the correction factors with respect to defined test conditions for the size of the test room, barometric pressure in the test location, and average air velocity in the vicinity of the test panels in order to ensure repeatable test results.

This standard specifies procedures, apparatus, and instrumentation for rating of the thermal performance of ceiling panels in a specific indoor configuration and thermal conditions. Thermal performance of a ceiling panel is measured in terms of heat delivered or heat removed by the ceiling panel as a function of the average fluid temperature of the heat transfer medium in the ceiling panel and the temperatures characterizing the surrounding indoor space. This standard covers testing of ceiling panels in the following effective panel surface high and low-temperature range limits:

a) Sensible Heating Ceiling Panels limits are from 24°C to 65°C (75°F to 149°F) for nonmetal heat transfer elements in the ceiling panel or from 24°C to 150°C (75°F to 302°F) for metal heat transfer elements in the ceiling panel.

b) Sensible Cooling Ceiling Panels limits are from 14°C to 24°C (57°F to 75°F).

ISO/DIS 18566-2, 2017

This Standard defines technical specifications and requirements of free hanging (suspended) heating and dry cooling only surface with an air gap between construction and the emitter (not embedded) with or without an insulation fed with water at temperatures below 120°C connected with a centralized heating and/or cooling supply source, intended to be installed in buildings. Ceiling mounted radiant panels covered by this standard are limited to a width from 0.3 m up to 1.5 m. The standard also defines the additional common data that the manufacturer shall provide into the trade, in order to ensure the correct application of the products. ISO 18566 Chapter 2 includes the radiant temperature asymmetry, Temperature measuring points, Verification of test installation, repeatability and reproducibility, Test method, Dimension and construction of the test samples, Selection of the models to be tested for determining the thermal output of a type, Manufacturer documents for the test samples, arrangement of the sample in the test booth, test procedure, test report etc. According to this standard, the steady-state condition will be achieved when the temperature of supply water and the air is in the limit of ±0.1K of the set point in the heating case and for the cooling case, the tolerance is ±0.5K. The tolerance for water flow rate is ±1% of the set value. Correction due to air pressure is also considered during the calculation of characteristic exponent for cooling and heating case. This standard also mentions the testing of mean surface temperature and the emissivity of the panel.

Different researchers and facility managers have performed experimental analysis to study the actual performance of the system. Some of the literatures are provided below to understand the experimental studies of the RCS.

2.4   Experimental investigation in radiant cooling system

[34] Cooling capacity and heat transfer coefficient were experimentally evaluated for inclined fin panel. For the typical test condition, the cooling capacity of the suspended metal ceiling radiant panel CRP is 77.5 W/m^2. The heating capacity of the suspended metal CRP is 188.0 W/m^2 and the radiant heat transfer coefficient is almost constant which is 5.5 W/(m^2 K). The correlations of the convective heat transfer coefficient in both cooling and heating condition are also obtained. While comparing with the convective heat transfer coefficient in literature, the measurement data is in the same range, but the heat exchange area is 0.4 times larger. In a typical office room, the cooling capacity of the tested panel with inclined fins is about 19% larger than the suspended panel. The panel shows the potential for free cooling when applied in buildings with a large area of glass envelopes [35].

[36] Cooling capacity and heat transfer coefficient were experimentally calculated for the ceiling radiant cooling panel system. They found that an average convective heat transfer coefficient of 4.2 W/m^{2}K which are between 2.8 and 4.8 W/m^{2}K when temperature difference moves from 3°C to 9°C, and total heat transfer coefficients range from 7.8 to 9.3 W/m2 K resulting in an average value of 8.5 W/m2 K. They also found that the total cooling capacity for the different temperature difference between operative temperature and panel surface temperature did not follow expected behaviour patterns, but it showed quite lower values.

[27] Heat transfer coefficients between the room and radiant ceiling in the typical condition of occupancy of an office building were experimentally evaluated. Internal gains were simulated using heated cylinders and heat losses using cooled surfaces. Heat transfer coefficient is expressed separately for convection and radiation or as one combined parameter, but this opinion may lead to different considerations about thermal performance of the system. They found a little higher average value of the total heat transfer coefficients which is 13.2W/m^2 K, for a cooled ceiling, compared to 11W/m^2 K from the literature. For a heated radiant ceiling, a total heat transfer coefficient of about 5.8W/m^2 K was measured, which is similar to the literature value of 6W/m^2 K.

[37] Study of radiant cooling by using outdoor air for ventilation in a hot and humid climate of Thailand was performed using experiments and simulation. They found the good potential for application of radiant cooling. Results show thermal comfort is in good agreement in the space. The results provide confidence and confirm the application of the radiant cooling system in hot and humid climate. In situations where cooling panels could affect air temperature, its use could lead to quiet quality comfort. Due to the need to avoid condensation of air moisture on the panel and the consequential limit on the temperature of supply cooling water to 24–25 °C, cooling capacity per area is limited to about 40 W/m^2, provides opportunity for energy conservation as very low energy means can probably be used to reduce the temperature of supply water to the required level.

[38] Experimental and theoretically analyzed metal ceiling panel in cooling mode for the climate of Greece. Experiments were performed in a 2.0×2.5×3 m^3 test chamber using a cooling panel area 1.80× 2.16m^2 hanging below the chamber ceiling. The study shows that the dynamic response of the panels is in good agreement with the thermal comfort conditions, fair for the climate of Greece. Under certain conditions, the condensed water vapour may rise dripping, solutions are proposed to avoid condensation. The response time of the system is reasonable and can be set as required value by regulating the supply flow temperature of cooling water. The time needed is less than 3 min for Tw<10°C and less than 10 min for Tw<15°C, while for medium to high indoor loads, the corresponding times may be doubled. The condensation problem on the surface of the panel has been examined experimentally and theoretically. Both analyses showed that under certain conditions the condensed water vapour may raise dripping problems, which may be solved by locating the panels on the ceiling under a slight inclination or in the upper part of the walls from the height of peoples' heads up to the ceiling.

Different heat transfer modes are associated in the working of the RCS, has provided thrust to develop heat transfer models. For analyzing analysis and benefits of different RCS, simulation analysis of RCS is documented.

2.5   Simulation analysis in RCS

This section addresses the different simulation analysis on energy performance, heat transfer analysis and thermal performance of the zone level in RCS using different energy and CFD simulation software's. Thermal analysis at the room level has meaningful importance in order to analyze the indoor environment by analyzing indoor

air quality, air flow pattern, room air distribution etc. CFD analysis for the RCS is of much importance as the RCS system is in general coupled with air systems for meeting the latent load and providing ventilation. Air creates thermal stratification, non-uniform distribution of room air and draft. CFD software uses the governing equation as Navier-Stokes equation in solving fluid flows phenomenon in the room with the RCS system.

[39] Experiments were conducted and different parameters like air temperature, mean radiant temperature, relative humidity and predicted mean vote were obtained for radiant ceiling panels, while air velocity and air pattern were studied by the CFD simulation study. Surface temperatures in the test room were found from experiment and used as boundary conditions of the CFD model. The study suggested a process of thermal comfort analysis using the CFD model as shown in Figure 2-5.
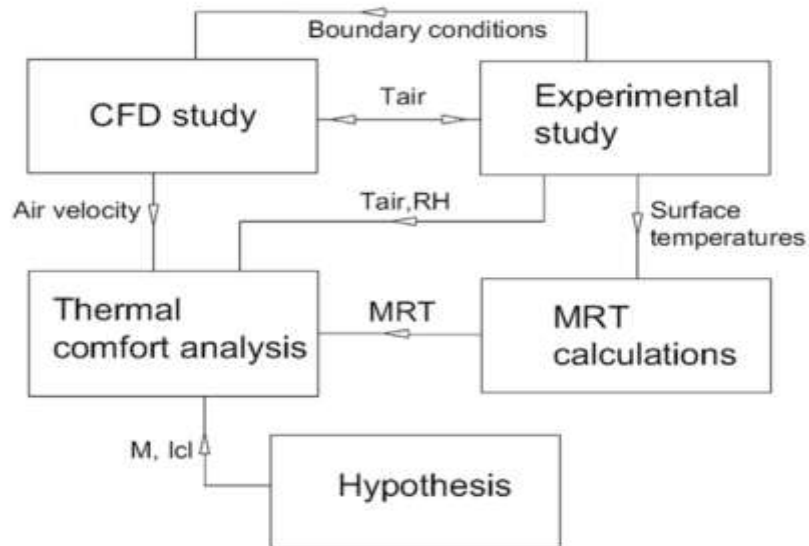
Figure 2-3: The process of thermal comfort analysis using the CFD model [38]

[40] In this study a semi-analytical radiant panel model is coupled with CFD calculations, for simulating the real interaction in between the radiant panel and its surrounding environment. The initial temperature of the radiant panels provides boundary conditions for solving the conservation equations using CFD which allows the calculation of a local heat transfer coefficient at each cell on walls These CFD calculation results are imported into a semi-analytical radiant panel model to compute the new temperature distribution on the panel which in turn provides new boundary conditions for CFD computations.

[41] A new CFD method and radiative heat transfer simulation are coupled to control heating, ventilating and air- conditioning (HVAC) in a room. This method is used to feeds back the outputs to run the HVAC system control (e.g., the supply of air temperature, the supply of air volume, etc.) to the input boundary conditions of the CFD. In this study, the radiation panel system is compared with the all-air cooling system. In case of the radiant panel cooling system, the heat flux of the panel surface was modified, while in the case of the all-air cooling system the temperature of the supply air was modified.

[42] A numerical technique is used for estimating the performance of a CWCT (closed wet cooling tower) for chilled ceiling systems. The technology is based on computational flow dynamics (CFD) for the two-phase flow of water and gas droplets. The Lagrangian approach is used for the water droplet phase flow and the Eulerian approach for the gas phase flow, with two-way coupling between two phases. The predicted maximum and minimum temperatures of tube coils representing the return and supply water for a chilled ceiling are close to the measured water temperatures at the outlet and inlet of the heat exchanger. The predicted maximum decrease in the coil temperature is in good agreement with the measured result for the water temperature. The numerical simulation indicates that CFD is a suitable tool for predicting the thermal performance and optimizing of the design and operation of the cooling tower for chilled ceilings.

[43] Investigated the current operational status of a TABS system installed in ECC building through a field survey. The TABS system heat and cool the rooms, whereas VAV systems perform the ventilation and dehumidification functions. The inlet water temperature was set to 29°C for heating and to 19°C for cooling. Using EnergyPlus simulation [44], the heating and cooling loads were determined based on the daily average outdoor temperature. The heating load distribution was approximately linear with the change in the outdoor air temperature in winter. For the cooling load, the relationship was less linear than that for the heating load. Finally, operational guidelines classified according to the load zones of the ECC building were suggested. First, the TABS thermal output was considered, and then the set point for the supply water temperature was changed to assure thermal comfort and to prevent the formation of surface condensation.

[45] Developed an EnergyPlus model of the building with radiant slab systems having evaporative cooling sources. In a dry and hot climate, the model predictive controller has been compared with the rule-based control method. It was found that MPC retains zone operative temperatures at EN 15251 Category II level more than 95% of the occupied hours for all zones. The rule-based method was able to maintain only the core zone at this thermal comfort level. It was also shown that MPC reduced the cooling tower energy consumption and pumping power consumption by 55% and 25% respectively.

[46] Evaluated the performance of radiant cooling system integrated with an air system for different operational strategies. For performance evaluation in the thermal performance and energy savings simulation software FLUENT and EnergyPlus is used in the Indian commercial building. Building model is calibrated with the measured data from the radiant system installed in the building. Different strategies are also proposed in this study for further energy savings potential in the radiant cooling system. Using simulation tool monthly and annual energy consumption is compared among the different operational strategies. The radiant cooling system saves up to 17% energy as compared to the conventional case. The study shows potential energy saving can be achieved when the radiant system is integrated with DOAS and by using different control strategies.

[47] Analyzed the performance of radiant floor cooling coupled with outdoor air in the hot and humid climate using TRNSYS simulation method. The calibrated model is used in the study for more accuracy. Results are reviewed in terms of energy consumption, indoor comfort, and system operation. Two different methods of outdoor air i.e. temperature based (DBT) outdoor air cooling mode and enthalpy based mode applied in this study. The temperature based mode is used when the outdoor air temperature is less than the Td and enthalpy based mode is used when the enthalpy of outdoor air is less than the enthalpy of indoor air. In this study, dehumidified ventilation with economizer control is analyzed with radiant floor cooling system. This analysis reported that by coupling outdoor air unit with radiant cooling system reduces the load on chiller by 24%, and in terms of total energy consumption up to 20% energy savings can be achieved. This study shows temperature based outdoor air mode is more energy efficient than the enthalpy based mode in the hot and humid regions.

[48] Compared radiant cooling system with VAV system for economic feasibility and energy cost using TRNSYS program. The first cost associated with system and space

requirement is also analyzed. In the cooling ceiling system for supplying outdoor ventilation air, mechanical dehumidification is used. Simultaneously several parameters as like cooling load, weather, operating hours, with or without free cooling etc. are also varied to see the impact on the cost. The cost associated with the system depends on the cooling load capacity of the system. Almost cooling load 45-55 W/m^2 is the breakup point of cost for VAV and cooling ceiling system. And up to 45% to 55% space requirement can be reduced. Energy cost of free cooling associated ceiling system saves 10-20%. The study shows that for higher cooling loads, ceiling cooling systems cost is favourable as compared to conventional VAV system.

Many studies on the radiant cooling system have focused on the realization of thermally comfortable conditions, some studies dealt with indoor air quality in a building with the RCS system.

2.6 Thermal comfort model for the radiant cooling system

Thermal comfort is the condition of mind that expresses satisfaction with the thermal environment and is assessed by a subjective evaluation [49]. An occupant's thermal comfort depends on the continuous process of heat exchange with its surrounding environment. A human body responds to mainly three conditions of thermal environment hot, cold and neutral environment. These thermal conditions are perceived by the human body and are dependent on the balance between energy gains and losses.

Indoor environmental condition significantly affects the body's working efficiency. This indoor environment consists of four major factors: Thermal environment, Air quality, Noise level and Lighting level. All these four factors are closely connected with each other and determine the overall effects of the building on the occupants. For example, natural or artificial lighting has its impact on thermal conditions, thermal conditions affect the air quality and in order to maintain air quality, a ventilation system is required which produces noise. Hence, requirements for the general thermal comfort (PMV-PPD, operative temperature etc.) and local thermal comfort (surface temperature, vertical air temperature differences, radiant temperature asymmetry etc.) must be considered for providing an overall comfortable thermal environment. Figure 2-3 shows the six primary factors used to predict thermal comfort.

2.6.1 Personal factors

- *Metabolic rate (met):*

The term metabolic rate quantifies the heat released from the human body per unit skin area. 1 metabolic unit= 1met= 58.2 W/m2, where typical values for adult males and females vary from 1.65 to 2.00 m^2 with an average value of 1.7 m^2 for a single adult person [50]. The amount of metabolic heat generated from the human body depends on the activity level and size of the person. For example, an average sized male seated quietly produces 108 W of body heat when compared to walking on a levelled ground at 1.34 m/s, the same body generates 270 W (ASHRAE, 1997).

- *Clothing insulation (Clo):*

The term defines the amount of thermal insulation the person is wearing. Clothing insulation value may be expressed in Clo units. 1.0 Clo is equivalent to 0.155 (m^2 K)/W. Clothing works as an insulation on the body and reduces heat loss from it. Insulation value is the basic criteria for the classification of clothing level. Clo value of 0.0 indicates a person who is naked i.e. no cloth. Different values above 0.0 Clo indicates different attires, for example, someone wearing a business suit has a Clo value of 1.0.
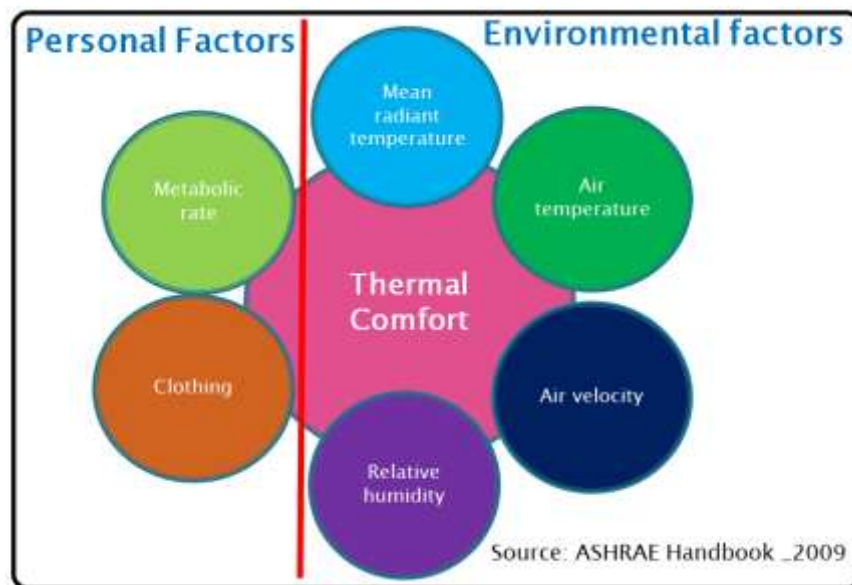
Figure 2-4: Six primary factors used to predict thermal comfort [87]

- *Environmental factors:*

***Air temperature*:** Temperature of the air which is surrounding the body.

Mean Radiant temperature: The weighted average of all the temperatures from surfaces surrounding the body.

Air velocity: Rate of air movement given distance over time.

Relative humidity: Percentage of water vapour in the air surrounding the body.

Operative temperature: When it comes to thermal comfort, the operative temperature is what humans experience thermally in a space. It is the combined effects of the mean radiant temperature and air temperature.

2.6.2   PMV and PPD scales

A method of describing thermal comfort was developed by Ole Fanger and is referred to as Predicted Mean Vote (PMV) and Predicted Percentage of Dissatisfied (PPD). If the thermal comfort in a workplace is not perfect, how far from perfect is it? Or within what limits should we maintain temperature and humidity to enable reasonable thermal comfort? The answers to these questions can be identified from the PMV-index (Predicted Mean Vote). The PMV-index predicts the mean value of the subjective ratings of a group of people in a given environment. The PMV scale is a seven-point thermal-sensation scale ranging from -3 (cold) to +3 (hot), where 0 represents the thermally neutral sensation. Even when the PMV-index is 0, there will be still some individuals who are dissatisfied with the temperature level, regardless of the fact that they are all dressed similarly and have the same level of activity.

[51] Conducted field assessment for evaluating thermal comfort at Mehran University of Engineering and Technology, situated in the subtropical region of Pakistan. The results indicate that people were feeling thermally comfortable at an effective temperature of 29.85°C (operative temperature 29.3°C). They found that the neutral effective temperature determined during this study closely matched that of the adaptive model based on indoor temperature or both indoor and outdoor temperatures. The results show that most of the occupants were satisfied at an average effective temperature of 32.5°C. This effective temperature is 6.5°C above the upper limit of the ASHRAE thermal comfort standard. Results show that if the radiant cooling option was adopted in place of air-conditioning, savings of 80% is possible in case thermal comfort is achieved through radiant cooling instead of conventional air-conditioning. Energy savings of 118.2 MWh/year or 80% and 106.8 MWh/year or 81% are obtained for offices and classrooms of the University, respectively.

[22] A field study is conducted to identify the thermal comfort level in the radiant cooling system using a total of 116 sets of data from 82 participants in summer and winter. The results show that occupant whole-body thermal sensations with radiant

cooling were consistent with the predicted mean vote (PMV) model. RCS has reduced local thermal discomfort with a reduced draft rate as well as reduced vertical air temperature difference. The measured average indoor operative temperature was about 22°C and ranged from 20.3 to 23.6°C, in both summer and winter; the average air temperature was about 22.3°C in both, the mean air velocity was about 0.06 m/s in winter and summer; average relative humidity was about 36% in summer and 11% in winter. The average vertical air temperature difference between the ankle and the head level was about 0.5°C and the average draft rate was about 4%. The average floor temperature was about 21°C in both seasons. The average temperature difference between the surfaces with the highest and lowest temperatures was about 2°C. The discrepancy between PMV and AMV was 0.06 scale units in summer and 0.09 scale units in winter. Combining summer and winter data, the discrepancy between PMV and AMV was 0.02.

[52] Developed a mathematical model for the evaluation of mean radiant temperature in radiant coupled environments and for the radiation from windows. The model works on the basis of the average temperature of each surface and angle factors between the person and each surface. It was compared with three different methods to calculate MRT, which are stated as follows:

- Based on black globe thermometer

$$MRT_{bgt} = \{(T_{globe} + 273.15)^4 + 0.274 \times 10^9 \times v_{air}^{0.5}(T_{globe} - T_{air})\}^{0.25} - 275.15 \qquad (1)$$

- Based on operative temperature, measured with a thermal comfort meter

$$MRT_{tcm} = 2T_{op} - T_{air} \qquad (2)$$

- Based on the measurement of plane radiant temperature

$$MRT_{prt} = \left[0.18(T_{up} + T_{down}) + 0.22(T_{right} + T_{left}) + 0.30(T_{front} + T_{back}) \right] / 1.4 \qquad (3)$$

[53] Proposed a simplified body model to simulate the real performance using the shape and thermal property of human body to investigate radiant heat exchange between the human body and its surroundings as shown in Figure 2-4. In the simplified model, skin temperature and thermal resistance of clothing were defined, using measured data. The developed model was successful in calculating the local thermal environment caused by radiant cooling effect quantitatively. For example, head and thigh were resulted

in greater heat loss and lowered body surface temperature in the radiant ceiling cooling system.
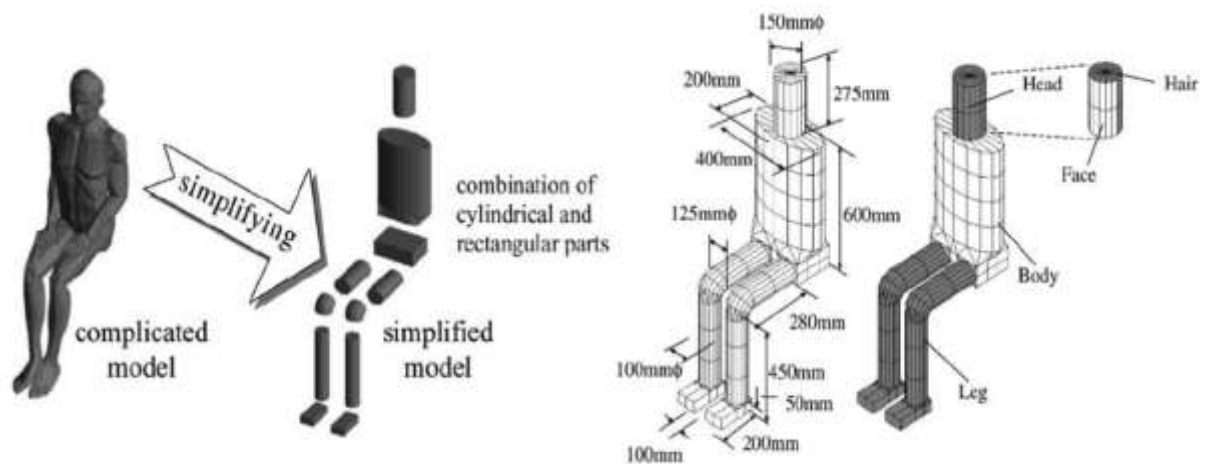
Figure 2-5: Six primary factors used to predict thermal comfort Simplified human body model proposed by [27]

[54] Reviewed for field measurement of MRT based on typical methodologies for measuring the MRT with practices consistent for instruments with ISO 7726: 1998.

2.7 History of DOAS

Dedicated outdoor air system (DOAS) can be defined as:

A dedicated outdoor air system (DOAS) use a separate equipment to condition all the outdoor air brought into the building for ventilation and delivers it to each occupied space, either directly or in conjunction with local or central HVAC unit serving those same spaces. The local or central HVAC units are used to maintain space temperature.

The concept of DOAS was known to researchers and introduced to the industry for long decades. Various DOAS configurations are available and perform differently in the different climatic conditions. DOAS is capable of providing 100% outside air in the space when coupled with the local terminal HVAC unit. ASHRAE Standard 62.1 ventilation requirements can be fulfilled by using DOAS; it was the first system identified which decouples the heat load.

Decoupling of the sensible and latent load became the major benefit of using DOAS. These kind of two systems i.e. primary and secondary system when used with another advanced system of their time provided energy savings compared to a conventional system. [56] The total load is decoupled, the primary system supplies air at 6°C in the space caters the latent load and partially sensible load while part load operation

and secondary system comprise of the terminal unit(s) using local recirculation air is used for the sensible load to meet the space setpoint.

Decoupling of load i.e. separate temperature and humidity control made the system downsized, instead of cooling the whole volume of air to 7°C for cooling and dehumidification we are going to cool some air to 7°C for dehumidification and rest would be at an elevated temperature to meet the sensible air. By downsizing the system duct size and fan size saves the first cost as well as the operational cost of the system.

Decoupling system configuration has another major benefit of maintaining good indoor air quality (IAQ) control. In the air-side economizer coupled VAV while low cooling load minimizes the ventilation rate below the prescribed rate. [57] By supplying 100% outdoor air, the system provides better IAQ performance and has the potential of energy saving in some climates.

After the introduction of ASHRAE Standard 62-1989, the potential of DOAS was identified and noticed by researchers and engineers worldwide. Newly introduced ASHRAE standard emphasized on the increasing required minimum ventilation per person for multi-zone to achieve better IAQ performance, researchers and engineers start looking at alternative system configurations to fulfil these requirements.

ASHRAE Standard 62-1989 prescribed the values for outdoor air requirement and accordingly categorized the buildings. In some categories, the requirement of outdoor air was increased by two to four times compared to 1981 version of the standard, provided the major upliftment in popularizing DOAS in the United States (Kosar et al. 1998). Introduction of new design criteria for ventilation rate for multi-zones system results in much higher ventilation flow rates compared to buildings designed under the older version of Standard 62.1. Furthermore, using outdoor air in non-arid climates can result in periods of increased indoor humidity levels [58].

Engineers realized that instead of using one system in which outdoor air and return air gets mixed in the mixing chamber should be replaced by two system for individual control of temperature and humidity provides better thermal comfort and the IAQ [59]. ASHRAE introduced "100% OA systems" in Addendum 62n of Standard 62-2001. The distinguishing characteristic of this system is that it supplies 100% outdoor air (OA) for ventilation to one or more zones.

Different researchers have published about positive outcomes of DOAS in the HVAC industry ([60], [61], [62], [63], [64]) However, knowledge of system configuration and integration of DOAS have varied with time and a large number of DOAS arrangements (decoupling strategies) are available for the integration with HVAC systems.

DOAS, as presented in this study, is defined as a system which uses separate equipment to condition the outdoor air supplied into the building for ventilation and meeting latent load, integrating with the radiant cooling system to meet the sensible load.

2.8   Studies on the decoupling of the load using DOAS

Some of the reasons one should design an HVAC system by the decoupling the load are for improving dehumidification, minimizing energy consumption and ventilation control.

Effective dehumidification, Better energy savings, Ventilation control

When a single HVAC component is handling the total load in a commercial building excess humidity can become a serious issue during "off-peak" hours. When the sensible load of the building remains low and the latent load is continuously high, when the sensible load in the space is low, the compressors in such a situation will work on constant-volume controlled. Due to lower sensible load thermostat temperature will be achieved very quickly and direct expansion (DX) cooling system will operate for a short period every hour. When the DX system is not working coil stop dehumidifying and moisture remaining on the surface of the coil can evaporate back into the air and the humid outside air enters the building and again increasing more latent load simultaneously. In same building load with different sensible and latent load ratio, system
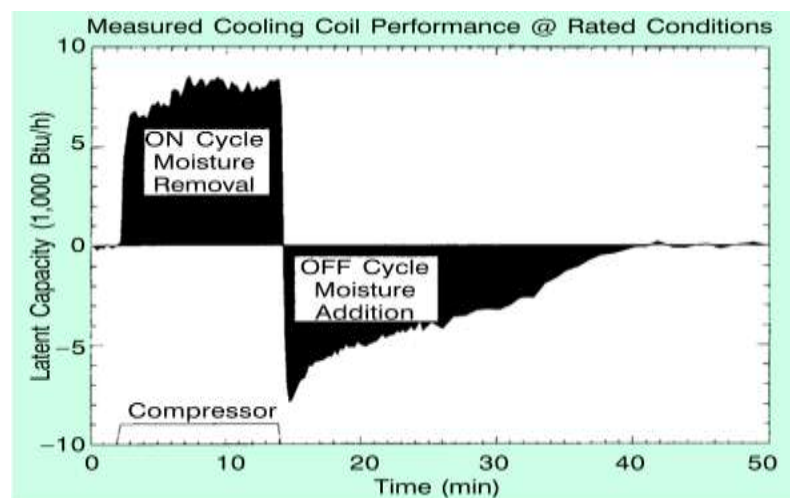
Figure 2-6: Measured dehumidification performance of a 3-ton cooling unit controlled by temperature [6]

dehumidifies the air differently. DX cooling unit after the compressor shuts off, moisture condensed on cooling coil re-evaporates removes very little moisture although moisture loads remain high. Figure 2-6 shows the measured dehumidification performance of a 3-ton cooling unit controlled by temperature alone. The compressor operated for only 12 minutes of the 50-minute test [6].

[65] DOAS removes the humidity from the outdoor air only, it allows the second component to operate only for the sensible load hence overall load on the HVAC system reduces and system downsizes.

DOAS airflows are independent of building cooling load, hence it is simple to operate and control DOAS in a constant volume system. Proper control of the DOAS is critical to realize the expected energy savings. Controls can be applied at the component level and DOAS level as well. Reducing the amount of outdoor air flow during the low occupancy availability in space can provide energy savings [66], the following strategy is known as *demand- controlled ventilation.* Implementation of such kind of strategy relay on the installation of the occupancy sensor, time of day schedules, people counters and carbon dioxide (CO_2) sensor.

Different decoupling strategies usually uses in the DOAS while some of them are described below. While decoupling the load decoupling strategies were used to cater the latent load. [67] Performance of a thermally regenerated desiccant system at two extreme ambient condition (high sensible and high latent load) is investigated. Figure 2-7 shows the schematic of a desiccant-based decoupling strategy. Latent COP is defined as the latent
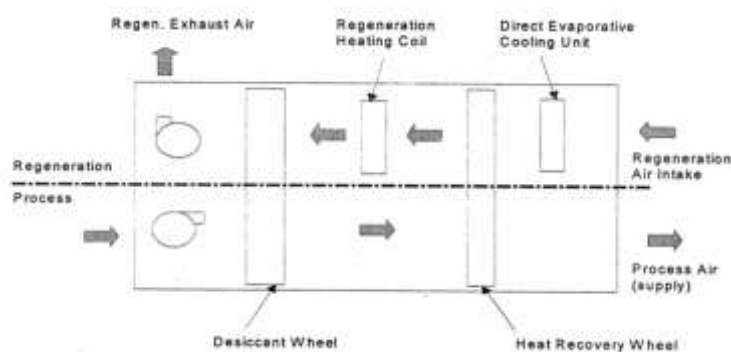
Figure 2-7: Schematic of the desiccant dehumidification system [67]

capacity divided by the total energy input of the process. The latent capacity significantly increased as desiccant wheel speed, face velocity and regeneration temperature increases for both climates.
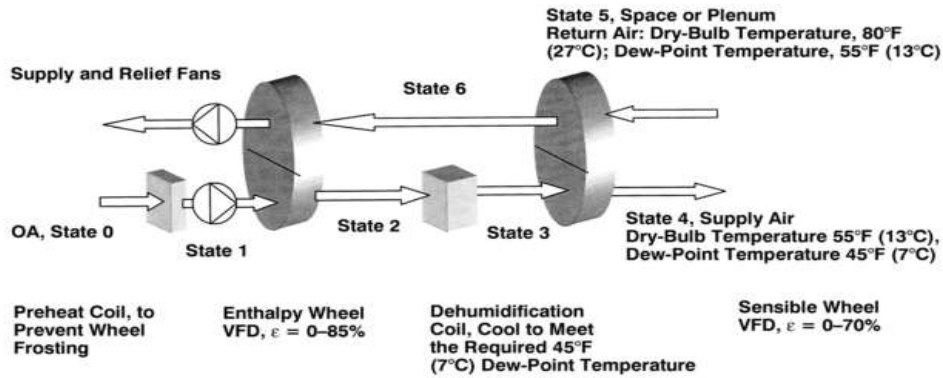
Figure 2-8: General arrangement of the DOAS [68]

[68] Discussed the importance of preconditioning of the outdoor air is vital in the performance of DOAS and its component. The dedicated OA must be cooled and dehumidified in the summer, and humidified and heated or cooled at other times to achieve efficiency. Figure 2-8 shows a cooling coil based arrangement of the DOAS.

[69] Achieving maximum energy savings air energy recovery depends on proper control of the energy-recovery device. On the hottest and coldest days of the year, energy savings can be significant. But, during less severe outdoor conditions, improper operation of the energy-recovery device may actually increase system energy use. Figure 2-9 shows the exhaust-air energy recovery in a dedicated OA system.
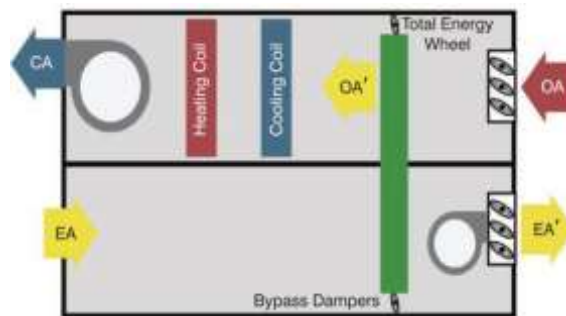
Figure 2-9: Exhaust-air energy recovery in a dedicated OA system [69]

[70] Comparing two methods refrigeration cycle - rotary desiccant and the heat exchanger cycle, refrigeration cycle for comparing and improvement of dehumidification in air conditioning systems. Figure 2-10 shows a schematic diagram and the psychrometric process of heat exchanger cycle.
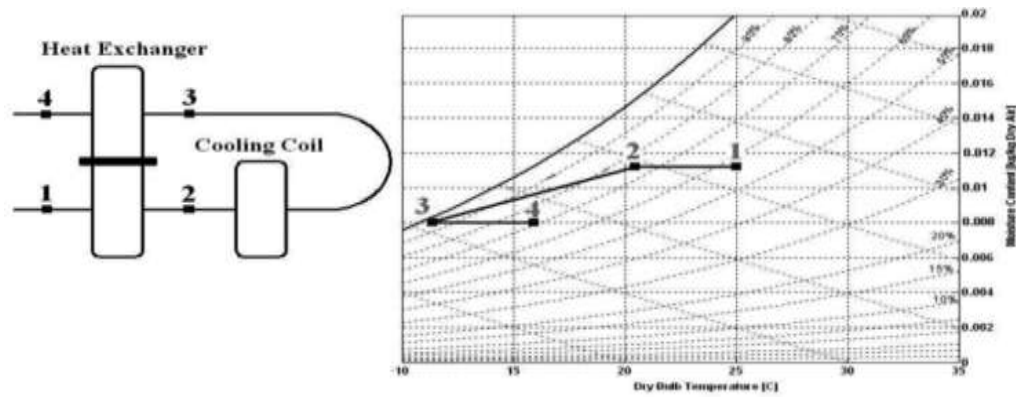
Figure 2-10: Schematic diagram and the psychrometric process of heat exchanger cycle [58]

Based on the literature review DOAS has the following benefits over conventional air system: Decoupling of sensible and latent load of air was first identified [59], [71], [72], Controlled ventilation can be provided with ease [73], [74], [74], provide flexibility in choosing the secondary HVAC system [75], provide energy savings with reduced demand for both primary and secondary HVAC system [63] [71].

Some of the literature discussed for integration of DOAS with RCS. [76] Study of chilled ceilings with displacement system was analyzed for the energy consumption. The chilled ceilings with displacement system, combined with a desiccant dehumidification system were tested for the climatic condition of hot and humid climate (Beijing). Considering heat removal by the chilled ceiling and displacement ventilation system the energy consumption was estimated and compared with the conventional air conditioning system. The combined system saved 68.5% of chiller energy and 39.0% of fan energy, however, it increased the pump energy by 25.6% and the boiler energy was about 4 times due to the regeneration of desiccant wheel. It was concluded that total energy saving was 8.2%, and the saving in electricity consumption was 62% less than the conventional system, which could help reduce electricity peak load caused by air conditioning systems. Figure 2-11 shows a combined chilled ceiling, displacement ventilation, and desiccant cooling system.

[77] A newly designed decentralized DOAS was coupled with the panel based radiant cooling for the tropical climatic condition (Figure 2-12). DOAS was designed to remove the latent load and part of the sensible load of the space and bring 100% outside air into space. A parallel radiant cooling system was integrated to handle the leftover sensible load. Two separate chillers were adopted in order to supply different chilled water temperature, which can lead to the improved efficiency of the chiller due to the

36

difference in supply chilled water temperature of RCS and DOAS. This design of the RCS with parallel DOAS can simultaneously satisfy the space sensible loads, latent load and ventilation requirements.
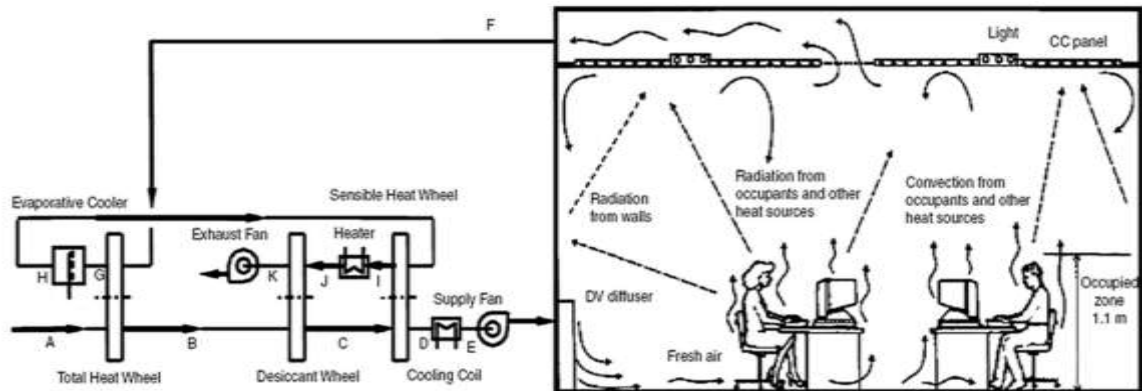
Figure 2-11: Combined chilled ceiling, displacement ventilation, and desiccant cooling system [64]
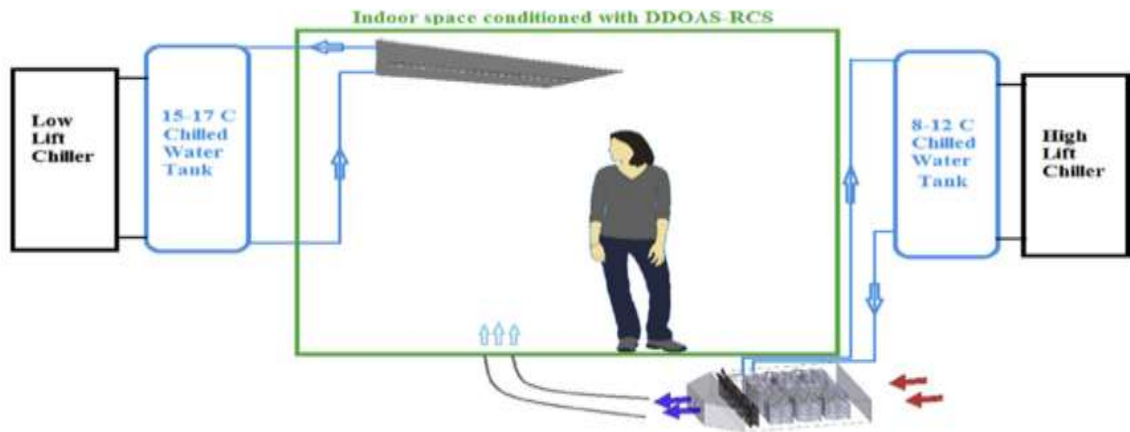
Figure 2-12: Decentralized DOAS coupled with radiant cooling panels [65]

[78] Radiant floor cooling system integrated with dehumidified ventilation (Figure 2-13) has been proposed to achieve savings compared to all-air cooling systems for Korea. Laboratory experiment and TRNSYS simulation for an apartment in Korea have been conducted to solve the condensation on a floor surface but also to control the indoor thermal environment within the acceptable range. The applicability of the proposed systems was proven for real situations, even for the hot and humid season of July–August, when there exist highest cooling loads and high potential for condensation.

(a) Concept of radiant cooling system with dehumidified ventilation system

(b) System components of a dehumidified ventilation system
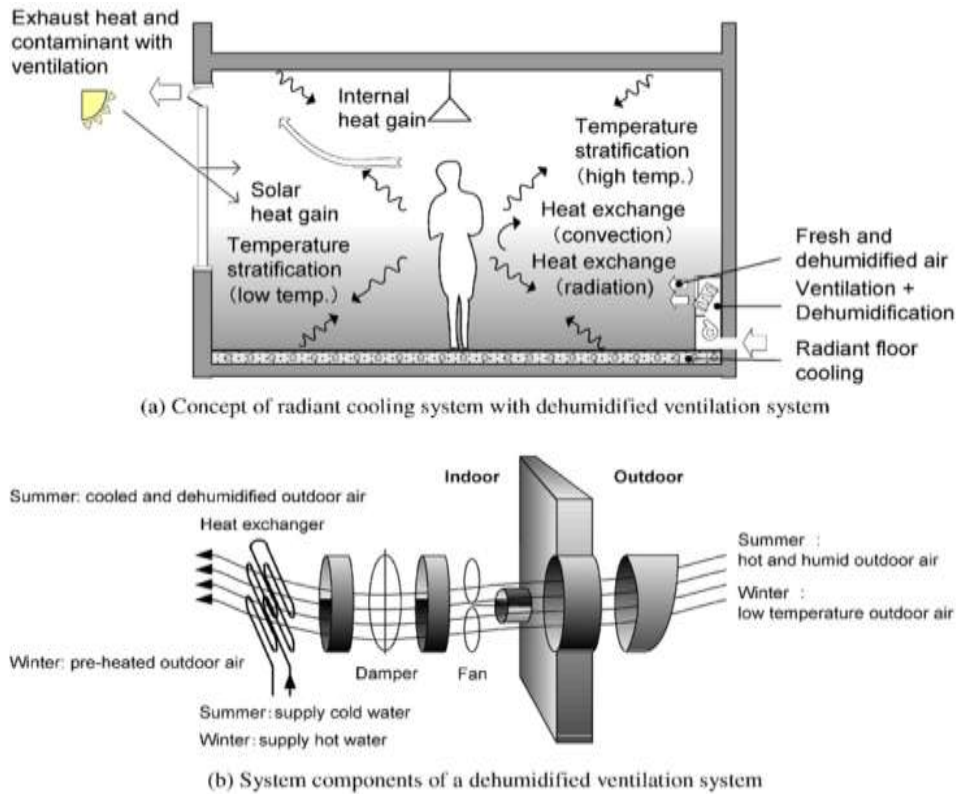
Figure 2-13: Radiant floor cooling integrated with dehumidified ventilation [66]

2.9   Enhanced indoor environmental quality (IEQ) with ventilation

Ventilation benefits of the DOAS can be seen when the building is designed to provide outdoor air in every zone of the building either directly or by using an HVAC terminal unit.

[71] When central HVAC systems serving multiple zones, in such a case it is not necessary that sensible load varies with the ventilation load of an individual zone. This causes increased system total intake of ventilation airflows to ensure proper ventilation to meet the comfort or ASHRAE Standard 62.1.

[79] One of the issues is over-ventilation of non-critical zones in a multi-zoned building. When a single terminal unit is providing outdoor air to multiple zones, providing proper ventilation to the critical zone (zone requires highest outdoor air) will result in over-ventilation of the non-critical zone. When DOAS supplies the outdoor air to an individual zone or in conjunction with a terminal unit one can overcome the above-mentioned ventilation issues. If DOAS will be designed properly ensures proper ventilation in each zone at the design zone population [71]. Application of DOAS has a primary goal of ventilation and secondary goal of humidity control. Humidity control benefits can only be achieved when all the known system configurations should be

properly implemented with proper sizing. Humidity is not easily controlled by all HVAC system for every climatic condition. ASHRAE 62, 1989 edition suddenly provided the mandate of supplying more outdoor air requirements. [58] Providing increased volume of outdoor air may result in increasing the humidity ratio (latent load) of the building for non-arid climates. [71] In the humid climates, outdoor air can increase the latent load very fast. While using a single system to handle the total load DOAS uses two separate equipment's to overcome sensible and latent load. [59] To handle indoor latent load exact amount of low humidity ventilation air can be provided in the space with a separate component, thus relying on the local HVAC terminal for humidity control is not necessary. If the DOAS is used in an HVAC system to achieve the goal of humidity control then it is necessary to use an energy recovery device as per ASHRAE 90.1. To achieve good control of humidity, it is important to pay more attention while part load operation and the ratio of load recovered by both the primary and secondary component. In a VAV system when the space loads changes, amount of total air delivered to the space changes in order to achieve efficiency. Due to change in air volume, sometimes it leads to a loss in the humidity control while still it manages to control the space temperature control. In such kind of situation, DOAS manages the latent load by supplying the air at low enough dew point to maintain acceptable indoor humidity levels.

Certain professional pointed out, for achieving fundamental change in the HVAC system, indoor air quality will play the major role. Decouple the load such that we can meet the requirement of thermal comfort and ventilation separately. Humidity control benefit is potentially available for almost all DOAS configurations. [80] Along with humidity control, DOAS creates pressure differential (barrier) between adjoining spaces or zones for the transportation of the potential airborne contaminants between zones. [81] With the application of DOAS airborne contaminants that might be entered into one zone of the building will not be distributed immediately in the whole building.

Many times it was observed that in real buildings, due to improper decoupling of load creates serious problems in the radiant cooling system. Improper sizing and selection of DOAS strategy also creates condensation problem along with increase energy consumption. The right selection of decoupling strategy while designing RCS leads to energy savings with improved thermal comfort and indoor air quality in the building. There are some successful integration of RCS in real buildings in India i.e. Infosys Hyderabad, Tech Mahindra in Hyderabad, KL University Vijayawada, Polaris software Chennai, IIM Raipur etc. Many a times, building owners face challenges in getting energy

savings, condensation in the case of DOAS due to wrong selection, sizing of DOAS strategy. DOAS strategy performs differently under different climatic condition; our research group has analyzed logged data of a few buildings and identified such problems.

2.10   Research gap

A comprehensive review was conducted on various studies on the RCS in terms of heat transfer models, experimental and simulation analysis, thermal comfort, the thermal analysis including heat transfer model and CFD analysis, system configuration and control strategies. Further studies are required to improve the performance and overcome limitations in utilizing the system for extensive building types and different climates. Following are some of the research gaps found in the literature review:

- Different types of the radiant cooling systems need to be experimentally examined for different Indian climate.
- Experimental analysis for integration of RCS with cooling tower needs to be analyzed.
- Different dehumidification techniques for integration with radiant cooling system need to be studied for the different climatic condition.
- Direct/indirect use of renewable energy (solar and geothermal) as a heat production source for desiccant regeneration to couple with RCS should be analyzed.

2.11   Chapter summary

A wide variety of theoretical, experimental and simulation studies are available in order to investigate the performance of DOAS and RCS. This chapter has also focused on different properties and parameters that adversely affect the performance of the RCS. However, I have not come across any kinds of literature which have provided a recommendation for the coupling of different DOAS and RCS strategies to enhance the performance of the system for the different climatic condition. For improving the performance of RCS in different climatic condition decoupling of sensible and latent load need to be studied.

The objective of this research is to provide right combinations of DOAS and RCS to enhance the performance of Radiant Cooling System (RCS) through decoupling of the sensible and latent loads. The RCS can handle the sensible load only; the total load is decoupled into primary (humidity control) and secondary (sensible load) load. Performance of RCS varies with climate, for improving the performance of RCS it is essential to use the right combination of DOAS strategy with RCS for the desired climatic condition. The overall work has been carried out broadly in three phases i.e. Phase 1 is a simulation analysis of decoupling strategies, Phase 2 is an experimental analysis of decoupling strategies and Phase 3 is experimental and simulation analysis of RCS. The objectives of the thesis has been accomplished and conducted in two separate steps for the dedicated outdoor air system (Phase1+Phase2) and radiant cooling system (Phase 3) as described below:
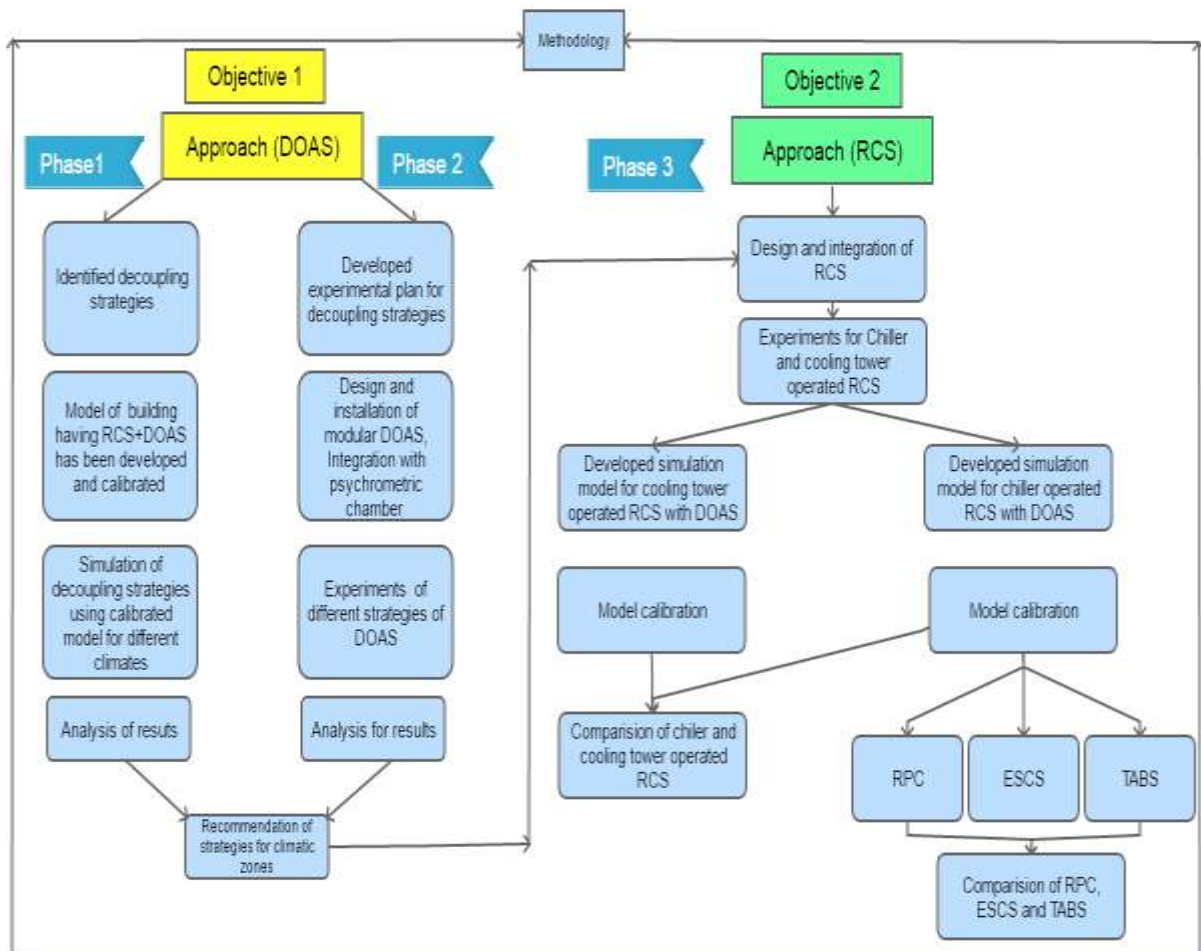
Figure 3-1: Flowchart for methodology of the thesis

Step 1 (Phase1+Phase2): Dedicated Outdoor Air System

- Decoupling strategies were identified from the literature review.
- Simulations were carried out to identify the potential of the different decoupling strategies for different climatic conditions.
- Identify the real-time performance of the different decoupling strategies, the experimental setup is designed and integrated.
- Modular DOAS setup is designed and integrated with the indoor and outdoor chamber for creating different psychrometric conditions.
- Experiments were conducted to evaluate energy consumption and thermal parameters for all decoupling strategies for different climatic conditions.
- Recommendations were provided for applicability of different decoupling strategies with parallel RCS for different climatic zones.

Step 2 (Phase 3): Radiant cooling system:

- The recommended strategy for Composite climate is coupled with RCS and an experimental setup is designed and integrated.
- Real-time experiments were conducted and data sets were collected and analyzed for the chiller and cooling tower operated radiant cooling system coupled with the recommended decoupling strategy.
- Whole building model is developed for both chiller and cooling tower based radiant cooling system and calibrated using the measured data using the EnergyPlus software.
- Annual and monthly comparison of the chiller and cooling tower RCS is done for different climatic conditions.
- Different types of radiant cooling system were compared.

All the three phases of the work have been briefly described in details below:

Figure 3-1 shows the flowchart of a methodology for the entire thesis. Performance of different decoupling strategies has been studied in phase 1 and 2. In phase 1 simulation analysis is conducted for decoupling strategies and based on the results phase 2 is executed for experimental analysis of different decoupling strategies of DOAS for the different climatic condition. Based on the results of phase 1 and 2 recommendations are provided for application of decoupling strategies based on different climatic condition. Figure 3-2 shows the flowchart of a methodology for the DOAS.

Performance of different decoupling strategies has been studied in phase 1 and 2. In phase 3 recommended strategy for composite climate is integrated with RCS in MNIT Jaipur. By conducting experiments and calibrated model analysis chiller and cooling tower based RCS has been compared. In addition, different types of RCS have also been compared. The detailed methodology of the different phases has been provided below:
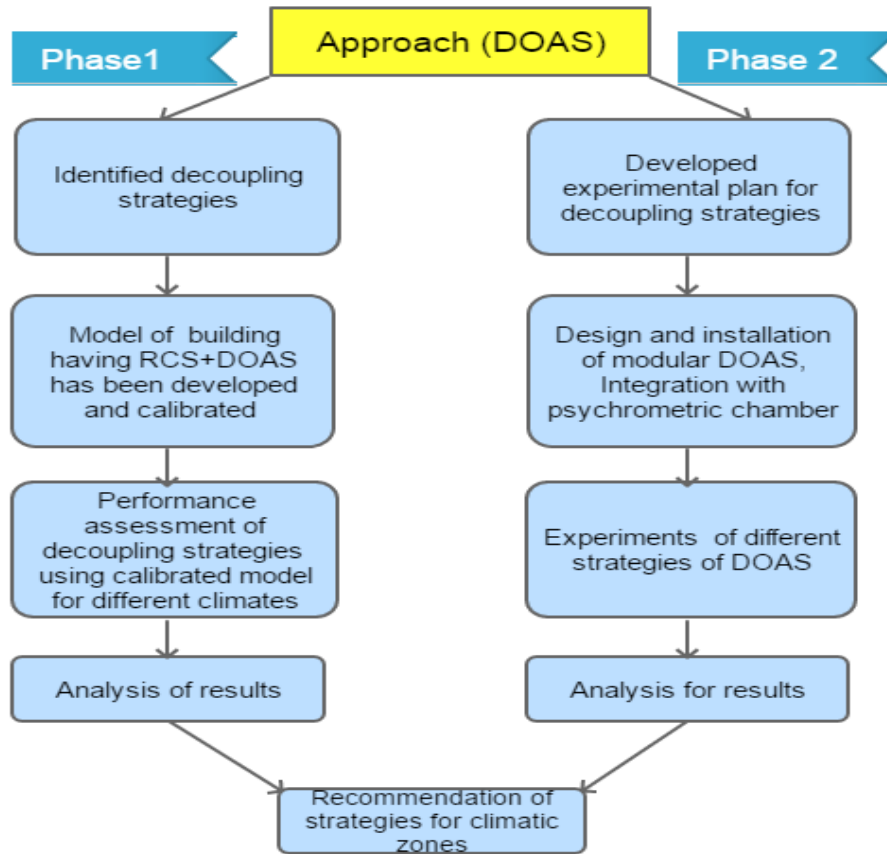
Figure 3-2: Methodology for Phase 1 and 2

3.1 Phase-1: Simulation analysis of decoupling strategies

In phase 1 simulation analysis for different decoupling strategies was performed. Initially, different decoupling strategies have been identified from the literature based on different dehumidification methods i.e. cooling coil and desiccant wheel. Simulation models are developed for all these six strategies using a calibrated building model of an office building integrated with RCS. The calibrated building has asymmetrical two wings one is integrated with RCS and other is integrated with the conventional all-air system. Parametric runs are performed for all the six models for four different climatic conditions of India. Results were analyzed for the different climatic condition for all the six strategies with the conventional all-air system. Details of phase 1 (modelling of different decoupling strategies) are discussed in chapter 4.

3.2   Phase-2: Experimental analysis of decoupling strategies

Based on the results of Phase 1, it was found there is a need to conduct experiments for a better understanding of the different decoupling strategies. A test facility was designed and developed for testing of different decoupling strategies. Testing of all the decoupling strategies was a big challenge. For testing all the existing decoupling strategies or any future addition of any new strategy a modular DOAS is designed and fabricated. Modular DOAS has been designed to incorporate the entire cooling coil and desiccant wheel based decoupling strategies (i.e. cooling coil and desiccant wheel with active heater regeneration based strategies as discussed in Phase 1) in order. All the components are placed in modular nature. For conducting experiment of particular strategy remaining all the components can be taken out of modular DOAS and the desired strategy can be created. An indoor-outdoor chamber is prepared for creating different outdoor condition in the outdoor chamber and indoor condition in the indoor chamber. Different outdoor condition and indoor condition are maintained by controlling the output of the heater and humidifier in the air handling unit (AHU). Details of controls and AHU and setup are discussed in chapter 5. Experiments were conducted and results were analyzed for the different climatic condition. Based on the results of chapter 4 & 5 recommendations were provided for decoupling strategies to couple with RCS for different climatic conditions.

3.3   Phase 3: Experimental and simulation analysis of radiant cooling system

An experimental setup was developed; recommended cooling coil based decoupling strategy for composite climate i.e. Strategy-2 (based on the result of chapter 3 & 4) was integrated with RCS. The RCS was designed and integrated into MNIT Jaipur (composite climate). Figure 3-3 shows the Methodology for Phase 3. RCS was coupled with a parallel chiller and a cooling tower to feed chilled water, DOAS is coupled with a separate chiller. Details of the setup are provided in chapter 6. Initially, experiments were conducted for chiller and cooling tower integrated RCS. Data was logged while conducting the experiments and further useful data was filtered. Based on the data, results of both the experiments were analyzed. While conducting experiments thermal comfort surveys were conducted and data were analyzed to calculate PMV and PDD.

Based on the building architectural drawing and HVAC plant details, building simulation model was developed for chiller and cooling tower based RCS in EnergyPlus. Using the experimental data of the chiller and cooling tower coupled RCS both of the

models were calibrated. Using both the model, the annual and monthly simulation was carried out and Chiller and cooling tower integrated RCS was compared. In the second case, the calibrated chiller based model is used to prepare three models for different types of RCS. Based on the annual simulations of all the three models different types of RCS were analyzed. Based on the simulation and experimental results of chapter 4 & 5 recommendations were provided for the climatic condition based usage of different decoupling strategies. Analysis of chapter 6 provided the recommendation for RCS strategies to be followed for different climatic condition.
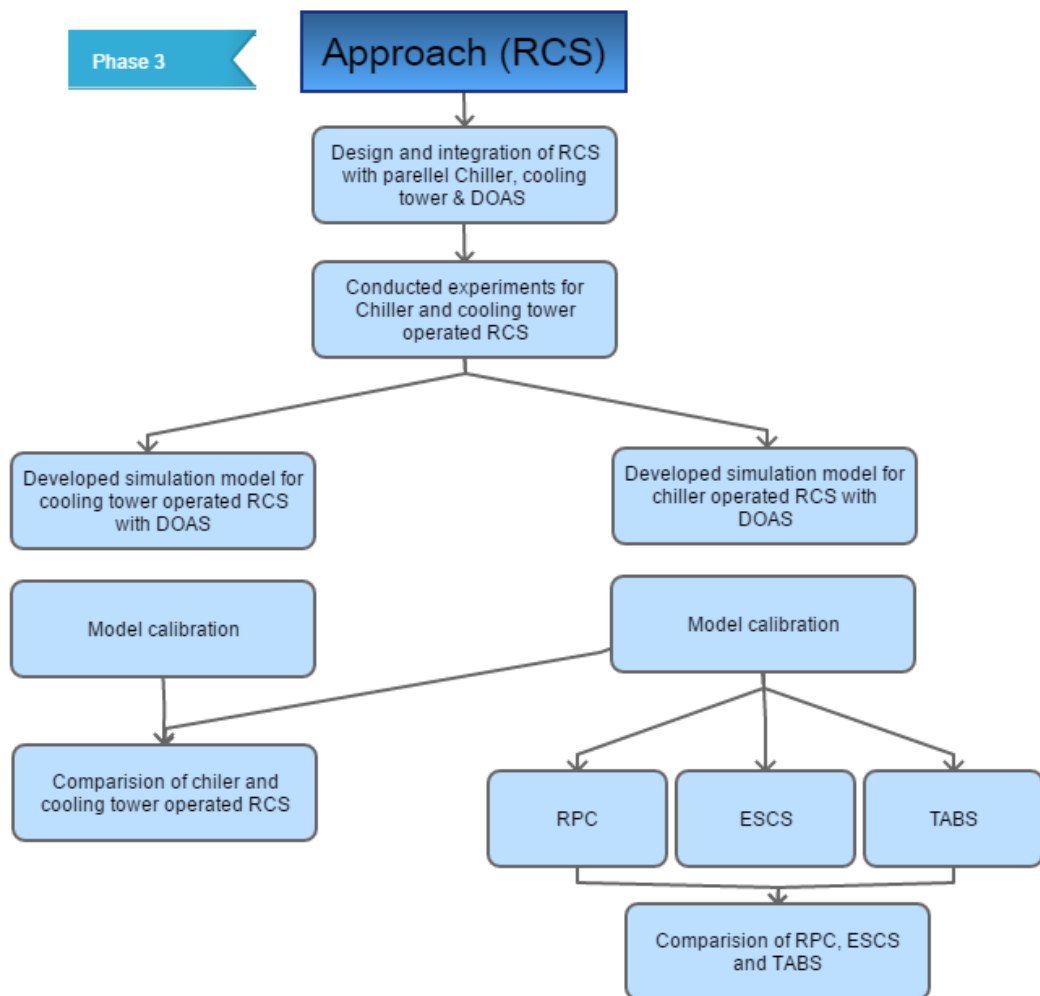
Figure 3-3: Methodology for phase 3 experimental and simulation analysis of RCS

For both the study of DOAS and RCS, experiments and simulations were conducted for the different climatic condition. Classification of Indian climatic condition and selection of the cities for the different climatic condition has been discussed in detail below.

3.4   Climatic conditions

As per the National Building Code (NBC), the Indian subcontinent is mapped into five climatic zones: (1) hot and dry; (2) warm and humid; (3) composite; (4) temperate; and (5) cold.
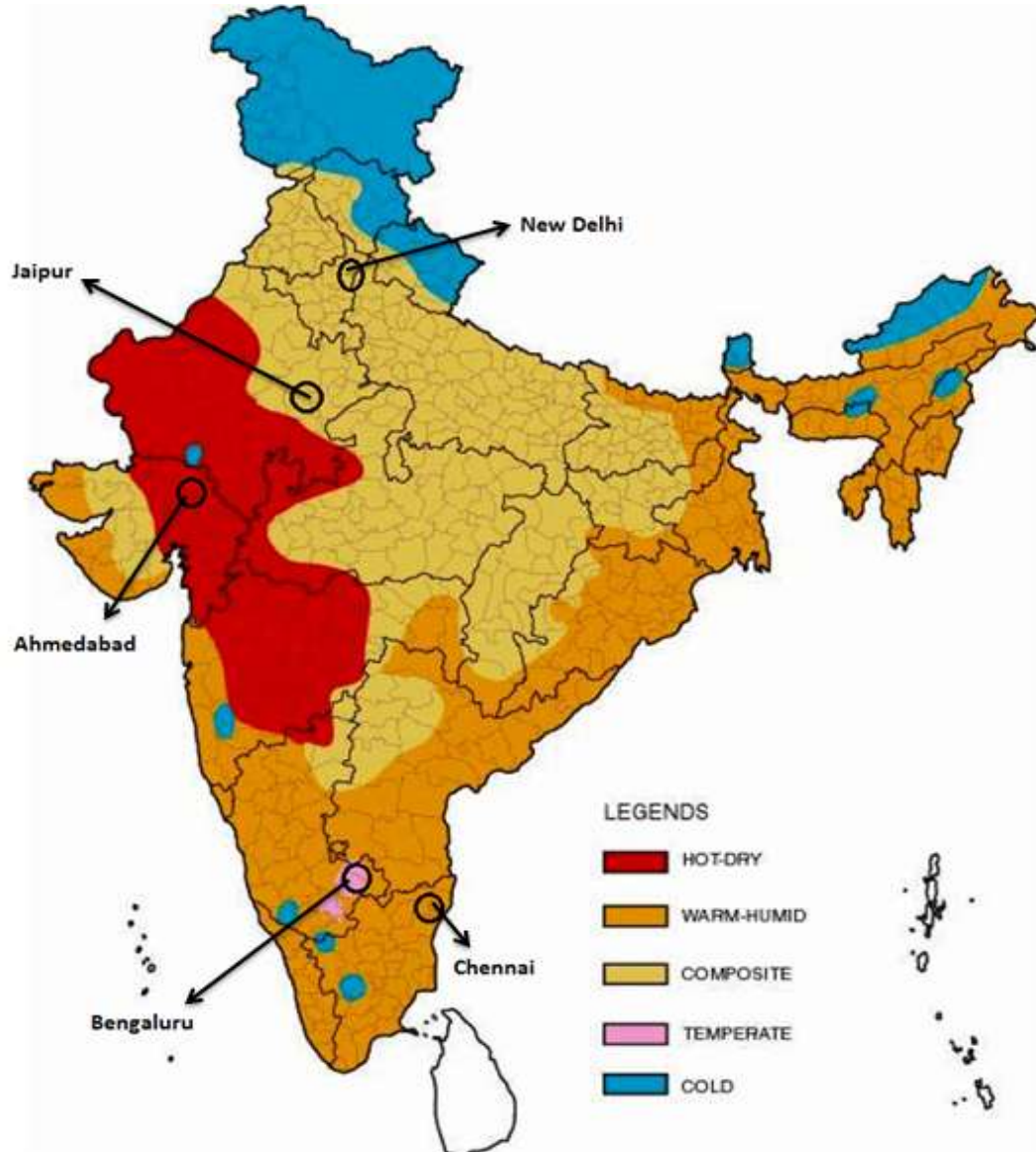
Figure 3-4: Indian climate map with selected cities.

The study of this thesis is focused on the cooling performance of the system, so the cold climate is not considered in the current study. Figure 3-4 shows the Indian climate map in which the selected cities (Ahmedabad [hot and dry], New Delhi [composite], Chennai [warm and humid], Bengaluru [temperate] and New Delhi and Jaipur [composite] have been marked.

Hot and dry climate usually have a high temperature with low humidity and rainfall, intense solar radiation with generally a clear sky, hot winds during the day and

cold winds during the night. The hot and dry climate is mapped in the region of the Thar Desert area in Rajasthan, east part of Gujarat and Maharashtra falls in this zone.

Warm and humid climate has a temperature moderately high in the day and night, high humidity and heavy rainfall, diffuse solar radiation if clouds cover is high and intense if the sky is clear and a high diversity in wind. Warm and humid climatic zone is mapped along the coastal region from Gujarat to Kanyakumari in the west and from the coastal region of West Bengal to Kanyakumari in the east. It also covers a vast area of northeastern India.

Composite climate applies when at least six months of the year does not fall within any of the other categories. Usually follows a high temperature in summers and low temperatures in winters. Receives a low humidity in summers and high in monsoon, high solar radiation in throughout the year except for monsoon. The composite climate is mapped in the north and central India. The states of Punjab, Haryana, Uttar Pradesh, Madhya Pradesh, part of Rajasthan, Bihar, Jharkhand, and Chhattisgarh.

The temperate climate is mapped with the tendency of moderate temperature, humidity and rainfall. Solar radiation is almost constant throughout the year with generally a clear sky. A major city in this climatic zone is Bengaluru.

3.5   Selection of building energy simulation tool

Selection of building energy simulation tool is a very important step in energy modelling of a building. There are too many simulation tools available for building energy simulation, so it is necessary to select an appropriate simulation tool for better simulation result which suits for the model. There are several software choices such as DOE-2, EnergyPlus, Energy 10, eQUEST, ESP-r, DeST, Energy Pro, Eco Tech, RIUSKA, TRNSYS, Perform 2002, Trane Trace 600 and Carrier Hourly Analysis Program (HAP). Tools Such as SPARK and BLAST have attempted to varying degree of success a holistic analysis of the radiant system and mass properties. SPARK allows users to construct models of complex building energy systems by connecting equation modules from a library. The program uses robust methods to solve the resulting set of differential and algebraic equations at different time step. Recent research includes work on a SPARK-to-EnergyPlus Link so that SPARK models of HVAC components, systems and controls can be run within EnergyPlus. BLAST is a software for mass analysis as it is essentially a transient multi-dimensional analysis tool that takes into account mass properties such as heat capacitance, thermal storage, etc. however, the radiant capacity is not fully developed, and a full analysis of radiant system efficiency is not possible [80].

Table 3-1 shows the comparison of basic characteristics of different Energy simulation tools and Table 3-2 shows the comparison of calculation capabilities of different energy simulation tools.

Table 3-1: Comparison of basic characteristics of simulation software's [82]

	DOE-2	eQUEST	EnergyPlus	ESP-r	DeST
Import CAD Drawing		✓	✓	✓	
Changeable Time Step		✓	✓	✓	
Export CAD Drawing			✓	✓	
Output Report		✓	✓	✓	✓

Table 3-2: Comparison of calculation capability [83]

	DOE-2	eQUEST	EnergyPlus	ESP-r	DeST
Room Heat Balance Calculation		✓	✓	✓	✓
Humidity Calculation		✓	✓		✓
Heat comfort calculation			✓	✓	
Nature ventilation calculation		✓	✓	✓	✓
Sunlight analysis	✓	✓	✓	✓	
Renewable energy calculation		✓	✓	✓	

EnergyPlus simulation software (it combines the best features of the DOE-2 program and BLAST program) was released by the United States Department of Energy in April 2001. In addition, to the ability to model configurable forced air system, the initial release of the new program also included models for High-temperature Radiant cooling and Low-temperature Radiant Heating Systems (Electric and Hydronic). TRNSYS also can Model Radiant cooling system, but it is not in open source. EnergyPlus is a freely available tool for the modelling of the radiant cooling system. So for modelling of the Radiant cooling system, EnergyPlus Simulation Tool is used in this thesis.

3.5.1 EnergyPlus

Building energy simulation tool was developed under support from the United States government was released in April 2001. EnergyPlus is based on the main features and capabilities of DOE-2 and BLAST but is a completely new program written in Fortran 90. New features include user-configurable modular systems, variable time steps, an integrated heat and mass balance based zone simulation, air pollutant transport, moisture transfer in building components, multi-zone airflow, solar PV simulation and input and output data structures tailored for the convenience of third-party module and interface development. EnergyPlus is initially a simulation engine without a user interface although user interfaces are under development by the private sector.

EnergyPlus uses an integrated solution technique by which the most serious deficiency of the BLAST and DOE-2 sequential simulations can be solved. Integrated simulation in EnergyPlus also allows users to evaluate a number of processes that neither DOE-2 nor BLAST can simulate well. Some of the more important include:

- realistic system controls

- moisture adsorption and desorption in building elements

- radiant heating and cooling systems

- Inter-zone air flow.

3.5.2   EnergyPlus components
EnergyPlus has three basic components as listed below

- Simulation Manager

- Heat and mass balance simulation module

- Building a system simulation module

Simulation Manager
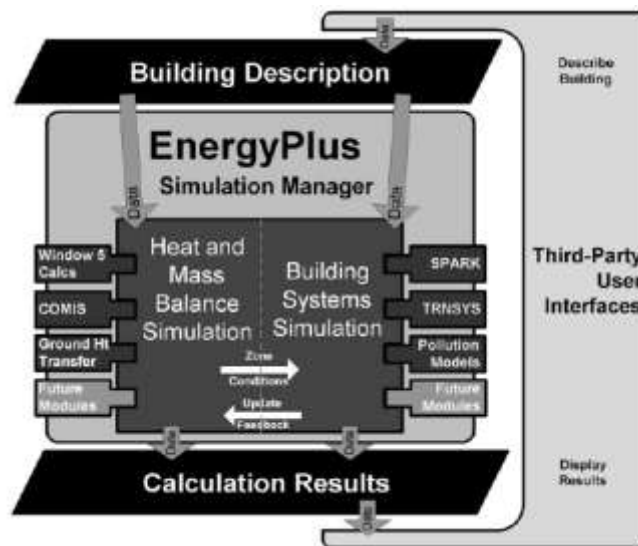
Figure 3-5: Overall EnergyPlus Structure [80]

Figure 3-5 shows the overall program structure of EnergyPlus. At the outermost program level, the simulation manager of EnergyPlus controls the interaction between loops from a sub-hour level up through the selected time step and simulation period - whether day, month, season, a year or several years. Actions of individual simulation modules are operated by the simulation manager, and instructing simulation modules to act such as initialize, simulate, record keeping, or report. [81]

Heat and Mass Balance

Heat balance model is used in EnergyPlus for the calculation of building thermal zone. The basic assumption of heat balance models is that air in each thermal zone can be modelled as well mixed with the same temperature throughout. Although this does not reflect physical reality well, the only current alternative is Computational Fluid dynamics (CFD) The modular structure of EnergyPlus is flexible which allows these new models to be included in future releases once they are available. The other main assumption in heat balance models is that room surfaces

- Uniform surface temperatures
- Uniform long- and short-wave irradiation
- Diffuse radiating surfaces
- One dimensional heat conduction.
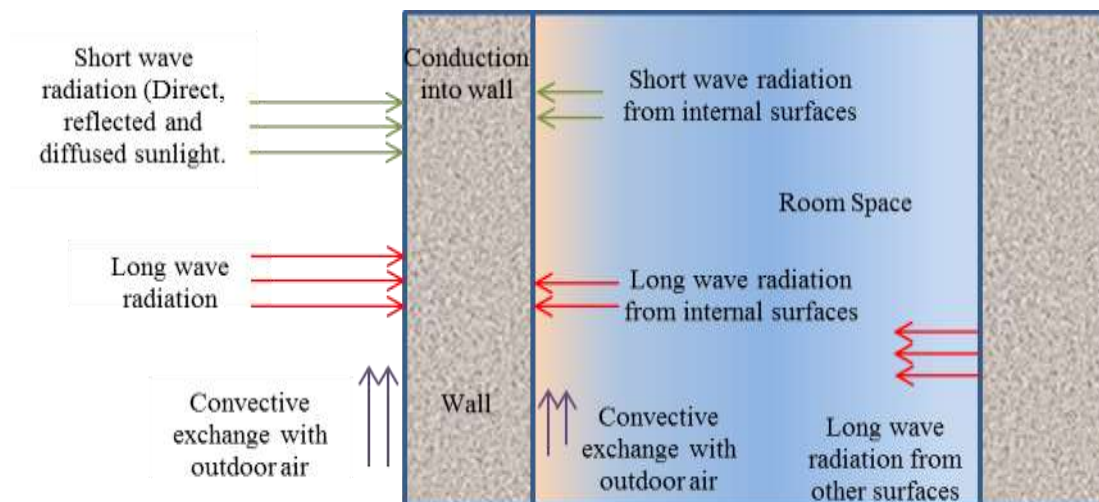
Figure 3-6: Heat balance Phenomenon of EnergyPlus [80]

Figure 3-6 shows the heat balance phenomenon in EnergyPlus. The EnergyPlus integrated solution manager manages the air and surface heat balance modules and acts as an interface between the building systems simulation manager and the heat balance. The surface heat balance module simulates inside and outside surface heat balance and boundary conditions; and convection, conduction, radiation, and mass (water vapour) transfer effects the air heat and mass balance module deals with various mass streams such as exhaust air, ventilation air, and infiltration.
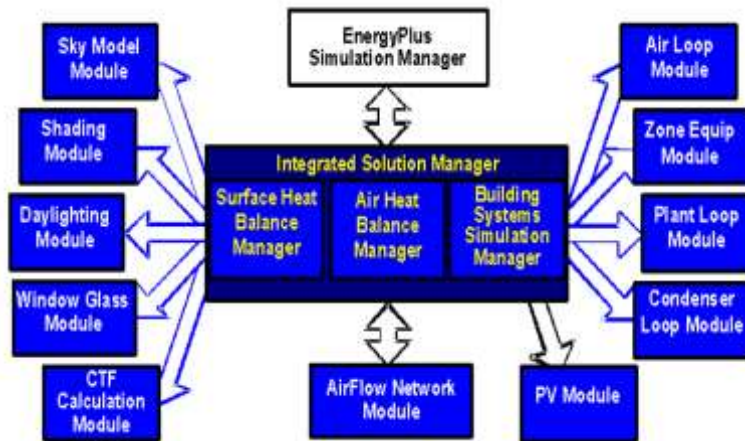
Figure 3-7: Integrated Simulation Manager [80]

Building systems simulation manager

When the heat balance manager completes simulation for a given time step, it calls the building systems simulation manager, building system simulation manager controls the simulation of electric and HVAC systems, equipment and components and updates the zone-air conditions. Figure 3-7 shows building system simulation manager EnergyPlus does not use an inline simulation method (first building loads, then air distribution system, and then central plant) as found in DOE-2 and BLAST since this imposes rigid boundaries on program structures and limits input flexibility. Building system simulation manager is a modular, extensible and fully integrated simulation of loads, systems, and plant.
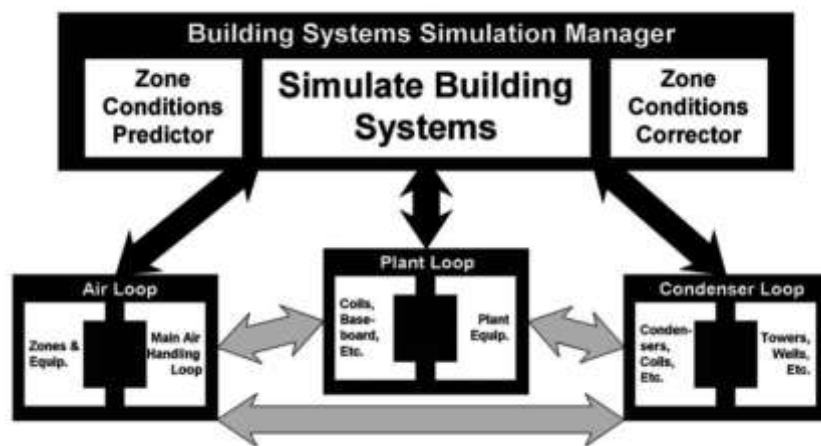
Figure 3-8: Building System Simulation Manager [80]

Integrated simulation models capacity limits more accurately and firmly couples the air and water side of the system and plant. Figure 3-8 shows the building system simulation manager, modularity is maintained at both the system and component level. This eases adding new components and flexible modelling system configurations and, at the system level, system and equipment are clearly connected to the zone model in the

51

heat balance manager. To bring these concepts into operation, EnergyPlus uses loops throughout the building systems simulation manager (primarily HVAC air and water loops). Loops imitate the network of pipes and ducts found in actual buildings and eventually will simulate thermal losses and head that occur as fluid moves in each loop.

3.6   Chapter summary

This chapter explains the entire methodology of the thesis. The overall work was conducted in three phase. Phase 1 is focusing on simulation analysis of decoupling strategies, Phase 2 is focusing on the experimental analysis of decoupling strategies and Phase 3 is explaining the integration of decoupling strategy with RCS with a comparison of the chiller and cooling tower integrated RCS and comparison of different types of RCS. The details of all the three Phases are discussed in chapter 4, 5 and 6.

CHAPTER 4. Simulation-based analysis of decoupling strategies

Decoupling strategies are used to separate out (decouple) the sensible and latent load in the HVAC system. Decoupling of load separates the temperature and humidity control in the system. The major advantage of decoupling is it downsizes the system. RCS is one of the best examples of decoupling of load, RCS is used to meet the sensible load and DOAS is used to provide ventilation requirement and meet the latent load. There are different decoupling strategies that can be used in DOAS. DOAS configuration under different climates does not provide the same benefits. Based on literature review it is found that air can be dehumidified either by (a) cooling coil by cooling it below the DPT of air, (b) adsorbing the moisture in the desiccant and (c) changing dew point using compression. This chapter provides information about decoupling strategies based on the cooling coil and desiccant wheel for dehumidification and their component. In this chapter different decoupling strategies are identified and calibrated simulation analysis and results are discussed for the different climatic condition.

4.1 DOAS configurations

DOAS is used for providing total outdoor air and to meet the space latent load. Initially, different decoupling strategies were identified from the literature. In our study, strategies based cooling coil and desiccant are identified and studied. In addition, energy recovery wheel, sensible wheel and indirect evaporative cooling system are also being used along with a cooling coil or desiccant wheel in DOAS. The identified strategies were simulated in the EnergyPlus software. Details of different decoupling strategies and their different components are described below.

4.2 Component of decoupling strategies

4.2.1 Low and high-temperature cooling coil

The cooling coil is used in the DOAS for cooling incoming air below dew point temperature for dehumidification. It plays a vital role in transferring the cooling load from the air loop to the chilled water loop by forcing the air to flow over the coil. Cooling coil usually consists of circular copper tubes section with fins (extended large area) to enhance the heat transfer (thermal performance). Usually in cooling coil, chilled water is passed in the coils and if the apparatus dew point temperature of the coil is less than dew point

Figure 4-1: Cross section view of the cooling coil and fan in DOAS
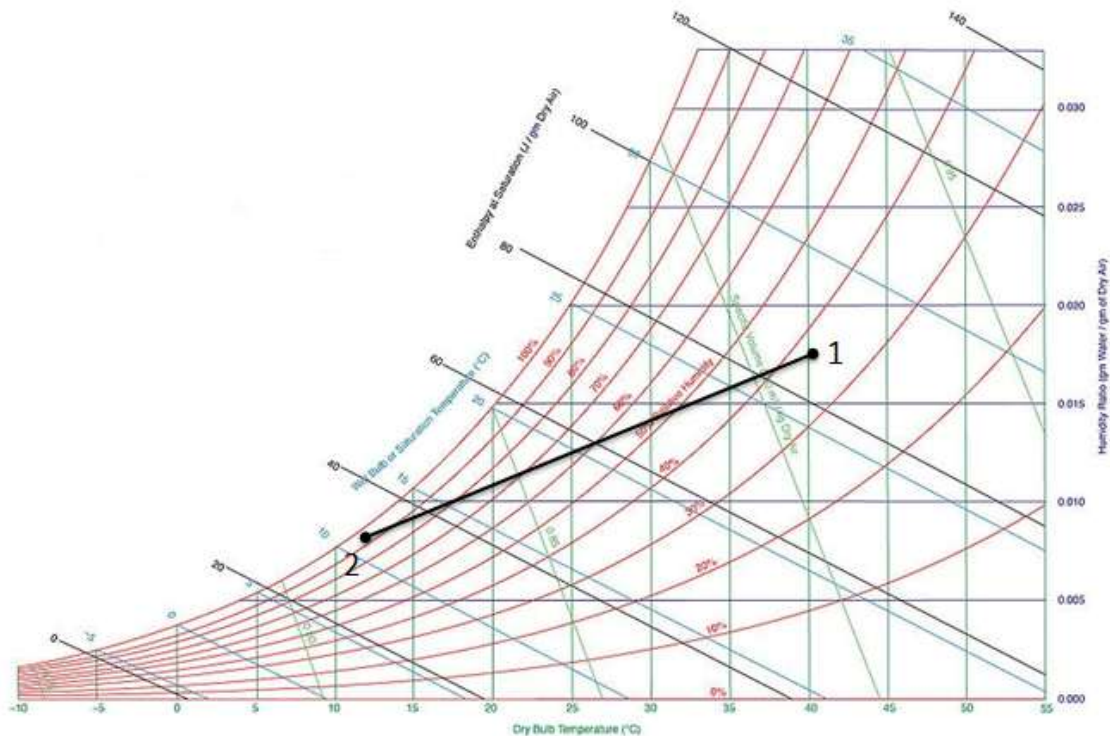
Figure 4-2: Psychrometric process of Low Temperature (LT) cooling coil

Process (1)-(2): Cooling and dehumidification

temperature of the air, moisture is removed from the air. Heat transfer characteristics directly influence the performance of the cooling coil. Chiller and pumping energy is

associated with the cooling coil. Performance of cooling coil impacts on the thermal comfort of the space. The main advantage of using the cooling coil is the response time of the cooling coil is very small. Figure 4-1 shows the crossectional view of the cooling coil and fan. Chilled water cooling coil has been used in two ways in this study i.e. (a) Low Temperature (LT) cooling coil and high-temperature (HT) cooling coil. Figure 4-2 shows the psychrometric process of the LT coil. In LT coil the supply chilled water temperature is 7°C. Figure 4-3 shows the psychrometric process of the high-temperature cooling coil (HT coil). In HT coil the supply chilled water temperature is 16°C. HT cooling coil only aims for sensible cooling of air. While modelling the LT and HT cooling coil availability schedule, supply chilled water temperature, design humidity ratio, design water flow rate, design air flow rate is needed to be input in the model.
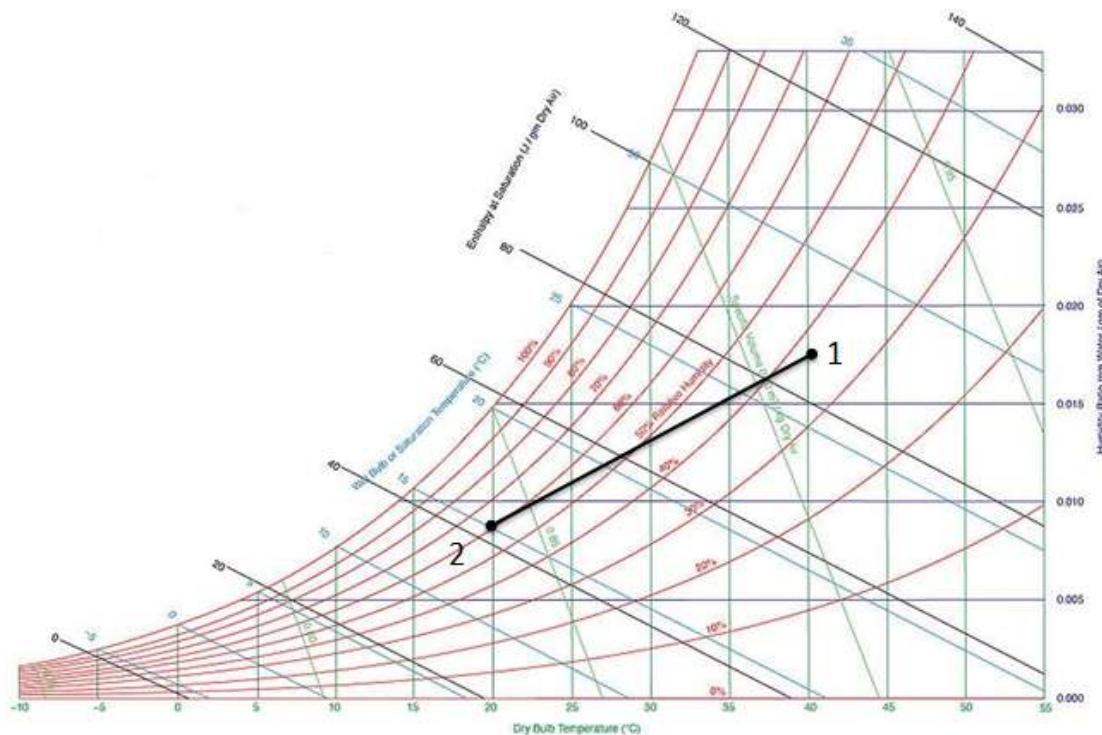
Figure 4-3: Psychrometric process of high-temperature cooling coil

Process (1)-(2): Cooling and dehumidification

4.2.2   Desiccant wheel

Desiccant dehumidification is also known as chemical dehumidification. It works on the principle of difference in vapour pressure, has a high affinity of removing moisture. The vapour pressure of the desiccant surface has a comparatively lower water vapour pressure than the humid air hence moisture gets absorbed by the desiccant. Desiccant dehumidification has some advantage over cooling coil i.e. (a) it also works when the

ambient temperature is 0°C, no limitation of dew point temperature, (b) better energy saving, (c) desiccant dehumidification does not produce any water condensate as compared to cooling coil which becomes breeding ground for bacteria. Desiccant materials which are commonly used in HVAC application are silica gel, molecular sieve, activated carbon, activated alumina, lithium chloride, calcium chloride etc.
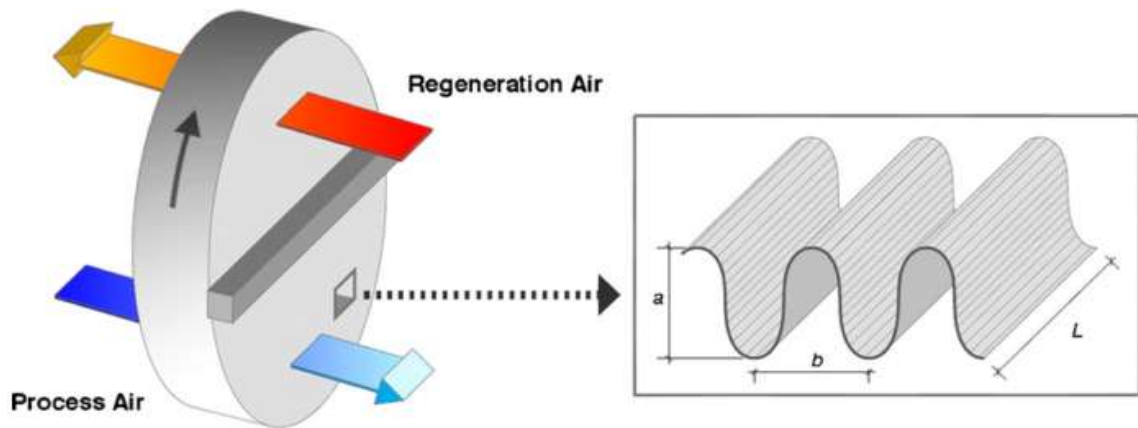
Figure 4-4: Desiccant wheel and channel schemes [72]

On the basis of the physical state, the desiccant can be divided into solid and liquid. The solid desiccant is mainly used in the form of the rotor in HVAC industry. Figure 4-4 shows the desiccant wheel and the channel schemes. Desiccant rotor matrix is made up of the honeycomb structure and is coated with desiccant particles of grain size 3Å / 4Å. The wheel is mainly divided into two zones i.e. process zone and the reactivation zone. Outside air enters the process zone and comes in contact with desiccant, removes moisture from the air and dehumidified air exits from the wheel. Conversion of latent heat adds some sensible heat in the air. For continuous use of desiccant, it requires to be regenerated. For the regeneration of desiccant rotor, heated air is passed through the reactivation zone. The solid or liquid desiccant can run on low-grade energy such as waste heat, solar energy etc., has energy storage potential. In liquid desiccant application, membrane-based heat exchanger is most commonly used. Advantages of the membrane-based heat exchanger are (a) it has lower pressure drop hence lower fan energy consumption, (b) there is no cross-contamination. In liquid desiccant system, regenerator loop is used for removing water content from the desiccant solution. Desiccants do not emit greenhouse gas, hence a better product for the environment. Figure 4-5 shows the crossectional view of the desiccant wheel in the modular DOAS.

Figure 4-5: Cross section view of the desiccant wheel
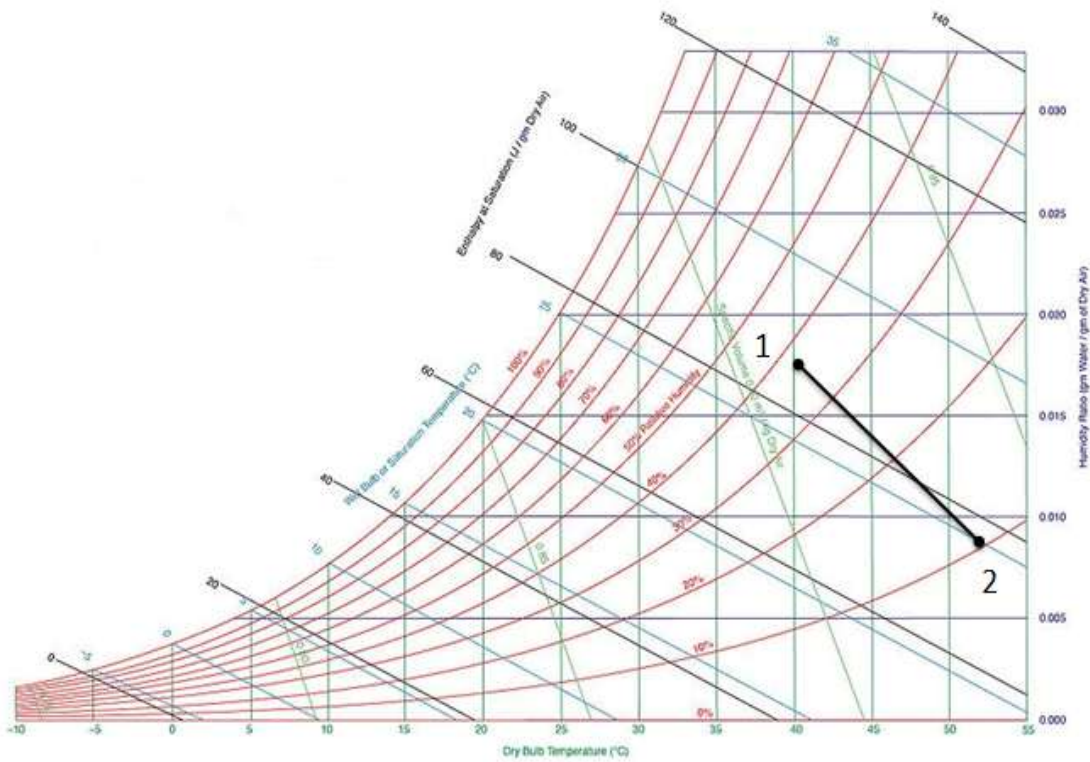
Figure 4-6: Psychrometric process of desiccant wheel

Process (1)-(2): Heating and dehumidification

The wheel contains a purge section to minimize the carryover of contaminants like carbon dioxide, particulate matter etc. in the wheel. With the addition of purge section efficiency of the wheel decreases but to ensure better indoor air quality purge is incorporated, it uses some amount of outdoor air to blow the return air out of the rotor. This study is focused on the solid desiccant in the form of the wheel rotor. While modelling the desiccant wheel in EnergyPlus, availability schedule, nominal electric power, the capacity of the wheel is kept at autosize. It sizes the wheel according to the volumetric flow of the air required to meet the humidity setpoint.

4.2.3   Enthalpy Recovery Wheel (ERW)

An Enthalpy Wheel is an air to air heat exchanger used to minimize the sensible and latent heat of incoming air. It is generally made up of porous material to increase surface area which increases heat transfer, has a high energy saving potential in HVAC application. The wheel is made up of aluminium foil of honeycomb structure in which desiccant of grain size of 3Å / 4Å is coated. Due to its low-pressure drop and high efficiency, it is preferably used in the ventilation system. Figure 4-7 shows the
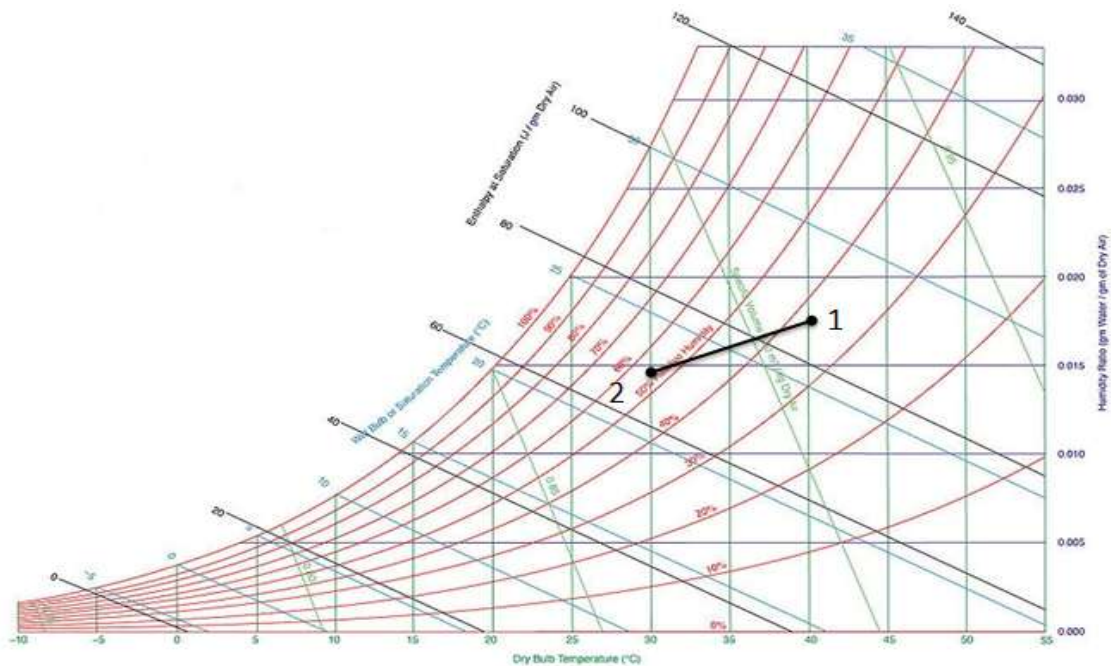
Figure 4-7: Psychrometric process of the enthalpy wheel

Process (1)-(2): Cooling and dehumidification

psychrometric process of the enthalpy wheel. Enthalpy wheel has the ability to reduce certain part of the sensible and latent load of the air whereas the cooling coil can cater the entire load of the air. While modelling the ERW in EnergyPlus it is required to input the

availability schedule, sensible and latent effectiveness at different part load and nominal electric power.

4.2.4   Sensible Wheel (SW)

It is an air to air heat exchanger used to recover sensible heat and do not absorb moisture from incoming air. It is made up of winding flat and corrugated sheets of the high-quality aluminium substrate to form a fluted "honeycomb" structure coated with corrosion resistant material. The wheel consists of alternate flat and fluted sheet of aluminium and they provide support and avoid nesting of flutes. Figure 4-8 shows the psychrometric process of the sensible wheel. While modelling the SW in EnergyPlus it is required to input the availability schedule, sensible effectiveness at different part load and nominal electric power.
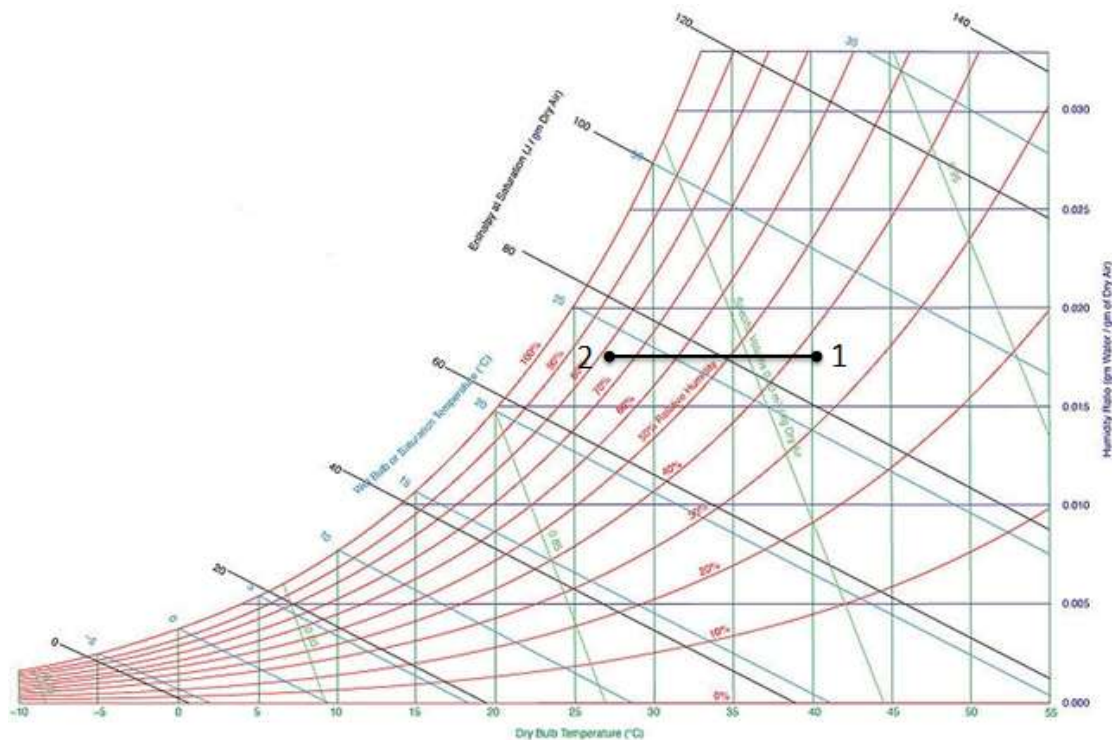
Figure 4-8: The psychrometric process of sensible wheel

Process (1)-(2): Sensible cooling

4.2.5   Indirect Evaporative Cooling System (IDEC)

It is used to cool the air through the process of evaporation, by using the water's enthalpy of vaporization. The lowest temperature which can be achieved by evaporative cooling is the wet bulb temperature of water. Due to evaporation of water some amount of energy is lost and the temperature of air decreases. Air passes through moist cooling pads, due to heat transfer water gets evaporated and this vapour gets absorbed into the air till air

Figure 4-9: Cross-sectional view of Indirect Evaporative Cooling System
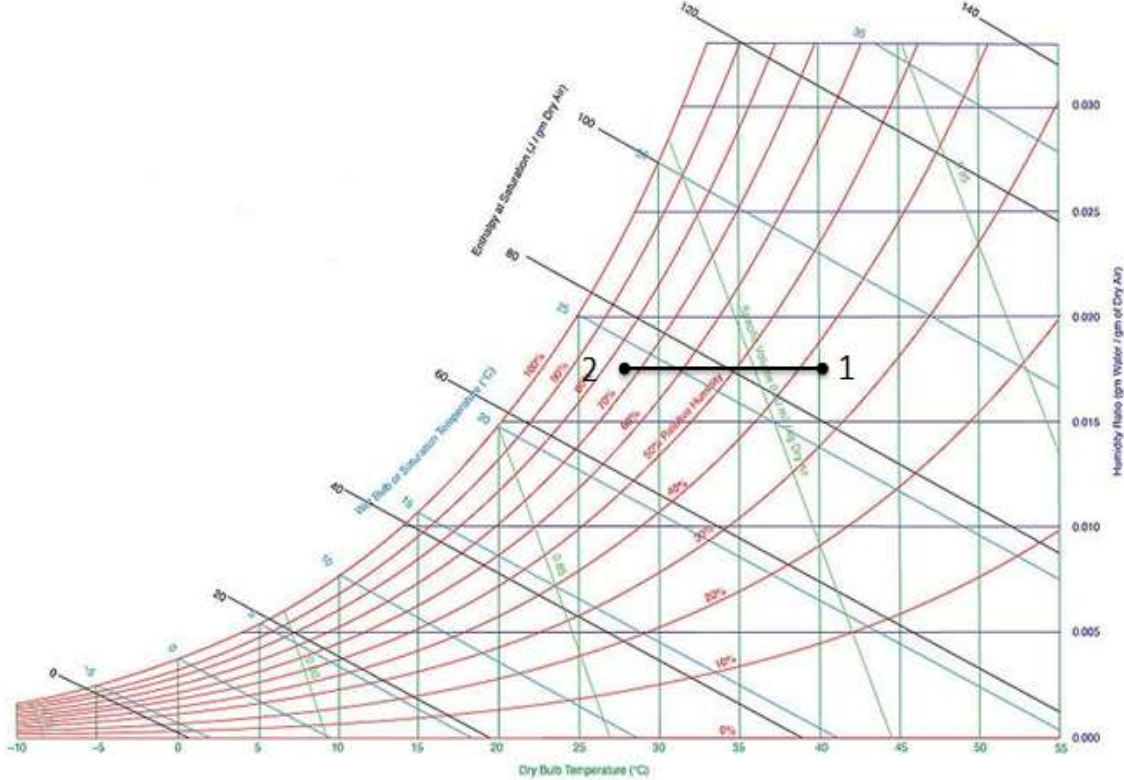
Figure 4-10: The psychrometric process of Indirect Evaporative Cooling System

Process (1)-(2): Sensible cooling

gets saturated. It decreases the dry bulb temperature of the air and increases the relative humidity of the water. There are two types of evaporative cooling i.e. direct and indirect evaporative cooling. In direct evaporative cooling, air is passed through a water-saturated medium and by evaporation cools the air. It adds moisture to the air. In indirect

evaporative cooling, a secondary air is cooled by water saturated medium and this secondary air cools primary air by using a heat exchanger, decreases moisture as well as dry bulb temperature of the air. In this study, an indirect evaporative cooling system is being used. Figure 4-9 shows the cross-sectional view of the indirect evaporative cooling system. Figure 4-10 shows the psychrometric process of the indirect evaporative cooling system. While modelling IDEC in EnergyPlus it is required to input availability schedule, pad area, recirculating pump power consumption, indirect heat exchanger effectiveness.

4.2.6   Fans

As the number of components increases in DOAS fan size and energy consumption of the system increases. Each component adds some amount of pressure drop and noise level in the system. Fan placement also adds some amount of heat in the passing air due to (a) resistive heat loss from motor winding, (b) pressure loss in impellers, (c) friction loss in bearing. The two arrangements which are mostly used in ventilation system blow through and draw through.

Based on the literature review DOAS strategies have been identified and listed below. DOAS strategies are described in three subcategories. First three strategies are based on cooling coil; the next three strategies are based on desiccant wheels. For achieving continuous dehumidification from a desiccant wheel high-temperature air is required to pass through the return section of the desiccant wheel. In strategy four to six, regeneration is being done using active heater regeneration. The last three strategies high-temperature heat pump is being used for regeneration of the desiccant wheel.

4.3   Decoupling strategies based on cooling coil

1. Strategy-1: Low-temperature cooling coil

In this case, the radiant cooling system is placed on the ceiling to meet the sensible load. Decoupling strategy comprises of low temperature (LT coil) cooling coil. Outdoor air (1)-(2) enters into the cooling coil in which air gets dehumidified and enters the zone. In this decoupling strategy, the energy consumption is mainly due to the chiller for producing chilled water for LT coil, pump and fan energy. The schematic of the strategy and the psychrometric process are shown in Figure 4-11.
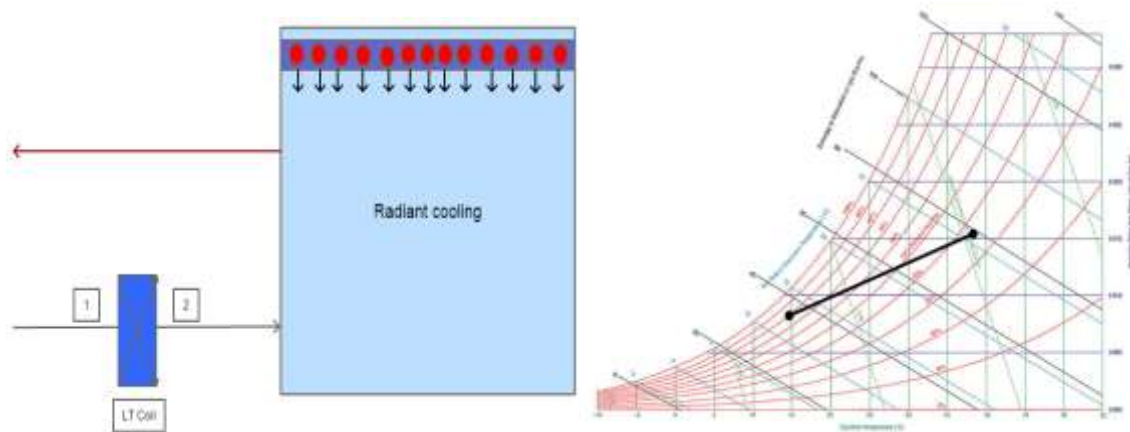
Figure 4-11: (a) Schematic of Case 1, (b) psychrometric process

Process (1)-(2): Cooling and dehumidification

2. Strategy-2: Energy recovery with low-temperature cooling coil

In this strategy, an extra energy recovery wheel is added to the cooling coil to decrease the cooling load on the cooling coil. Outdoor air (1)-(2) first enters into energy recovery wheel; it exchanges heat and moisture with Return air (4)-(5) and then moves to the low-temperature cooling coil for dehumidification (2)-(3) and then enters the zone. The energy consumption is involved in the motor (rotational of ERW), chiller, pump and fan energy. The schematic of this strategy and the psychrometric process are shown in Figure 4-12.
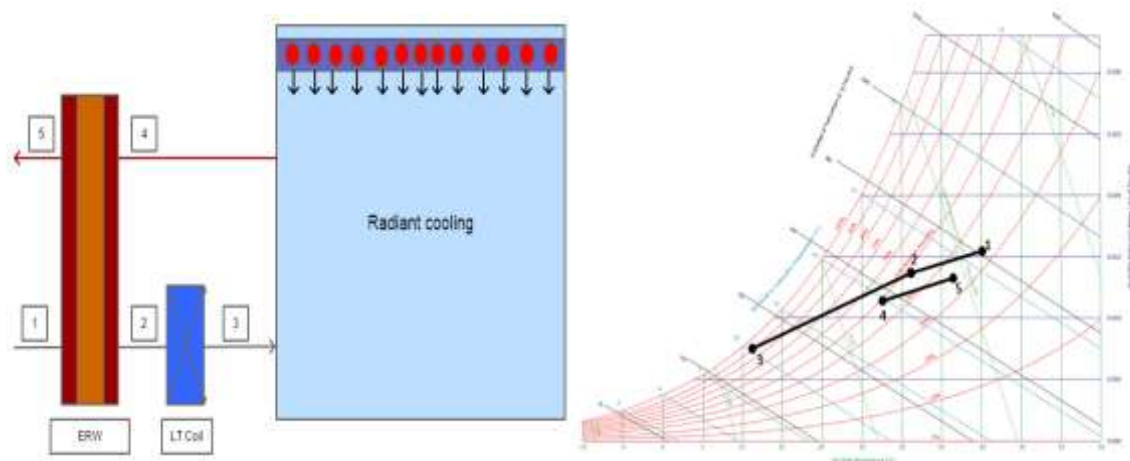
Figure 4-12: (a) Schematic of Case 2, (b) psychrometric process

Process (1)-(2): Cooling and dehumidification

Process (2)-(3): Cooling and dehumidification

Process (3)-(4): Heating and humidification

3. Strategy-3: Energy recovery with low-temperature cooling coil and sensible wheel

This strategy is the addition of a sensible wheel to strategy 2 after the cooling coil. The main aim of the sensible wheel is to reheat the supply air (3)-(4) and cool the return air (5)-(6). By cooling the return air before ERW, cooling load of the cooling coil can be further reduced. In (2)-(3) sensible cooling takes place. Increasing the temperature of the supply air (3) by exchanging heat with the return air (5), overcooling of the zone can be minimized leads to maintain better thermal comfort in the zone. In this strategy, additional motor cost (rotation of sensible wheel) and fan energy (due to increased fan pressure drop) will increase the energy consumption. The schematic of this strategy and the psychrometric process are shown in Figure 4-13.
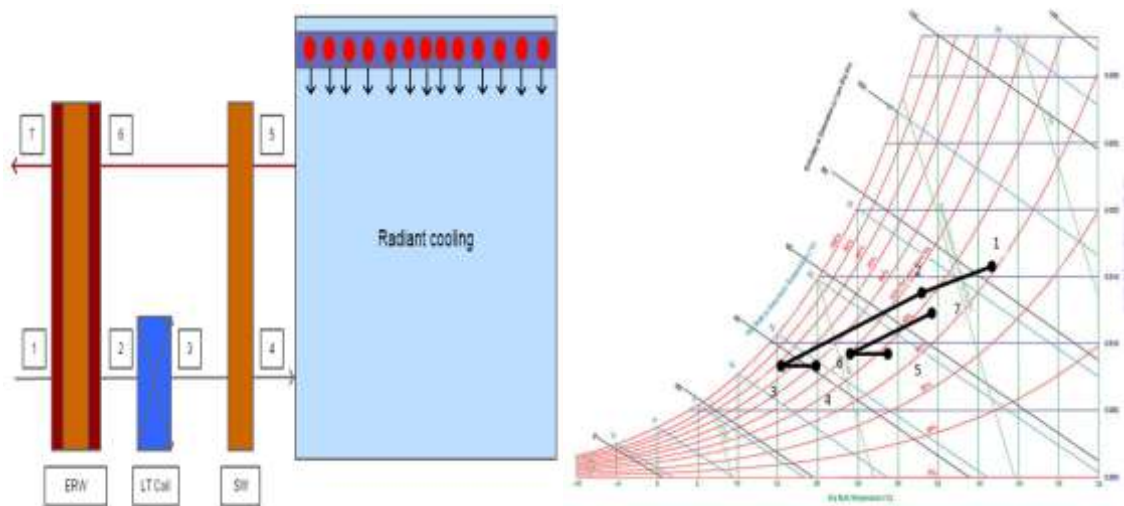
Figure 4-13: (a) Schematic of Case 3, (b) psychrometric process

Process (1)-(2): Cooling and dehumidification

Process (2)-(3): Cooling and dehumidification

Process (3)-(4): Sensible cooling

Now next three strategies are based on the desiccant wheel for dehumidification of air. DOAS strategies based on the desiccant wheel with active heater regeneration are as follow:

4.3.1 DOAS strategies based on the Desiccant wheel with active heater regeneration

4. Strategy-4: Desiccant wheel with high-temperature cooling coil

This strategy comprises of a desiccant wheel and a high-temperature cooling coil (HT). HT coil has a supply chilled water temperature of 16°C. In this case, OA (outdoor air) is first entered into desiccant wheel where it exchanges latent heat with the return air (1)-(2). When water molecules get adsorbed in the desiccant than it requires to be regenerated so that wheel does not attain saturation. Return air (4) is passed through an active heater to increase the temperature for the regeneration of wheel (4)-(5). In process (1)-(2) humidity is reduced and sensible heat is added in the air. Then air is passed through an HT coil for sensible cooling (2)-(3). The energy consumption is involved in the motor (rotational of DW), chiller, pump, fan energy and heating. The schematic of the strategy and the psychrometric process are shown in Figure 4-14.
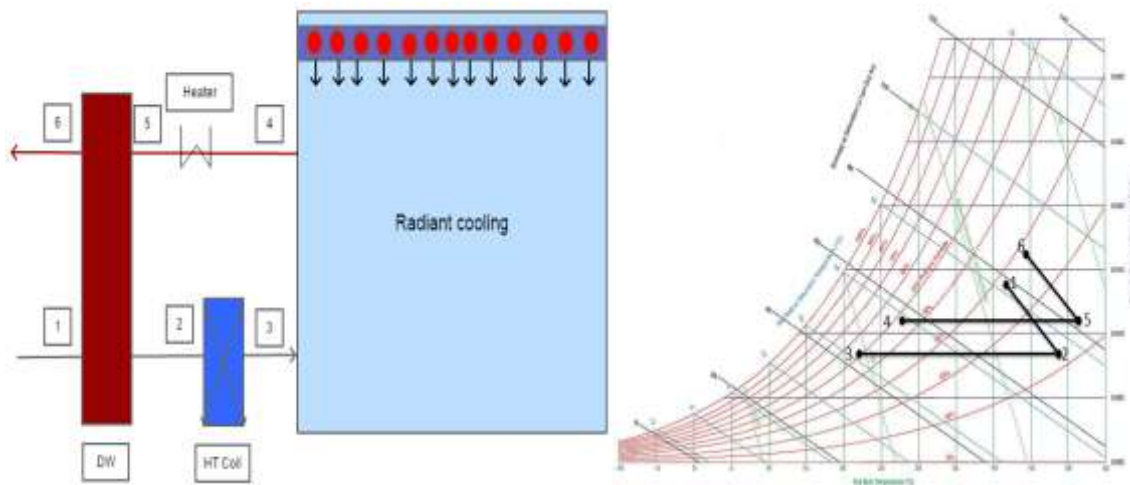
Figure 4-14: (a) Schematic of Case 4, (b) psychrometric process

Process (1)-(2): Dehumidification and heating

Process (2)-(3): Sensible cooling

Process (4)-(5): Sensible heating

Process (5)-(6): Humidification and cooling

5. Strategy-5: Desiccant wheel with, sensible wheel and high-temperature cooling coil

In this strategy, a sensible wheel is added after the desiccant wheel in the strategy 4. When the air after passing through the desiccant wheel (1)-(2), it needs to be sensible cool to feed in the space. Part of the sensible cooling is done by the sensible wheel (2)-(3) and rest is done by the HT coil (3)-(4). The sensible wheel cools the supply air and sensible heat the return air (5)-(6). Overall the sensible wheel reduces the load of the HT

coil as well as the heater. The energy consumption is involved in the motor (rotational of DW and SW), chiller, pump, fan energy and heating. Chiller energy consumption will reduce as compared to strategy four; additionally, motor energy for rotating sensible wheel will increase. The schematic of the strategy and the psychrometric process are shown in Figure 4-15.
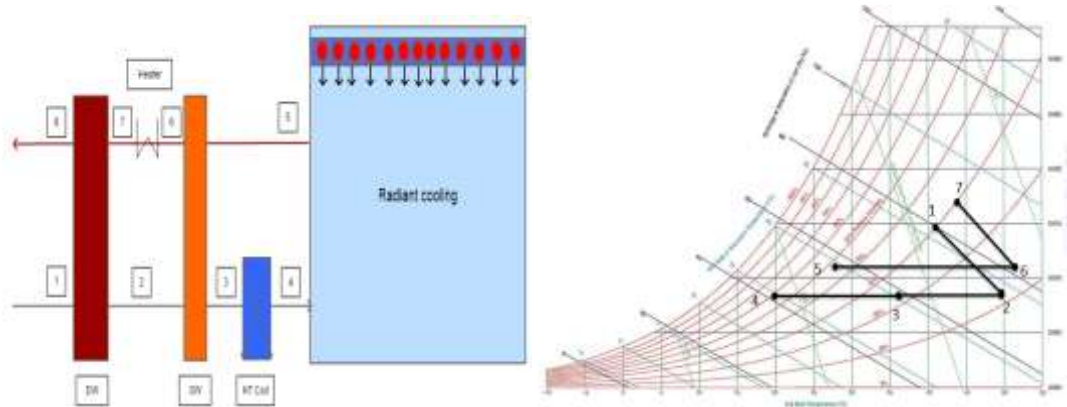
Figure 4-15: (a) Schematic of Case 5, (b) psychrometric process

Process (1)-(2): Dehumidification and heating

Process (2)-(3): Sensible cooling

Process (3)-(4): Sensible cooling

Process (5)-(6): Sensible heating

Process (6)-(7): Sensible heating

Process (7)-(8): Humidification and cooling

6. Strategy-6: Desiccant wheel with indirect evaporative cooling (IDEC)

In this strategy, an indirect evaporative cooling is added after the desiccant wheel in the strategy 4. Indirect evaporative cooling (IDEC) performs well in the dry climate for sensible cooling. Air after passing through the desiccant (1)-(2), some part of sensible cooling will be done by IDEC (2)-(3); the rest of the sensible cooling will be done by HT coil (3)-(4). In (5)-(7) the return air is heated and passed through desiccant wheel i.e. humidity is added. The energy consumption is involved in the motor (rotational of DW), chiller, pump, fan energy and heating. As compared to strategy five, chiller energy of sensible wheel will be replaced by IDEC. The schematic of the strategy and the psychrometric process are shown in Figure 4-16.
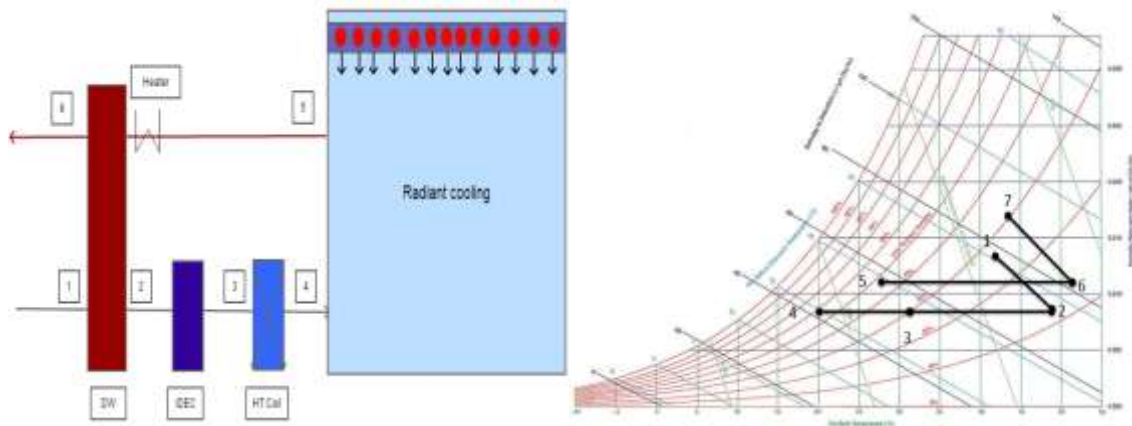
Figure 4-16: (a) Schematic of Case 6, (b) psychrometric process

Process (1)-(2): Dehumidification and heating

Process (2)-(3): Sensible cooling

Process (3)-(4): Sensible cooling

Process (5)-(6): Sensible heating

Process (6)-(7): Humidification and cooling

To regenerate the desiccant, high-grade energy is required. The major energy consumption in the desiccant wheel based strategy is due to the active heater. Regeneration of desiccant wheel is not recommended using active heaters, as COP of the heater is less than one and should not be used for regeneration. Using of desiccant wheel is always recommended if either there is the availability of waste heat; hot water can be generated using solar thermal system etc. In future three cases we are using a high-temperature heat pump for regeneration of desiccant wheel.

7. Strategy-4*: Desiccant wheel with heat pump

This strategy comprises of a desiccant wheel, heat pump and an HT coil. The heat-rejecting side of the heat pump is used for the regeneration of the desiccant wheel whereas the cooling side of the heat pump is used to sensible cool the air. The cooling side of the heat pump is termed as a free cooling (FC). The outside air enters the desiccant wheel for dehumidification (1)-(2). Then air enters the evaporator side (free cooling) of the heat pump for sensible cooling (2)-(3) and then enters a high-temperature cooling coil for sensible cooling (3)-(4). The return air (5) enters the condenser coil for regeneration of the desiccant wheel (5)-(6). In (6)-(7) air is passed through desiccant wheel for humidification and sensible cooling. The energy consumption is involved in the motor

(rotational of DW), chiller, pump, fan energy and heat pump. The schematic of the strategy and the psychrometric process are shown in Figure 4-17.
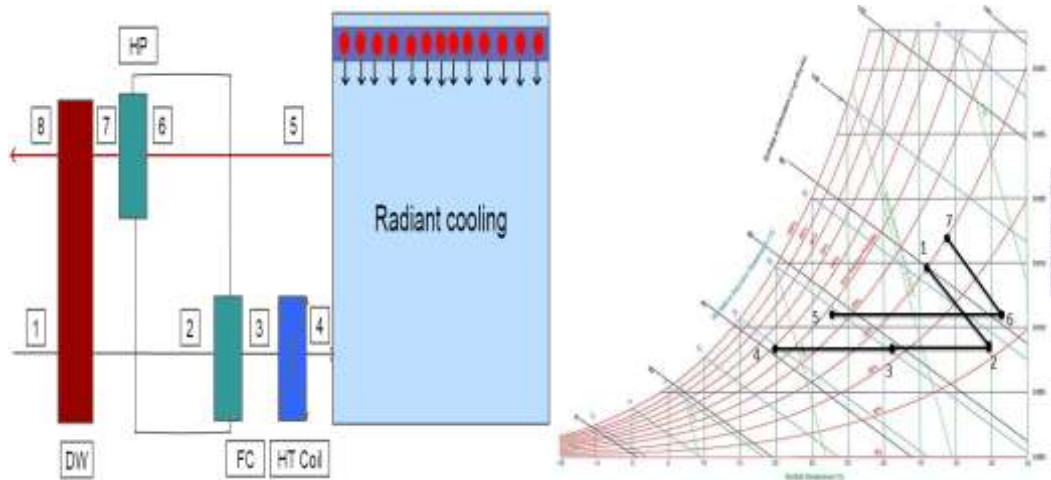
Figure 4-17: (a) Schematic of Case 6, (b) psychrometric process

Process (1)-(2): Dehumidification and heating

Process (2)-(3): Sensible cooling

Process (3)-(4): Sensible cooling

Process (6)-(7): Sensible heating

Process (7)-(8): Humidification and cooling

8. Strategy-5*: Desiccant wheel with the sensible wheel and heat pump
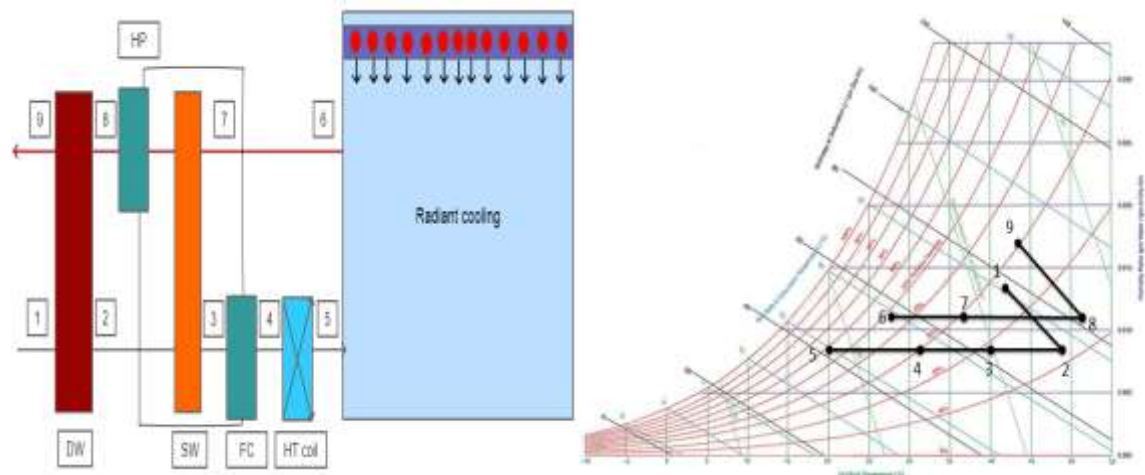
Figure 4-18: (a) Schematic of Case 8, (b) psychrometric process

Process (1)-(2): Dehumidification and heating

Process (2)-(3): Sensible cooling

67

Process (3)-(4): Sensible cooling

Process (4)-(5): Sensible cooling

Process (6)-(7): Sensible heating

Process (7)-(8): Sensible heating

Process (8)-(9): Humidification and cooling

This strategy comprises of a desiccant wheel, sensible wheel heat pump and an HT coil. In the process (1)-(2) air is passed through the desiccant wheel, air gets dehumidified and sensible heat is added. Process (2)-(3) air is passed through sensible wheel; air gets sensible cooled in supply side and sensible heat in the return side and reduces the load of the HT coil. Process (3)-(4) air passes through the FC coil for sensible cooling and then remaining cooling is done by HT coil and enter the zone. Process (6)-(7) return air passes through the sensible wheel and gets sensible heating. Process (7)-(8) air first passes through heat pump for sensible heating and then process (8)-(9) enters the desiccant wheel for regeneration. The energy consumption is involved in the motor (rotational of DW and SW), chiller, pump, fan energy and heat pump. The schematic of the strategy and the psychrometric process are shown in Figure 4-18.

9. Strategy-6*: Desiccant wheel, IDEC and heat pump

This case comprises of the Desiccant wheel, indirect evaporative cooling (IDEC) heat pump and HT coil. In this strategy, the sensible wheel of the strategy eight is replaced with an indirect evaporative cooling. In (1)-(2) Outdoor air passed through desiccant wheel for dehumidification and sensible heating. In (2)-(3) air is passed through indirect evaporative cooling, in (3)-(4) air is passed to free cooling and from (4)-(5) air is passed through HT coil for sensible cooling. The return air (6)-(7) is passed through condenser side of heat pump for sensible heating of air and from (7)-(8) air is passed through desiccant wheel for humidification and sensible cooling. The motor energy for rotating the sensible wheel will be replaced by the pump energy provides water in the IDEC. The energy consumption is involved in the motor (rotational of DW), chiller, pump, fan energy and heat pump. The schematic of the strategy and the psychrometric process are shown in Figure 4-19.
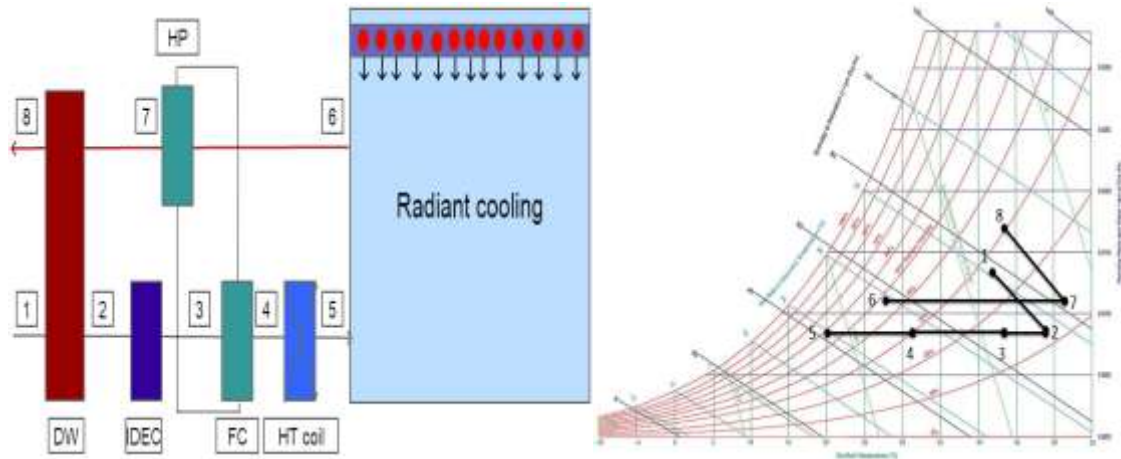
Figure 4-19: (a) Schematic of Case 6, (b) psychrometric process

Process (1)-(2): Dehumidification and heating

Process (2)-(3): Sensible cooling

Process (3)-(4): Sensible cooling

Process (4)-(5): Sensible cooling

Process (6)-(7): Sensible heating

Process (7)-(8): Humidification and cooling

Based on the above-discussed decoupling strategies an experimental setup is designed and integrated along with indoor-outdoor chamber for testing of the strategies.

4.4   Mathematical equations for performance indexes

Desiccant wheel is used for dehumidification of the air, for avoiding saturation in desiccants while dehumidification some amount of heat is added in the return side of air for regeneration. The calculation of the desiccant wheel sorption rate is based on the moisture removal capacity (MRC), MRC equation is given below where OA is outdoor air and RA is return air, m is mass flow rate and X is humidity ratio.

$$MRC = \overset{o}{m}_{OA}(\Delta X_{OA} - X_{RA}) \tag{4.1}$$

The performance of the desiccant wheel in the removal of moisture from its desiccant surface is based on the moisture removal regeneration (MRR). RegA is regeneration air and EA is exit air.

$$MRR = \overset{o}{m}_{\mathrm{Re}gA}(\Delta X_{EA} - X_{\mathrm{Re}gA}) \tag{4.2}$$

69

The third parameter is moisture mass balance (MMB), it is defined as the ratio is MRC and MRR [82].

$$MMB = \frac{MRC}{MRR} \approx 1 \pm 5\% \, Max \tag{4.3}$$

Total energy balance, the evaluation of the desiccant wheel is based on the moisture mass balance. The total energy balance (TEB) is presented as:

$$TEB = \frac{\overset{o}{m_A}}{\overset{o}{m_{RegA}}} \frac{(h_{Moist,PA} - h_{Moist,OA})}{(h_{Moist,RegA} - h_{Moist,EA})} \tag{4.4}$$

The coefficient of performance (COP) of the wheels can be calculated. For the sensible wheel, Sensible coefficient of performance (COP$_{Sensible}$) will be calculated. For energy recovery wheel both sensible and latent COP will be calculated and added. For the desiccant wheel latent coefficient of performance (COP$_{Latent}$) will be calculated where PA is processed air and HA is hot air.

$$COP_{Sensible} = \frac{m_{OA} C_{P(A)} \overset{o}{(T_{PA} - T_{OA})}}{\overset{o}{m_{RegA}}(h_{Moist,RegA} - h_{Moist,HA})} \tag{4.5}$$

$$COP_{Latent} = \frac{m_{OA} H_{Evap}(X_{OA} - X_{PA})}{\overset{o}{m_{RegA}}(h_{Moist,RegA} - h_{Moist,HA})} \tag{4.6}$$

Total coefficient of performance is the performance of the desiccant wheel in reducing the air moisture content and at the same time changing the air thermal energy content.

$$COP_{Total} = \frac{\overset{o}{m_A}}{\overset{o}{m_{RegA}}} \frac{(h_{Moist,OA} - h_{Moist,PA})}{(h_{Moist,RegA} - h_{Moist,HA})} \tag{4.7}$$

Sensible wheel effectiveness is based on the thermal energy exchange between the supply and return air, in the below equation HS and CS are hot side and cold side of air, I and O are inlet and outlet.

$$\varepsilon = \frac{\{m_{CS}((T_{CS(O)} - T_{CS(I)}) + m_{HS}(T_{HS(O)} - T_{HS(I)}))\}}{2m_{Min}(T_{HS(I)} - T_{CS(O)})} \tag{4.8}$$

4.5   Shortlisting of strategy for the simulation study

First three strategies are based on the cooling coil, Strategy-4,5,6 are based on the desiccant wheel with active heater regeneration and last three strategies are based on the desiccant wheel with a high-temperature heat pump. Simulation study is carried out for six strategies out of the nine discussed above. For the simulation study, in desiccant wheel based strategy instead of active heater for regeneration, desiccant-based strategies with high temperature heat pump (HTHP) for regeneration are used i.e. Strategy-4*, Strategy-5* & Strategy-6* for analysis. High temperature heat pump is used in simulation study becaues it is more than three times efficient compared to active heaters. Table 4-1 shows the component used in all the strategy. For experiments designing every desiccant strategy with high temperature heat pump regeneration in modular DOAS system was very expensive.

Table 4-1: Components used in the strategy

Strategy	All air	Component							
		LT Coil	ERW	SW	DW	HT Coil	IDEC	Heater	HP
Base case	√								
Strategy-1		√							
Strategy-2		√	√						
Strategy-3		√	√	√					
Strategy-4					√	√		√	
Strategy-5				√	√	√		√	
Strategy-6					√	√	√	√	
Strategy-4*					√	√			√
Strategy-5*				√	√	√			√
Strategy-6*					√	√	√		√

4.6   Building details for model development

In this study, an office building in Hyderabad, India (composite climate) is used. In this building, there are two nearly identical wings with two different and separate HVAC systems. The similar architectural features and two different individual HVAC systems are installed for two different wings. There are appropriate sensors and instrumentation is installed to log all the necessary HVAC and other important parameters needed for developing the model. The office building used in the case study (Figure 4-20) is the first large commercial building in India with parallel conventional all air system and RCS side by side. The total area of the building, about 24,000 m^2 (258,334 ft^2), is distributed over six floors within two symmetrical structures joined by an elevated two-story centre wing. The western side (conventional side) of the building is cooled by a VAV air-conditioning system, whereas the eastern side (radiant side) is cooled by an RCS

with a DOAS. The building is oriented so that the longer side is situated in an east-west direction. The building has a standardized floor layout that gives the building a pyramid shape. The architectural symmetry and parallel two different airconditioning systems make it a good candidate for comparative analysis.
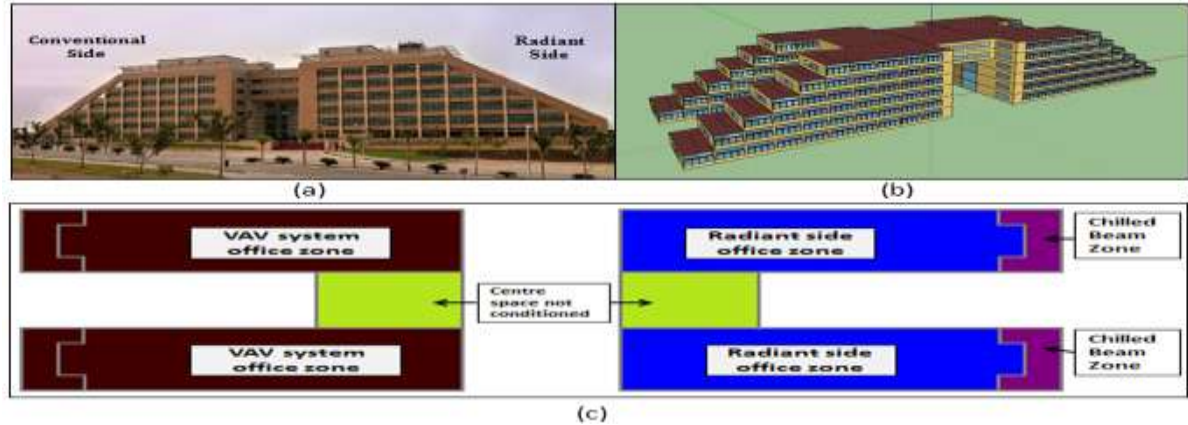
Figure 4-20: (a) Case study office building in Hyderabad, India, (b) Building model & (c) zoning layout of a floor of the building

4.6.1 HVAC systems description

The conventional (west) side of the building is served by the VAV systems which is operated by six air-handling units (AHUs). The east side a radiant cooling system is installed in which chilled water flows in the radiant pipes embedded in the slab (embedded surface cooling system) and cools the surface of the entire slab. The outdoor air is supplied using a DOAS at the rate of 5 cubic feet per minute (CFM)/person (2.5 L/s/person) + 0.06 CFM/ft^2 (0.3L/S/m^2) as required by code with an additional 30% of the required value. The DOAS unit is being used to meet the latent load and ventilation. The DOAS unit is coupled with an energy recovery unit that has a set-point of 25°C (77°F). Additionally, chilled beams are used to meet the cooling requirement and conference rooms.

On the conventional side, one chilled water plant serves the cooling coil of six AHUs and the low-temperature (LT) cooling coil of DOAS, which has a capacity of 272 TR (952 kW). On the radiant side, another chilled water plant, with a capacity of 325 TR (1137 kW), supplies the RC system, which cools the building by flowing chilled water through embedded pipes. This chiller also provides the chilled water to the high-temperature cooling coil (HT) of the DOAS unit. The leaving chilled water temperature chiller set-point, which is taken from the monitored data, is approximately 7°C (44.6°F) on the conventional side and 15°C to 16°C (59°F to 60.8°F) on the radiant side.

4.6.2 Simulation model development

Based on the architectural and operational data, a building energy model was created to predict the energy consumption of a building using the modelling tool EnergyPlus Version 8.1 (US-DOE 2013). Many parameters such as geometry, thermal zones, building construction, lighting systems, internal equipment, occupancy, and HVAC systems are considered to develop the model. All the important data such as drawings related to building construction and mechanical systems were collected. The drawings, which consist of the floor plan, the side views, the building section and elevation, the building material, and the personal computers (PCs) locations, were helpful in preparing the model. Important information about the building's mechanical system was collected during interviews with the HVAC engineers who were taking care of the system's operations. The total number of occupants in the building was estimated from the architectural layout of the building. These layouts were very helpful in estimating the occupancy levels of each zone. The total occupancy of the building was 2500 estimated, which was distributed on both the sides in equal numbers. The lighting power density (LPD) was 5 W/m^2 and the equipment power density (EPD) was 20 W/m^2.

Building façade is composed of two different glazing i.e.the lower side is known as a vision panel (V.P.) and the higher one is known as the daylight panel (D.P.). Building construction was developed based on the information and data obtained from architectural drawings and facility manager. The detailed building construction parameters are given in Table 4-2.

Table 4-2: Building construction details

S.NO.	Parameters	Unit	Value
1	Exterior wall U-value	W/m^2-K	0.34
2	Ground floor U-value	W/m^2-K	1.7
3	Roof U-value	W/m^2-K	0.34
4	Internal floor or slab U-value	W/m^2-K	1.81
5	VP (window) U-value	W/m^2-K	1.854
6	DP (window) U-value	W/m^2-K	1.763
7	VP (window)	-	0.25
8	DP (window)	-	0.36
9	Window-to-wall ratio	% Area	East & West:15
			North & South: 50

The building was operated from 9:00 a.m. to 6:00 p.m. 5 days every week. The lighting schedule was used extracted from the monitored hourly lighting load. The complete system was controlled and managed by a building management system. The thermostat setpoint was 24°C ± 1°C (75.2°F ± 1°F) for the conventional side and 26°C ± 1°C (78.8°F ± 1°F) for the radiant side throughout the year. The supply air set-point temperature of AHUs was 14°C (57.2°F) and for DOAS the set-point was 12°C (53.6°F) which is based on the monitored data. The similar set-point temperature was used in the simulation model. Chiller capacity is considered as actual from the site and in site chiller capacity of radiant side is higher compared to conventional side. I have used the measured data for supply air and indoor setpoint while performing simulations. As per the Infosys facility team they were experiencing similar thermal comfort with elevated indoor setpoint in radiant cooling system. The aim is to maintain similar operative temperature in both sides. Table 4-3 shows the specifications of the buiding HVAC system.

Table 4-3: Building HVAC system specifications

S.No	Parameters	Unit	Conventional side	Radiant side
1	Chiller capacity	kW (TR)	952(272)	1137(325)
2	Chiller (COP)		6.47@7.77°C supply temperature	7.8@12.77°C supply temperature
3	Air flow rate	m^3/s(CFM)	AHU1:8.825(18700) AHU2:7.551(16000) AHU3:6.489(13750) AHU4:7.787(16500) AHU5:6.843(14500) AHU6:5.427(11500)	DOAS: 8.967 (19000)
4	Supply air set-point	°C	14	12
5	Indoor set-point	°C	24	26

The zoning of the building has been simplified but maintains a reasonable level of accuracy. The building has 62 zones in total, 49 of which are conditioned. The space zoning of the building was used in the model is based on the area served by the AHUs, RC system, and chilled beam system without differentiating interior and perimeter zones.

4.6.3 Model calibration

Model calibration was done to achieve more accurate results of the simulation results as the measured data so that simulation analysis will be more realistic. Several different indices and statistical variables are used for setting the calibration criterion. The coefficient of variation root means squared error (CV-RMSE) and the normalized mean bias error (NMBE) are mostly calculated and analyzed for calibration criteria. As per

ASHRAE Guideline 14-2014 (ASHRAE 2014), the acceptable limits for these two indices are 5% and 15%, respectively, for monthly calibration and 10% and 30%, respectively, for hourly calibration. Calibration is achieved by changing the parameters to make it more actual as per the measurement and then try to reach as close as measured data. The iterations of revising the model keep on until we reach the limit as per calibration criteria. In some respects, revising a model can be considered the most important part of the whole procedure. Modellers may spend most of their time on this step when creating a calibrated model. Figure 4-21 shows the comparison of simulated and measured energy consumption for different HVAC components such as a chiller, fan, cooling tower, chilled water pump, condenser pump.
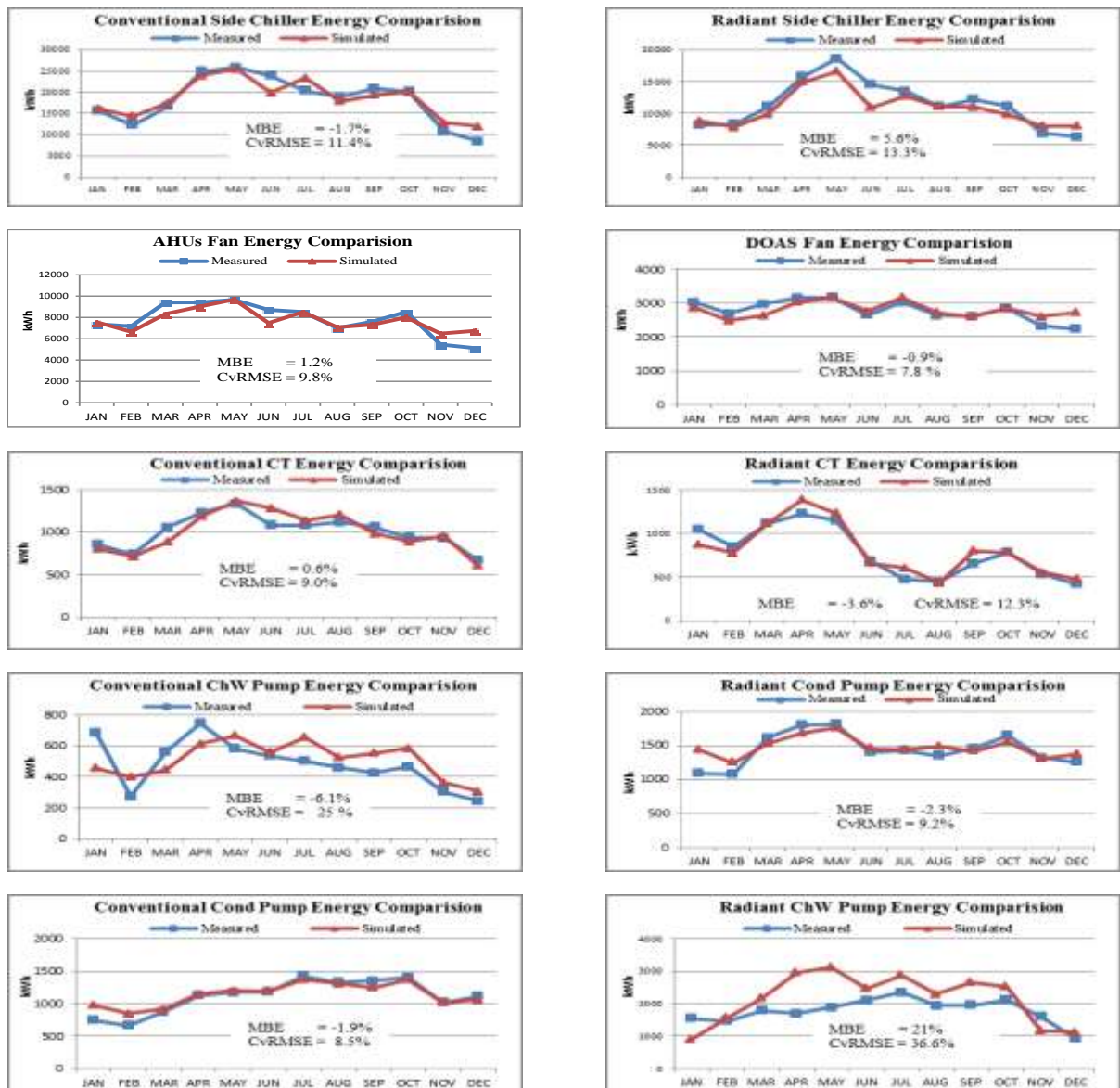
Figure 4-21: Graphs of simulated and measured energy consumption for different HVAC components

The measured data included only the cooling energy of the chiller, as this study was concerned only with cooling energy consumption. In this study cooling energy use of the building, based on the availability of data is used for calibration purpose. Calibration was achieved by iterating the process of using the occupancy and plug load (electrical equipment) patterns, which have the highest diversity to match the measured and simulated HVAC energy consumption on an hourly basis from April through June. Therefore calibrated model can be used for further analysis of decoupling strategies. Table 4-4 shows the component level error in the calibrated model. Table 4-5 shows the total error in the HVAC system in the calibrated Model.

Table 4-4: Error at the Component Level in the calibrated Model

Component	MBE (%)	CvRMSE (%)
Conventional Chiller	-1.7	11.4
Radiant Chiller	5.6	13.3
AHUs Fan	1.2	9.8
DOAS Fan	-0.9	7.8
Conventional Cooling Tower	0.6	9.0
Radiant Cooling Tower	-3.6	12.3
Conventional ChW Pump	6.1	25
Radiant ChW Pump	21	36.6
Conventional CndW Pump	-1.9	8.5
Radiant CndW Pump	-2.3	9.2

Table 4-5: Total error in the HVAC system in the calibrated Model

Calibration type	Index	Error (ASHRAE 14)	Error (MODEL)
Hourly	MBE	±10%	8.7%
	CvRSME	30%	23.9%

4.6.4 Modification in the calibrated model

The calibrated model is modified and different models are prepared for different decoupling strategies coupled with a radiant cooling system for predicting the energy savings potential in different climatic conditions. For the study of decoupling strategy, the study is focused on the eastern side (radiant side) of the building. Further, all the decoupling strategies along with radiant cooling system are compared with the conventional all-air system (west side). In total there are a total of seven models out of which the first is a conventional all-air system (base case), the rest of the seven models are of decoupling strategies coupled with RCS. Out of the six decoupling strategies first

three are cooling coil based and rest of the three are desiccant wheel based systems with HTTP for regeneration to provide ventilation and achieve dehumidification in the radiant cooling system. In all the model's different components are placed as per the decoupling strategy by changing node arrangements in the air path of DOAS. Table 4-5 has shown the different HVAC details used in the different models. The performance of different decoupling strategies is strongly influenced by climate condition. The performance analysis of different strategies has been conducted under climatic conditions of 4 cities. Cities i.e. Ahmedabad (hot & dry), Chennai (warm & humid), Jaipur (composite) and Bangalore (temperate) are considered.

Table 4-6: HVAC details

S.No.	Parameters	Unit	Values
1	Heat pump (COP)		4
2	Regeneration air temperature	°C	50
3	Pressure drop (ERW)	Pa	150
4	Sensible effectiveness (ERW)	%	0.65
5	Pressure drop (DW)	Pa	150
6	Pressure drop (SW)	Pa	150
7	Pressure drop (IDEC)	Pa	200
8	LT coil (Supply-return temp)	°C	7-12
9	HT coil (Supply-return temp)	°C	16-19

The annual operating energy consumptions of the DOAS with RCS for different decoupling strategies were estimated by developing detailed hourly energy simulations. In the first strategy, a low-temperature cooling coil alone is being used hence the total air load is being handled by the cooling coil. Detailed analyses of the different climatic conditions are described below:

4.7 Results for Hot and Dry climate

The hot and dry climate zone is favourable for the radiant cooling system as in this climate percentage of the latent load stays lowers as compared to other climatic condition. The annual energy consumption for different strategies for Ahmedabad climate has been shown in below Figure 4-22.

The energy consumption for conventional air conditioning system for conventional side of the building is 418 MWh out of which 109 MWh is consumed by the fan motor for the hot and dry climate. In Strategy-1 radiant cooling system integrated with DOAS was found to consume 330 MWh and providing 21% saving compared to the

conventional case and around 73.2% fan energy is saved compared to the conventional case. The savings are achieved due to change of air system to a radiant cooling system, fan energy is also reduced as a fan has to only supply the outdoor air and overcome the latent load. Rest of the sensible load is met by the radiant cooling system. In the Strategy-2 the annual energy consumption is 303 MWh which gives 27% energy saving over a conventional system. In this strategy, the cooling energy delivered by the ERW is almost 151 MWh which reduces the electric energy consumption of the DOAS chiller by 29.4 MWh. ERW is exchanging heat with the return air and cooling the outdoor air passing through the ERW, in Strategy-2 ERW has reduced the load of the cooling coil as compared to Strategy-1 due to that chiller energy consumption has reduced in Strategy-2. The fan energy has been increased due to the addition of ERW in the air path, it has increased pressure drop across the fan and energy consumption of fan is increased to 9.7 MWh. In the Strategy-3; the annual energy consumption is 312 MWh which gives 25% energy saving over a conventional system. In this strategy addition of the sensible wheel is exchanging sensible heat with the return air and reduces the load on DOAS chiller to 71.4 MWh which saves 11.7 MWh in electric energy consumption and increasing the supply temperature of the air entering the zone. However, in this strategy due to increased supply temperature of the air the radiant side chiller energy consumption has increased by 10.1 MWh, and the addition of sensible wheel in the air path has increased pressure drop in air path subsequently fan energy consumption is increased by 6.23 MWh. Therefore, the energy saving achieved due to addition of sensible wheel in DOAS, savings achieved in the DOAS chiller is compensated in radiant side chiller and fan energy.
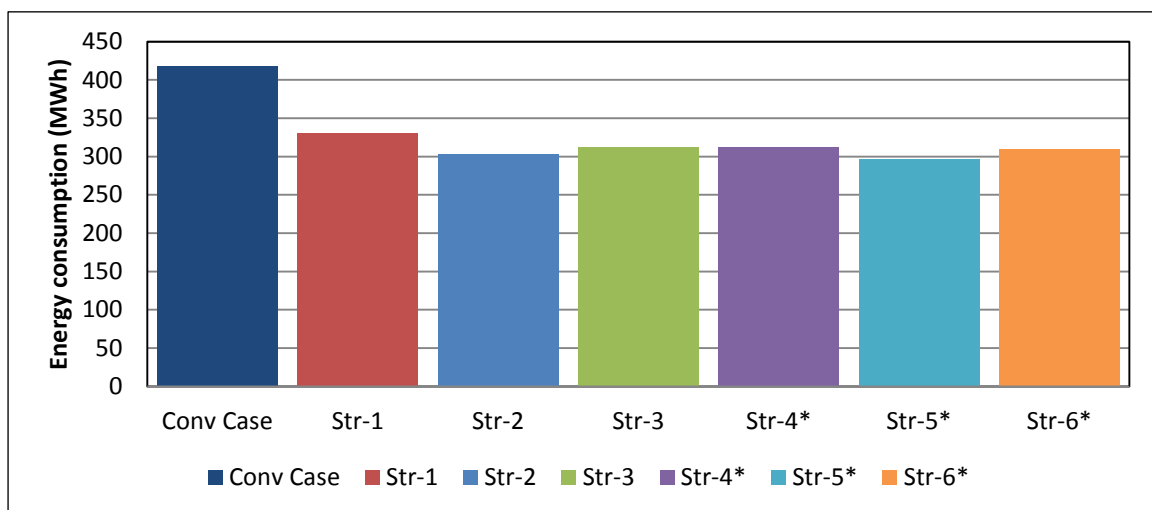
Figure 4-22: Comparison of annual energy consumption for different strategies coupled with RCS for hot and dry climate zone.

Figure 4-23 shows the variation of the thermal energy in the low-temperature cooling coil (LT coil) for the Strategy-1, 2 &3. In the Strategy-1, the thermal energy of the LT coil is 179 MWh. In the Strategy-2 with the addition of energy recovery wheel, the load on the LT coil reduced to 18% compared to Strategy-1 and in the Strategy-3, the sensible wheel has further reduced the load to 21% compared to Strategy-1. Based on the annual energy simulation, strategy two is most suitable for the hot & dry climate in the cooling coil based strategies.
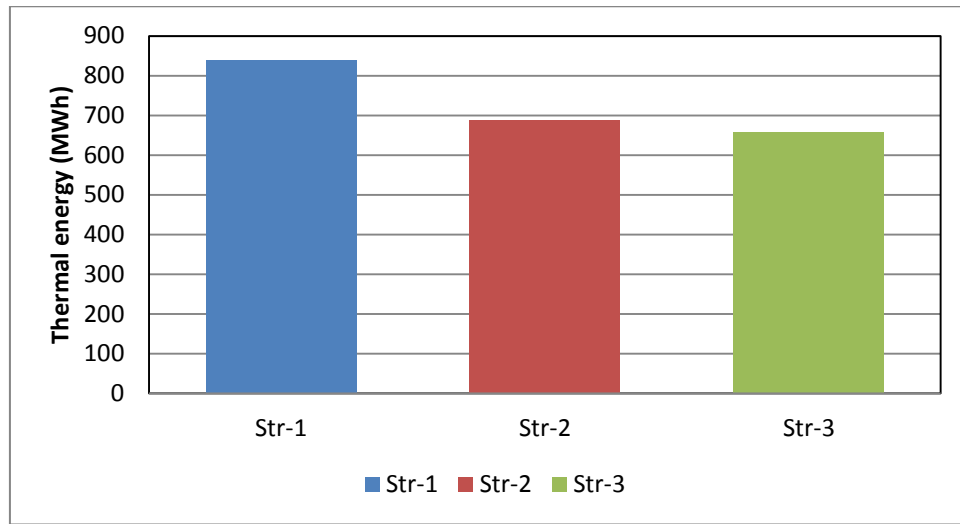
Figure 4-23: Comparison of the annual thermal energy of the low-temperature cooling coil in Strategy 1, 2 & 3 for hot and dry climate
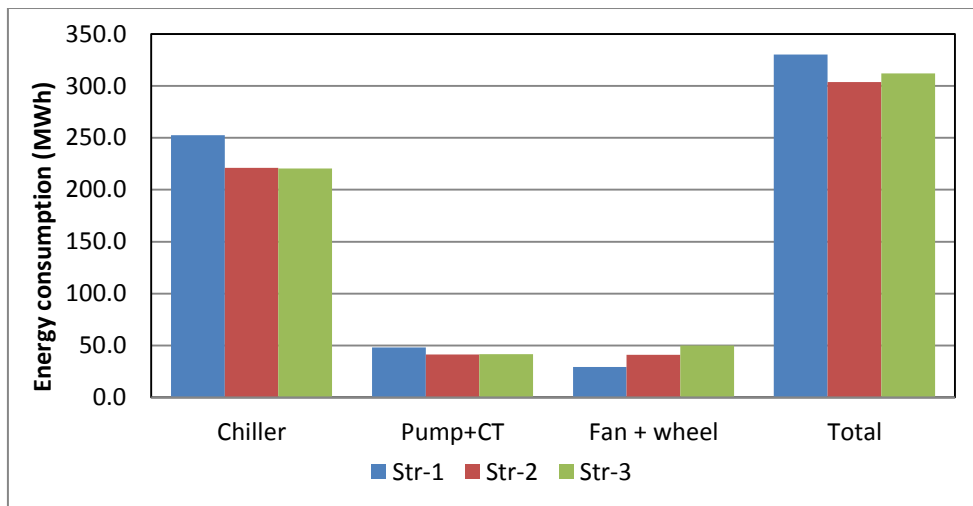
Figure 4-24: Comparison of energy consumption of chiller, pump + cooling tower, fan + wheel & total of the cooling coil based Strategy 1, 2 &3.

Figure 4-24 shows the comparison of energy consumption of chiller, pump + cooling tower, fan + wheel & total of the cooling coil based Strategy 1, 2 &3 to show variation of component wise energy consumption among different strategies. In Figure 4-24 energy consumption of pump and cooling tower are added and shown as pump +

cooling tower and energy consumption of fan and wheel are added and shown as Fan + wheel. In Strategy-1 entire load (sensible and latent) of DOAS was catered by cooling coil. In Strategy 1 chiller energy consumption for RCS and cooling coil of DOAS is 252.6 MWh, pump and cooling tower is 48.2 MWh and fan and wheel is 29.2 MWh. In Strategy-2 addition of ERW is used for exchanging energy with return air, precooling the air for cooling coil. On one hand ERW has minimized the load of chiller and pump by 12.6%, on the other hand ERW has increased pressure drop in the air path and energy consumption of fan has been increased. In Strategy-3 sensible wheel is further added in Strategy-2. Sensible wheel is exchanging sensible heat with return air and precooling the air for cooling coil, ERW has reduced energy consumption compared to Strategy-1 but Strategy three is consuming higher energy compared to Strategy-2.

In this paragraph desiccant wheel based strategies getting regenerated with HTTP have been discussed. In the Str-4* DOAS components used are desiccant wheel HTTP and high-temperature cooling coil (HT coil), the desiccant wheel is responsible for dehumidification and evaporator side of HTTP provide sensible cooling of supply air and condenser side is used for regeneration of the desiccant wheel. The annual energy consumption is 312.6 MWh which provide 24% energy saving as compared to the conventional system. The energy consumption in the radiant cooling system is 132.2 MWh. The energy consumption in dehumidification and sensible cooling of supply air are 1.95 MWh, 105 MWh respectively. The energy consumption in regeneration and fan motor is 52.8 MWh and 38 MWh respectively. In the Strategy-5* sensible wheel is added in between the desiccant wheel and free cooling coil. Sensible wheel exchanges heat with the return air, as a result, it improves the efficiency of the HTTP and reduces cooling load on the supply side. The annual energy consumption is 296 MWh which provide 29% energy saving over a conventional system. The energy consumption in the radiant system is 132.6 MWh. In this strategy, the energy consumption in regeneration is reduced by 1.5 MWh by sensible heating of return air by the sensible wheel. The SW also provides almost 18.1 MWh of sensible cooling of supply air; however, because of the high-pressure drop, the fan energy is increased. The energy consumption in the sensible cooling of supply air is reduced by 21.5 MWh. In the Strategy-6* DOAS component comprises of desiccant wheel, HTTP, indirect evaporative cooling (IDEC) and HT coil. In this strategy, sensible wheel is replaced with IDEC. The annual energy consumption is 310 MWh which is equal to 26% energy saving over a conventional system. The energy

consumption in the radiant cooling system is 135.1 MWh. The energy consumption in dehumidification and sensible cooling of supply air has been slightly reduced as compared to Strategy-4* as the addition of IDEC has not provided major reduction of load on the cooling coil. However, the regeneration energy consumption in this strategy is almost the same as Strategy-4*. The energy consumption in IDEC is 12.8 MWh. The energy consumption in the fan is 40.8 MWh. Performance of the indirect evaporative cooling system is highly influenced by the climatic condition. Based on the results replacing the sensible wheel (Strategy-5*) with IDEC (Strategy-6*) is not beneficial in the hot and dry climatic condition.

Figure 4-25 shows the comparison of the annual thermal energy in regeneration and cooling (FC coil and HT coil) of air. As compared to Strategy-4*, the addition of sensible wheel in Strategy-5* reduces 14% of thermal energy in cooling and reduces 3% in regeneration. In Strategy-6* the thermal energy in sensible cooling of air is reduced to 12% compared to Strategy-4* and the thermal energy for regeneration is same as Strategy-4*. Strategy-5* is most suitable for the Hot and Dry climate in desiccant wheel based strategies.
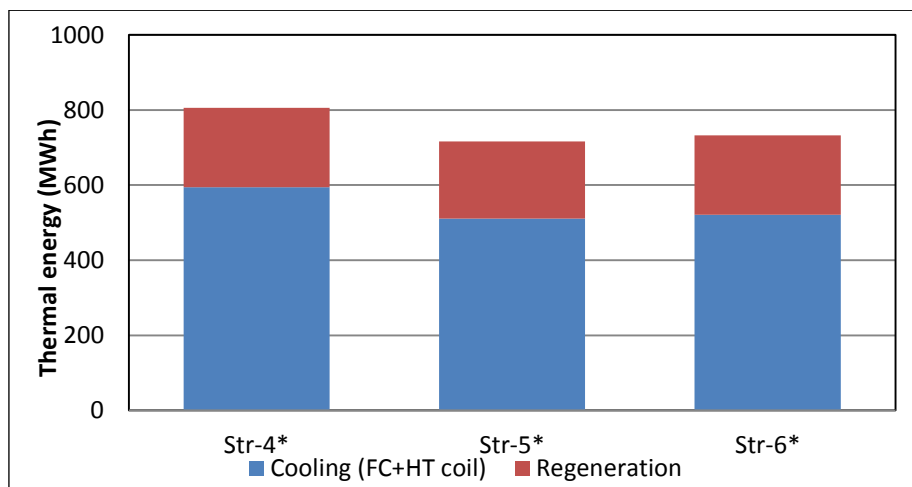
Figure 4-25: Comparison of annual thermal energy in regeneration and cooling (FC coil and HT coil) in Strategy 4*, 5* &6*

Figure 4-26 shows the comparison of energy consumption of chiller, energy consumption of pump and cooling tower are added and shown as pump + cooling tower, energy consumption of fan and wheel are added and shown as pump fan + wheel, IDEC, heat pump & total of the desiccant wheel based Strategy 4*, 5* &6* to shows the comparison. In Strategy-5* chiller energy consumption is 173.4 MWh, heat pump consumes 64.1 MWh, fan and wheel consumes around 38.1MWh. In Strategy-5* sensible

wheel is added in the Strategy-4*, sensible wheel is reducing the load on the chiller as well as heat pump by heating the air which is entering the condenser side and cooling the air at evaporator side of the heat pump. In Strategy 5 chiller energy consumption has been reduced by 21.6 MWh and heat pump energy consumption has been reduced by 6.5 MWh compared to Strategy 4. In Strategy-6* in place of sensible wheel in Strategy 5, IDEC is added. IDEC is reducing the temperature of the air supplied by desiccant wheel to the cooling coil but has not shown much reduction in the energy consumption of heat pump. Strategy-5* is most energy efficient among the three in Hot and Dry climate.
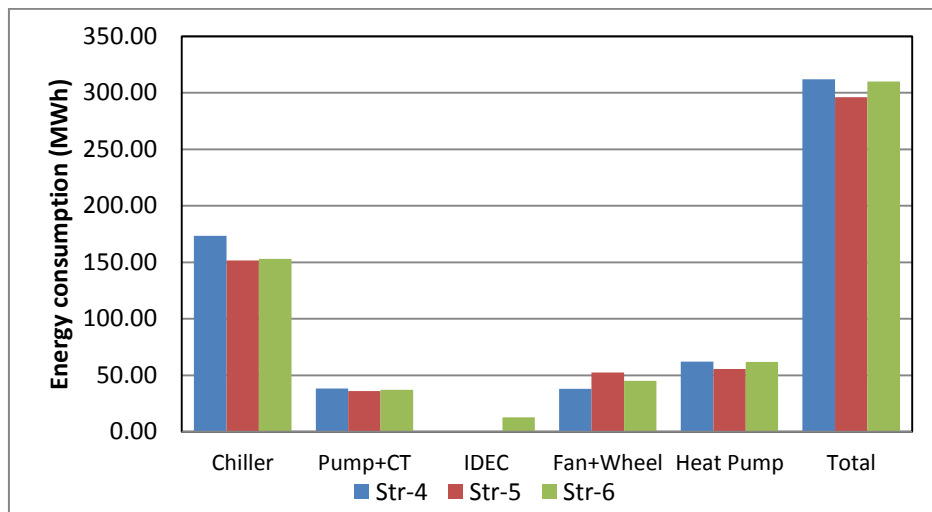
Figure 4-26: Comparison of energy consumption of chiller, pump + cooling tower, fan + wheel IDEC, heat pump & total of the desiccant wheel based Strategy 4*, 5* &6*.

The results of the rest of the climatic conditions i.e. warm and humid, composite and temperate climate are provided in **Appendix I**.

4.8   Chapter summary

In this chapter different types of decoupling strategies (cooling coil and desiccant wheel) were identified from the literature. In the current investigation, performance analysis of different cooling coil and desiccant wheel based strategies are presented and analyzed for different climate zones by whole building simulation approach. Different cooling coil and desiccant wheel based decoupling strategies are compared with a conventional all-air system for different climatic conditions. Many times designer and consultant do not feel comfortable to use desiccant-based dehumidification system in the building due to lack of confidence, unavailability of a high-temperature heat source for regeneration. The recommendation is provided separately for the cooling coil and desiccant-based strategy (Table 4-7) so that if the designers do not want to use a desiccant based system, can use the most efficient strategy from a cooling coil based strategy.

Table 4-7: Recommended Strategy for different climatic conditions

Climate	Cooling coil Strategies	Desiccant wheel Strategies
Hot and Dry	Strategy 2	Strategy 5
Warm and Humid	Strategy 2	Strategy 5
Composite	Strategy 2	Strategy 5
Temperate	Strategy 1	Strategy 6

Based on the simulation results, for hot and dry climate, in cooling coil based strategy, ERW of Strategy-2 is performing better compared to the addition of sensible wheel in Str-3 to reduce the load of the LT coil. In desiccant wheel based strategy sensible wheel of Strategy-5* is performing better in simultaneously improving the performance of HTTP and reducing load of the HT coil as compared to IDEC in Strategy-6*. In warm and humid climate and composite climate also similar pattern was observed and ERW of Strategy-2 and sensible wheel of Strategy-5* is performing better as compared to other strategies of their counterparts. In temperate climate addition of ERW in Strategy-2 and sensible wheel in Strategy-3 is providing penalty on the energy consumption and Strategy-1 was found most suitable in cooling based strategies. In desiccant wheel based strategies addition of sensible wheel in Strategy-5* is reducing cooling load in the supply side and providing penalty in return side by increasing load on the condenser side of HTTP. IDEC in Strategy-6* is performing well in reducing cooling load in supply-side better than the sensible wheel in Strategy-5*. Simulation result provided thrust for conducting experimental analysis for the testing of DOAS strategies. If the designer is planning to design RCS, designer can select the recommended strategy from the Table 4-6; these results are based on the simulation analysis of decoupling strategies. The recommendation is divided into two parts i.e. first is cooling coil based strategies and the second is desiccant based strategies. Based on the preference of designer has to finalize which type (cooling coil or desiccant based strategy) of strategy they want to use while designing RCS and then they can select a recommended strategy.

CHAPTER 5. Experimental analysis for sensible-latent load decoupling strategies

This chapter explains the development of experimental setup for testing and comparing different decoupling strategies for different climatic conditions. The simulation result provides the energy benefits and annual energy saving for the decoupling strategies. To gain more insights and improve our understanding of the physics of decoupling strategies, experimental setup was installed.

To investigate and understand the decoupling strategies in more details, an experimental study was required. The main challenge for the experimental study was to generate the steady-state climatic condition for testing. Generation of steady-state climatic condition required chamber based study and hence planned. To test the decoupling strategies two climatic chambers i.e. outdoor chamber (to generate different ambient condition), indoor chamber (to generate the indoor condition) was designed. Indoor-outdoor chambers were developed by using proper controls to create different climatic conditions and then modular DOAS was coupled with the indoor-outdoor chamber.

5.1 Indoor-Outdoor chamber integrated with Modular DOAS System

Based on the different decoupling strategies a modular DOAS is designed to accommodate all the strategy (Strategy-1 to Strategy-6 as shown in chapter 4) in order. All the components of the DOAS were designed to keep modular nature. While performing experiments of a particular strategy, all the components are modular and components which are not required can be taken out. A lot of time is dedicated in designing and procurement of dedicated outdoor air system. For manufacturing of the modular DOAS discussions were carried out with different companies i.e. DRI, APPIDI and Oorja.

The casing is made of extruded Aluminum hollow profile frames, The Casing leakage is in accordance with relevant EUROVENT standard that is CLASS B. The panels are of double skin construction with both inner and outer steel sheets being
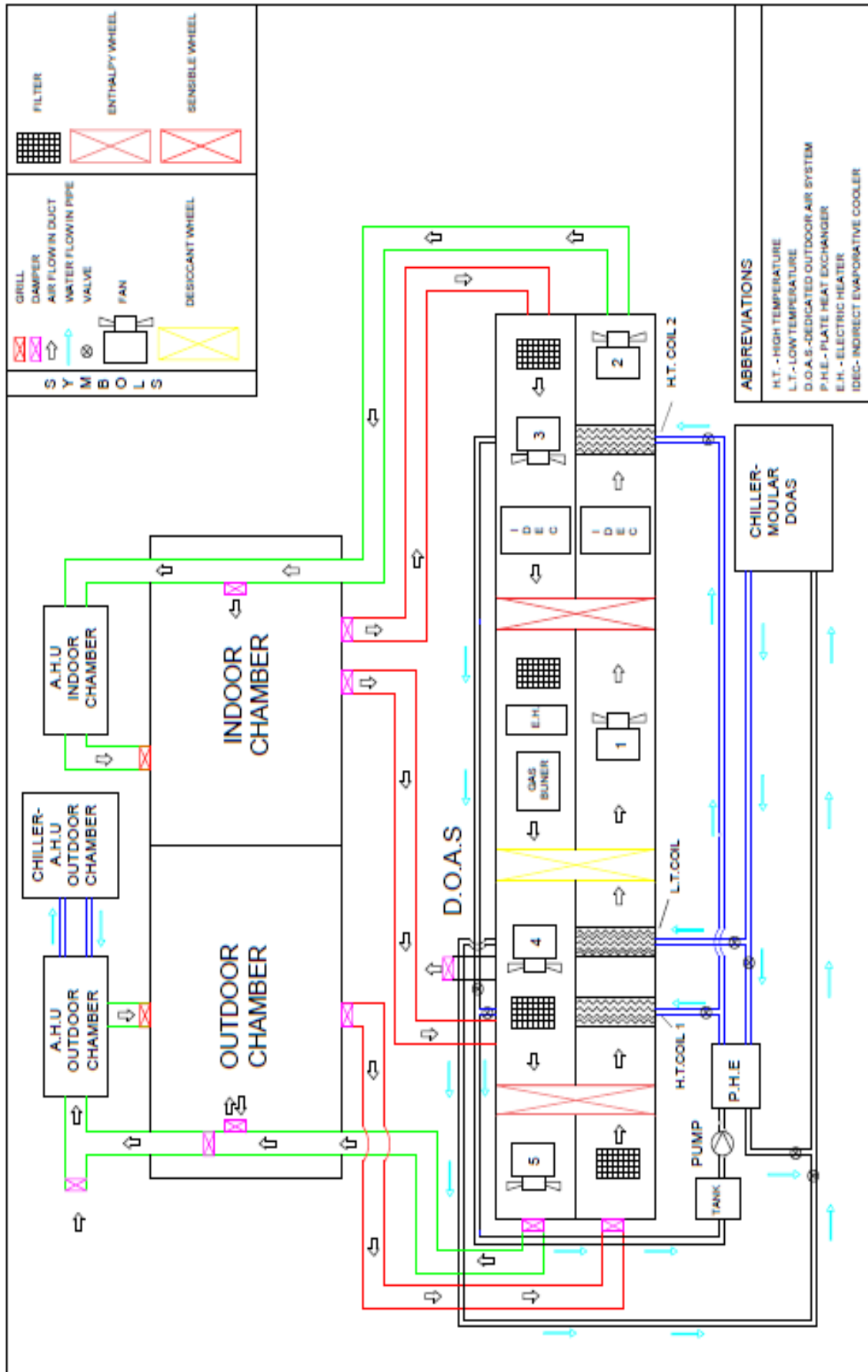
Figure 5-1: Schematic of the indoor-outdoor chamber integrated with modular DOAS

minimum 0.8mm thick. Outside sheet is pre-coated & plasticized and inner sheet is galvanized with 43 mm thick fire retardant, fibreglass insulation sandwiched between the sheets, the fibreglass density is 48 kg/m^3. The fans are backward curved direct driven (plenum) fan. The impellers are statically and dynamically balanced. Fan and motor are mounted on a common galvanized steel or Aluminum block base. The fan motors are energy efficient and suitable for 415$\pm$10% volts, 50 cycles, 3 phase squirrel cage, totally enclosed fan, with IP – 55 protections. Motors are designed for quiet operation, drives are provided for controlling the RPM of fans.

The filter section is normally designed using deep folded disposable synthetic pre filters (panel type) of Class MERV 8. The filter elements are mounted on rails and can be easily pulled out for replacement. The rails are provided with high quality gasket to minimize the risk of leakage. Other HVAC components are as follow.

After designing the modular DOAS, it is integrated with the indoor-outdoor chamber. The outdoor chamber is designed and developed for creating different outdoor conditions as per Indian climatic conditions and the indoor chamber is designed to develop stable indoor conditions to test different decoupling strategies. Figure 5-1 shows the schematic of the indoor-outdoor chamber integrated with modular DOAS. On top of Figure two AHU are shown, they are being used to develop different indoor and outdoor conditions. Chiller-AHU outdoor chamber is used for feeding chilled water to cooling coil of AHU of the outdoor chamber. Second chiller (chiller modular DOAS) as shown in Figure 5-1 is used for supplying chilled water in the cooling coils of the modular DOAS. Figure also shows the air flow (ducting loop) of the entire system. Supply chilled water pipe is designated with the blue colour and return chilled water pipeline is designated with the black colour. Chilled water piping used in this setup is polypropylene random copolymer (PPR). The wiring diagrams and specification of the components used in the setup as shown in Figure 5-1 are provided in Appendix II. The details of the modular DOAS is discussed below.

5.1.1 Supply side of modular DOAS
Enthalpy recovery wheel

The enthalpy recovery wheel was designed to provide minimum recovery of 75 % of the total heat, i.e. both sensible and latent. The wheel is made of pure Aluminum foil coated with molecular sieve desiccant "Ecosorb 300" with pore diameter of

3Å. The cross contamination between the two air streams, leakages are less than 0.04%. The vertical and radial run of the wheel is less than 1 mm per meter of diameter. The wheels have non-contact labyrinth seals for effective sealing between the two air streams. The wheel is certified as per DIN EN ISO 846 with 0% fungal and bacterial growth at 95% Relative humidity and above.

High-temperature cooling coil

Cooling coil sections were provided with chilled water cooling coil, coils are AHRI Certified. Water coil supply and return connection are extended to the unit exterior. The cooling coil is mounted on an insulated SS drain pan. The cooling coil has 6 RD chilled water coil. In the HT coil the supply water temperature is provided at 16°C.

Low-temperature cooling coil

Cooling coil sections were provided with chilled water cooling coil, coils are AHRI Certified. Water coil supply and return connection are extended to the unit exterior. The cooling coil is mounted on an insulated SS drain pan. The cooling coil has 8 RD chilled water coil. In the LT coil the supply water temperature is provided at 7°C.

Desiccant wheel

The desiccants honeycomb rotor media has adsorbent nature, non-toxic, non-flammable, fully water washable. The desiccant media has in-situ synthesized metal silicate desiccant. The Usable desiccant mass is at least 80% of the media weight, so as to ensure high performance and minimal heat carry over. The desiccant rotor has integral long-life bearings supported by a simple fixed shaft design to allow a simple slide out of the rotor/bed. The wheel has a perimeter flange which encircles the entire perimeter so as to allow greater durability and to roll the rotor on the ground, without damage. The wheel is certified as per DIN EN ISO 846 with 0% fungal and bacterial growth at 95% Relative humidity and above.

Sensible wheel

The substrate: The substrate or wheel matrix is made of only pure Aluminium foil with following properties.

a) Quick and efficient uptake of thermal energy.

b) Sufficient mass for optimum heat transfer

c) Maximum sensible heat recovery at a relatively low rotational speed of 20 to 25 RPM

The wheel is certified as per DIN EN ISO 846 with 0% fungal and bacterial growth at 95% Relative humidity and above. The wheel is AHRI certified too.

Indirect evaporating cooling

The Indirect evaporative coolers are made of Polyethylene, infused with a biocide and have integrated watering supplying system. It is integrated with a modular approach, and have the easy-to-install cassette. The minimum wet bulb effectiveness as per manufacturer catalogue is 100%.

High-temperature cooling coil

Cooling coil sections were provided with chilled water cooling coil, coils are AHRI Certified. Water coil supply and return connection are extended to the unit exterior. The cooling coil is mounted on an insulated SS drain pan. The cooling coil has 6 RD chilled water coil. In the HT coil the supply water temperature is provided at 16°C.

5.1.2   Return side of modular DOAS

Sensible wheel: Discussed above

Regeneration section

Regeneration section comprises of following components:

- ✓ Active heater
  For regeneration of the desiccant wheel, an electric heater of 75kW is used. The heater is coupled with a thyristor control for modulation of the capacity. Active heater is used while conducting the experiments.
- ✓ Hot water coil
  The regeneration process can also be done by using hot water in the coil placed in the return path. Hot water can be used by generating in a solar thermal system or by exchanging heat from waste heat.
- ✓ Gas burner
  The machine also provides the facility for heating of the regeneration air using gas. The gas burner is provided, the gas connection is required to be done.

Desiccant wheel: Discussed above

Enthalpy recovery wheel: Discussed above
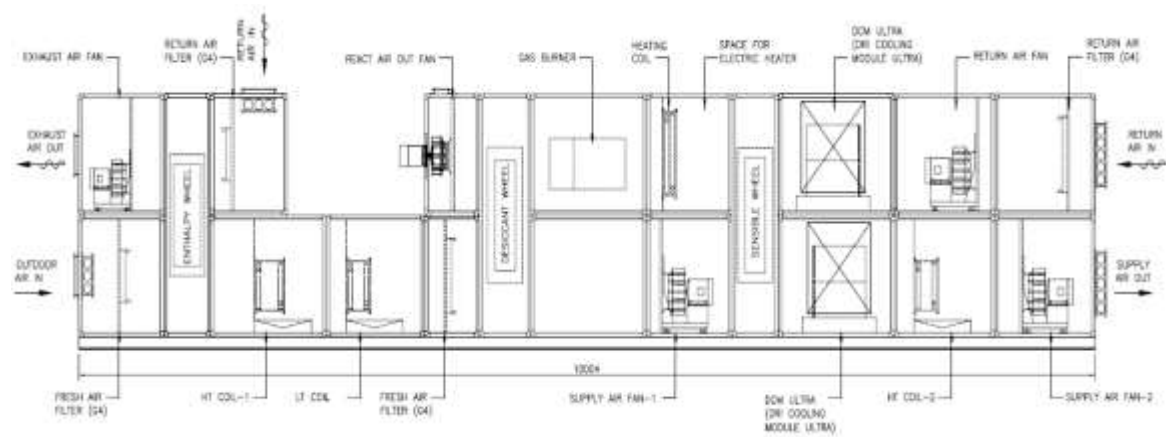
Figure 5-2: Schematic of modular DOAS setup

Figure 5-3: Installation and commissioning of modular DOAS

Figure 5-4: Modular DOAS setup

Figure 5-2 shows the schematic of the modular DOAS setup designed to accommodate strategy one to seven of chapter three. The same schematic is provided for the manufacturing and fabrication of the setup. Figure 5-3 shows the various photographs while commissioning of the modular DOAS setup at the Center for Energy and Environment, MNIT Jaipur to couple the DOAS with the indoor and outdoor chamber. This Figure shows the crane lifting and the cross-sectional view of the DOAS. Figure 5-4 shows the commissioned modular DOAS setup ready for integration with the indoor and outdoor chamber to generate a steady-state psychrometric condition for the testing.

5.2 Integration of indoor-outdoor chamber with modular DOAS

Integration of indoor-outdoor chamber with modular DOAS was one of the most challenging part of the whole thesis work. From conceptual idea to integration and testing took around two years and four months. Workflow of integration of indoor-outdoor chamber is shown in the Figure 5-5. The indoor-outdoor chamber is created by placing a partition wall in the center of a single room of dimensions of 8x8 m. Based on the design of the testing facility, procurement of the different component such as air handling unit, chillers, pumps, plate heat exchangers, insulation, sensors and instrumentation etc. was completed.
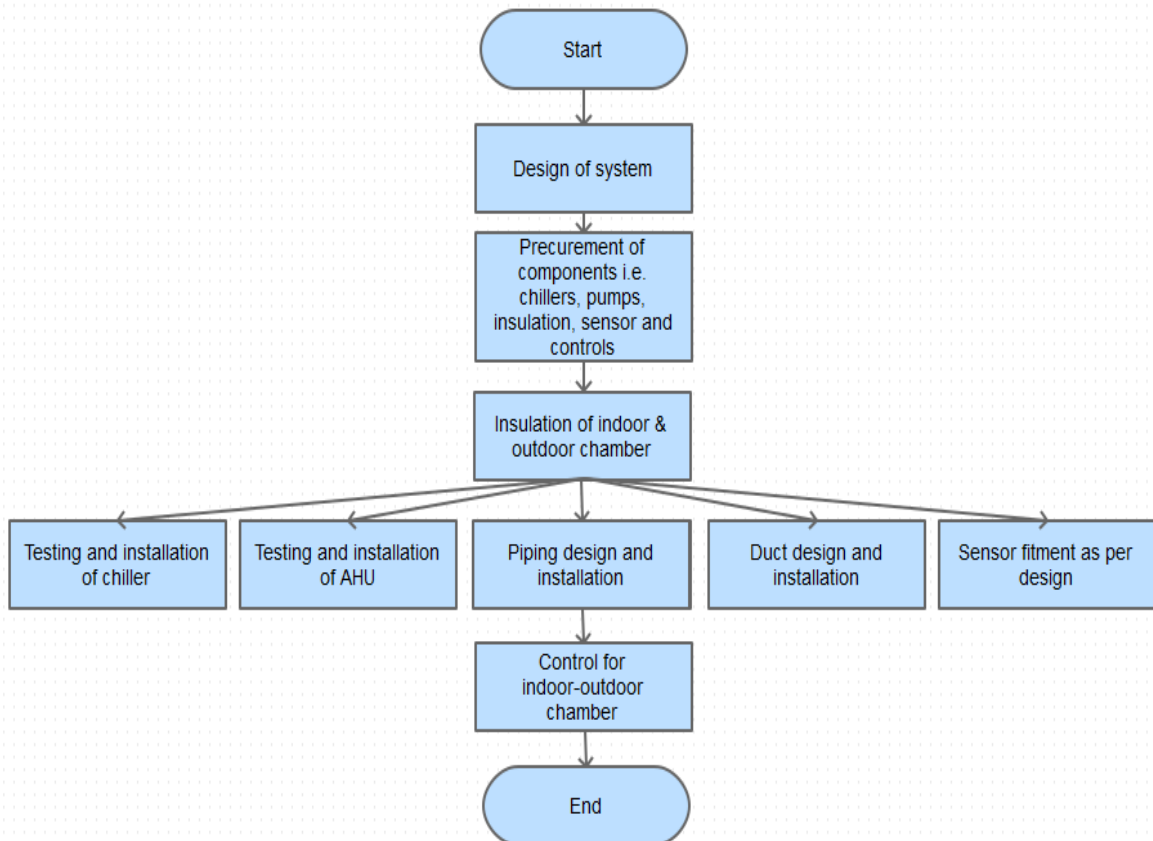
Figure 5-5: Flowchart of installation indoor-outdoor chamber integrated with modular DOAS

5.2.1 Insulation of chambers

One of the most important aspects for the proper functioning of the indoor-outdoor chamber for maintaining steady state condition was to avoid infiltration and heat gains through chamber envelope. All the walls and roof are insulated by using extruded polystyrene rigid board XPS INSUBoard of 50 mm thickness. XPS board is made from CO_2 based blowing agent, having a thermal conductivity as per IS 3346 of 0.028 W/mK. The compressive strength at 10% deflection is 300kpa; density is 34-36 kg/m^3 and water absorption 0.2% by volume, with fire retardant property. Figure 5-6 shows the placement of insulation in the chamber envelop.

Figure 5-6: Placement of insulation in the indoor-outdoor chamber

5.2.2 Chiller installation and testing

Two chillers (specifications attached in Appendix II) were procured to feed chilled water in the cooling coil of modular DOAS and the AHU coupled with the outdoor chamber to generate a different climatic condition for the testing. Both the chillers are having the inbuilt recirculating pump. After placement of the chillers at site, chillers were commissioned with three-phase electrical wiring.

CPVC (Chlorinated polyvinyl chloride) piping work was carried out for coupling chiller 1 with a cooling coil of AHU of the outdoor chamber and chiller 2 with a cooling coil of modular DOAS as shown in Figure 5-1. Piping was pressure tested to detect the leakage in the piping while testing some of the leakages were identified and rectified. Demineralized water is used in the chiller to avoid scaling in long run of the system. Figure 5-7 shows the pictures while testing and filling the demineralized water in the chiller. After the installation, testing and troubleshooting was performed as discussed below.

Figure 5-7: Chiller commissioning and testing

Trouble shooting: While starting the chiller initially we observed the pump overload error. To overcome pump overload, water balancing was done by setting the bypass valve and the pressure at the evaporator side of the chiller. Chiller was tested at different supply chilled water temperature range from 7-15ºC. During the initial run of the chiller, it was frequently getting on and off. After checking different electrical aspects we came to know the earthing of the neutral wire was getting fluctuated and due to that chiller was frequently starting and stopping. To avoid this issue earthing was rectified.

5.2.3   AHU installation and testing

Two air handling units (AHU) were procured (specifications provided in Appendix II), each one for the indoor and outdoor chamber. AHUs were used to develop steady state psychrometric condition in the chambers. The outdoor chamber contains a low-temperature cooling coil, electric heater and a humidifier. The air is first passed through a low-temperature cooling coil for dehumidification and sensible cooling. After cooling coil, it is passed through heater and humidifier to add desired heat and humidity to achieve steady state condition. AHU of indoor chamber consists of a humidifier and a heater. Both the AHUs are placed on the base above the vibration damper pads in front of the indoor-outdoor chamber. Figure 5-8 shows the pictures of installation/placement of AHU.

Figure 5-8: AHU commissioning for indoor-outdoor chamber

Figure 5-9: AHU of indoor-outdoor chamber after commissioning

5.3   Indoor-outdoor chamber

Figure 5-9 shows the front view of the indoor-outdoor chamber after coupling of chambers with the AHU and chiller by integration of air loop (ducting) and water loop (piping). Figure 5-10 shows the chambers inside view after insulation of envelops. Each chamber is 4x4m in area. Fig 5-10 (a) shows the indoor chamber, all the starter panels such as wheels, fans, pumps, heater etc. are place in indoor chamber. Figure 5-10 (b) shows the indoor chamber. The back part of the indoor-outdoor chamber is covered with the shade and picture cannot be shown. Figure 5-11 shows the three dimensional view of the experimental setup. It shows the chillers feeding the AHU, modular DOAS and the duct air loop connecting the components. Table 5-1 shows the sizing of the components used in the HVAC system to develop different psychrometric condition in the outdoor and indoor chamber.

Figure 5-10: a) Indoor chamber, b) outdoor chamber
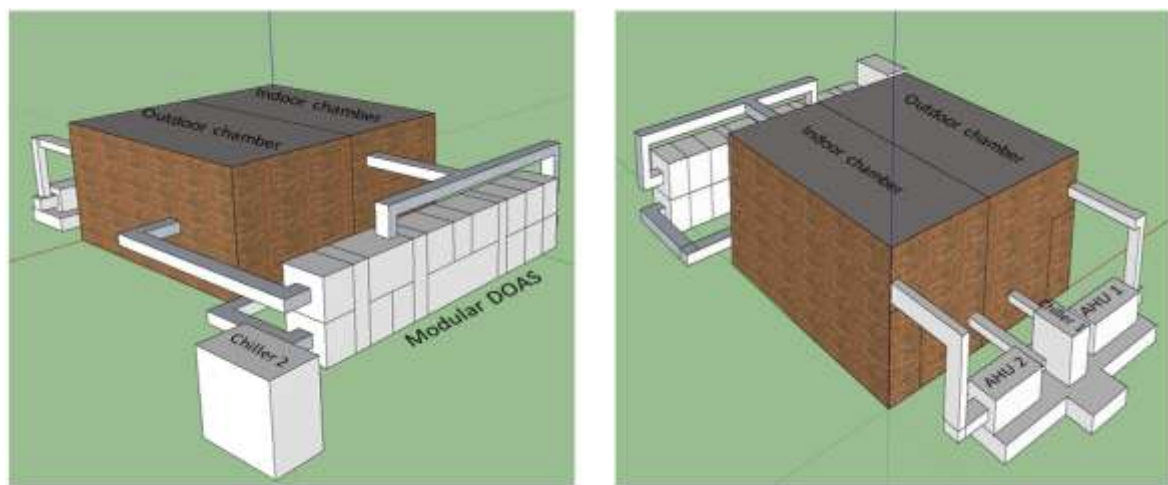
Figure 5-11: 3D View of the experimental setup (a) back portion, (b) front portion of the chamber

Table 5-1: Component sizing detail as used in indoor-outdoor chamber

Parameters	Details
Chamber size (indoor & outdoor)	4x4 m
Chiller 1 (capacity in ton)	10 (detailed specs in Appendix II)
Chiller 2 (capacity in ton)	5 (detailed specs in Appendix II)
Pump capacity (coupled with chiller 1 and modular DOAS)	0.5 HP (detailed specs in Appendix II)
Heater capacity (AHU outdoor chamber)	20kW (4kWx5)
Humidifier (AHU outdoor chamber)	8kg/h
Heater capacity (AHU outdoor chamber)	10kW (2kWx5)
Humidifier (AHU outdoor chamber)	4kg/h

5.4   Instrumentation and controls in the indoor-outdoor chamber

Instrumentation and sensors are one of the foremost important aspects of the DOAS testing setup. Proper positioning of sensors, accuracy of sensor is the key to get quality data for conducting reliable study. Control works based on the feedback of the sensors input. For achieving steady state condition selection of right sensor,

instrumentation and control is the key. We have used the high-end sensor and instrumentation in the setup. The different sensors such as temperature and RH sensor, air velocity sensor, pressure differential sensor is used to get the data from the DOAS at every supply and return of each component. Temperature and RH sensor are also used in the indoor-outdoor chamber for generating the conditions. Air velocity is used in ducts and DOAS for calculating the volumetric flow. The energy meter is used to log the energy of every component. BTU meters are used across every cooling coil to log the thermal energy. Detailed specification of the sensor and instrumentation are provided below. Table 5-2, 5-3, 5-4, 5-5, 5-6 shows the detailed specification of the temperature and RH sensor, air velocity, differential pressure, BTU meter and energy meter respectively. Figure 5-12 shows the positioning of T&RH, air velocity and pressure differential sensor in the modular DOAS. BTU meter is placed along every cooling coil and energy meter is coupled with wheels, fans, heater, chiller and pumps.
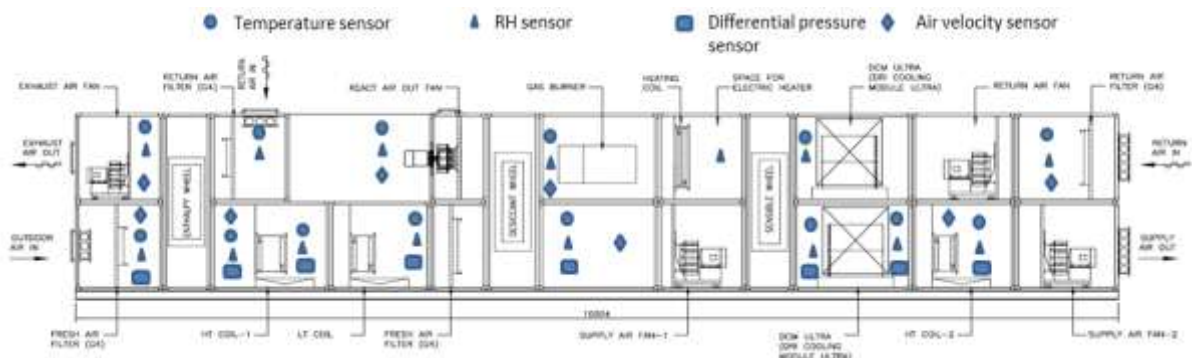
Figure 5-12: Positioning of sensors in the modular DOAS

5.4.1 Sensors

Following sensors are used in the experimental setup:

a) Temperature & RH sensor: Make-Rotronic

Table 5-2: Specifications of T&RH sensor

Parameters	Range
Integrated sensors	Yes
Humidity sensor	Hygromer
Temperature sensor	Pt100 1/3 Class B
Accuracy at 23 ±5 °C	±2.0 %RH / 0.3 K (±1.0 %RH / 0.2 K Type R)
Resolution	0.02 %RH / 0.01 K
Response time	10 s
Measurement range	-40…60 °C / 0…100 %RH
Electronics operating range	-40…60 °C / 0…100 %RH
Alarm functions (programmable)	Open or shorted sensor
Output signals Freely scalable by	4-20 mA

user

Power supply	10-28 VDC
Power consumption	max 40 mA,
Sensor protection	Polyethylene filter
Dew point /frost point calculation	Yes

b) Air velocity sensor: Make-Siemens

Table 5-3: Specifications of air velocity sensor

Parameters	Range
Operating voltage	AC 24 V ±20 %
Frequency	50 Hz
Power consumption	5 VA (max. 200 mA)
Measuring ranges	0-15 m/s
Measuring accuracy at 20 °C, 45 % RH	± 0.2 m/s
Permissible air velocity	20 m/s
Voltage DC	0-10 V
Current	±1 mA
Probe length	370 mm
Mounting type	Duct

c) Differential pressure sensor: Make- Dwyer

Table 5-4: Specifications of differential pressure sensor

Parameters	Range
Pressure range	0-750 Pa
Accuracy	±1%
Operating Conditions	
Medium	Air
Supply voltage	24 VAC or VDC ± 10%
Current Consumption	40 mA max.
Stability	±1% / year FSO.
Output Signals	4 to 20 mA
Enclosure Rating	IP66.
Parity	None
Stop Bits	1

d) BTU meter: Make-Sontex

Table 5-5: Specifications of BTU meter

Parameters	Range
Pressure:	1.6MPa
Press loss:	0.025MPa
Static current:	10uA
Accuracy class:	Class 2
Permissible flow temp:	2°C - 95°C
Permissible ΔT:	3°C -70°C
Permissible flow:	1 -15 m^3/h

Enclosure protection:	IP65
Flow sensor:	Ultrasonic
Flow sensor accuracy:	$\pm2\%$
Temperature sensor:	PT 500
Temperature sensor accuracy:	±0.3 ℃
Flow meter Diameter:	40mm
Interface:	Analogue module with two outputs 4-20mA

e) Energy Meter: Make-Selec

Table 5-6: Specifications of energy meter

Display	
Display	LCD
Digit	8
Digit hight	10.5mm
Input Specification	
Electrical connection	3ϕ-3/4 wire, 2ϕ 3wire
Input Voltage	19 to 519V AC (phase to phase)
	11 to 300V AC (phase to neutral)
Input current	10mA-5A (6A max)
Frequency	45-65 Hz
Resolution	0.01K.
Accuracy	Power (Active, Reactive):$\pm1\%$
	Energy (Active, reactive, apparent): Class1
Memory Retention	10years (for energy)
Display reset	Programmable (for energy)
Communication	RS-485

5.4.2   Controls for indoor-outdoor chamber

Control is the heart of the DOAS testing facility. For creating the steady state psychrometric condition we have used the PLC (programmable logic control) based control. PLC has evolved as an important controller in industries these days because of its simplicity and robustness. It is used for controlling many mechanical movements of the heavy machines or to control the voltage and frequency of the power supplies.

Control is used for generating steady state psychrometric condition in the indoor-outdoor chamber. We have controlled the cooling coil, heater and humidifier to achieve the steady state condition in the outdoor chamber. The air supplied by modular DOAS is passed through AHU of the indoor chamber to provide steady state condition for the return air in modular DOAS by controlling heater and humidifier. This application is based on monitoring of Energy Meter, BTU Meter, different sensors such as T & RH, air velocity, differential pressure transmitter in DOAS SYSTEM and T & RH sensor in the indoor-outdoor chamber & controlling AC Drive. Temperature, RH, Differential pressure, air velocity sensors, BTU meter and energy meter values are displayed on a screen by

using WAGO WEB visualization & these values are continuously stored in SD Card. We can check previous dated data by using SD Card. We can also check previous date data by using data plotter application. We can switch on /off AC drive through PLC. Manually we can feed frequency to selected AC Drive. In case of Auto mode, AC drive maintains frequency based on the input to maintain the volumetric flow.
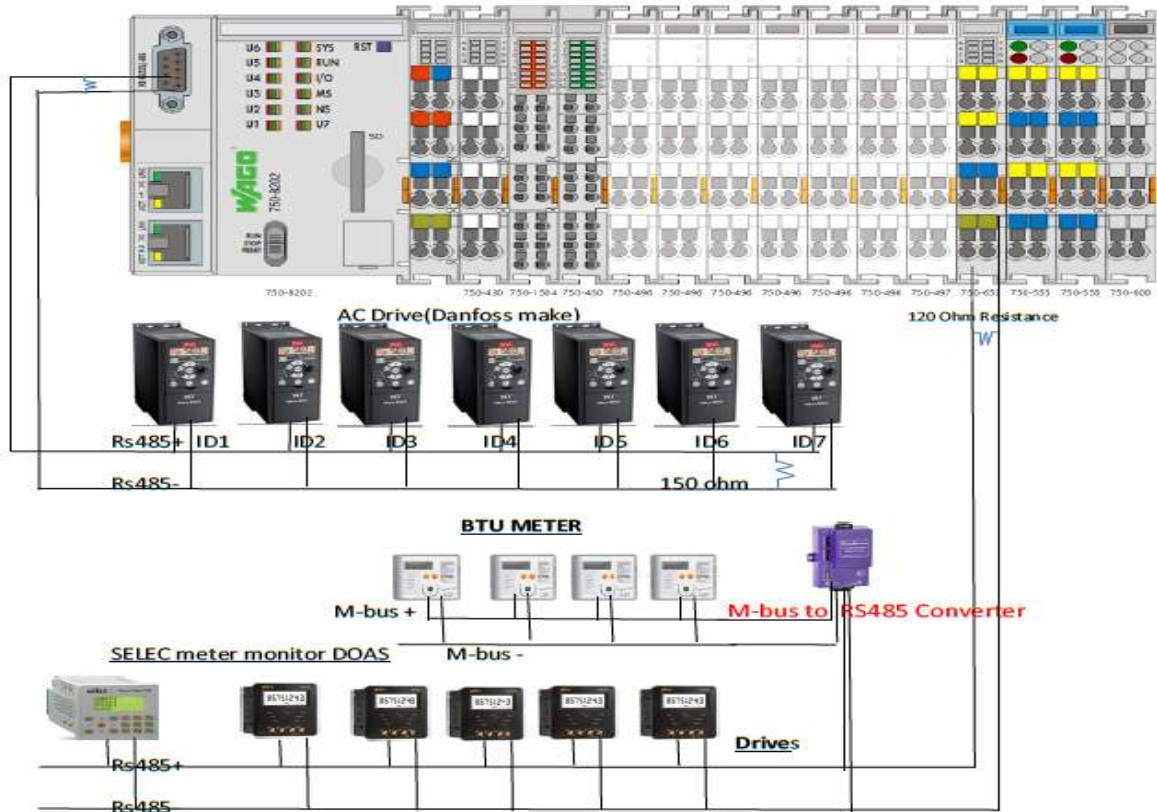
Figure 5-13: Control Architecture of the psychrometric chamber

Figure 5-13 shows the control architecture of the DOAS testing facility. The bar on the top shows the Wago PLC (Wago 750-8202) with different input-output digital and analog card. PLC IP address is 192.168.1.50. These input-output cards are used to log the values from different sensors and instruments and control the drives based on the logic. Different drives are laid on the RS 485 protocol connected to Wago 750-8202 for controlling different fans in the modular DOAS and controlling the humidifier in the AHU of the indoor-outdoor chamber. Inbuilt 9 pin RS 485 id Interface ID is COM0, its baud rate is 9600, stop bit is 1 & data bit 8 Node ID of AC drives are 1,2,3,4,5,6,7. Serial interface module 750-652 has Interface ID COM2 & its baud rate is 19200, stop bit is 2 & data bit is 8 Node ID of DOAS unit is 1, Node ID of Energy meters are 2,3,4,5,6, & Node ID of BTU Meters 10,11,12,&15. The BTU meter placed along the cooling coil gives the

data output in M-bus protocol. An M-bus to RS 485 converter is used to convert the BTU meter signal for logging the data card. Selec energy meters are used to log energy consumption of different modular DOAS components such as a chiller, pump, fan, wheel and heater is connected with RS 485 protocol. All the sensors such as T & RH, air velocity, and pressure differential are placed in the modular DOAS are connected to Selec meter-monitor (DOAS) is further connected to Wago 750-8202 for data logging. Table 5-7 shows the control strategy and components for AHU of the indoor-outdoor chamber.

Table 5-7: Control strategy for indoor-outdoor chamber

AHU 1 (Outdoor chamber)	AHU 2 (Indoor chamber)
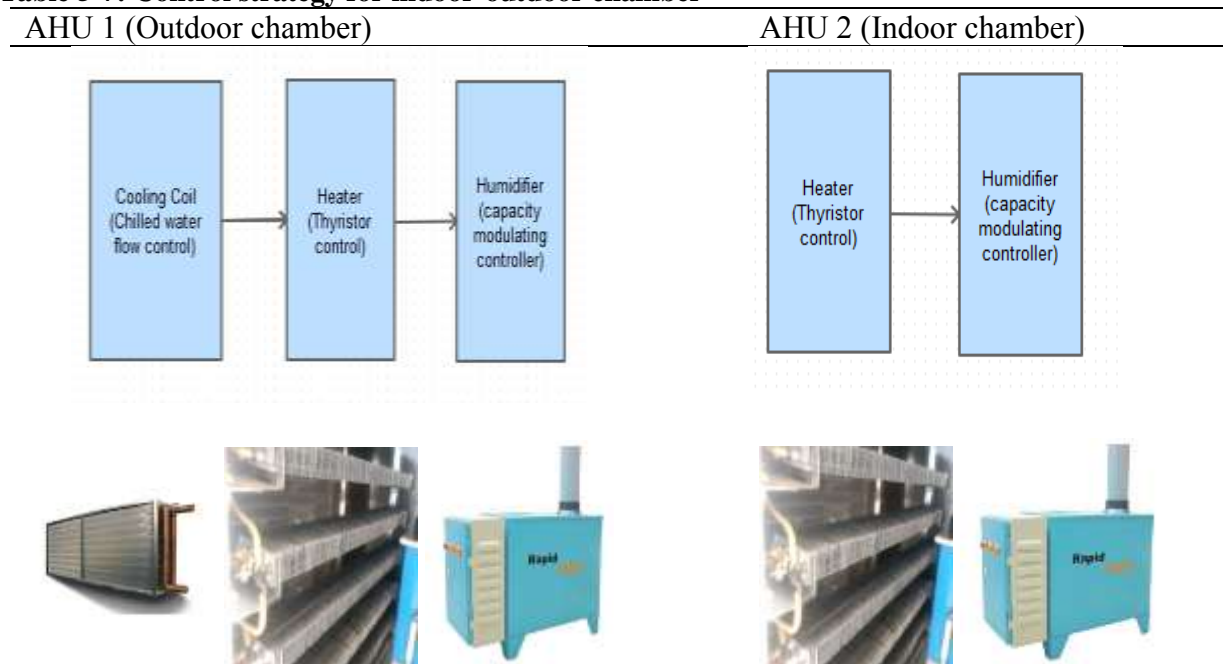
5.5   Design of experiment

HVAC systems are usually designed for the peak load, usually designers consider 2% design condition for designing HVAC system for simplicity. In the Indian society of heating refrigeration and air conditioning (ISHRAE) Indian weather data 2017 design conditions of Dry Bulb Temperature (DBT) and Mean Coincident Wet Bulb Temperature (MCWB) is provided at 2% annual cumulative frequency of occurrence. The experiments have been conducted for 2% design condition provided in ISHRAE Indian weather data 2017. Based on the given DBT and MCWB, RH and specific humidity was calculated from psychrometric chart and the 2% design conditions i.e. dry bulb temperature (DBT), wet bulb temperature (WBT), relative humidity (RH) and specific humidity (ω) are provided in Table 5-8. The 2% design conditions were maintained in the outdoor chamber and experiments were conducted. Selection of this method of conducting experiments is finalized based on the detailed discussion with industry people and some researchers working in the area of HVAC, building energy efficiency.

Table 5-8: Design of experiment [83]

2% Design conditions	Cities			
	Ahmedabad (Hot and dry)	Chennai (Warm & humid)	New Delhi (Composite)	Bengaluru (Temperate)
DBT (°C)	39.9	36.2	39.4	32.6
WBT (°C)	22.9	25.8	23.1	19.8
RH (%)	23	44	25	30
ω (g/kg)	10.5	16.7	10.3	9.2

Once the system was stabilized two-hour data has been considered for the analysis. I have conducted two sets of experiments for each condition to achieve better accuracy.

5.6   Results and discussion

Experiments were conducted based on the outdoor condition shown in the design of experiments. After achieving steady state condition in the outdoor chamber the experiments were conducted and data for all the sensors and instruments were logged. Subsequently, the data was cleaned and analyzed for different climatic conditions. The data were analyzed for two hours. Overall the analysis of results was conducted separately for cooling coil based strategies and desiccant wheel based strategies. Results are described in details for different climatic conditions below:

5.6.1   Hot and dry climate

Ahmedabad city is considered for the hot and dry climate. Figure 5-14 shows the comparison of energy consumption of chiller, wheel, fan & total of the cooling coil based strategy. Chiller energy consumption comprises of the summation of electrical energy consumption of chiller and pump. The fan energy consumption is a summation of all the fans used in modular DOAS. In Strategy-1 the total load is removed by the cooling coil alone, chiller energy consumption is 11.8 kWh. In Strategy-2 comprise of ERW and a cooling coil, an ERW is placed before cooling coil, ERW exchanges energy with return air hence reduces the load on the cooling coil as a result chiller energy consumption is

Figure 5-14: Comparison of energy consumption chiller, wheel, fan & total of the cooling coil based Strategy 1, 2 &3.

Table 5-9: Psychrometric values of Strategy-2

State point		1	2	3	4	5
Str 2	**T (°C)**	39.9	32.6	12.8	27.2	35.3
	w (g/kg)	10.5	9.8	7.2	9.3	9.9
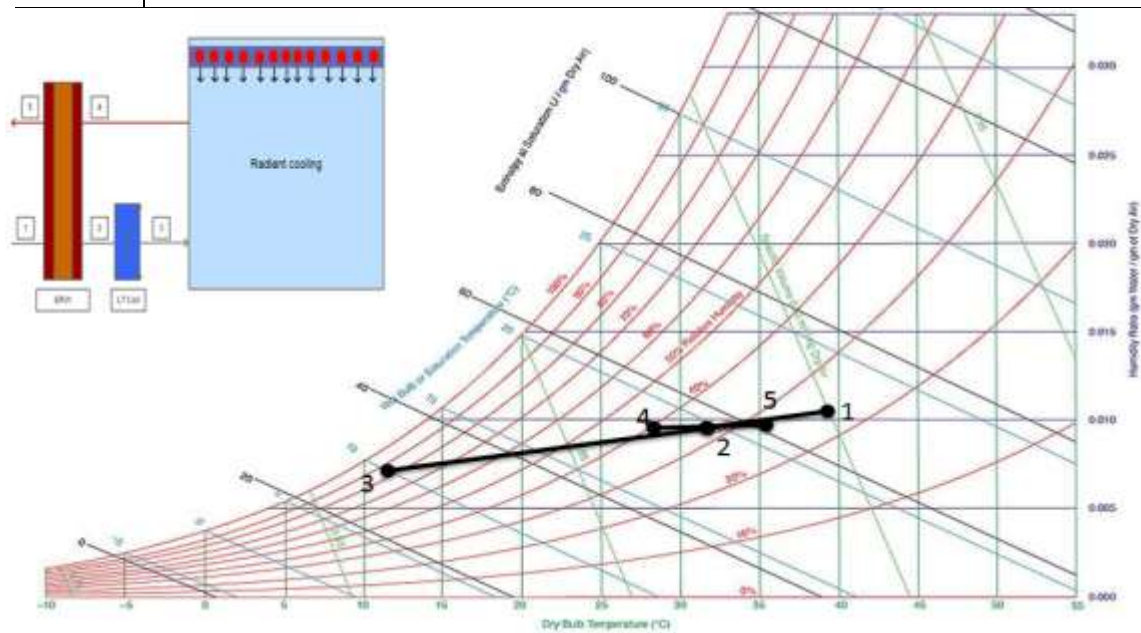
Figure 5-15: Psychrometric process of the Strategy-2

Process (1)-(2): Energy recovery (sensible cooling and dehumidification)

Process (2)-(3): Dehumidification and sensible cooling

Process (4)-(5): sensible heating and humidification

reduced and it is 9.9 kWh. In Strategy-3 a sensible wheel is added to the Strategy-2, sensible wheel is placed after cooling coil and the chiller energy consumption of 9.3 kWh.

In Str-2 the ERW motor consumes 0.3 kWh and in Strategy-3 ERW and sensible wheel consumes 0.6kWh. Fan consumes 1.8 kWh, 2.1 kWh, and 2.5 kWh in Strategy-1, Strategy-2 and Strategy-3. Strategy-2 is saving 10% energy compared to Strategy-1 and Strategy-3 is saving 9% energy compared to Strategy-1. Addition of ERW in Strategy-2 has provided better savings compared to addition of an extra sensible wheel in Strategy-3.

Table 5-9 shows the psychrometric values at entry and exit of each components of Strategy-2. Range of measured values (minimum, maximum, mean) and graphical plots of the measured data are provided in **Appendix III**. Figure 5-15 shows the process of Strategy-2 on psychrometric chart. In process (1)-(2) air passes through the ERW, drops the temperature from 39.9 to 32.6 °C and specific humidity from 10.5 to 9.8 g/kg while exchanging heat from return air i.e. process (4)-(5), addition of ERW reduces load from the cooling coil. In the process (2)-(3) the air is further cooled and dehumidified while passing through the cooling coil and then enter the zone. In Strategy-1 the total load is on the cooling coil hence chiller energy is much higher and in Strategy-3 addition of sensible wheel does not impacted much on savings. Strategy-2 is found to be most suitable in hot and dry climate.

Figure 5-16 shows the comparison of energy consumption of chiller, fan, wheel, heater & total energy consumption of the desiccant wheel based strategy. When air is passed through the desiccant wheel the humidity gets adsorbed in the wheel, in the return side to desorb the desiccant wheel high-temperature air (heated by resistance heater) is passed through return side. The active heater is being used for regeneration of wheel. When supply air is passed through the desiccant wheel it gets dehumidified and some heat is added to the air due to active regenerating source (return air temperature is at high temperature). To cool the air high-temperature cooling coil is applied in the Strategy-4. The chiller energy consumption is 8.15 kWh in Strategy-4, the addition of sensible wheel in between the desiccant wheel and cooling coil exchanges heat with return air and reduce the load of the chiller to 6.45 kWh in Strategy-5. In Strategy-6 addition of IDEC in between the desiccant wheel and cooling coil reduce the load on chiller compared to Strategy-4 but not as efficient as a sensible wheel in Strategy-5, chiller consumes 7.55 kWh in Strategy-6. Heater has the highest magnitude in terms of energy consumption. Total installed capacity of heater is 75 kW, there are three banks of 18kW having on/off control and fourth bank of 21kW controlled by thyristor. By these two combinations (on/off and thyristor) of controls desired amount of heating can be provided. In the return

side of DOAS, in order to achieve continuous dehumidification desiccant wheel has to be regenerated. To supply air continuously at 7.5-8 g/kg, regeneration is being done i.e. in return side, air is being heated using resistive heaters. In Strategy 4 and 6 return air has to be heated from 27°C to 54°C, around 19kW heater banks were energized for the same purpose while in Strategy 5 air is first heated by the sensible wheel and temperature at supply of heater was reached to 42.5 °C and load of the heater was reduced and only 13kW of heater capacity were energized. Heater consumes 39.8 kWh, 26.2 kWh and 38.9 kWh in Strategy-4, Strategy-5 and Strategy-6 respectively. Strategy-5 saves around 29% of energy consumption compared to Strategy-4 and Strategy-6 saves 3% of energy consumption compared to Strategy-4. Addition of sensible wheel in Strategy-5 has provided better energy savings compared to IDEC in Strategy-6. Strategy-5 is most suitable for hot and dry climate in desiccant wheel based strategy.
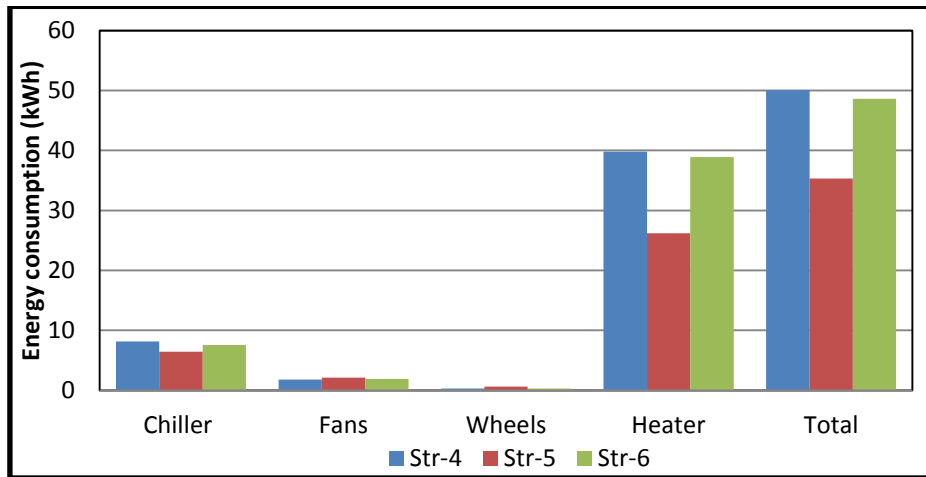
Figure 5-16: Comparison of energy consumption of chiller, fan, wheel, heater & total of the desiccant wheel based Strategy 4, 5 & 6

Table 5-10 shows the psychrometric values at entry and exit of each components of Strategy-5. Range of measured values (minimum, maximum, mean) and graphical plots of the measured data are provided in **Appendix III.** Figure 5-17 shows the process of Strategy-5 on psychrometric chart. In process (1)-(2) air passes through the desiccant wheel, air gets dehumidified and sensible heat from 39.9 °C and 10.5 g/kg to 49.3 °C and 7.8 g/kg. In process (2)-(3) air passes through the sensible wheel to exchange heat with return air i.e. process (5)-(6), in this process air gets sensible cooling. In process (3)-(4) air passes through the high-temperature cooling coil (HT) for sensible cooling and then enters the zone. In process (6)-(7) air passes through the active heater to heat the air to achieve regeneration of the desiccant wheel in the process (7)-(8). In Strategy-4 the

desiccant wheel is responsible for dehumidification and HT coil is responsible for sensible cooling, the total sensible load is met by the chiller hence having higher energy consumption compared to Strategy-5. In Strategy-5, SW has reduced the load from the coil and provided savings in chiller energy consumption. In Strategy-6 the ambient condition of Ahmedabad has not provided much favorable condition and IDEC has not performed well hence again chiller energy consumption has increased compared to Strategy-5. Strategy-5 is found to be most suitable for hot and dry climatic conditions.
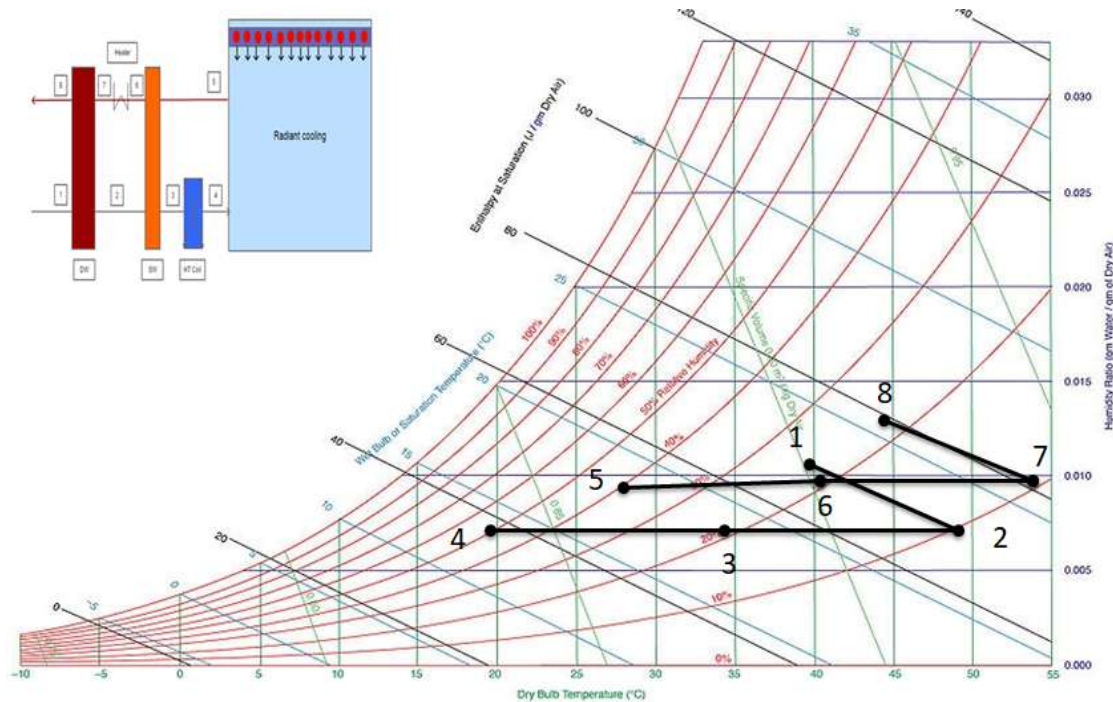
Figure 5-17: Psychrometric process of the Strategy-5

Process (1)-(2): Dehumidification and sensible heating

Process (2)-(3): Sensible cooling

Process (3)-(4): Sensible cooling

Process (5)-(6): Sensible heating

Process (6)-(7): Sensible heating

Process (7)-(8): Humidification

Table 5-10: Psychrometric values of Strategy-5

State point		1	2	3	4	5	6	7	8
Strategy-5	**T (°C)**	39.9	49.3	34.3	19.4	27.2	42.3	54	44.72
	w (g/kg)	10.5	7.8	7.8	7.7	9.1	9.3	9.2	12.6

104

5.6.2 Warm and humid climate
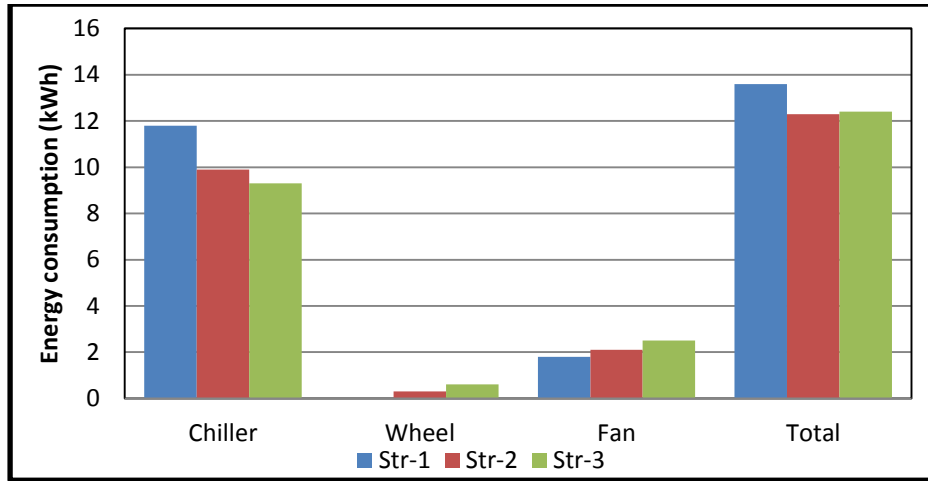
Chennai city has been considered for the warm and humid climate. Figure 5-18 shows the comparison of energy consumption chiller, wheel, fan & total of the cooling coil based Strategy 1, 2 &3. In Strategy-1 the chiller energy consumption is 12.6 kWh which is highest among the three as total load is met by the cooling coil. The chiller energy consumption is 10.8 kWh in Strategy-2 and 10.3 kWh in Strategy-3 respectively. Addition of energy recovery wheel and the sensible wheel has reduced the load on the coil in Strategy-2 and Strategy-3, therefore, energy consumption of chiller has been reduced in Strategy-2 and Strategy-3. In Str-2 the ERW motor consumes 0.3 kWh and in Strategy-3 ERW and sensible wheel consumes 0.6kWh. Wheel and fan energy have been increased in Strategy-2 and Strategy-3 due to the addition of wheels in the air path. Fan consumes 1.8 kWh, 2.1 kWh, and 2.5 kWh in Strategy-1, Strategy-2 and Strategy-3. Strategy-2 is saving 8% energy compared to Strategy-1 and Strategy-3 is saving 7% energy compared to Strategy-1. Table 5-11 shows the psychrometric values at entry and exit of each components of Strategy-2. Range of measured values (minimum, maximum, mean) and graphical plots of the measured data are provided in **Appendix III**.

Table 5-11: Psychrometric values of Strategy-2

State point		1	2	3	4	5
Strategy-2	**T (°C)**	36.2	30.3	12.3	27.2	32.8
	w (g/kg)	16.7	11.9	7.2	9.4	14.1

Figure 5-18: Comparison of energy consumption chiller, wheel, fan & total of the cooling coil based Strategy 1, 2 &3.

Figure 5-19 shows the process of Strategy-2 on psychrometric chart. In process (1)-(2) air passes through the ERW, drops the temperature from 36.2 to 30.3 °C and specific humidity from 16.7 to 11.9 g/kg while exchanging heat from return air i.e. process (4)-

(5), addition of ERW reduces load from the cooling coil. In the process (2)-(3) the air is further cooled and dehumidified to 12.3 °C and 7.2 g/kg while passing through the cooling coil and then enter the zone. Warm and humid climate has high level of latent load, in Strategy-1 the total load is on the cooling coil hence chiller energy is much higher and in Strategy-3 addition of sensible wheel does not impacted much on savings. Strategy-2 is found to be most suitable in warm and humid climate. Range of measured values (minimum, maximum, mean) and graphical plots of the measured data are provided in Appendix III.
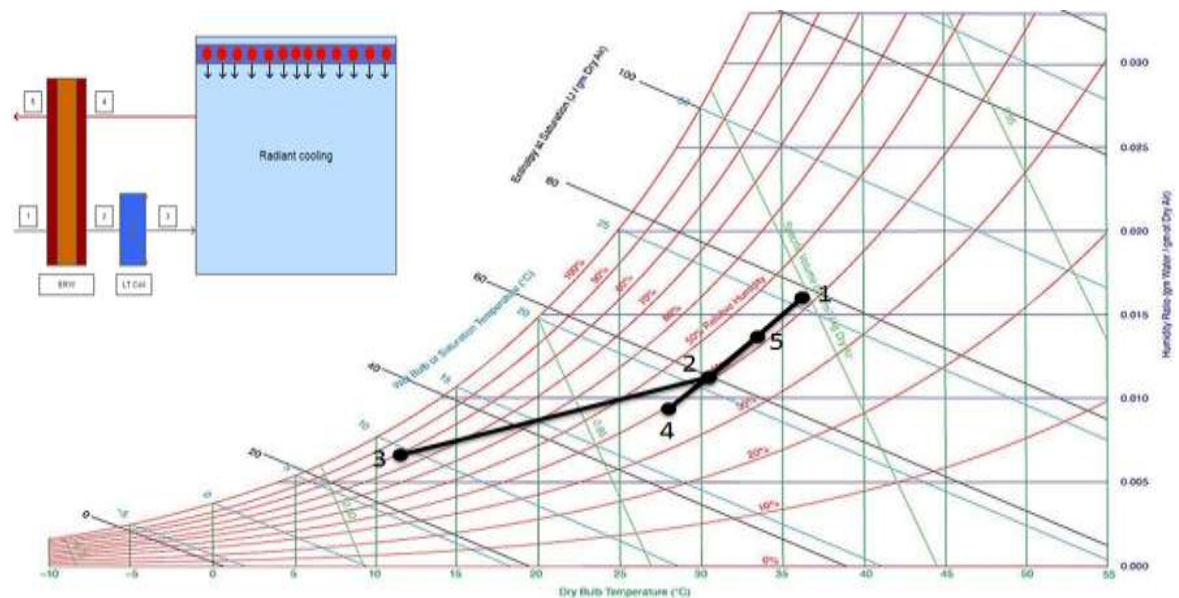
Figure 5-19: Psychrometric process of the Strategy-2

Process (1)-(2): Energy recovery (sensible cooling and dehumidification)

Process (2)-(3): Dehumidification and sensible cooling

Process (4)-(5): sensible heating and humidification

Figure 5-20: Comparison of energy consumption of chiller, fan, wheel, heater & total of the desiccant wheel based Strategy 4, 5 & 6

Table 5-12: Psychrometric values of Strategy-5

State point		1	2	3	4	5	6	7	8
	T (°C)	36.1	61	38.3	19.7	27.2	49.8	68	45.2
Strategy 5	w (g/kg)	16.6	7.96	7.9	7.7	9.1	9.8	9.8	18.1

Figure 5-21: Psychrometric process of the Strategy-5

Process (1)-(2): Dehumidification and sensible heating

Process (2)-(3): Sensible cooling

Process (3)-(4): Sensible cooling

Process (5)-(6): Sensible heating

Process (6)-(7): Sensible heating

Process (7)-(8): Humidification

Figure 5-20 shows the comparison of energy consumption of chiller, fan, wheel, heater & total of the desiccant wheel based strategy. The chiller energy consumption is 11 kWh, 10 kWh, and 10.7kWh in Strategy-4, Strategy-5 and Strategy-6 respectively. In the return side of DOAS in order to achieve continuous dehumidification desiccant wheel has to be regenerated. To supply air continuously at 7.5-8 g/kg, regeneration is being done i.e. in return side air is being heated using resistive heaters. In Strategy 4 and 6 return air has

to be heated from 27°C to 68°C, around 31kW heater banks were energized for the same purpose while in Strategy 5 air is first heated by the sensible wheel and temperature at supply of heater was reached to 42.5 °C and load of the heater was reduced and only 22.5 kW of heater capacity were energized. The heater consumes the electrical energy of 62 kWh, 45 kWh and 62 kWh in Strategy-4, Strategy-5 and Strategy-6 respectively. Strategy-4 and Strategy-6 consume around same energy while Strategy-5 consumes lower energy due energy recovery load on heater reduces. Strategy-5 saves around 22% energy and Strategy-6 consumes around same energy compared to Strategy-4. Strategy-5 is found to be most suitable in composite climate.

Table 5-12 shows the psychrometric values at entry and exit of each components of the Strategy-5. Range of measured values (minimum, maximum, mean) and graphical plots of the measured data are provided in **Appendix III**. Figure 5-21 shows the process of Strategy-5 on psychrometric chart. In process (1)-(2) air passes through the desiccant wheel, air gets dehumidified and sensible heat from 36.1 °C and 16.6 g/kg to 61 °C and 8 g/kg. In process (2)-(3) air passes through the sensible wheel to exchange heat with return air i.e. process (5)-(6), in this process air gets sensible cooling. In process (3)-(4) air passes through the high-temperature cooling coil (HT) for sensible cooling and then enters the zone 19.7 °C and 7.7 g/kg. In process (6)-(7) air passes through the active heater to heat the air to achieve regeneration of the desiccant wheel in the process (7)-(8). In Strategy-4 the desiccant wheel is responsible for dehumidification and HT coil is responsible for sensible cooling, the total sensible load is met by the chiller hence having higher energy consumption compared to Strategy-5. In Strategy-5, SW has reduced the load from the coil and provided savings in chiller energy consumption. In Strategy-6 the ambient condition of Chennai is having high specific humidity and WBT hence IDEC has not performed well hence again chiller energy consumption has increased compared to Strategy-5. Strategy-5 is found to be most suitable for hot and dry climatic conditions.

5.6.3 Composite climate

Jaipur city has been considered for the temperate climate. Figure 5-22 shows the comparison of energy consumption chiller, wheel, fan & total of the cooling coil based strategy In Strategy-1 the total load is catered by cooling coil, the energy consumption of the chiller in Strategy-1 is 11.2 kWh. Addition of energy recovery wheel and the sensible wheel has reduced the load on the coil in Strategy-2 and Strategy-3, therefore, energy consumption of chiller has been reduced in Strategy-2 and Strategy-3 to 9.3 kWh and 8.8

kWh respectively. Wheel and fan energy have been increased in Strategy-2 and Strategy-3 due to the addition of sensible wheel in the air path. Table 5-13 shows the psychrometric values at entry and exit of each components of Strategy-2. Range of measured values (minimum, maximum, mean) and graphical plots of the measured data are provided in Appendix III.
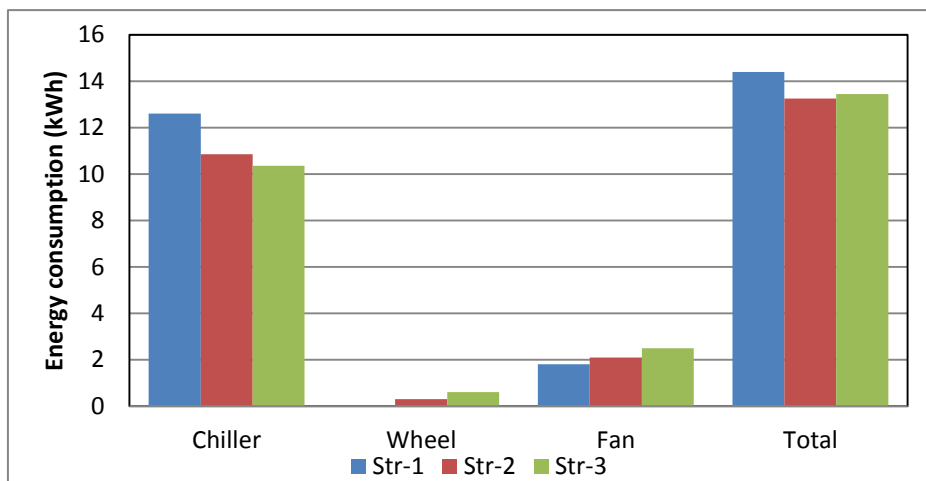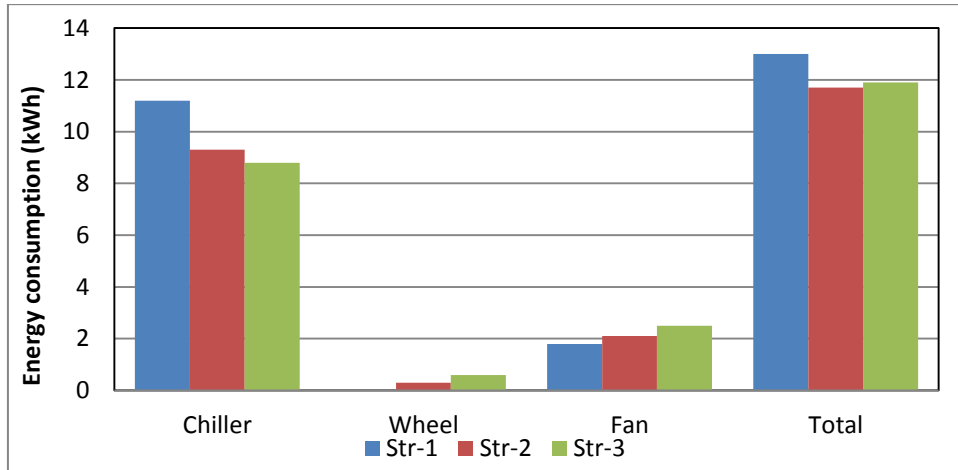

Figure 5-22: Comparison of energy consumption chiller, wheel, fan & total of the cooling coil based Strategy 1, 2 &3.
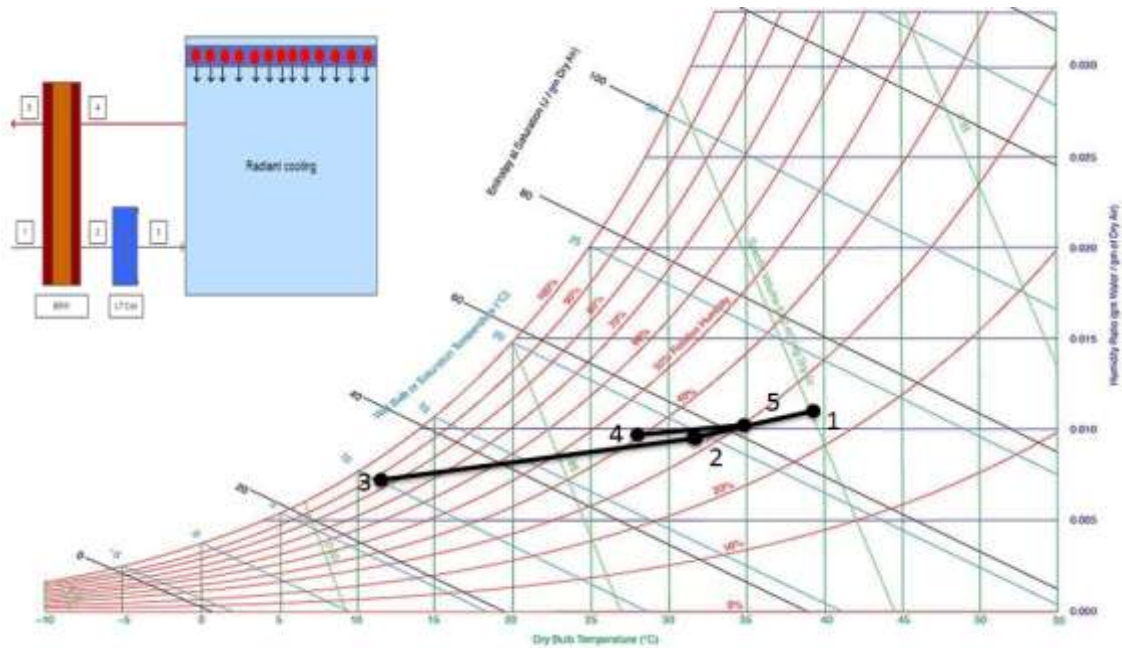
Figure 5-23: Psychrometric process of the Strategy-5

Process (1)-(2): Energy recovery (sensible cooling and dehumidification)

Process (2)-(3): Dehumidification and sensible cooling

Process (4)-(5): sensible heating and humidification

Table 5-13: Psychrometric values of Strategy-2

State point		1	2	3	4	5
Strategy 2	**T (°C)**	39.4	32.6	12.8	27.2	35.3
	w (g/kg)	10.2	10.4	7.2	9.5	10.3

Figure 5-24: Comparison of energy consumption of chiller, fan, wheel, heater & total of the desiccant wheel based Strategy 4, 5 & 6

Table 5-14: Psychrometric values of Strategy-5

State point		1	2	3	4	5	6	7	8
Strategy 5	**T (°C)**	39.8	44	32.4	18.2	27.2	39.2	44.4	41.2
	W (g/kg)	10.1	7.3	7.2	7.2	8.9	9	9	9.9
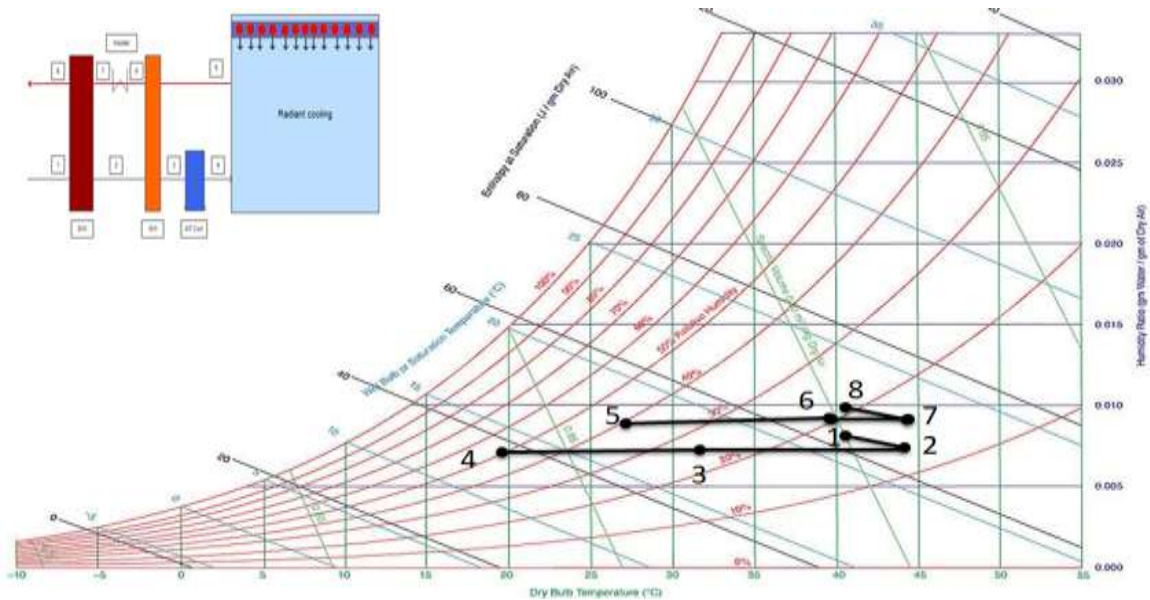
Figure 5-25: Psychrometric process of the Strategy-5

Process (1)-(2): Dehumidification and sensible heating

Process (2)-(3): Sensible cooling

110

Process (3)-(4): Sensible cooling

Process (5)-(6): Sensible heating

Process (6)-(7): Sensible heating

Process (7)-(8): Humidification

Figure 5-23 shows the process of Strategy-2 on psychrometric chart. In process (1)-(2) air passes through the ERW, drops the temperature from 39.4 to 32.6 °C and specific humidity from 11.2 to 10.4 g/kg while exchanging heat from return air i.e. process (4)-(5), addition of ERW reduces load from the cooling coil. In the process (2)-(3) the air is further cooled and dehumidified to 12.8 °C and 7.2 g/kg while passing through the cooling coil and then enter the zone. In Strategy-1 the total load is on the cooling coil hence chiller energy is much higher and in Strategy-3 addition of sensible wheel does not impacted much on savings. Strategy-2 is found to be most suitable for Composite climate.
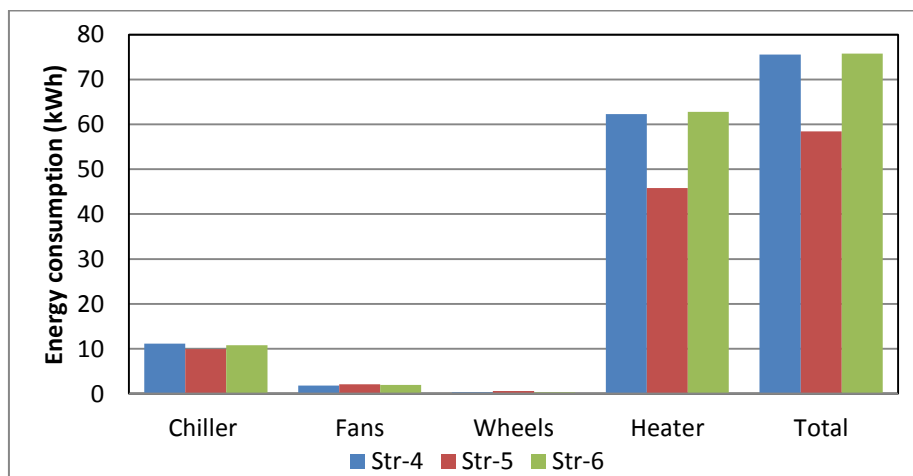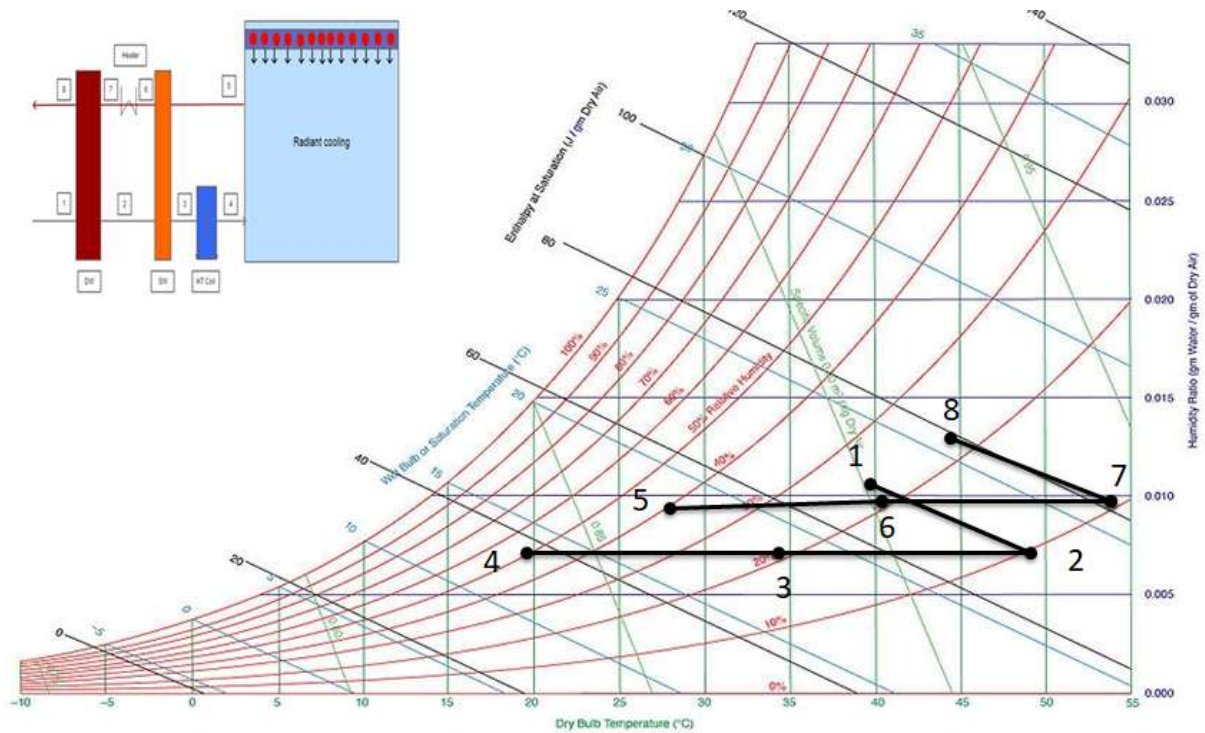
Figure 5-24 shows the comparison of energy consumption of chiller, fan, wheel, heater & total of the desiccant wheel based strategy. Strategy-5 has achieved 27% energy savings compared to Strategy-4, Strategy-5 is most suitable in Composite climate. The chiller energy consumption is 8kWh, 6.3 kWh, and 7.5kWh in Strategy-4, Strategy-5 and Strategy-6 respectively. In the return side of DOAS in order to achieve continuous dehumidification desiccant wheel has to be regenerated. To supply air continuously at 7.5-8 g/kg, regeneration is being done i.e. in return side air is being heated using resistive heaters. In Strategy 4 and 6 return air has to be heated from 27°C to 44.5°C, around 19 kW heater banks were energized for the same purpose while in Strategy 5 air is first heated by the sensible wheel and temperature at supply of heater was reached to 39 °C and load of the heater was reduced and only 13 kW of heater capacity were energized. The heater consumes the electrical energy of 49 kWh, 34 kWh and 48.5 kWh in Strategy-4, Strategy-5 and Strategy-6 respectively. Strategy-4 and Strategy-6 consume around same energy while Strategy-5 consumes lower energy due energy recovery load on heater reduces. Strategy-5 saves around 29% energy and Strategy-6 save around 3% energy compared to Strategy-4. Strategy-5 is found to be most suitable in composite climate.

Table 5-14 shows the psychrometric values at entry and exit of each components of Strategy-5. Figure 5-25 shows the process of Strategy-5 on psychrometric chart. In process (1)-(2) air passes through the desiccant wheel, air gets dehumidified and sensible

heat from 40.1 °C and 10.1 g/kg to 44 °C and 7.3 g/kg. In process (2)-(3) air passes through the sensible wheel to exchange heat with return air i.e. process (5)-(6), in this process air gets sensible cooling. In process (3)-(4) air passes through the high-temperature cooling coil (HT) for sensible cooling and then enters the zone 18.2 °C and 7.2 g/kg. In process (6)-(7) air passes through the active heater to heat the air to achieve regeneration of the desiccant wheel in the process (7)-(8). In Strategy-4 the desiccant wheel is responsible for dehumidification and HT coil is responsible for sensible cooling, the total sensible load is met by the chiller hence having higher energy consumption compared to Strategy-5. In Strategy-5, SW has reduced the load from the coil and provided savings in chiller energy consumption. In Strategy-6 the ambient condition of Jaipur is having and WBT at 2% design condition hence IDEC has not performed well hence again chiller energy consumption has increased compared to Strategy-5. Strategy-5 is found to be most suitable for hot and dry climatic conditions.

5.6.4   Temperate climate

Bengaluru city is considered for the temperate climate. Figure 5-26 shows the comparison of energy consumption of chiller, wheel, fan & total of the cooling coil based strategy. In Strategy-1 the total load is removed by the cooling coil alone, chiller energy consumption is 7.9 kWh. In Strategy-2 an ERW is placed before cooling coil, ERW exchanges energy with return air hence reduces the load on chiller as a result chiller energy consumption is 7.6 kWh. In Strategy-3 a sensible wheel is added to the Strategy-2 after cooling coil and the chiller energy consumption of 7.4 kWh. In Strategy-2 the ERW motor consumes 0.3 kWh and in Strategy-3 ERW and sensible wheel consumes 0.6kWh. Fan consumes 1.8 kWh, 2.1 kWh, and 2.5 kWh in Strategy-1, Strategy-2 and Strategy-3. Strategy-2 is consuming extra 3% energy compared to Strategy-1 and Strategy-3 is consuming extra 8% energy compared to Strategy-1. Strategy-1 is found to be most suitable in hot and dry climate. Addition of ERW and the sensible wheel is not providing any benefit in a temperate climate.

Table 5-15 shows the psychrometric values at entry and exit of cooling coil of Strategy-1. Range of measured values (minimum, maximum, mean) and graphical plots of the measured data are provided in **Appendix III**. Figure 5-27 shows the process of Strategy-1 on psychrometric chart. In process (1)-(2) air passes through the cooling coil to cool and dehumidify from 32.6 °C and 9.3 g/kg to 13.8 °C and 7.2 g/kg and then enter the zone. In temperate climate the ambient condition is quite moderate round the year and

hence having lower load compared to rest of the climatic zones. In Strategy-1 the total load is on the cooling coil and chiller energy is lower among the three. Addition of ERW and SW in Strategy-2 and Strategy-3 respectively does not impacted much in energy savings, Strategy-1 is found to be most suitable for temperate climate.
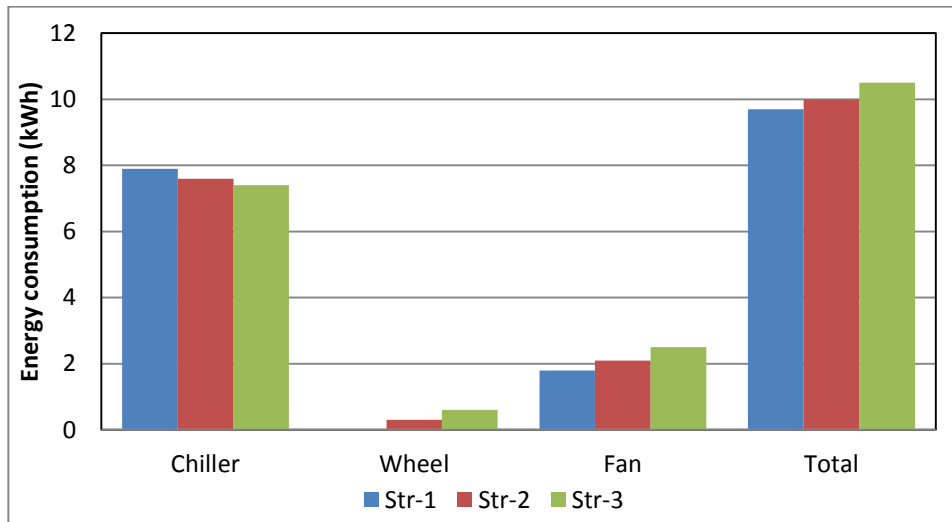
Figure 5-26: Comparison of energy consumption chiller, wheel, fan & total of the cooling coil based Strategy 1, 2 &3.

**Table 5-15: Psychrometric values of Strategy-1**

State point		1	2
Strategy 2	T (ºC)	32.6	13.8
	w (g/kg)	9.3	7.2
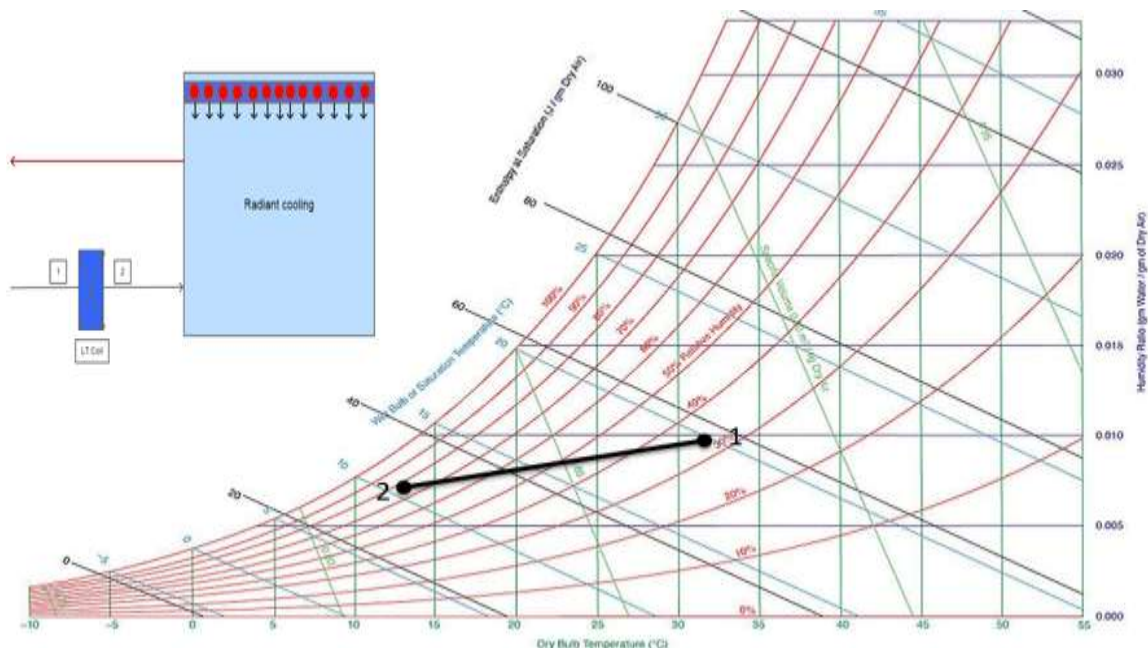
Figure 5-27: Psychrometric process of the Strategy-1
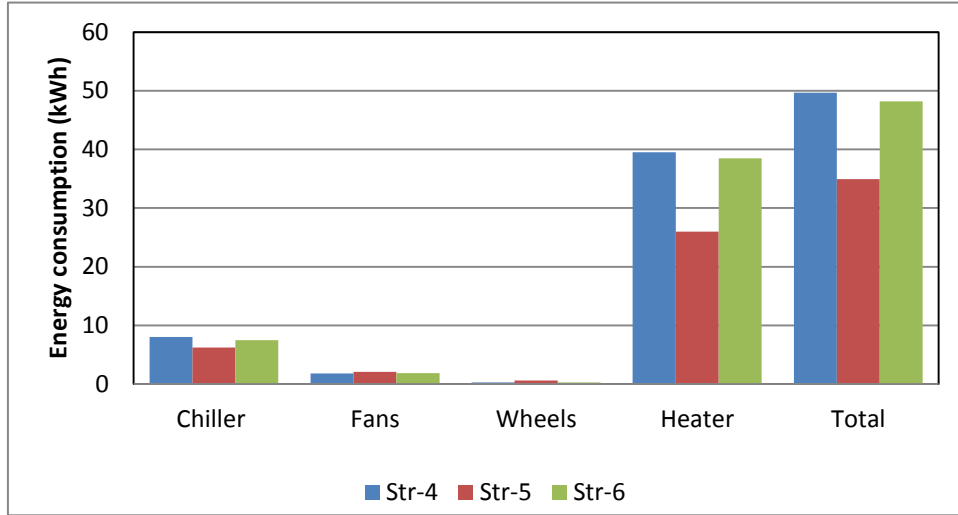
Process (1)-(2): Sensible cooling and dehumidification

Figure 5-28 shows the comparison of energy consumption of chiller, fan, wheel, heater & total of the desiccant wheel based strategy. Strategy-4 consumes around 5.5 kWh in chiller energy consumption. In Strategy-5 the chiller energy consumption is reduced to 5kWh due to the addition of sensible wheel, 4.1 kWh is consumed in Strategy-6 as IDEC performed really well in the temperate climate. Energy consumption associated with wheels are 0.3 kWh, 0.6 kWh and 0.3 kWh in Strategy-4, Strategy-5 and Strategy-6 respectively. The heater has an energy consumption of 26 kWh, 21.8 kWh, and 25.7 kWh in Strategy-4, Strategy-5 and Strategy-6 respectively. Strategy-4 and Strategy-6 have almost same energy consumption whereas in Strategy-5 due to the addition of sensible wheel, air temperature of the return side is increased and load on the heater is reduced. If the desiccant is regenerated with an active heater as done in the experiments then 13% of energy can be saved in Strategy-5 and 5% of energy can be saved in Strategy-6 compared to Strategy-4. While using active heater regeneration Strategy-5 is most efficient but in the same set of strategy if regeneration can be done either using waste heat or solar thermal system than Strategy-6 would be most efficient.
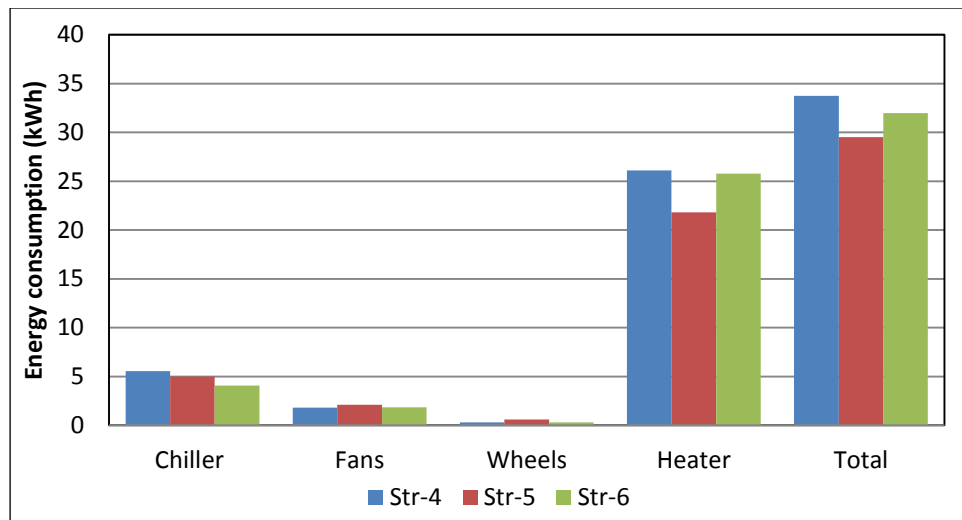
Figure 5-28: Comparison of energy consumption of chiller, fan, wheel, heater & total of the desiccant wheel based Strategy 4, 5 & 6

Table 5-16 shows the psychrometric values at entry and exit of cooling coil of Strategy-6. Fig 5-29 shows the process of Strategy-6 on psychrometric chart. In process (1)-(2) air passes through the desiccant wheel, air gets dehumidified and sensible heat from 40.1 °C and 10.1 g/kg to 44 °C and 7.3 g/kg. In process (5)-(6) air passes through the active heater and desiccant wheel to heat the air for achieve regeneration and avoid attainment of saturation of the wheel. In process (2)-(3) air passes through the IDEC, it has performed well in sensible cooling of air climate and reduced the load on the HT coil.

In process (3)-(4) air passes through the HT coil for sensible cooling of the air and fed into the zone at 17.3 °C and 7.3 g/kg. In case of active heater regeneration Strategy-5 is found to be most suitable as sensible wheel is reducing the load on the heater and heater has the highest magnitude in terms of energy consumption. If regeneration can be done either using waste heat or solar thermal system in that case the energy consumption of heater will be replaced with the pumping energy pumping the hot water in hot water coil and in that case Strategy-6 will most efficient.
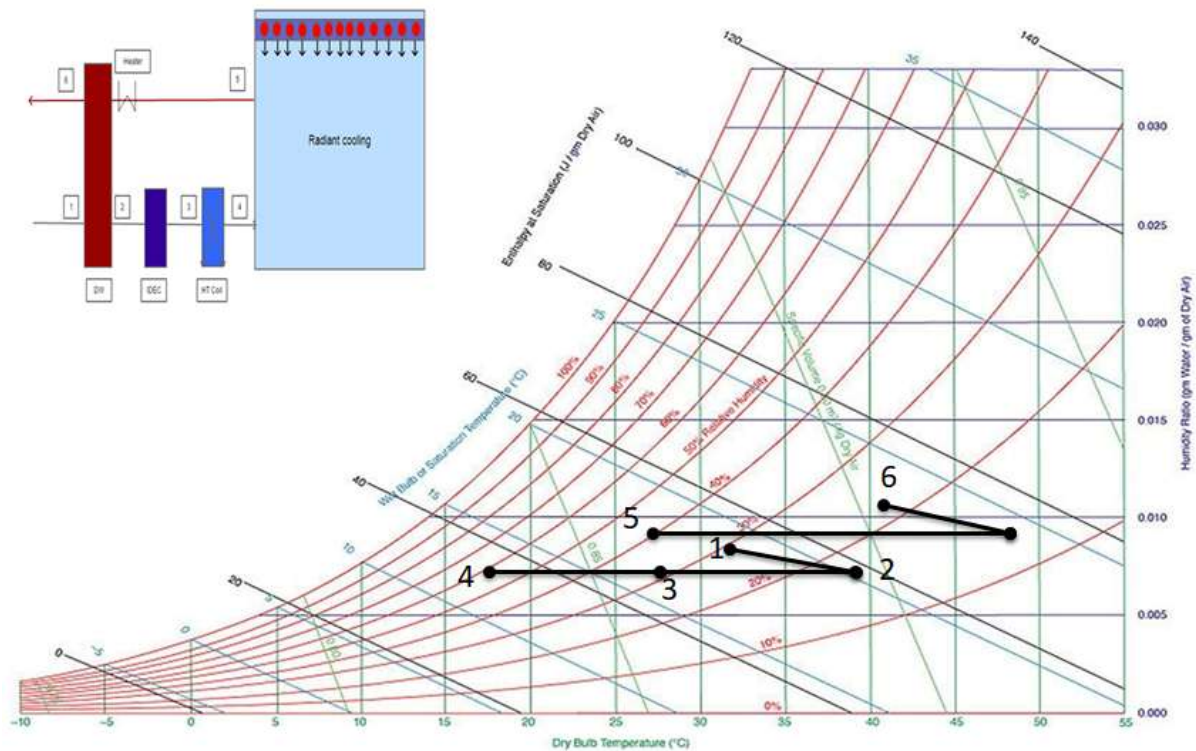
Figure 5-29: Psychrometric process of the Strategy-6

Process (1)-(2): Dehumidification and sensible heating

Process (2)-(3): Sensible cooling

Process (3)-(4): Sensible cooling

Process (5)-(6): Sensible heating

Process (6)-(7): Humidification

Table 5-16: Psychrometric values of Strategy-6

State point		1	2	3	4	5	6
Strategy 6	T (°C)	32.2	39.8	28	17.3	27.1	41.1
	w (g/kg)	8.58	7.4	7.4	7.3	9.1	10.9

Table 5-17: Pressure drop against the different components.

S.No.	Air Flow (cfm)	ERW		Desiccant Wheel		Sensible Wheel		HT coil	LT Coil	IDEC
		Supply	Return	Supply	Return	Supply	Return	Supply	Supply	Supply
3	1000	140	140	150	180	90	90	160	105	250

Pressure drop values against different components of the modular DOAS is tabulated in Table 5-17. The experiments were conducted at a volumetric flow rate of 1000 cfm and the value of pressure drop is obtained at a volumetric flow rate of 1000 cfm. The energy recovery wheel has a pressure drop of 140 Pa in both the sides, the desiccant wheel has a pressure drop of 150 Pa in supply side and 180 Pa in return side. Due to the higher temperature of return air density of air increases and pressure drop is also increases. The sensible wheel has a pressure drop of 90 Pa in supply and returns side. There is a pressure drop of 160 Pa, 105 Pa and 250 Pa against HT coil, LT coil and IDEC. Details of measured values of all the sensors and plots showing steady state condition maintained during experiments in different climatic conditions and plots of measured data for different climatic conditions are provided in Appendix III.

5.7 Chapter summary

This chapter discussed the development of testing facility of the modular dedicated outdoor air system. The chapter has explained the integration of the psychrometric chamber with the modular dedicated outdoor air system. Based on the design of experiments, experiments were conducted for cooling coil and desiccant wheel

Table 5-18: Recommended Strategy for different climatic conditions

Climate	Cooling coil Strategies	Desiccant wheel Strategies
Hot and Dry	Strategy 2	Strategy 5
Warm and Humid	Strategy 2	Strategy 5
Composite	Strategy 2	Strategy 5
Temperate	Strategy 1	Active heater: Strategy 5
		Waste heat/Solar thermal/HTTP: Strategy 6

based strategies. In Hot and dry climate addition of ERW in Strategy-2 was found to save more energy compared to addition of extra sensible wheel in Strategy-3. Warm and humid and composite climate has followed the similar pattern in case of cooling coil based strategy and Strategy-2 is most suitable. In Strategy-1 addition of ERW in Strategy-

2 and addition of another sensible wheel in Strategy-3 has not provided any benefits in terms of energy savings and Strategy-1 is most suitable for temperate climate for cooling coil based strategies. In case of the desiccant wheel based strategy, for hot and dry addition of ERW has provided simultaneously energy savings in chiller as well as regeneration and is comparatively higher to the addition of IDEC provided savings in chiller in Strategy-6 Strategy-5 is most suitable. In warm and humid and composite climate similar trend of energy savings has been found and Strategy-5 is found to be most suitable. For temperate climate Strategy-5 is most suitable with an active heater for regeneration. Strategy-6 will be most suitable for temperate climate if waste heat or solar thermal system will be used for regeneration of desiccant wheel. If designer is planning to design RCS, they can select the recommended strategy from the Table 5-18; these results are based on the experimental analysis of decoupling strategies. The table has two parts first is cooling coil based strategies and the second is desiccant based strategies. Firstly designer has to finalize which type of strategy they want to use in designing RCS and accordingly they can select recommended strategy.

CHAPTER 6.   Analysis for Radiant Cooling System integrated with DOAS

Analysis of radiant cooling system coupled with the recommended cooling coil based decoupling strategy is done by experimental and simulation analysis. Based on the results of chapter 4, we integrated the decoupling strategy with the RCS into real-time building at MNIT Jaipur to identify the potential of real-time performance. Jaipur is the state capital of the largest state of India. It is situated in the western part of the country and Jaipur is located in the eastern side of Rajasthan. Table 6-1 shows the geographic location of Jaipur. Jaipur falls under composite climate, Strategy-2 i.e. energy recovery with a low-temperature cooling coil (case two) decoupling strategy was the most energy efficient for the composite climate, Strategy-2 was installed along with RCS. Appropriate instrumentation was installed in the setup for logging the data for analysis.

Table 6-1: Geographic details of Jaipur

S.No.	Parameters	Data
1	Latitude	75.80° E
2	Longitude	75.80° E
3	Altitude	431 m
4	Annual maximum air temperature	43.6 °C
5	Annual minimum air temperature	5.5 °C

6.1   Building description

A two-story administrative building was considered for the study as shown in Figure 6-1. The first floor of the building is integrated with a conventional all-air HVAC system. The building is having floor to ceiling height of 3.5m and total floor area of 1500 m^2. The panel based radiant cooling system is installed in the low energy cooling lab, floor plan of the second floor shown in Figure 6-2. Experiments were conducted in an experimental room of 67.8 m^2 (730 ft^2) area. The building's roof is directly exposed to the

sun such that maximum heat gain is from the windows and exposed wall and roof. The HVAC plant of the system is installed on the roof of the building.

Figure 6-1: Actual Building
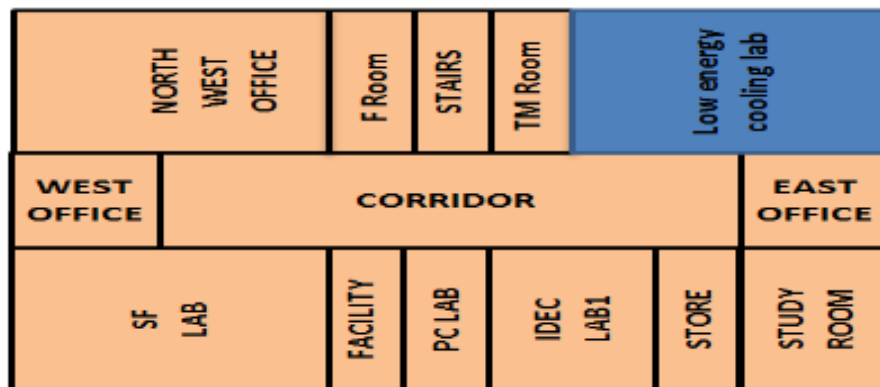
Figure 6-2: Floor plan of second floor of the building

6.2 HVAC system details

Experiments were conducted for two configurations of RCS i.e. chiller based RCS (base case) and cooling tower based RCS. Both of the experiments were conducted in the experimental setup as shown in Figure 6-3. Details of the configurations are discussed below. This system consists of chilled ceiling based RCS coupled with a parallel chiller and a cooling tower to feed chilled water in the RCS. The system also contains a dedicated outdoor air system for supplying ventilation air and to meet the latent load. The dedicated outdoor air system has a cooling coil for dehumidification of air and an energy recovery wheel to exchange energy between outside air and return air. RCS and DOAS are coupled with two different chillers operating at different temperatures. Radiant chiller or a cooling tower supplies cool water in the radiant panels and DOAS chiller is supplying chilled water to cooling coil at a temperature 7-10°C.
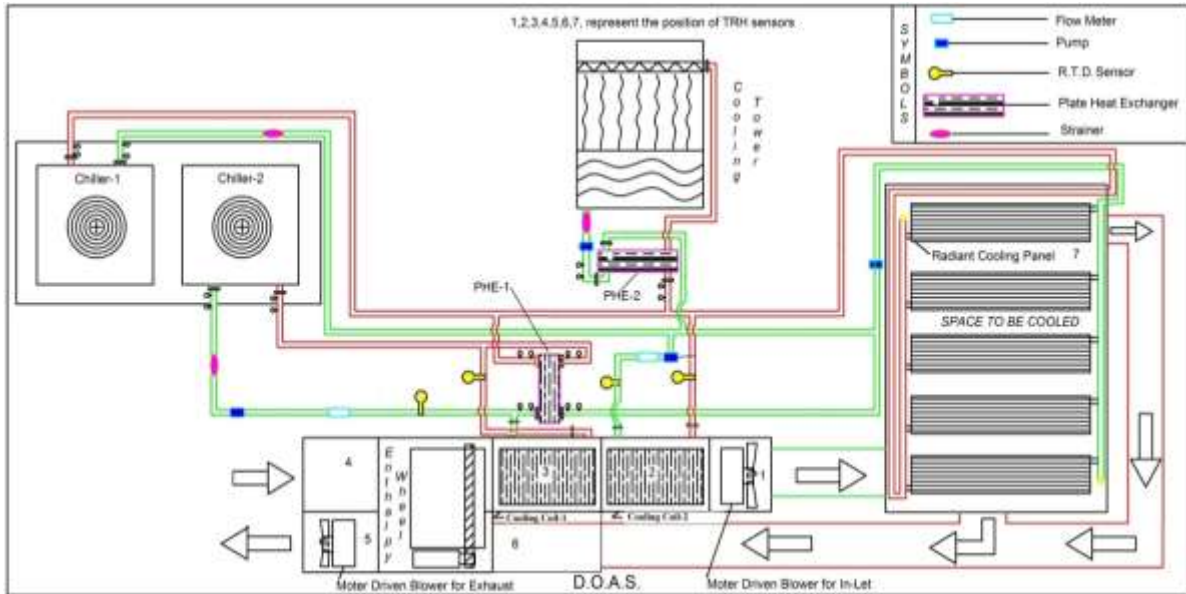
Figure 6-3: Schematic of radiant cooling system

Figure 6-4: (a) Radiant cooling system; (b) Chilled water plant

To avoid the uncertainty in calibration and condensation in the panels due to infiltration of air due to human interaction while conducting experiments, loads are emulated while conducting the experiments. For emulating the human loads sensible and latent loads are provided by using an electric bulb and humidifiers of the same capacity. The installed RCS is shown in Figure 6-4(a); the installed HVAC system is shown in Figure 6-4(b). Black cylinders (Figure 6-4a) were placed to provide the internal load with increased surface area and minimizing radiative heat exchange of the heat source with the panels in the experimental room. Experiments were conducted in a room of 67.8 m^2 (730 ft^2) area fig. 6-3, shows the placement/positioning of different sensors and instrument in the HVAC system.

6.2.1 Radiant cooling system coupled with chiller and DOAS (Base case)

A conventional radiant system was used for the base case: an RCS coupled with a chiller as shown in Figure 6-3 (RADIANT CHILLER as in Figure 6-5) i.e. to feed chilled water to the system, supply chilled water at 16°C. Two different chillers are being used to supply chilled water in radiant panels at 16°C and cooling coil of DOAS at 7°C. In this case, chilled water was produced in a radiant chiller and supplied to the radiant panels to cater to the sensible load, whereas DOAS was used to cater to the latent load in the zone. A conventional chiller as shown in Figure 6-3 (CONV CHILLER as in Figure 6-5) was used to feed chilled water to a cooling coil for dehumidification of air in the DOAS, supply chilled water at 7°C. In the DOAS, supply air first enters the energy recovery wheel, where it exchanges heat with return air and then enters the cooling coil. Case 1 is considered as the base case for the study. Figure 6-5 is a schematic diagram of the base case.
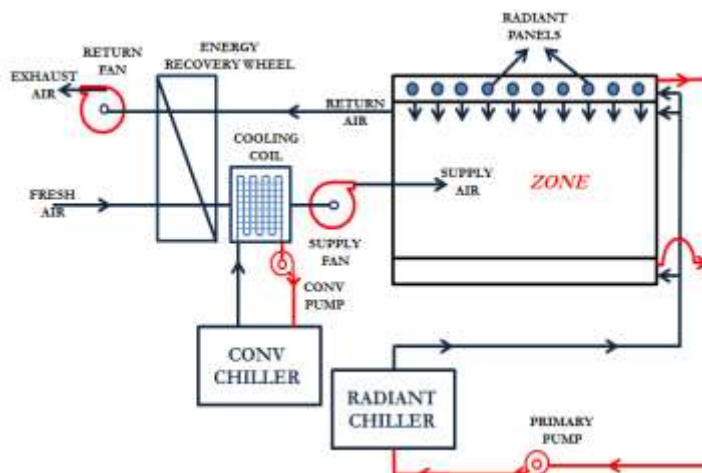
Figure 6-5: Radiant cooling system operated with chiller

6.2.2 Radiant cooling system coupled with cooling tower and DOAS (Advance case)

In this case, the chilled water in the RCS is supplied from a cooling tower instead of the chiller in the base case to cater to the sensible load, and chilled water in the cooling coil of the DOAS is supplied from a chiller 2 as shown in Figure 6-3 (CONV CHILLER, Figure 6-6) to cater to the latent load. Demineralized water is used in the radiant loop, and normal tap water is used in the cooling water loop. To protect the RCS from scaling, dirt, and impurities a plate heat exchanger is used in between. Figure 6-6 is a schematic diagram of the RCS operated with a cooling tower.
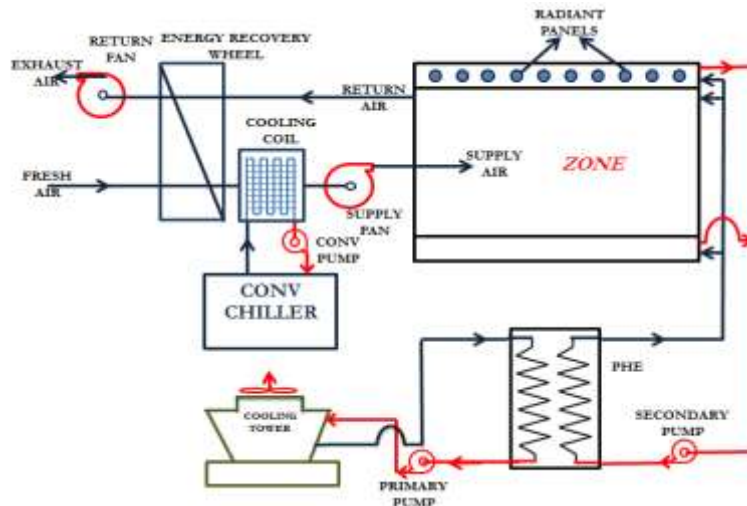
Figure 6-6: Radiant cooling system operated with cooling tower

6.3 Measuring instruments and sensors

Table 6-2 shows the list of instruments and sensors used in the experiment of the radiant cooling system. Resistance Temperature Detectors (RTDs) are placed in the zone for the temperature at different positions (4 near the walls, 4 at the centre at a different height (0.1 m, 0.6 m, 1.1 m, 1.7 m and 2.4 m) and 4 for the panel temperature. Inline RTDs are placed for the temperature of supply and return temperature of the chilled water coming from the chiller and cooling tower. All the RTDs were calibrated prior to the tests as shown in Figure 6-7. Temperature and RH (TRH) sensors are placed in dedicated outdoor air system 1, 2, 3, 4, 5 and 6 as shown in Figure 6-3. There are two inline Ultrasonic flow meters are placed in the supply line of chilled water for radiant panels and the cooling coil along with two RTDs for supply and return temperature for the calculation of thermal energy. Testo 480 kit as shown in Figure 6-8(a) was placed (center of the room at 1 m high) in the zone, which contains air velocity sensor, globe sensor for mean radiant temperature (MRT). Figure 6-8(b) shows the Keysight data logger for logging the values of RTD. Figure 6-8(c) shows the Horner data logger Energy meters are used to get energy consumption for each component. All TRH sensors, Energy meters, BTU meters are connected in loop with data logger with RS 485 communication protocol. Figure 6-9 (a) shows Energy meter & Figure 6-9 (b) shows BTU meter display.

Table 6-2: Instruments and sensor

S.No.	Sensor/instrument (Unit)	Position	Accuracy
1	Temperature RTD (°C)	4 (near walls), 4 (centre at a height 0.1 m, 0.6 m, 1.1 m, 1.7 m and 2.4 m) and 4(panel temperature)	±0.2°C

2	Water flow meter (m^3/s)	Chilled water pipe	±1%
3	Energy meter (kW, kWh)		±1%
4	T&RH sensor (°C & %)	6 at supply and return of each component in DOAS	±0.5°C& ±3 %
5	Air velocity sensor (m/s)	1 m height at center of the room	±2 %
6	MRT Globe (°C)	1 m height at center of the room	±0.5°C

Figure 6-7: Calibration of RTD sensors using Fluke thermal calibrator

Figure 6-8: (a) Testo 480; (b) Keysight data logger; and (c) Horner data logger
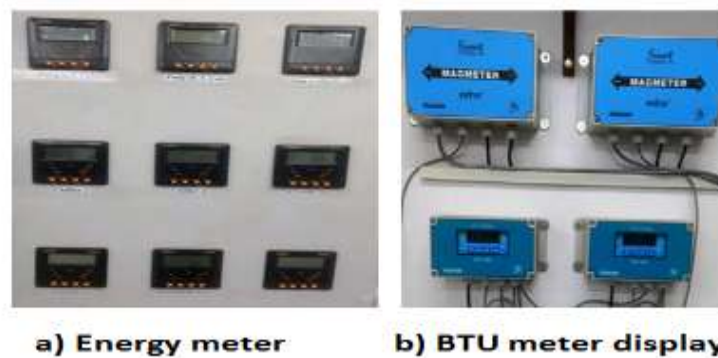
Figure 6-9: (a) Energy meter; (b) BTU meter display

6.4   Experimental results

The radiant cooling system was integrated into the existing building of the institute. In the first phase, experiments were conducted for the Base and Advance case of

panel-based RCS integrated with DOAS. Experiments were conducted in some part of the month of April-June for the system. As per ISHRAE weather data handbook the local summer design conditions for Jaipur are DBT: 40°C, WBT: 21.3°C & RH: 18%, while conducting the Base case experiments the outdoor DBT and RH was in the range of 27°C-42°C and 12-49% respectively and while conducting the Advance case experiments the outdoor DBT and RH was in the range of 24°C-42°C and 04-48% respectively. Experiments were conducted from 9 am to 5 pm in the weekdays. While running the Base case of RCS the chiller supply water temperature is 16°C has a differential setting of 3°C that's the reason of the varying chiller temperature from 16-19°C. The supply chilled water in the cooling coil is 7°C. Chilled water at 16°C for radiant cooling system and 7°C for cooling coil of DOAS are being fed by two different chillers as shown in Figure 6-4 (b) and For Advance case cooling tower is feeding the cool water in RCS and conv chiller is feeding the DOAS. For the RCS we logged the data for all the sensors and instrumentation, further, the data was cleaned as per requirement of analysis. We calculated the thermal energy supplied in the system, indoor and outdoor temperature, RH, operative temperature and we also analysed the stratification inside the space. Thermal comfort surveys were conducted while conducting both the experiments. Figure 6-10 shows the variation of outdoor dry bulb temperature, outdoor relative humidity and the room operative temperature for the Base case. The operative temperature in the space varies from 26-29°C. Figure 6-11 shows the variation of outdoor dry bulb temperature, outdoor relative humidity and the room operative temperature for the Advance case. In Advance case, the operative temperature in the space varies from 26-29°C. While conducting the experiments thermal comfort survey was conducted. Based on the survey data, predicted mean vote (PMV) and predicted person dissatisfied (PDD) were calculated as shown in Table 6-3.
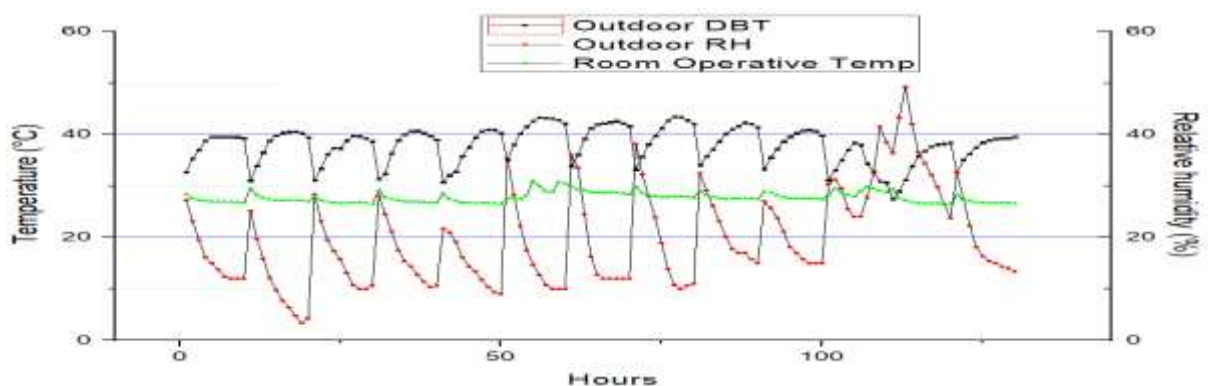
Figure 6-10: Outdoor dry bulb temperature, outdoor RH and room operative temperature for the Base case

The RCS was integrated into the existing building. While conducting an initial set of experiments condensation was observed. We found out ambient air was infiltrating inside the space due to improper fit of the windows, we replaced all the window fittings which were unable to close properly. After improving the airtightness of the zone, the problem of condensation was eliminated to a greater extent.
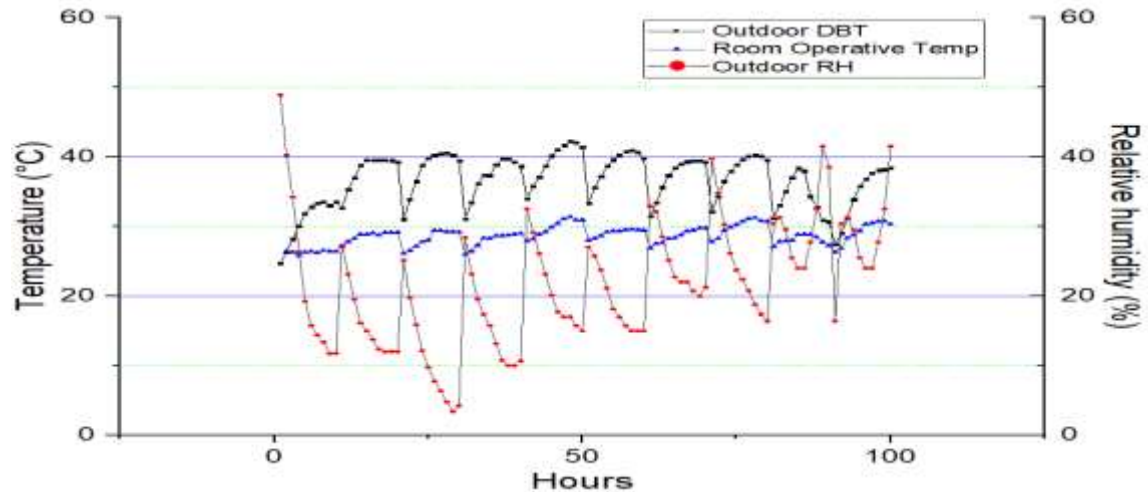
Figure 6-11: Outdoor dry bulb temperature, outdoor RH and room operative temperature for the Advance case

Table 6-3: Range of PMV and PDD in experiments of Base and Advance case

Case	PMV	PDD
Base	-0.45-0.5	5-10
Advance	0.45-1.62	5-56

6.5   Heat transfer model for radiant cooling system

Heat transfer in RCS is quite different compared to conventional air system. In RCS more than 50% of heat transfer takes place through radiative heat exchange. Thermal radiation is transmitted at the speed of light and travels in straight path, it can be reflected, elevate the temperature of solid objects by absorption. Radiation heat transfer exchange heat continuously between all bodies in a building environment. The rate at which thermal radiation occurs depends on the following factors:

- Temperature of the emitting surface and receiver
- Emittance of the radiating surface
- Reflectance, absorptance, and transmittance of the receiver
- View factor between the emitting and receiver surfaces

According to ASHRAE research project (RP-876), concluded that surface roughness and texture have insignificant effects on thermal convection and thermal radiation, respectively. Surface emittance for typical indoor surfaces, such as carpets,

vinyl texture paint, and plastic, remained between 0.9 and 1.0 for panel surface temperatures of 30 to 55°C.

In general, rough surfaces have low reflectance and high emittance or absorptance characteristics. Similarly, smooth or polished metal surfaces have high reflectance and low absorptance or emittance.

Heat transfer by panel surfaces

Sensible cooling or heating is done by the radiant surface or temperature-controlled surface (Active Surfaces) to or from an indoor space and its enclosure surfaces by thermal radiation and natural convection.

Heat Transfer by Thermal Radiation

The basic equation for a multi-surface enclosure with gray, diffuse isothermal surfaces is derived by radiosity formulation as given in equation 6.1

$$q_r = J_p - \sum_{j=1}^{n} F_{pj} J_j \qquad\qquad 6.1$$

q_r = net heat flux because of thermal radiation on the active (cooled) panel surface, W/m^2

J_p = total radiosity leaving or reaching panel surface, W/m^2

J_j = radiosity from or to another surface in room, W/m^2

F_{pj} = radiation view factor between panel surface and another surface in room

n = number of surfaces in room other than panel

equation 6.1 can be applied to simple and complex enclosures with varying surface temperatures and emittance. The net heat flux by thermal radiation at the panel surfaces can be determined by solving the unknown J_j

Several methods have been developed to simplify above equation by reducing a multi-surface enclosure to a two-surface approximation. In the MRT method, the thermal radiation interchange in an indoor space and it is modeled by assuming that the surfaces radiate to a fictitious, finite surface that has an emittance and surface temperature that gives about the same heat flux as the real multi-surface case. In addition, angle factors do not need to be determined in evaluating a two-surface enclosure. The MRT equation may be written as equation 6.2

$$q_r = \sigma F_r \left[T_p^4 - T_r^4 \right] \qquad\qquad 6.2$$

σ= Stefan-Boltzmann constant = 5.67×10^{-8} W/(m$^2 \cdot$K^4)

F_r = radiation exchange factor

T_p = effective temperature of cooling panel surface, K

T_r = temperature of fictitious surface K

The temperature of the uncooled surface is given by an area emittance weighted average of all surfaces other than the panel(s) as given in equation 6.3

$$T_r = \frac{\sum_{j=p}^{n} A_j \varepsilon_j T_j}{\sum_{j=p}^{n} A_j \varepsilon_j}$$

6.3

A_j = area of surfaces other than panels, m^2

ε_j = thermal emittance of surfaces other than panel

When the surface emittance of an enclosure are nearly equal, and surfaces directly exposed to the panel are marginally uncooled, then above equation becomes the area-weighted average uncooled temperature (AUST) of such surfaces exposed to the panels. Therefore, any uncooled surface in the same plane with the panel is not accounted for by AUST. For example, if only part of the floor is heated, the remainder of the floor is not included in the calculation of AUST, unless it is observed by other panels in the ceiling or wall.

The radiation exchange factor for two-surface radiation heat exchange is given by the Hottel equation. Equation 6.4 represents the Hottel equation below.

$$F_r = \frac{1}{\frac{1}{F_{p-r}} + \left(\frac{1}{\varepsilon_p} - 1\right) + \frac{A_p}{A_r}\left(\frac{1}{\varepsilon_r} - 1\right)}$$

6.4

F_{p-r} = Radiation angle factor from panel to fictitious surface (1.0 for flat panel)

A_r = Area of fictitious surface

ε_r = Thermal emittance of fictitious surface

In normal practice, the thermal emittance ε_p of nonmetallic or painted metal nonreflecting surfaces is about 0.9. When this emittance is used in equation 6.4, the radiation exchange factor F_r is about 0.87 for most indoor spaces. By Substituting this

value in equation 6.2, σF_r becomes $4.93\mathrm{x}10^{-8}$. In Literature this constant was $5.03\mathrm{x}10^{-8}$. Then the equation for heat flux from thermal radiation for panel cooling can be written as equation 6.5

$$q_r = 5 \times 10^{-8} \left[(t_p + 273.15)^4 - (AUST + 273.15)^4 \right] \qquad 6.5$$
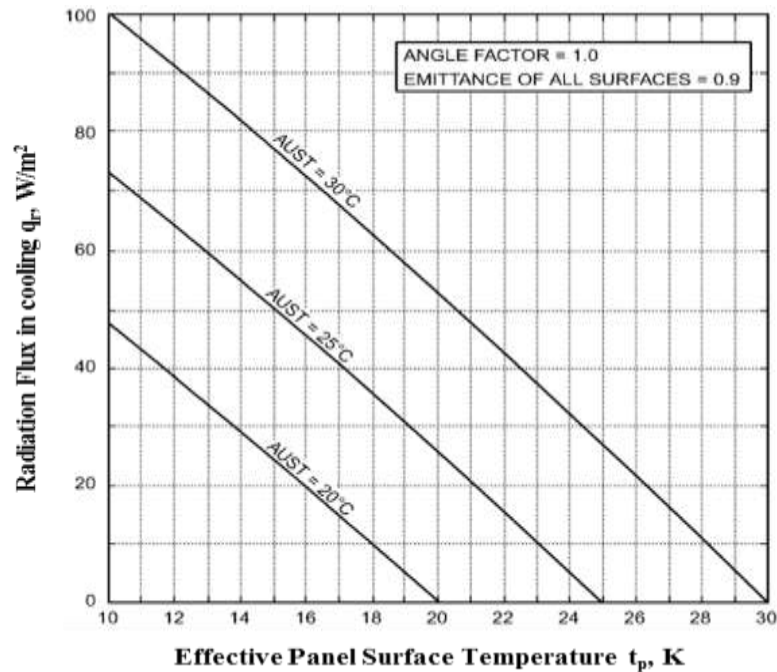
Figure 6-12: Heat removed by radiation at cooled ceiling panel surface [87]

In above equation qr is positive on heating by the panel and negative while cooling by panel surface. Radiation heat removed by a cooling panel for a range of normally encountered temperatures is given in the Figure 6-12.

Heat Transfer by Natural Convection

Heat flux from natural convection q_c occurs between the indoor air and the temperature-controlled panel surface. Thermal convection coefficients are not easily established. In natural convection, cooling the boundary layer of air at the panel surface generates air motion. In practice, however, many factors, such as the indoor space configuration, interfere with or affect natural convection. Infiltration/exfiltration, occupant's movement, and mechanical ventilating systems can introduce some forced convection that disturbs the natural convection.

Natural-convection heat flux in a panel system is a function of the effective panel surface temperature and the temperature of the air layer directly contacting the panel. The most consistent measurements are obtained when the dry-bulb air layer temperature is

measured close to the region where the fully developed boundary layer begins, usually 50 to 65 mm from the panel surfaces. Natural convection heat flux between a cooled ceiling surface and indoor air was calculated from equation 6.6

$$q_c = 2.42 \frac{|t_p - t_a|^{0.31}(t_p - t_a)}{D_e^{0.08}}$$ 6.6

D_e = equivalent diameter of panel ($4 \times$ area/perimeter), m

The effect of room size was usually insignificant except for very large spaces like hangars and warehouses, equation 6.6 can be simplified to the equation 6.7 by putting De = 4.91 m.

$$q_c = 2.13|t_p - t_a|^{0.31}(t_p - t_a)$$ 6.7

Figure 6-13 shows the heat removal by natural convection at cooled ceiling panel surfaces, as calculated by equation 6.7
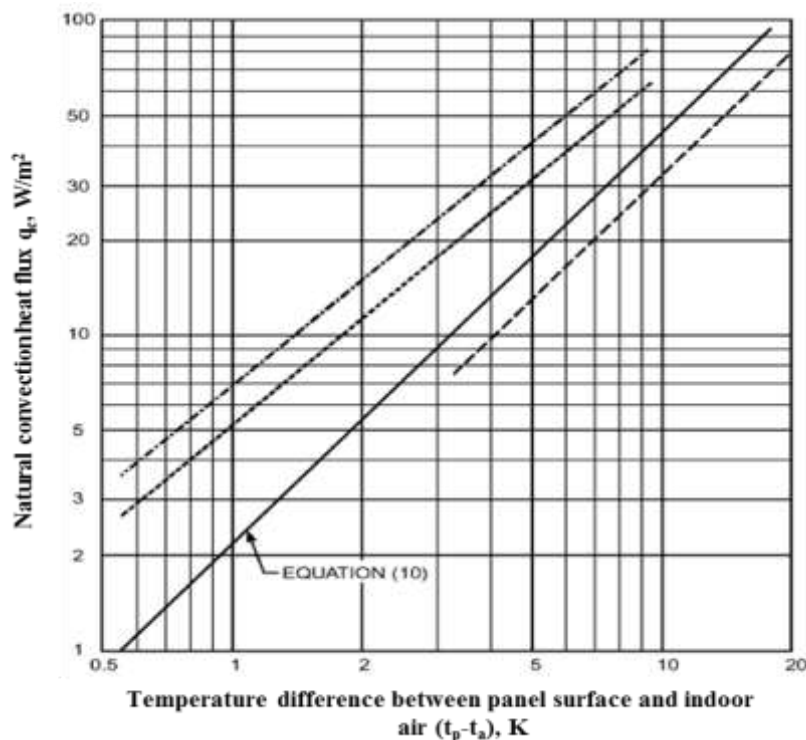
Figure 6-13: Empirical data for heat removal by ceiling cooling panels from natural convection [87]

6.6   Model simulation and calibration

Based on the actual building design and characteristics parameters, a building model is created with EnergyPlus 8.6 as shown in Figure 6-14.

Figure 6-14: (a) Actual view of the modelled building; and (b) Isometric view of building model

This was an existing building of the campus, all the physical dimensions were measured and used in the model. In simulations, a fixed-occupancy pattern of 10 persons are considered and office hours from 9 a.m. to 5 p.m. and no occupancy was considered during weekends. The weather file used for the calibration was prepared by inserting the values of temperature, RH and solar radiation obtained from a weather station in the weather file obtained from "Indian Society of Heating Refrigerating and Air Conditioning (ISHRAE) weather file (2014)". The lighting power density electric power density was assumed to be $5W/m^2$ & 60 W/person respectively. Building details and description is provided in Table 6-4. Table 6-5 shows the HVAC system parameters used in the model. The fan is designed for a constant volume of 0.094 m^3/s of air based on the ventilation air of 0.0094 m^3/s per person. Zone set point temperature is considered as 27°C. With the radiant cooling system, also known as high-temperature cooling system, people feel the same comfort at elevated temperatures as they would feel at the lower temperatures with conventional all air system. To avoid condensation in the zone Cooling Control Throttling Range of 2°C is provided in the EnergyPlus model.

Table 6-4: Building construction and operational parameters

Building parameter	Unit	Value
U-value of structure	W/m^2-K	Exterior wall—1.6 Roof—0.44, Windows—2.7
Solar heat gain coefficient of windows	Fraction	0.76

Visible transmittance of windows	Fraction	0.81
Lighting power density	W/m^2	5
Electric power density	W/person	60
Occupancy	Person	10

Table 6-5: HVAC system configuration parameters

Parameter	Value
HVAC system type	Radiant chilled ceiling system with DOAS
Fan design	Constant volume with 0.0094 m^3/s
Supply air set point temperature	14°C
Chiller parameter	DOAS chiller autosized @ 3 COP and supply chilled water temp @ 7°C. Radiant chiller autosized @ 3.5 COP and supply chilled water temp @ 16°C.
Radiant pipes diameter and spacing	15 mm and 150 mm
Ventilation	0.0094 m^3/s per person
Zone set point temp.	27°C
Water flow rate (Base case)	0.45 m^3/hr
Water flow rate (Advance case)	0.60 m^3/hr
PHE effectiveness	0.90

For model calibration, hourly data from the logged data in experimental setup for both chiller-operated and cooling tower-operated systems are used. This validation of the simulation models is based on the experiments conducted for a set of days in the month of April, May and June 2017 to cover the monthly variation in weather. Experiments of the Base case and Advanced case carried out on the alternate days. For the validation of the model, the data of the thermal energy supplied to the panel and dedicated outdoor air system was used. The US Department of Energy's Federal Energy Management Program (FEMP) measurement and verification guidelines provide some criteria for the calibration in the NMBE (Normalized Mean Bias Error) and (CV-RMSE) (Coefficient of Variation of Root Mean Square Error) indexes [84] are calculated by using equation (1) & (2), where s_i, m_i and $\bar{m}$ shows the simulated, measured and average measured data at instance i with p=1, for n number of hours respectively. The experiments are performed in the single zone on the second floor of the building;

$$CV(RMSE) = 100 \times \frac{\sqrt{(\sum_{i=1}^{n}(m_i - s_i)^2 / (n-p)}}{\bar{m}} \qquad (1)$$

$$NMBE = 100 \times \frac{\sum\limits_{i=1}^{n}(m_i - s_i)}{(n-p) \times \bar{m}} \qquad (2)$$

A model is considered as calibrated when the statistical indices demonstrating calibration have been met. The calibration criterion, in general, apply to facility and component level energy comparison but it may be a good idea to specify spot measurements of key parameters for comparing the simulation and measured data, such as surface temperatures, to ensure that the simulated profiles match with the measured profiles of a particular parameter. Figure 6-15 & Figure 6-16 shows thermal energy and panel temperature between simulation and measured data for Base case. Figure 6-17 & Figure 6-18 shows thermal energy and panel temperature between simulation and the measured data for Advanced case.

To capture the variation of ambient condition, calibration was performed for some days of April, May, & June. Figure 6-13 shows the variation of measured and simulated total thermal energy consumed by RCS and DOAS for the Base case. Minimum value of the thermal energy of the system varies from 4.13-3.5 kW, maximum value of the thermal energy varies from 5.53-5.07kW for measured and simulated results respectively. NMBE and CV-RMSE for the thermal energy for the Base case are 7 and 18 respectively. Figure 6-14 shows the comparison of panel surface temperature for measured and simulated data. The minimum value of the radiant surface temperature varies from 22.3-21.6°C and maximum value of the radiant surface temperature varies from 27.6-26.3°C for the measured and simulated results. NMBE and CV-RMSE for the radiant surface temperature are -4 and 10 respectively.
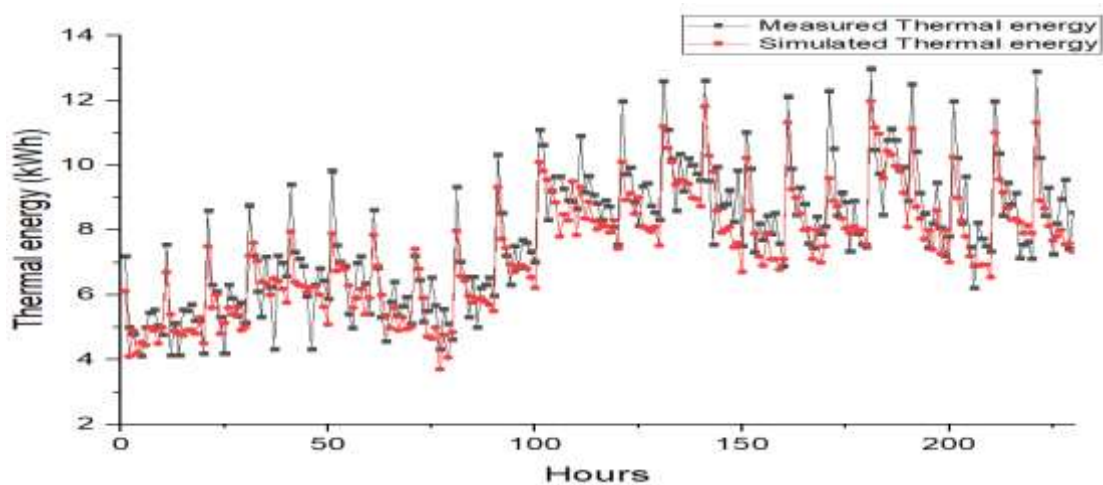
Figure 6-15: Comparison of thermal energy for measured and simulation results for the Base case
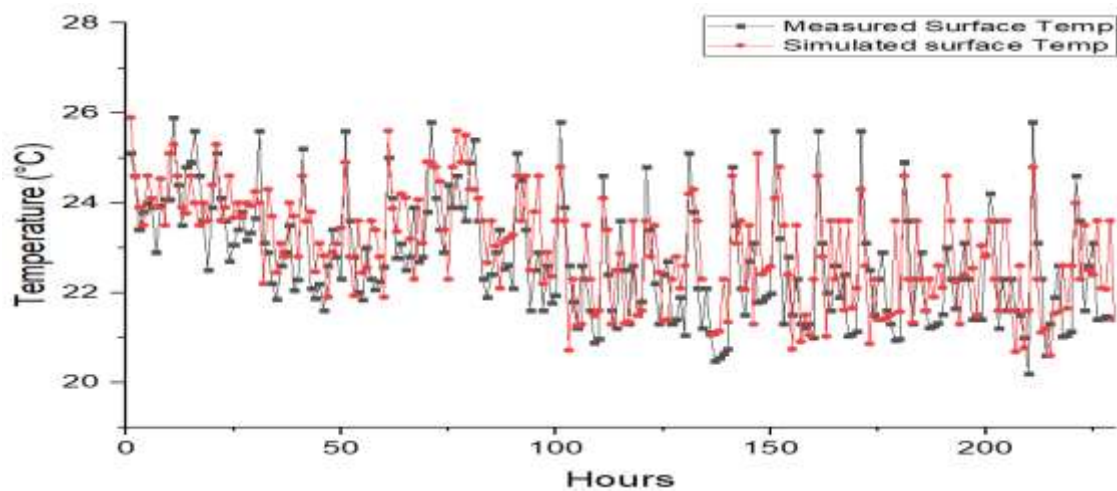
Figure 6-16: Comparison of panel surface temperature for measured and simulation results for the Base case

Figure 6-15 shows the variation of measured and simulated total thermal energy consumed by RCS and DOAS for cooling tower based system. Minimum value of the thermal energy of the system varies from 2.1-2.3kW and maximum value varies from 6.3-5.6.4kW for measured and simulated result respectively. NMBE and CV-RMSE for the thermal energy are -6 and 19 respectively. Figure 6-16 shows the variation of panel surface temperature for measured and simulated data. The minimum radiant surface temperature varies from 24.3-24.8°C and maximum radiant surface temperature varies from 27.1-26.1°C for the measured and simulated results. NMBE and CV-RMSE for the radiant surface temperature are 5 and 12 respectively.
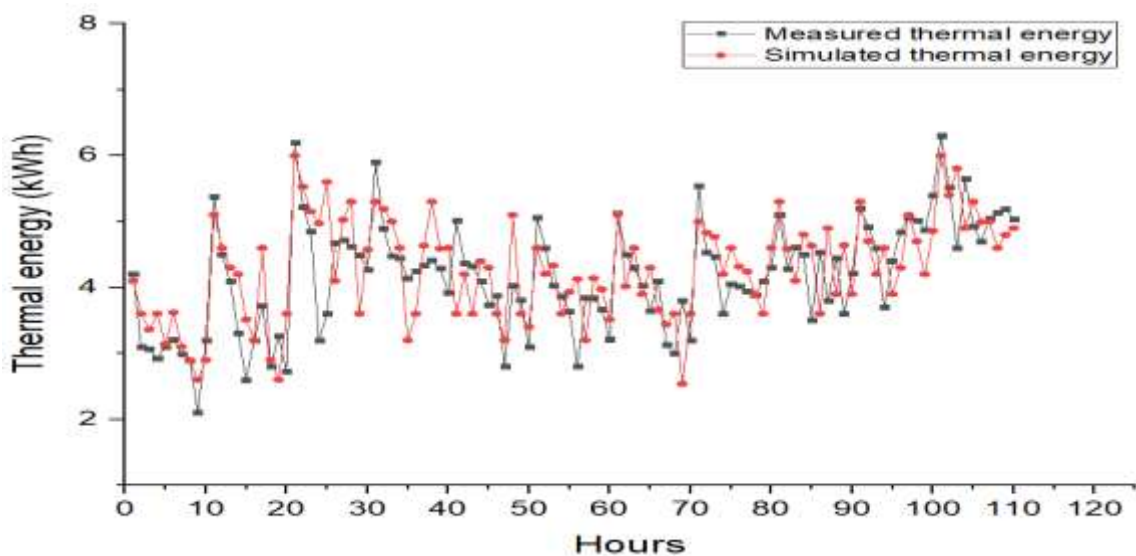
Figure 6-17: Comparison of thermal energy for measured and simulation results for Advanced case
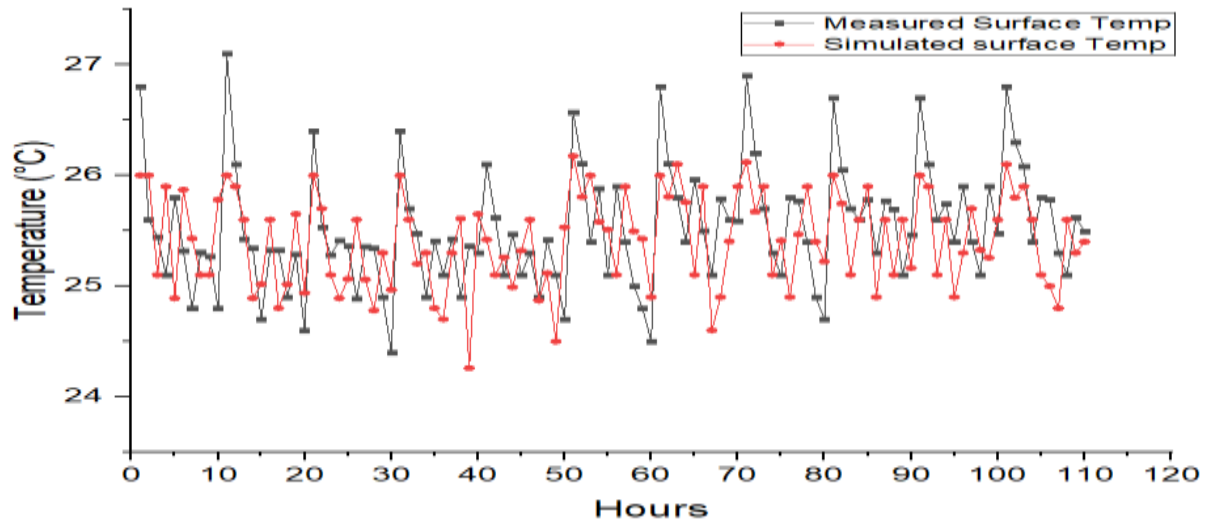
Figure 6-18: Comparison of panel surface temperature for measured and simulation results for advanced case

The normal mean bias error (NMBE) is and the cumulative root mean square error (CV-RMSE) are in good agreement with IPMVP and FEMP guidelines as shown in Table 6-6.

Table 6-6: Calibration criteria

| | Calibration Type | Calibrated parameter | Index | Limit | | Calibrated Model Error (%) |
				IPMVP[8]	FEMP[9]	
Base case	Hourly	Cooling Energy	NMBE	-	10	7
			CV-RMSE	20	30	18
	Hourly	Panel Surface Temperature	NMBE	-	-	-4
			CV-RMSE	-	-	10
Advance case	Hourly	Cooling Energy	NMBE	-	10	-6
			CV-RMSE	20	30	19
	Hourly	Panel Surface Temperature	NMBE	-	-	5
			CV-RMSE	-	-	12

The calibration results were found to be well within the acceptable limits of the NMBE and (CV-RMSE) criteria and thus are satisfactory. These models can confidently be used for further energy performance analysis for different climatic zones.

The simulation analysis was conducted in two phase. In the first phase, chiller and cooling tower based radiant cooling system is compared for the different climatic condition. Chiller is used for producing chilled water for DOAS coil in both base and Advance case. Chiller in the Base case and cooling tower in advance case is used to produce cool water for the radiant cooling system.

In the second phase comparison of different types of radiant cooling system is done. Schematic of the three types of radiant cooling systems is shown in Figure 6-19. The calibrated model of chiller based radiant cooling system (base case) is used to make three models for radiant panel cooling (RCP), embedded surface cooling system (ESCS) and thermal activated cooling system (TABS) by changing the "construction internal source" and construction as provided in Table 6-7.
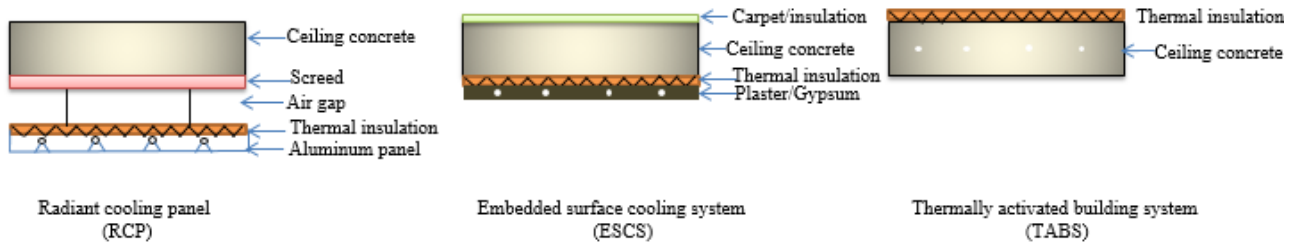
Figure 6-19: Schematic of the three types of radiant cooling systems [28].

Table 6-7: Radiant surface constructions specifications (inside to outside).

	Thickness (m)	Specific heat (J/kg K)	Density (kg/m3)	Conductivity (W/m K)
RCP ceiling Aluminum panel	0.001	910	2800	273.0
Air gap	0.800	790	1920	0.02
Water tube Insulation	0.05	1210	56	0.02
Concrete slab	0.08	1000	1400	1.13
Insulations	0.1118	840	12	0.04
Roof deck	0.019	900	530	0.14
ECS ceiling plaster	0.012	840	1050	0.7
Water tube plaster	0.014	840	1050	0.7
Insulation	0.05	1210	56	0.02
Concrete slab	0.08	1000	1400	1.13
Insulations	0.1118	840	12	0.04
Roof deck	0.019	900	530	0.14
TABS ceiling Concrete	0.04	1000	1400	1.13
Water tube Concrete	0.04	1000	1400	1.13
Insulations	0.1118	840	12	0.04
Roof deck	0.019	900	530	0.14

6.7 Mathematical equations used to calculate cooling capacity of panels

Based on the ASHRAE 138 (ASHRAE 2009) by considering the cooling panel as an individual surface, heat is exchanged convectively with room air and radiantly with other inner surfaces (floor and wall). The total sensible heat gain qtot, W/m^2 ($Btu/h \cdot ft^2$) of the panel is the sum of convective qc, W/m^2 ($Btu/h \cdot ft^2$) and radiation heat fluxes q_r, W/m^2 ($Btu/h \cdot ft^2$) The total heat flux measured through the hydronic circuit is calculated by the equation 6.8. The radiative and convective heat transfer coefficient was calculated from equation 6.9 and 6.10 respectively.

$$q_{tot} = \sum_{j=1}^{m}[\rho V C_p (t_r - t_i)/\sum_{j=1}^{m}[A_p]_j \qquad \text{6.8}$$

$$q_r = 5 \times 10^{-8}[(t_p + 273.15)^4 - (AUST + 273.15)^4] \qquad \text{6.9}$$

$$q_c = 2.13|t_p - t_a|^{0.31}(t_p - t_a) \qquad \text{6.10}$$

The mean water temperature of the hydronic loop was calculated from equation 6.11. Where t_i and t_r are the inlet and return water temperature. The area-weighted average temperature (AUST) and the operative temperature of the room were calculated from equation 6.12 and 6.13 respectively.t_1, t_2, t_3, and t_4 are the interior uncooled surface temperature, t_e is exposed surface temperature, and the t_{ce} is uncooled ceiling temperature.

$$t_m = \frac{(t_i + t_r)}{2} \qquad \text{6.11}$$

$$AUST = \frac{A_1 t_1 + A_2 T_2 + A_3 t_3 + A_4 t_4 + A_e t_e + A_{ce} t_{ce}}{A_1 + A_2 + A_3 + A_4 + A_e + A_{ce}} \qquad \text{6.12}$$

$$t_o = \frac{(t_a + t_{mr})}{2} \qquad \text{6.13}$$

Characteristic performance coefficient (nco'') of the radiant panel can be calculated

from equation 6.14. qad was the adjusted heat flux which was calculated from equation 8, Δt is temperature difference between the panel surface temperature and room air temperature and it was calculated from equation 9. Now in equation 6.14 there are two unknown Cco'' and nco'' which can be determined by the method of least square.

$$q_{ad} = C''_{co} \Delta t^{nco''}$$ 6.14

$$q_{ad} = q_{tot} \beta$$ 6.15

$$\Delta t = \pm(t_p - t_a)$$ 6.16

In equation 6.15, β is adjustment factor for heat flux and can be calculated from equation 6.17. In equation, 6.17 abc represent the adjusting term of convective heat flux component a, b and c take care of size effect, mass density (altitude) and indoor air velocity effect. The value of a, b, c, and α was calculated according to criteria given in ASHRAE 138.

$$\beta = 0.87 \times \frac{\alpha}{F_c} + (1 - \alpha) \times abc$$ 6.17

For solving the equation 6.14 method of least square is adopted. Equation 6.17 can be written as

$$\ln(q_{ad}) = \ln(C''_{co}) + nco.\ln(\Delta t'')$$ 6.18

$$\varepsilon_r^2 \equiv \sum_{i=1}^{z}(y_i - y_{fitted,i})^2$$ 6.19

Equation 6.19 can be minimized by equation 6.20

$$\varepsilon_r^2 \equiv \sum_{i=1}^{z}[y_i - (A + Bx_i)]^2$$ 6.20

Where

$y_i = \ln(q_{ad})_i$

$x_i = \ln(\Delta t'')_i$

$A = \ln(C_{co}'')$

$B = nco''$

Z = number of data point

With the appropriate sums, coefficients A and B in the linear fit can be solved

$$A = [z \sum_{i=1}^{z} y_i - B \sum_{i=1}^{z} x_i]/z \qquad \text{6.21}$$

$$B = [z \sum_{i=1}^{z} x_i y_i - \sum_{i=1}^{z} x_i \sum_{i=1}^{z} y_i]/[z \sum_{i=1}^{z} x_i^2 - (\sum_{i=1}^{z} x_i)^2] \qquad \text{6.22}$$

The value of Characteristic performance coefficient is within the range as given in ASHRAE Standard 138. Table 4 shows the value of characteristic performance exponent (nco'') for different cases.

The convective heat transfer between the radiant surface and the room depends on room air dry bulb temperature, and the radiative heat transfer depends on the AUST of the room. The total heat transfer coefficient between the radiant surface and room depends on operative temperature of room. The convective, radiative and total heat transfer coefficient can be calculated from equation 6.23, 6.24 and 6.25 respectively.

$$h_c = \frac{q_c}{T_a - T_p} \qquad \text{6.23}$$

$$h_r = \frac{q_r}{AUST - T_p} \qquad \text{6.24}$$

$$h_{tot} = \frac{q}{T_{op} - T_p} \qquad \text{6.25}$$

6.8   Result and discussion

In the first phase chiller and cooling tower integrated RCS is compared for the different climatic condition. Initially, statistical analysis for the different climatic condition is performed to identify the potential of cooling tower as discussed below.

6.8.1   Comparison of chiller and cooling tower based radiant cooling system for different climatic condition

The applicability and performance of the proposed radiant cooling system integrated with the cooling tower is a function of the wet bulb temperature and approach of the cooling tower. The performance of the cooling tower is dependent on the ambient condition of the location. It is necessary to know that whether the wet bulb temperature of

various selected cities for the study in India is appropriate for providing the desired temperature of cool water for the radiant cooling system for a substantial period of the year. The weather data of representative cities for different climatic conditions of India has been analyzed for the summer season in which cooling is desired.

- **Statistical analysis of different climatic zones**

Statistical analysis was conducted to see the potential of the integration of cooling tower with RCS to generate cool water. Statistical analysis was conducted based on the hourly data of the ambient dry bulb temperature (DBT), wet bulb temperature (WBT) and approach of the cooling tower. Usable cool water temperature for the radiant cooling system is in the range of 16-24°C. The analysis is done for achieving minimum, maximum and average WBT for day and night time in the summer season. Based on the WBT, using the approach of 2°C for cooling tower availability of cool water from the cooling tower is calculated. Based on the classification of the Energy Conservation Building Code [2], India has been divided into five climatic zones: (a) hot and dry, (b) warm and humid, (c) composite, (d) temperate, and (e) cold. This study is focused on the cooling application for RCS. The study is focused for first four climates and cold climate is avoided for the present study. The representative cities selected are Ahmedabad (hot and dry), Chennai (warm and humid), Jaipur (composite) and Bengaluru (Temperate) for the study. Table 9-8 shows cooling degree day and heating degree day for base 18°C. Chennai has maximum hours of cooling degree days i.e. 3786 hours and Bengaluru has a minimum of 2142 hours out of the four cities.

Table 6-8: Cooling and heating degree days for representing cities

S.No.	City	Climatic condition	$CDD_{18°C}$	$HDD_{18°C}$
1	Ahmedabad	Hot and dry	3453	8
2	Chennai	Warm and humid	3786	0
3	Jaipur	Composite	2953	141
4	Bengaluru	Temperate	2142	18
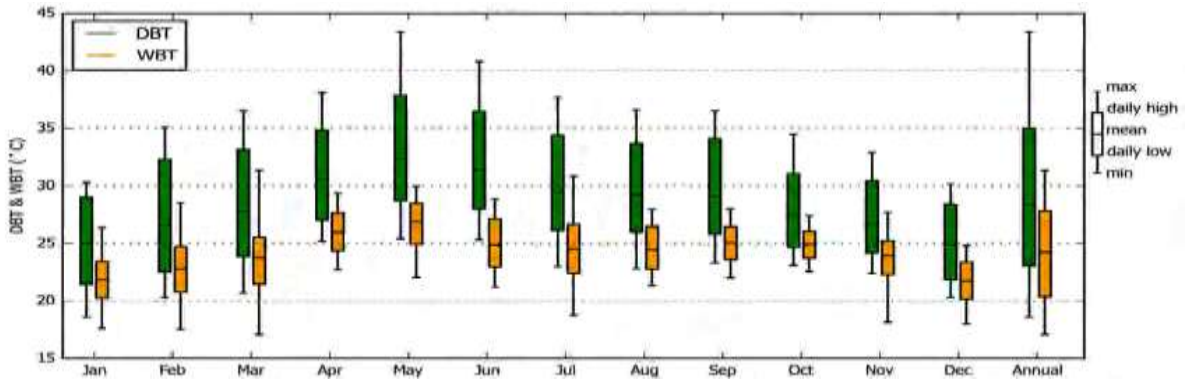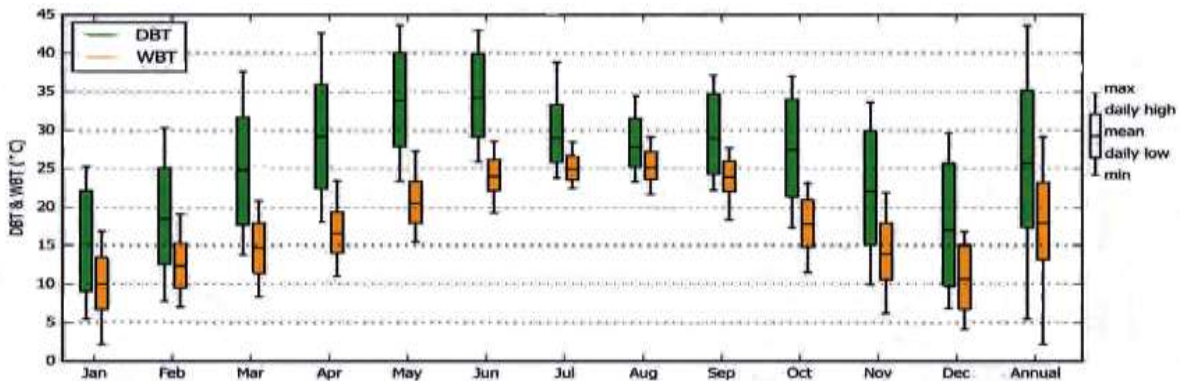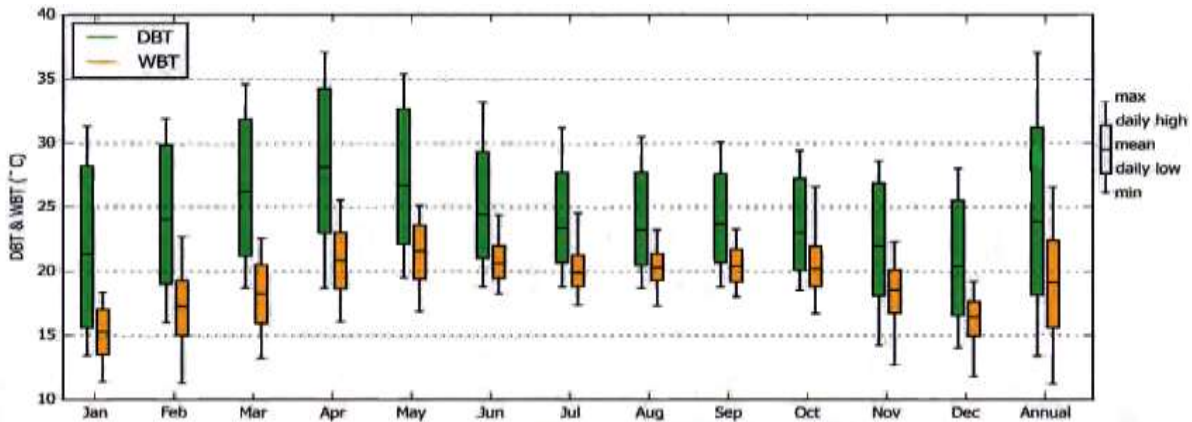
Figure 6-20: Monthly statistics of DBT and WBT (a) Ahmedabad, (b) Chennai (c) Jaipur, & (d) Bengaluru

The applicability and performance of the proposed RCS integrated with the cooling tower is a function of the wet bulb temperature and approach of the cooling tower. The performance of the cooling tower is dependent on the ambient condition of the location. It is necessary to know that whet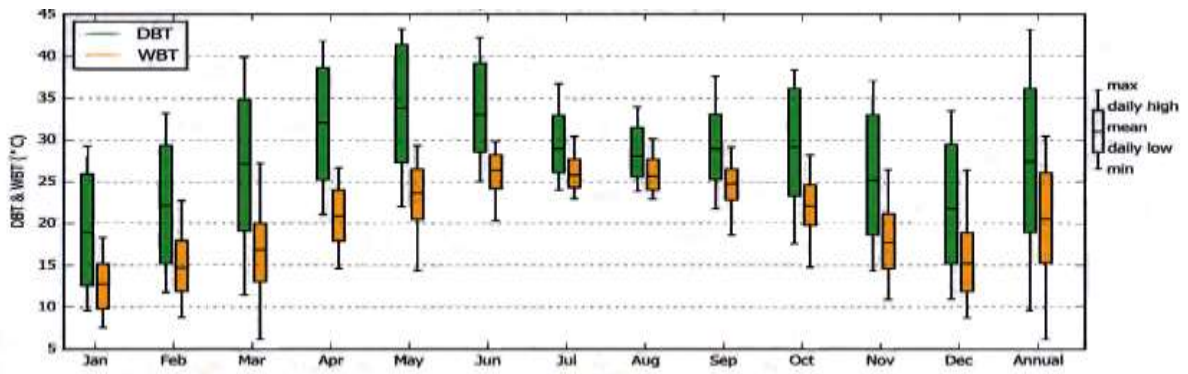her the wet bulb temperature of various selected cities for the study in India is appropriate for providing the desired temperature of cool water for the RCS for a substantial period of the year. The weather data of representative cities for different climatic zones of India has been analyzed for the summer season in which cooling is desired. Table 6-9 shows the minimum, maximum and average WBT for a different climatic condition for the summer season. The data is categorized for the daytime and night time to see the diurnal variation. In dry climatic condition, lower WBT is achieved in the night time. The work can be further extended for the night time using a thermal storage for the cooling tower integrated radiant cooling system.

Table 6-9: Ambient air wet bulb temperature for the different climatic zones

Climatic Zone	Wet Bulb Temperature (°C) in Summer (April to July)					
	Day-time (9am to 6pm)			**Night-time (12am to 9am and 6pm to 12am)**		
	Minimum	Maximum	Average	Minimum	Maximum	Average
Hot-dry	12	30.4	23.6	9.8	30.3	21.9
Warm-humid	16.2	33	**26.4**	14.3	31.2	**25.5**
Composite	12.5	32.3	23.24	8.04	308	21.6
Temperate	16.3	25	**20.8**	15.57	25.6	**20.3**

Figure 6-20 (a) shows the monthly variation of DBT and WBT for Ahmedabad (Hot and dry). It can be observed that the WBT is higher than 20°C from May-September. For the daytime average WBT is 23.61°C, and for the night time average, WBT is 21.95°C for the summer season Table 9. The temperature of the water was found to be less than 24 °C for the 49% of the total daytime period and 51% of the total Night time period Figure 5-21.

Monthly variation of DBT and WBT for Chennai (warm and humid) is shown in Figure 6-20(b). Throughout the year WBT is more than 20°C; from March-October the average WBT is more than 24°C which is not suitable for implementation of the cooling tower to achieve cool water for RCS. Average WBT for the daytime for the summer

season is 26.37°C and the WBT for the night time is 25.5°C as shown in Table 9. Figure 5-21 shows the cooling availability potential for cool water from cooling tower, there is no period providing water at 20°C. The availability of water during the day period below 24°C is 12%, and cooling availability below 24°C for the night time is 17%. Incorporating parallel chiller and cooling tower with an RCS has following challenges: the first cost of the system increases, additional water loop and components are added, the complexity of the system increases and proper control is required so that system can switch the running of cooling tower and chiller based on the load and the WBT. For warm and humid climate, the cooling tower will not be able to provide cool water for enough hours so as to offset the above-said challenges. Based on the WBT of the daytime and nighttime and cooling availability of cool water from cooling tower, it can be concluded that application of cooling tower integrated RCS has no scope for the warm and humid climate. The warm and humid climate is not suitable for cooling tower integration of chiller and hence simulation analysis will not be done for the warm and humid climate.

Monthly variation of DBT and WBT for Jaipur (composite) is shown in Figure 6-20(c), the WBT is higher than 20°C from May-September. Average WBT for the daytime is 23.24 °C and the WBT for the night time is 21.6°C for the summer season as shown in Table 9. The temperature of the water was found to be less than 24 °C for the 64% of the total Daytime period and 70% of the total Night time period. The overall difference in the cooling availability of water for the day and night period for a temperature lower than the 24 °C was not significant. The availability of cool water below 20 °C is 44% during the daytime and 57% of total nighttime Figure 5-21, shows a good potential for cooling tower integration with RCS.

Monthly variation of DBT and WBT for Bengaluru (Temperate) is shown in Figure 6-20(d). For almost round the year WBT is lower than 24°C, which is a most suitable condition for integration of cooling water for achieving cool water for RCS. Average WBT for the daytime for the summer season is 20.8 °C and the WBT for the night time is 20.34°C as shown in Table 9. The availability of cool water time below 20°C from the cooling tower is 28% for the daytime and 31% for the night time. Availability of cool water time below 24°C from the cooling tower is 64% for the daytime and the night time as shown in Figure 6-21. Statistical analysis of the different climatic condition of India shows that cooling tower integration has a strong potential for Bengaluru followed by Jaipur and Ahmedabad, Chennai climate is not suitable for the

cooling tower integrated RCS. For studying the behaviour of cooling tower integrated RCS in more details, the experimental setup is designed and integrated into Jaipur (composite climate).
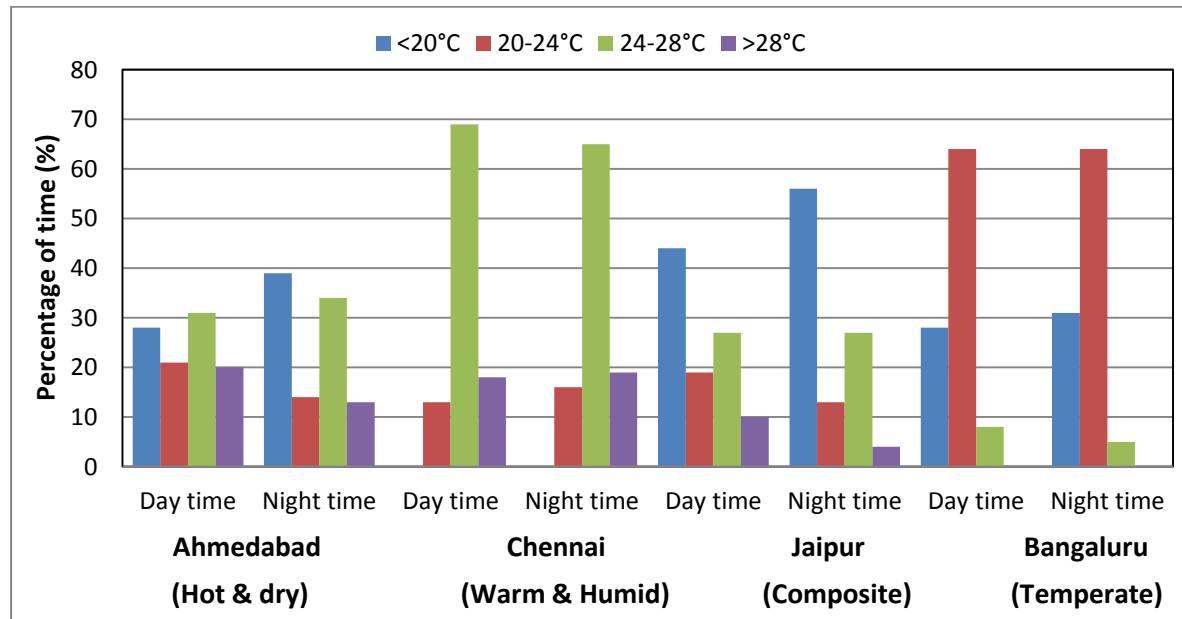
Figure 6-21: Annual cooling availability potential of water from the cooling tower

- **Simulation results**

Using the calibrated model annual energy simulation was carried out for different climatic zones of India using TMY (Typical meteorological year) files for different cities. Results are described for comparison of chiller integrated (Base case) and cooling tower integrated (Advanced case) RCS. The annual energy consumption for both cases of the different climatic condition is shown in Figure 6-22. Annual energy savings of 7%, 11% and 20% has been achieved in the Advanced case compared to Base for Hot & dry, Composite and Temperate climate respectively. Figure 6-23 shows the energy consumption of chiller of RCS and DOAS for both cases in Hot and Dry, Composite, & Temperate climate. Annual energy consumption breakdown details for a different component of both cases for different climatic zones are given in Table 6-10.

While replacing chiller with a cooling tower in the Advanced case for hot and dry climate, energy consumption has been reduced by 1,605 kWh but RCS alone is unable to meet the total sensible load. Energy consumption of conventional chiller supplying chilled water to DOAS cooling coil is increased by 1,017 kWh in Advanced case. In Advanced case due to increased flow, pumping energy has been increased to 58 kWh.
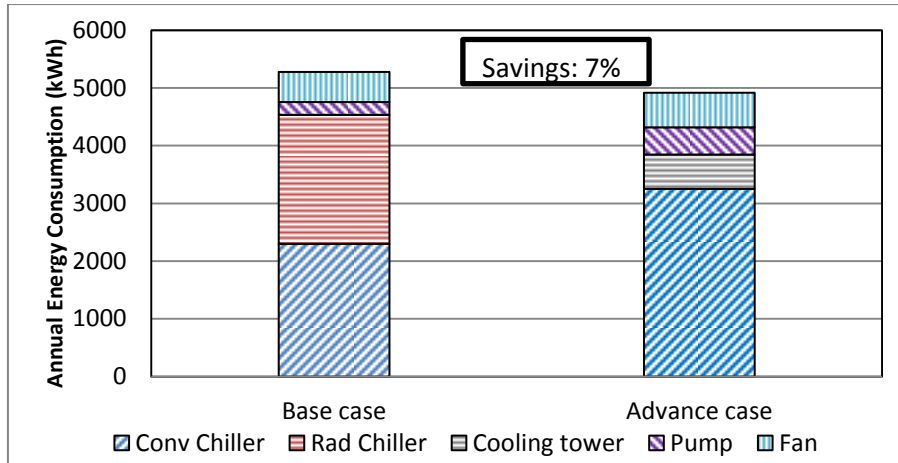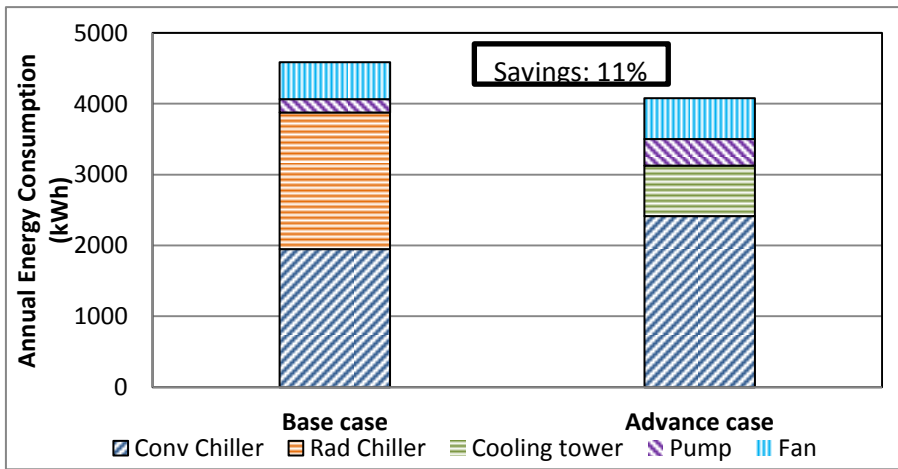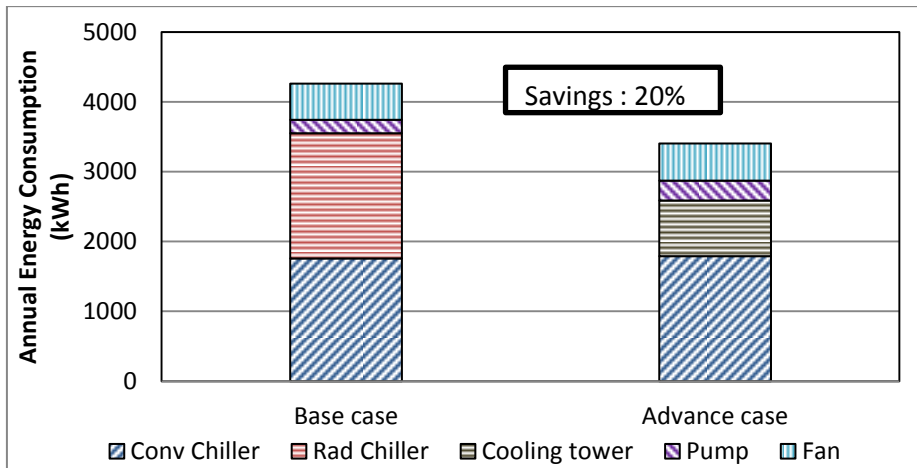
Figure 6-22: Annual energy consumption of chiller and cooling tower–operated radiant
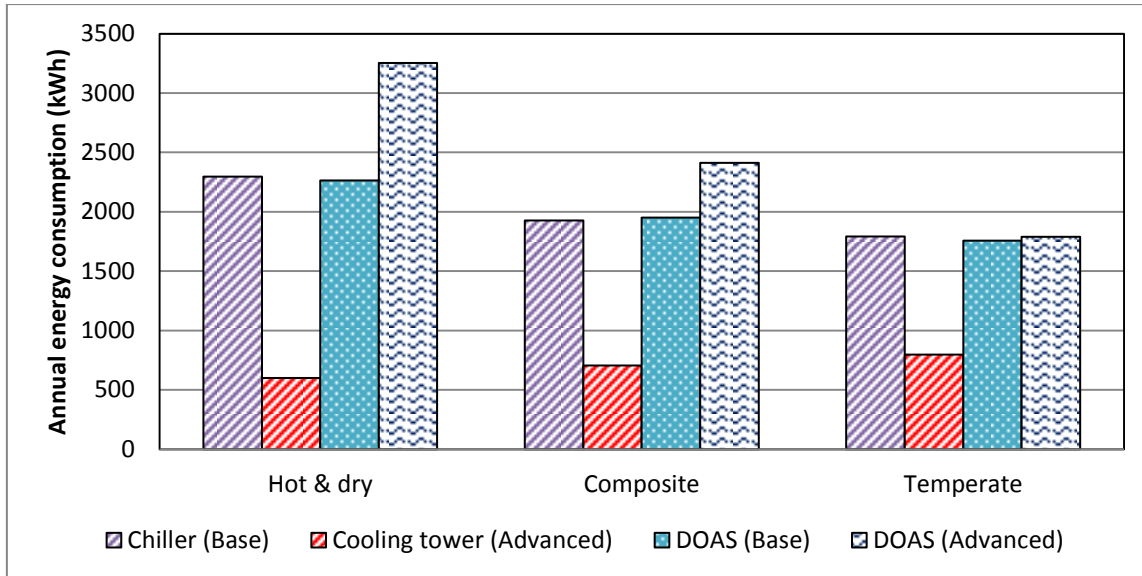
Figure 6-23: Annual energy consumption for RCS and DOAS for Base and Advanced case in Hot & dry, Composite & Temperate climate zone.

Table 6-10: Annual energy consumption breakdown for different cases

City	Cases	Radiant Plant (Chiller/cooling tower)	DOAS plant	Fan	Total	Saving
		Annual electric energy consumption (kWh)				
Hot & dry	Base	2,373	2,403	524	5,300	
	Advanced	821	3,501	596	4,918	7%
Composite	Base	2,039	2,025	523	4,585	
	Advanced	848	2,655	577	4,080	11%
Temperate	Base	1,879	1,860	523	4,262	
	Advanced	897	1,974	531	3,402	20%

The radiant plant and DOAS plant is the summation of the chiller energy consumption and pump energy consumption. In Hot and Dry climate radiant chiller has the highest energy consumption of 2,373 kWh due to the highest number of cooling degree days (CDD). In Hot and Dry climate cooling tower has the lowest energy consumption of 767 kWh because of the higher WBT 26°C from the month of May to September cooling tower is unable to deliver cool water suitable for the RCS.

Composite climate has radiant chiller energy consumption of 2,039 kWh in the Base case and 848 kWh for the cooling tower in the Advanced case. For composite climate, cooling tower operation faces a challenge from June-September due to the WBT above 23.5 °C. The temperate climatic condition has a chiller and cooling tower energy consumption of 1,879 kWh and 897 kWh respectively in the Base and Advanced case. In the Advanced case, RCS might not be able to meet the whole building sensible load, therefore, DOAS is running in the recirculation mode to meet the remaining sensible mode. In Hot and Dry climate, the difference in the energy consumption of RCS and

145

DOAS is maximum followed by Composite and Temperate climate. In Temperate climate, almost all the sensible load is met by the cooling tower operated RCS.
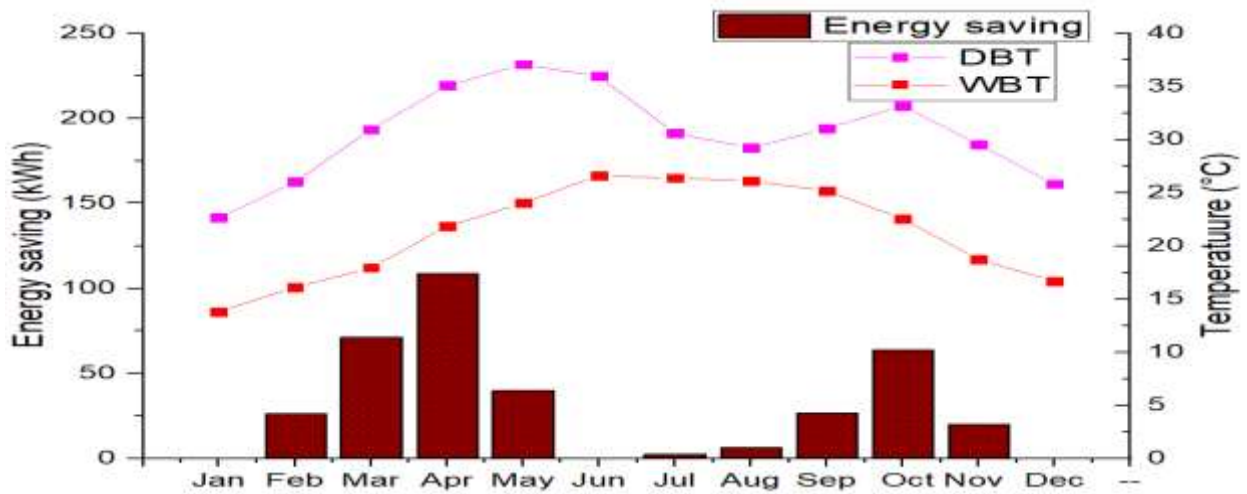
Figure 6-24: Ambient dry bulb temperature (DBT), wet bulb temperature (WBT), and energy savings for the hot and dry climate.

Figure 6-24 shows the variations of monthly energy savings with respect to ambient DBT and ambient WBT for Hot and Dry climate. Maximum monthly energy saving of 110 kWh is achieved in the month of April. In this month, ambient WBT is suitable for RCS with high sensible load, which makes the maximum utilization of cool water from the cooling tower. In the month of May, ambient WBT has increased and cooling tower is unable to supply cool water that can be used for cooling in RCS. In the month of March and October, 71 and 63 kWh monthly energy savings have been achieved. In the month of February, May and November, the cooling tower has substantial opportunity for energy savings. June, July and August is the monsoon season and there is no saving achieved due to high WBT. The cooling tower is unable to provide cool water which could be utilised for cooling through radiant cooling system hence both RCS and DOAS are being operated by the chiller. In the month of January and December, there is a cooling requirement.

By comparing the Base and Advanced case in Composite climate, energy consumption for providing cool water in RCS has been reduced by 1,191 kWh but RCS is unable to meet total sensible load. The remaining sensible load, ventilation load and latent load are met by DOAS which increases the energy consumption of conventional chiller is increased by 630 kWh. Pumping energy in the Advanced case is increased by 42 kWh due to the enhanced flow of the cooling tower water.

Figure 6-25 shows the variations of monthly energy savings with respect to ambient DBT and ambient WBT for the composite climate. In the month of May, the maximum monthly energy savings of 160 kWh was achieved for the Advanced case. Maximum energy savings in May is due to the combination of lower ambient WBT and high sensible load. Performance of the cooling tower is better and the RCS can handle the sensible load most effectively in the month of May. In the month of April, monthly energy savings was 120 kWh, which is slightly lower as compared to May due to the reduced cooling load requirement in April. In the Months of January, February, November, and December, energy savings were minimal as there is almost no requirement for cooling; the only requirement in winter is to provide outdoor air. Also, in the months of March and October, the cooling tower saves 65 kWh and 76 kWh respectively and has a good potential to couple with the RCS to achieve energy savings.
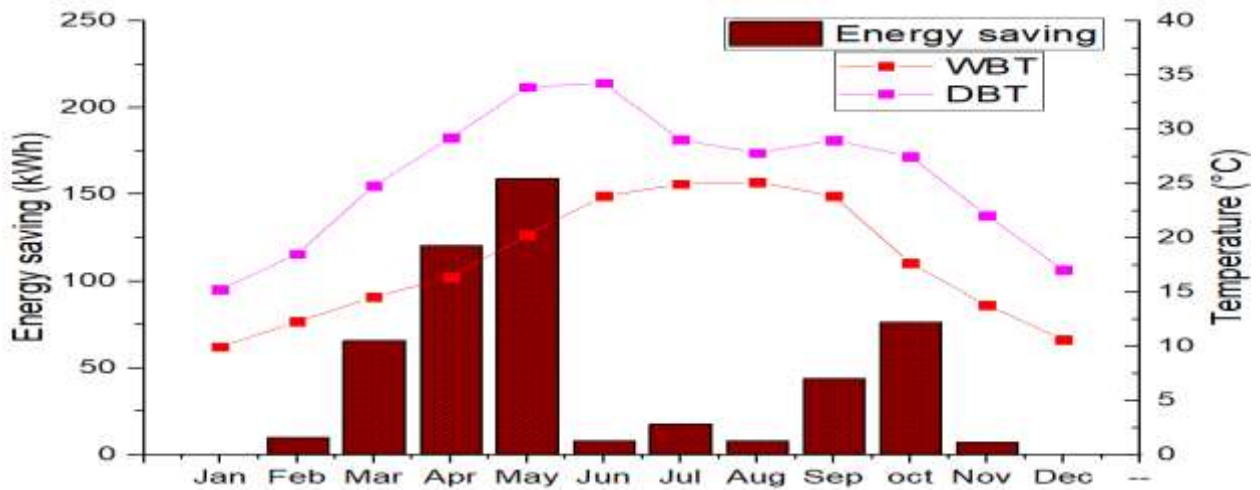
Figure 6-25: Ambient dry bulb temperature (DBT), wet bulb temperature (WBT), and energy savings composite climate

Comparing Base and Advanced case in a temperate climate, refrigeration energy consumption for providing cool water for RCS has been reduced by 982 kWh as a result; DOAS energy consumption has been increased by 114 kWh to cater the leftover sensible load of the zone. Pumping energy in cooling tower integrated RCS has been increased by 8 kWh due to the enhanced flow of the cooling tower.

Figure 6-26 shows the variations in monthly energy savings with respect to ambient DBT and ambient WBT in Temperate climate. In a temperate climate, except for April, May and June whole rest of the year monthly WBT is lower than 20°C. Maximum WBT is 21.9°C in the month of May which is suitable for obtaining cool water from the cooling tower to utilize in RCS. In the month of May, the maximum monthly energy

savings of 153 kWh was achieved for the Advanced case. Temperate climate has a cooling requirement from the month of March to June and maximum savings have been achieved in this period. For rest of the period of the year temperate climate usually does not require much cooling; ventilation only can serve the purpose. Temperate climate has the great potential of integration of cooling tower with the RCS. In most part of the year cooling tower alone is sufficient to operate RCS.
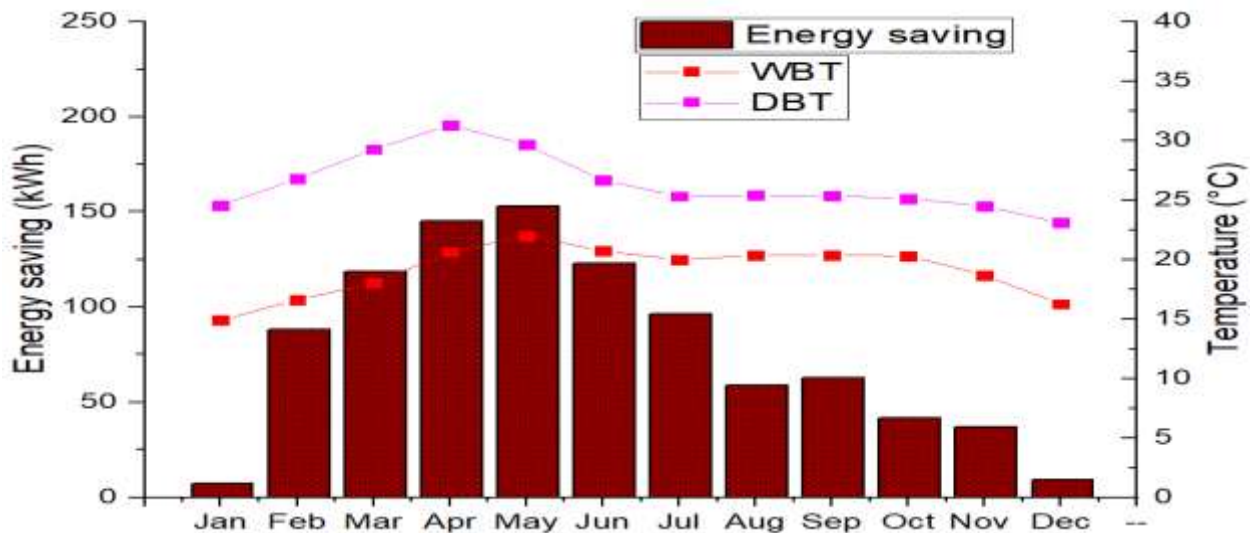
Figure 6-26: Ambient dry bulb temperature (DBT), wet bulb temperature (WBT), and energy savings for a temperate climate.

Comparison of Thermal comfort between Base and Advance case

While performing the experiments, thermal comfort survey was conducted for Jaipur (composite climate). In the survey, data of air dry bulb temperature (DBT), mean radiant temperature (MRT), air velocity, relative humidity, metabolic rate, clothing level and thermal sensation votes were obtained and using the CBE thermal comfort tool based on ASHRAE standard 55-2017, PMV was calculated. As per ASHRAE 55-2017, the comfort range for PMV is -0.5<PMV<0.5. In the base case, the PMV range was found to be -0.45 - 0.5 i.e. within the acceptable limit. In the Advance case, the PMV is in the range of 0.45-1.62. PMV is breached in Advance case whenever there is higher ambient WBT; the cooling tower is unable to provide sufficient cool water. In some cases due to higher ambient WBT, higher water temperature was supplied by the cooling tower, therefore, the upper range of PMV has increased due to higher zone DBT and MRT.

Figure 6-27 shows the variation of the daily average of ambient dry bulb temperature, a daily average of zone operative temperature of the Base case and Advance case for the month for the summer season (April, May and June) for composite climate

148

obtained from simulation results. In the Base case, the operative temperature is within the limit in most of the time whereas in the Advance case in some of the cases operative temperature is breaching the limit whenever WBT is not suitable for the supply of cold water from cooling tower. The operating temperature varies from 25.8-27.7°C and 26-28.4°C in Base and Advance case respectively. In composite climate, there is a need of integration of parallel chiller and cooling tower with RCS. Controls are needed to be designed, whenever WBT is not suitable for cooling tower operation, controls should switch the operation from cooling tower to chiller and vice-versa.
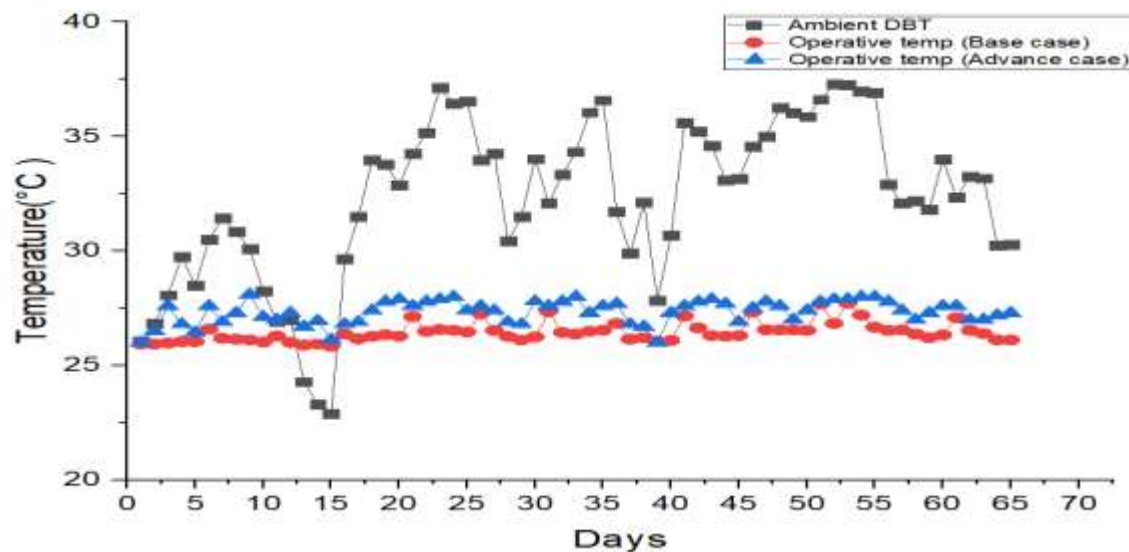
Figure 6-27: Average daily ambient dry bulb temperature (DBT), daily average zone operative temperature (Base case), and daily average zone operative temperature (Advance case) for the composite climate.

Figure 6-28 shows the variation of the daily average of ambient dry bulb temperature, a daily average of zone operative temperature of the Base case and Advance case for the month for the summer season (April, May and June) for temperate climate obtained from simulation results. In case of Base cases, the operative temperature is within the limit whereas in Advance case few times operative temperature is breaching the limit whenever WBT is not suitable for the supply of cold water from cooling tower. The operating temperature varies from 25.7-27.3°C and 25.9-27.7°C in Base and Advance case respectively. Cooling tower alone can meet the setpoint in most of the period of the year along with 20% annual energy can be achieved. The temperate climate is most suitable for integration of cooling tower with RCS.
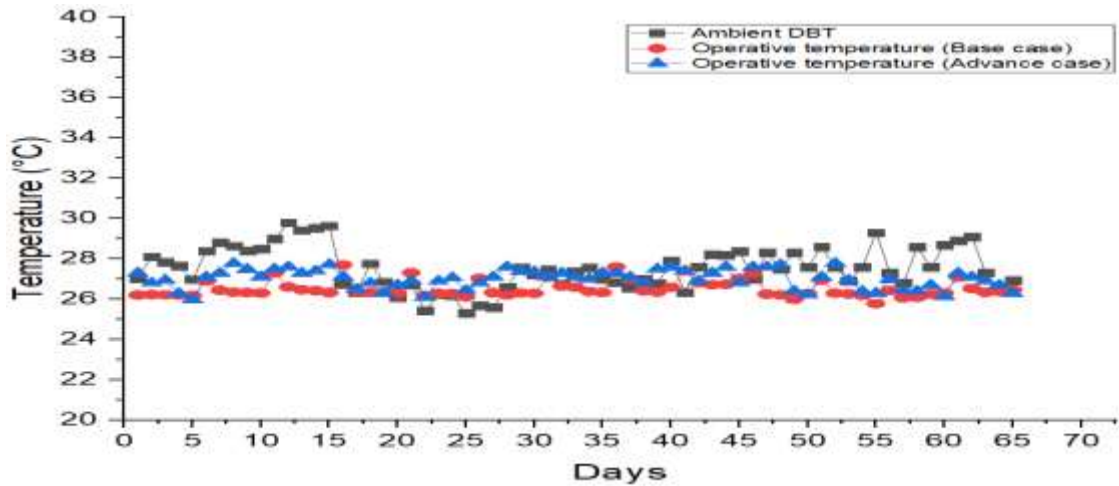
Figure 6-28: Average daily ambient dry bulb temperature (DBT), daily average zone operative temperature (Base case), and daily average zone operative temperature (Advance case) for a temperate climate.

6.8.2 Comparison of different types of radiant cooling system

Results are described into two-phase i.e. annual and monthly energy savings and cooling capacity. For the energy consumption/savings analysis yearly run time was considered for the simulation of the model. After calibration of the simulation model, three different models are created by changing the construction internal source and material for a different type of radiant cooling system using the data of Table 7 in the calibrated model. Models of all three types of RCS are simulated and compared based on the annual and monthly energy consumption/savings. Cooling capacity is calculated by using the values from the simulation results for peak day and compared to analyse the different types of RCS

- **Energy savings**

Annual simulations were carried out to see the variation of annual and monthly energy consumption for the RCS and DOAS system. Figure 6-29 shows the annual energy consumption for the RCP, ESCS and TABS. The difference among the three in terms of energy consumption is due to the material property and difference in hydronic circuit laying arrangement. Annual energy consumption for the RCP is 5.1% less compared to ESCS and 6.2% lower than TABS. RCP is found to be most efficient among the three types of RCS for the system in a composite climate of Jaipur. Figure 6-30 shows monthly energy saving of RCP compared to ESCS and TABS. RCP is considered as the base case for analyzing the monthly energy savings. RCP energy savings are maximum in the month of May i.e. 56 kWh as compared to TABS and 51 kWh as compared to ESCS. In the month of June RCP has an energy savings of 51 kWh and 46 kWh compared to

TABS and ESCS. In the month of January, February, November and December energy consumption for the RCS is minimum; in winter season mostly energy is consumed for supplying the ventilation air alone.
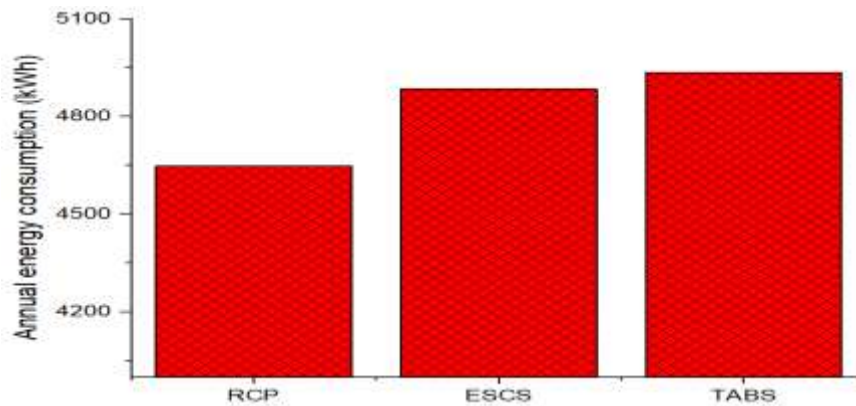
Figure 6-29: Comparison of annual energy consumption of RCP, TABS and ESCS.
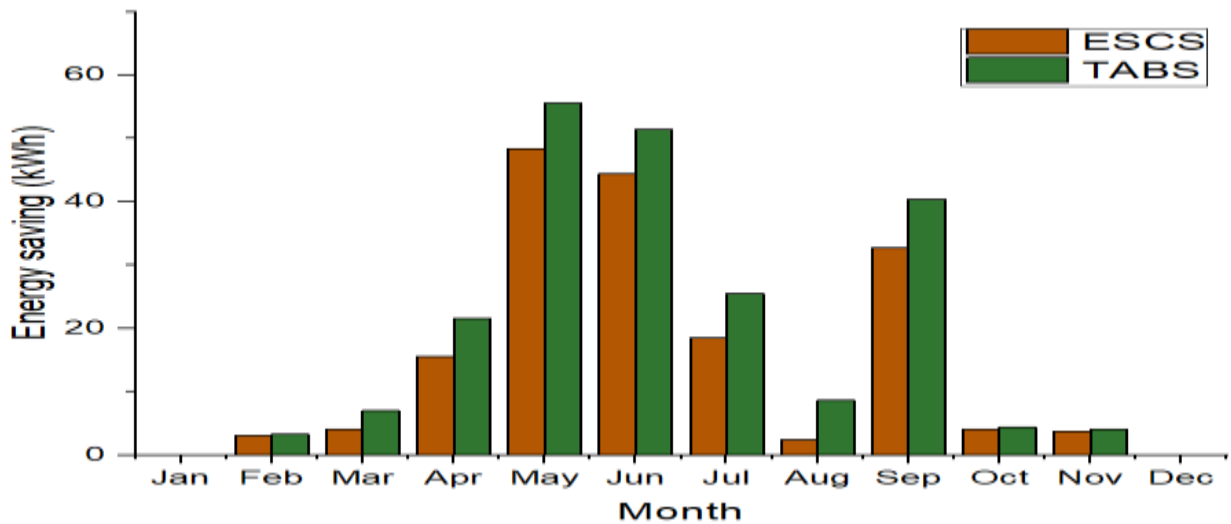
Figure 6-30: Annual energy savings of ESCS and TABS compared to RCP.

Figure 6-31 shows the monthly variation of the energy consumption of the RCS for RCP, ESCS and TABS. Maximum energy consumption for the RCS is in the month of May 397 kWh for the TABS system and then 392 kWh for the ESCS and 343 kWh for RCP. Energy consumption for the DOAS is maximum in the month of August. The monthly energy consumption of DOAS is in the monsoon season as it has maximum humidity ratio in the ambient condition. In India, July-September is considered as monsoon season. Table 6-11 provides the monthly data of thermal energy consumption of the DOAS and its component.
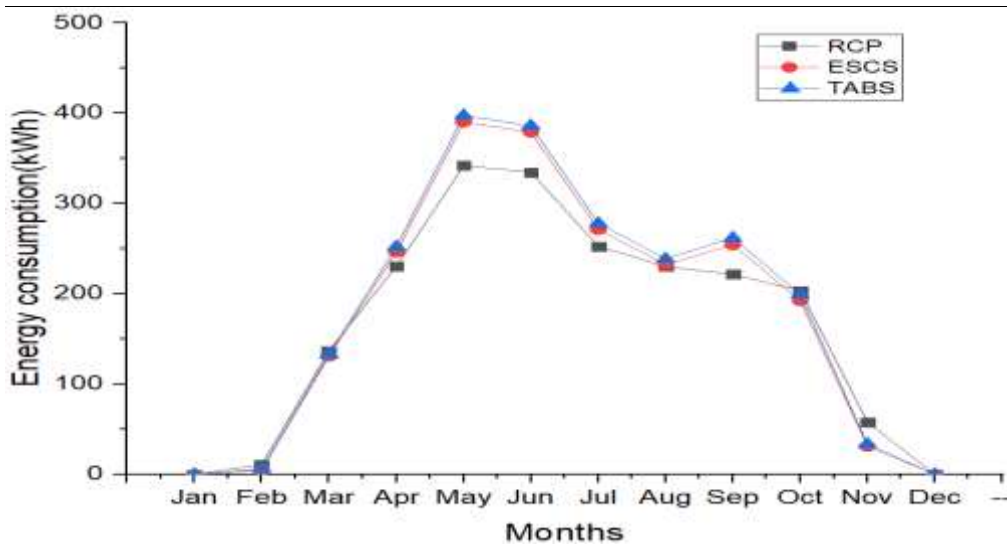
Figure 6-31: Monthly comparison of an energy consumption radiant cooling system for RCP, ESCS and TABS.

Table 6-11: Comparison of the thermal energy of DOAS, cooling coil and ERW for RCP ESCS and TABS

Month	RCP			ESCS			TABS		
	ERW	Cooling coil	DOAS	ERW	Cooling coil	DOAS	ERW	Cooling coil	DOAS
Jan	0	264	264	1	284	284	1	284	284
Feb	6	274	280	6	292	298	6	292	297
Mar	22	334	356	18	357	375	18	357	375
Apr	56	329	385	46	354	400	44	357	401
May	130	414	545	109	448	557	105	455	560
Jun	193	390	583	170	427	597	165	436	600
Jul	181	463	645	145	519	664	139	526	666
Aug	202	477	679	150	549	698	147	551	698
Sep	154	412	566	125	457	582	123	460	583
Oct	66	414	480	56	446	502	55	447	502
Nov	17	338	355	16	362	377	16	361	377
Dec	3	265	268	3	285	288	3	285	288

Figure 6-32 shows bar graph representation of the monthly variation of thermal energy delivered by DOAS component for RCP for the composite climate. Table 6-11 shows the thermal energy consumed by DOAS and its components for RCP, ESCS and TABS. First, the air enters the ERW, ERW work as a heat exchanger and exchanges enthalpy with the return air from the space. Value of thermal energy for ERW is almost

same or small variation for all the three types of RCS. After ERW air enters the cooling coil where it gets dehumidified and enters the space. As heat transfer rate and heat transfer coefficient for the RCP, ESCS and TABS are different so to meet the set point of the space cooling capacity of the coil varies accordingly. Thermal energy for DOAS coupled with TABS is maximum as the load recovered by TABS is minimum among the three.
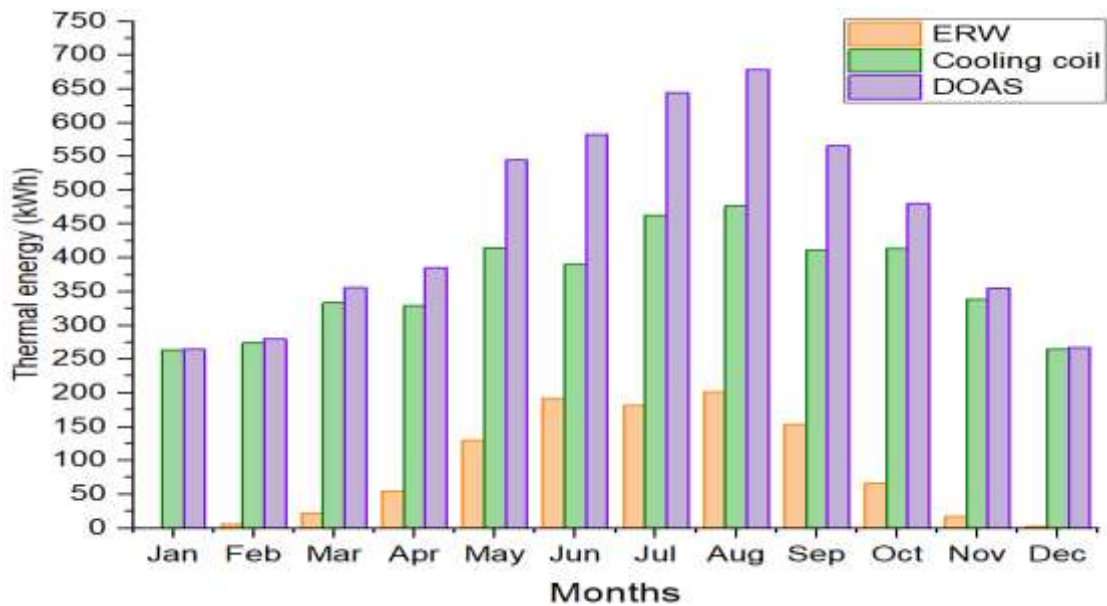
Figure 6-32: Monthly comparison thermal energy handled by energy recovery wheel (ERW) and cooling coil in DOAS for RCP for the composite climate.
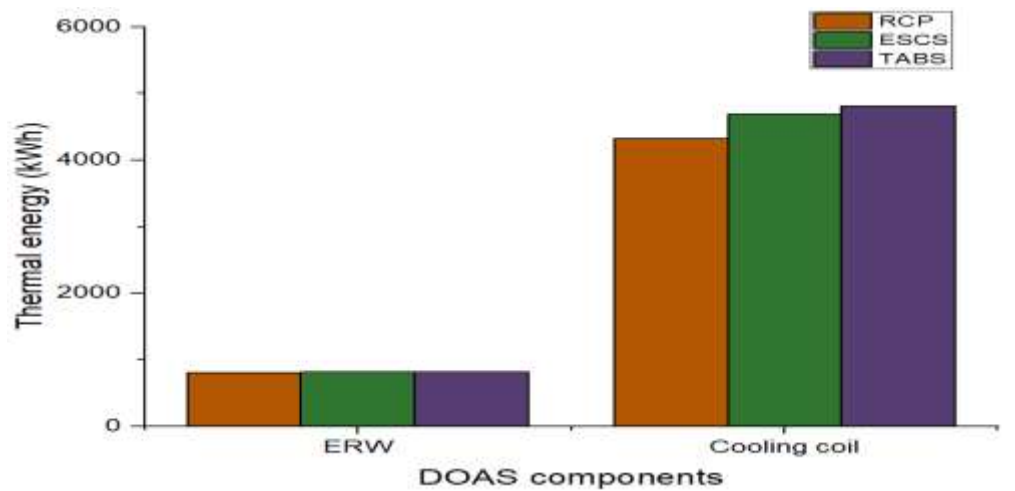
Figure 6-33: Annual comparison of thermal energy handled by energy recovery wheel (ERW) and cooling coil in DOAS for RCP, ESCS and TABS.

Figure 6-33 shows the comparison of annual load share between ERW and cooling coil for RCP, ESCS and TABS. Placement of ERW before cooling coil in the supply air path of the DOAS saves energy. Around 17% of the load of the cooling coil is

reduced by using ERW in DOAS by recovering the thermal energy from the return air in all the three cases of RCS.

- **Cooling capacity**

For analyzing the cooling capacity, simulations are carried out for the peak day to analyze and compare the cooling capacity phenomenon for different types of RCS. Figure 6-34 shows the comparison of cooling capacity for TABS, ESCS and RCP for the peak design day. Cooling capacity can be calculated by using above stated equations (1). Cooling capacity for the TABS while in the morning is maximum of 80 W/m^2, 76.6 W/m^2 for ESCS and 72.2 W/m^2 for RCP as it has to overcome the heat stored in the thermal mass first and then it starts cooling the space, ESCS in the intermediate and the RCP is minimum. As the day proceeds, the thermal mass of the building is getting cooled with time, the cooling capacity for TABS and ECWS reduces, and for RCP the cooling capacity is reduced less compared to TABS and ESCS. In the evening hours, external load reduces and space achieves a stabilized condition hence in the evening the difference in cooling capacity value for all the three system is comparatively smaller than the first
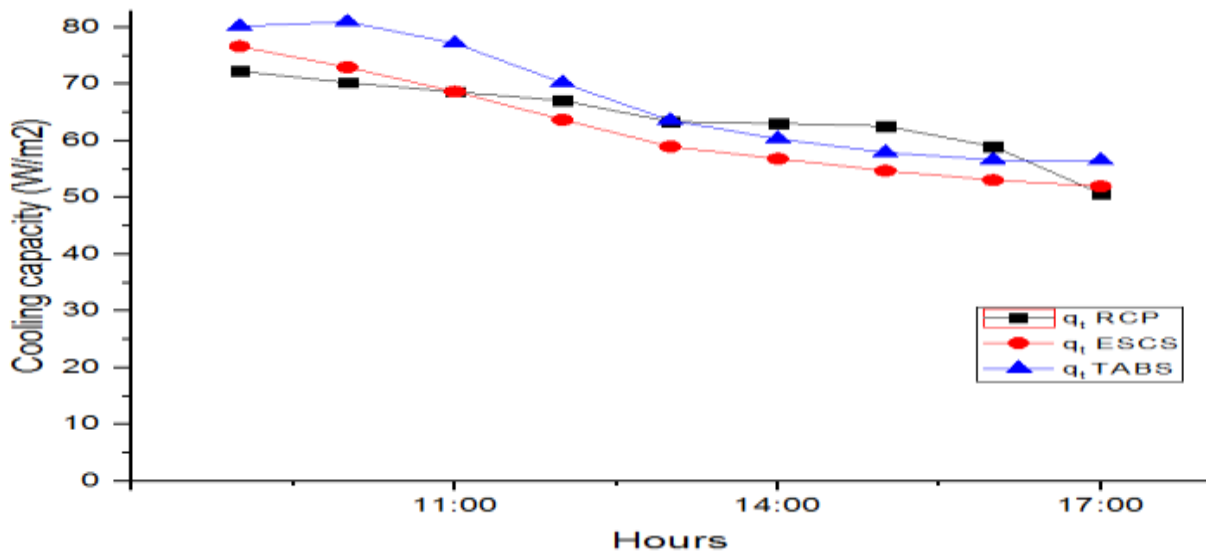
Figure 6-34: Comparison of cooling capacity for TABS and ESCS and RCP.

half of the day. The minimum value for the cooling capacity for RCP, ESCS and TABS is 50.3 W/m^2, 52 W/m^2 and 56.5 W/m^2 respectively. Due to significant variation of the cooling capacity, there is variation in the delivered thermal energy and electrical consumption among the different types of RCS.

6.9   Chapter summary

The chapter is focused on the experimental and simulation analysis of RCS. Achieving energy efficient operation for RCS, chiller and cooling tower based chilled water source is used. Cooling tower shows great opportunity for coupling with the radiant cooling system to save energy, Provides maximum savings in a temperate climate. Cooling tower integrated RCS saves around 11% in composite climate, 7% in hot and dry climate and 20% in temperate climate compared to chiller integrated RCS. Radiant panel system saves around 3.9% electrical energy compared to an embedded surface cooling system and 4.8% compared to the thermally activated system.

CHAPTER 7.   Summary and Conclusions

7.1   Summary of work

This thesis work has been conducted to identify the opportunities to enhance the performance of the radiant cooling system (RCS). In RCS load is decoupled i.e. RCS is responsible for catering the sensible load, a parallel air system i.e. dedicated outdoor air system (DOAS) is used for meeting the latent load and providing the ventilation air requirement. Experimental and calibrated simulation study was carried out for RCS and DOAS. This study is conducted in three phases to meet out the objectives as discussed below.

Entire thesis work was conducted in three phases. In the first phase, different combinations of cooling coil and sensible/energy recovery/desiccant wheels based DOAS strategies were identified from the literature. A commercial building model integrated with RCS was calibrated using measured data. Different building models integrated with RCS and different DOAS strategies were developed using a calibrated building model. A total of six models of different decoupling strategies along with RCS were simulated for annual period and analyzed to compare with conventional all-air system for the different climatic conditions of India.

In the second phase, further to understand the thermal behaviour and actual operational parameters of different DOAS strategies, an experimental setup was developed. A modular DOAS was designed and developed to accommodate all the components of different decoupling strategies in order. The modular DOAS is integrated with the indoor-outdoor chamber. The indoor and outdoor chambers were responsible for creating steady-state indoor and outdoor conditions. Based on the results of the experimental and simulation results of different decoupling strategies, recommendations were provided to use DOAS strategy along with RCS to make it energy efficient for different climatic conditions.

In phase three further to see the integrated performance of RCS and DOAS, the recommended DOAS strategy based on the results of phase one and two for Composite climate i.e. Strategy-2 [comprise of energy recovery wheel (cater both sensible & latent load) and low temperature cooling coil] is integrated with RCS at MNIT Jaipur (falls in

Composite climate). Chilled water in RCS is provided through a chiller and cooling tower (used as a water side economizer) for supplying chilled water in RCS. Based on the experimental data and HVAC plant specifications, EnergyPlus models were developed and calibrated. Using the calibrated model annual energy simulations were carried out for chiller and cooling tower based RCS. Further three different models of radiant panel cooling (RCP), embedded surface cooling system (ESCS) and thermal activated building system (TABS) were developed by changing the construction of internal source in the EnergyPlus. Annual energy simulations were carried out for different types of RCS to analyze energy saving potential.

7.2   Major findings

Based on the experimental and simulation analysis of the DOAS and RCS following are the main findings-

Decoupling strategies

- In Hot and Dry climate Strategy-2 offers maximum energy saving potential in cooling coil based strategy and Strategy-5 offers maximum energy saving potential in desiccant wheel based strategy in both simulation and experimental based study. In the cooling coil based strategies, Strategy-2 and Strategy-3 were found to save 10% and 9% energy respectively compared to Strategy-1 in experimental study. In case of desiccant wheel based strategy using active heater regeneration, Strategy-5 and Strategy-6 are found to save 29% and 3% energy compared to Strategy-4 respectively.

- In Warm and Humid climate Strategy-2 offers maximum energy saving potential in cooling coil based strategy and Strategy-5 offers maximum energy saving potential in desiccant wheel based strategy in both simulation and experimental based study. In the cooling coil based strategies, Strategy-2 and Strategy-3 were found to save 8% and 7% energy compared to Strategy-1 in the experimental study. In case of desiccant wheel based strategy, Strategy-5 is found to save around 22% compared to Strategy-4 and Strategy-6 is having almost the same energy consumption as Strategy-4.

- In Composite climate, Strategy-2 offers maximum energy saving potential in cooling coil strategy and Strategy-5 offers maximum energy saving potential in desiccant wheel based Strategy in both simulation and experimental based study. In the cooling coil based Strategyategies, Strategy-2 and Strategy-3 were found to save 10% and 8% energy compared to Strategy-1 in the experimental study. In case of desiccant wheel

based strategy, Strategy-5 and Strategy-6 are found to save 29% and 4% energy compared to Strategy-4 respectively.

- In Temperate climate, Strategy-1 offers maximum energy saving potential in cooling coil based strategy in both simulation and experimental based study and Strategy-5 offers maximum energy saving potential while using active heater for regeneration (experimental study) and Strategy-6 offers maximum energy saving potential while using high temperature heat pump for regeneration (simulation study) in desiccant wheel based strategy. In the cooling coil based strategies, Strategy-1 was found to be most suitable, Strategy-2 and Strategy-3 were found to consume extra 2% and 6% energy compared to Strategy-1 respectively. In case of desiccant wheel based strategy, in case of active heater regeneration for the desiccant wheel, Strategy-5 and Strategy-6 are found to save 13% and 5% energy compared to Strategy-4 respectively.

Radiant Cooling System

- Statistical analysis was conducted based on the hourly data of the ambient dry bulb temperature (DBT), wet bulb temperature (WBT) and approach of the cooling tower to identify the suitability of integration of cooling tower with RCS. Based on the results cooling tower is suitable for integration with RCS in Hot and Dry, Composite and Temperate climate. Cooling tower is not suitable for Warm and Humid climate for integration with RCS.

- Calibrated model annual energy simulation using the TMY (Typical meteorological year) files for different cities of different climatic condition were conducted, annual energy savings of 7%, 11% and 20% has been achieved in the cooling tower integrated RCS (Advance case) compared to chiller integrated RCS (Base case) for Hot & dry, Composite and Temperate climate respectively.

- In Hot and Dry climate maximum monthly energy saving of 28% of total energy savings was achieved in the month of April for the cooling tower based RCS, WBT in April is favorable to generate desired cool water temperature from cooling tower. In the month of March, April, May and October cooling tower has a good potential to couple with the RCS. June, July and August is the monsoon season, due to high WBT cooling tower is unable to perform and there is no saving achieved in this period.

- In Composite climate, in the month of May, the maximum monthly energy savings of 31% of total annual savings was achieved for the cooling tower based RCS. In the

month of March, April, May, September and October, the cooling tower has a good potential to couple with the RCS to provide appreciable energy savings.

- In Temperate climate, except for April, May and June whole rest of the year monthly WBT is lower than 20°C which is highly recommended for cooling tower integration with RCS. Maximum WBT is 21.9°C in the month of May which is also recommended for obtaining cool water from the cooling tower to utilize in RCS. In the month of May, the maximum monthly energy savings of 18% of annual energy savings was achieved for the cooling tower based RCS.

- While comparing the three types of RCS, radiant panel cooling (RCP) provides energy savings of 5.1% compared to embedded surface cooling system (ESCS) and 6.2% compared to thermal activated cooling system (TABS).

- In RCP energy savings is maximum in the month of May as compared to TABS and ESCS.

- Around 17% of the load of the cooling coil is reduced by adding energy recovery wheel (ERW) before cooling coil in DOAS by recovering the thermal energy from the return air in all the three cases of RCS.

- For analyzing the cooling capacity, simulations were carried out for the peak day. Cooling capacity for the TABS in the morning was maximum of 80 W/m^2, 76.6 W/m^2 for ESCS and 72.2 W/m^2 for RCP. TABS has to overcome the heat stored in the thermal mass first and then it starts cooling the space, ESCS in the intermediate and the RCP is minimum in terms of cooling capacity. As the day proceeds, the thermal mass of the building is getting cooled with time, reduction in the cooling capacity for TABS and ESCS is higher as compared to RCP.

- RCS has a great potential to improve the energy scenario and minimize peak power demand in India. Right selection of RCS and recommended configuration and sizing of DOAS for integration with RCS is the key to achieve potential energy savings and improved thermal comfort.

- Except for Warm and humid climate, RCS should be designed with parallel chiller and cooling tower (water side economizer) to feed chilled water in RCS. Operation of chiller and cooling tower need to be controlled based on ambient WBT. If Ambient WBT is in the range of 14-22°C, it is highly recommended to operate the RCS using a cooling tower. While using cooling tower with RCS, DOAS need to be properly size and volumetric flow of DOAS should be controlled using variable frequency drives.

7.3   Scope for further research

Experimental and simulation study has been performed for DOAS and RCS for enhancing the performance of RCS through decoupling of the load. Following are some recommendation for future work-

- Some more decoupling strategies can be identified and can be compared with the existing strategies; membrane-based dehumidification system can also be compared with the strategies investigated in this study.

- In this study only desiccant wheel (solid desiccant impregnated in rotor) is used. Liquid desiccant based system can be investigated to see the comparative analysis to use in conjunction with RCS.

- To further improve the performance of the DOAS integrated with RCS, control strategy needs to be developed to capture the monthly variation of different decoupling strategy.

- The recommendations of different DOAS strategies provided in this thesis are solely based on the energy analysis. However there may be a significant cost of adding the additional components and systems. The economic analysis is not in the scope of the thesis.

- Study can be conducted to minimize the peak demand of the radiant cooling system by using thermal storage.

References

[1]   T. T. Aarti Nain, Anamika Prasad, "PACE-D Technical Assistance Program HVAC Market Assessment and Transformation Approach for India," 2014.

[2]   ECBC, "User Guide, Energy Conservation Building Code," 2013.

[3]   C. Stetiu, "Energy and peak power savings potential of radiant cooling systems in US commercial buildings," *Energy Build.*, vol. 30, no. 2, pp. 127–138, 1999.

[4]   J. L. Niu, L. Z. Zhang, and H. G. Zuo, "Energy savings potential of chilled-ceiling combined with desiccant cooling in hot and humid climates," *Energy Build.*, vol. 34, no. 5, pp. 487–495, Jun. 2002.

[5]   J. Babiak, B. Olesen, and D. Petras, "Low temperature heating and high temperature cooling, REHVA Guidebook, Federation of European Heating and Air-Conditioning Associations," 2007.

[6]   "ISO. 11855-1:2012(E) building environment design e design, dimensioning, installation and control of embedded radiant heating and cooling systems: Part 1," 2012.

[7]   *ASHRAE 62.1: Ventilation for Acceptable Indoor Air Quality, ASHRAE, 2010.* 2016.

[8]   J. James and L. G. Harriman, "Dehumidification Equipment Advannces," *ASHRAE J.*, vol. August, pp. 22–27, 2002.

[9]   M. M. Svein Morner, Amalia Hicks, *ASHRAE Design Guide for operation and maintenance for Dedicated Outdoor Air Systems*. 2017.

[10]   C. W. Bayer, S. A. Crow, "Causes of Indoor Air Quality Problems," 2002.

[11]   "ISO 18566: Building Environment Design — Design, test methods and control of hydronic radiant heating and cooling panel systems," 2017.

[12]   K. W. Kim and B. W. Olesen, "Radiant Heating and Cooling Systems: Part two," *Ashrae J.*, vol. 57, pp. 34–42, 2015.

[13]   R. Bean, B. W. Olesen, and K. W. Kim, "History of Radiant Heating & Cooling Systems: Part 1," *ASHAE J.*, vol. Jan, pp. 40–49, 2010.

[14]   R. Bean, B. W. Olesen, and K. W. Kim, "History of Radiant Heating & Cooling Systems-Part2," vol. February, 2010.

[15]   N. K. Bansal, "Characteristic parameters of a hypocaust construction," *Build. Environ.*, vol. 34, no. 3, pp. 305–318, May 1998.

[16]   D. K. Kim, "The natural environment control system of Korean traditional architecture: Comparison with Korean contemporary architecture," *Build. Environ.*, vol. 41, no. 12, pp. 1905–1912, Dec. 2006.

[17]   C. Bae and C. Chun, "Research on seasonal indoor thermal environment and residents' control behavior of cooling and heating systems in Korea," *Build. Environ.*, vol. 44, no. 11, pp. 2300–2307, Nov. 2009.

[18]   J. Y. An, S. Kim, H. J. Kim, and J. Seo, "Emission behavior of formaldehyde and TVOC from engineered flooring in under heating and air circulation systems," *Build. Environ.*, vol. 45, no. 8, pp. 1826–1833, Aug. 2010.

[19] R. Hu and J. L. Niu, "A review of the application of radiant cooling & heating systems in Mainland China," *Energy Build.*, vol. 52, pp. 11–19, 2012.

[20] C. Stetiu, H. Feustel, and F. Winkelmann, "Development of a simulation tool to evaluate the performance of radiant cooling ceilings," *Lawrence Berkeley Lab*, vol. LBNL-37300, 1995.

[21] W. H. Chiang, C. Y. Wang, and J. S. Huang, "Evaluation of cooling ceiling and mechanical ventilation systems on thermal comfort using CFD study in an office for subtropical region," *Build. Environ.*, vol. 48, no. 1, pp. 113–127, 2012.

[22] Z. Tian and J. a. Love, "A field study of occupant thermal comfort and thermal environments with radiant slab cooling," *Build. Environ.*, vol. 43, no. 10, pp. 1658–1670, 2008.

[23] H. E. Feustel and C. Stetiu, "Hydronic radiant cooling - preliminary assessment," *Energy Build.*, vol. 22, no. 3, pp. 193–205, 1995.

[24] B. Olsen, "Radiant floor heating in theory and practice," *ASHRAE J.*, vol. 44, pp. 19–26, 2002.

[25] P. Fazio, "Thermal Performance of a Hollow Core Concrete Floor System for Passive Cooling," *Build. Environ.*, vol. 23, pp. 243–252, 1988.

[26] J. D. Feng, F. Bauman, and S. Schiavon, "Experimental comparison of zone cooling load between radiant and air systems," *Energy Build.*, vol. 84, pp. 152–159, 2014.

[27] F. Causone, S. P. Corgnati, M. Filippi, and B. W. Olesen, "Experimental evaluation of heat transfer coefficients between radiant ceiling and room," *Energy Build.*, vol. 41, no. 6, pp. 622–628, Jun. 2009.

[28] C. Stetiu, "Energy and peak power savings potentlai of radiant cooling systems in US commercial buildings," *Energy Build.*, vol. November, 1999.

[29] C.-A. Roulet, J.P. Rossy, and Y. Roulet, "Using large radiant panels for indoor climate conditioning," *Energy Build.*, vol. 30, no. 2, pp. 121–126, Jun. 1999.

[30] T. Imanari, T. Omori, and K. Bogaki, "Thermal comfort and energy consumption of the radiant ceiling panel system. Comparison with the conventional all-air system," *Energy Build.*, vol. 30, no. 2, pp. 167–175, 1999.

[31] L. Z. Zhang, "Energy performance of independent air dehumidification systems with energy recovery measures," *Energy*, vol. 31, no. 8–9, pp. 1228–1242, Jul. 2006.

[32] J. Babiak, B. W. Olesen, and D. Petras, "REHVA Guidebook No 7: Low TemperatureHeating and High Temperature Cooling, 1st ed.," *Fed. Eur. Air-conditioning Assoc. Belgium*, 2009.

[33] ASHRAE 2009, "ANSI/ASHRAE Standard 138-2009, Method of testing for rating ceiling panels for sensible heating and cooling. Atlanta: ASHRAE."

[34] L. Zhang, X.-H. Liu, and Y. Jiang, "Experimental evaluation of a suspended metal ceiling radiant panel with inclined fins," *Energy Build.*, vol. 62, pp. 522–529, Jul. 2013.

[35] X. Han, X. Zhang, L. Wang, and R. Niu, "A novel system of the isothermal dehumidification in a room air-conditioner," *Energy Build.*, vol. 57, pp. 14–19, 2013.

[36] M. Andrés-Chicote, A. Tejero-González, E. Velasco-Gómez, and F. J. Rey-Martínez, "Experimental study on the cooling capacity of a radiant cooled ceiling system," *Energy Build.*, vol. 54, pp. 207–214, Nov. 2012.

[37] P. Vangtook and S. Chirarattananon, "An experimental investigation of application of radiant cooling in hot humid climate," *Energy Build.*, vol. 38, no. 4, pp. 273–285, Apr. 2006.

[38] K. A. Antonopoulos, M. Vrachopoulos, and C. Tzivanidis, "Experimental evaluation of energy savings in air-conditioning using metal ceiling panels," *Appl. Therm. Eng.*, vol. 18, no. 11, pp. 1129–1138, Nov. 1998.

[39] T. Catalina, J. Virgone, and F. Kuznik, "Evaluation of thermal comfort using combined CFD and experimentation study in a test room equipped with a cooling ceiling," *Build. Environ.*, vol. 44, no. 8, pp. 1740–1750, 2009.

[40] M. Tyegingras and L. Gosselin, "Comfort and energy consumption of hydronic heating radiant ceilings and walls based on CFD analysis," *Build. Environ.*, vol. 54, pp. 1–13, 2012.

[41] T. Kim, S. Kato, and S. Murakami, "Indoor cooling / heating load analysis based on coupled simulation of convection , radiation and HVAC control," *Build. Environ.*, vol. 36, pp. 901–908, 2001.

[42] G. Gan and S. B. Riffat, "Numerical simulation of closed wet cooling towers for chilled ceiling systems," *Appl. Therm. Eng.*, vol. 19, no. 12, pp. 1279–1296, Dec. 1999.

[43] J. H. Lim, J. H. Song, and S. Y. Song, "Development of operational guidelines for thermally activated building system according to heating and cooling load characteristics," *Appl. Energy*, vol. 126, pp. 123–135, 2014.

[44] "EnergyPlus 2016. EnergyPlus (energy simulation software and supplemental documentation), www.energyplus.gov, Department of Energy."

[45] J. D. Feng, F. Chuang, F. Borrelli, and F. Bauman, "Model predictive control of radiant slab systems with evaporative cooling sources," *Energy Build.*, vol. 87, pp. 199–210, 2015.

[46] Y. Khan, V. Rai, J. Mathur, and M. Bhandari, "Performance evaluation of radiant cooling system integrated with air system under different operational strategies," *Energy Build.*, vol. 97, pp. 118–128, 2015.

[47] J.-M. Seo, D. Song, and K. H. Lee, "Possibility of coupling outdoor air cooling and radiant floor cooling under hot and humid climate conditions," *Energy Build.*, vol. 81, pp. 219–226, Oct. 2014.

[48] F. Sodec, "Economic viability of cooling ceiling systems," *Energy Build.*, vol. 30, no. 2, pp. 195–201, Jun. 1999.

[49] "ASHRAE ANSI/ASHRAE Standard 55-2017: Thermal environmental conditions for human occupancy," *Am. Soc. Heat. Refrig. Air-Conditioning Eng.*, vol. 48, pp. 1–15, 2017.

[50] "ISO 7730: Ergonomics of the thermal environment-analytical determination and interpretation of thermal comfort using calculation of the PMV and PPD indices and local thermal comfort criteria," *Int. Organ. Stand. Geneva, Switz.*, pp. 3545–3566, 2005.

[51] R. A. Memon, S. Chirarattananon, and P. Vangtook, "Thermal comfort assessment and application of radiant cooling: A case study," *Build. Environ.*, vol. 43, no. 7, pp. 1185–1196, 2008.

[52] R. Zmeureanu, S. Iliescu, D. Dauce, and Y. Jacob, "Radiation from cold or warm windows: computer model development and experimental validation," *Build. Environ.*, vol. 38, no. 3,

pp. 427–434, Mar. 2003.

[53] T. Miyanaga, W. Urabe, and Y. Nakano, "Simplified human body model for evaluating thermal radiant environment in a radiant cooled space," *Build. Environ.*, vol. 36, no. 7, pp. 801–808, Aug. 2001.

[54] F. R. D Ambrosio Alfano, M. DellIsola, B. I. Palella, G. Riccio, and A. Russi, "On the measurement of the mean radiant temperature and its influence on the indoor thermal environment assessment," *Build. Environ.*, vol. 63, pp. 79–88, May 2013.

[55] "ISO 7726: Ergonomics of the thermal environment-instruments for measuring physical quantities. Geneva, Switzerland:," *Int. Stand. Organ. Stand.*, 1998.

[56] G. Meckler, "Innovative ways to save energy in new buildings," *HPAC Eng.*, vol. 58(5), pp. 87–92, 1986.

[57] N. H. . Scofield, C.M. & Des Champs, "HVAC design for classrooms: Divide and conquer. Heating, Piping and Air Conditioning," *Energy Build.*, 1993.

[58] B. D. R. Kosar, M. J. Witte, D. B. Shirey, and R. L. Hedrick, "Dehumidification Issues Of Standard 62-1989," *Ashrae J.*, no. March, pp. 71–75, 1998.

[59] W. Coad, "Conditioning Ventilation Air for Improved Performance and Air Quality," *HPAC Eng.*, vol. September, pp. 49–56, 1999.

[60] D. Stanke, "Dedicated-OA Systems," *Ashrae J.*, no. October, 2004.

[61] S. a. Mumma, "Overview of integrating dedicated outdoor air systems with parallel terminal systems," *ASHRAE Trans.*, vol. 107 PART., pp. 545–552, 2001.

[62] S. Mumma, "Preconditioning dedicated OA for improved IAQ—Part 2," *IAQ Appl. 2001*, vol. 3, no. 2, pp. 21–23, 2001.

[63] J. W. Jeong, S. A. Mumma, W. P. Bahnfleth, and D. Ph, "Energy conservation benefits of a dedicated outdoor air system with parallel sensible cooling by ceiling radiant panels," in *ASHRAE Transactions*, 2003, vol. 109 PART 2, pp. 627–636.

[64] S. A. Mumma, "Terminal equipments with DOAS: Series Vs. Parallel," *Eng. Syst.*, no. May, pp. 86–89, 2008.

[65] J. Murphy, "Smart dedicated outdoor air systems," *ASHRAE J.*, vol. 48, no. July, 2006.

[66] H. Crowther, "Design considerations for dedicated OA systems," *ASHRAE J.*, no. March, 2016.

[67] E. A. Vineyard, J. R. Sand, D. J. Durfee, and M. Meckler, "Performance characteristics for a desiccant system at two extreme ambient conditions," *ASHRAE Trans.*, vol. 108 PART 1, pp. 587–596, 2002.

[68] S. A. Mumma, "Preconditioning Dedicated OA for Improved IAQ — Part 1," *IAQ Appl.*, no. Spring, 2001.

[69] B. J. Murphy, "Total Energy Wheel Control In a Dedicated OA System," *ASHAE J.*, no. March, 2012.

[70] M. A. Sayegh, M. Hammad, and Z. Faraa, "Comparison of two methods of improving dehumidification in air conditioning systems: Hybrid system (refrigeration cycle - Rotary

desiccant) and heat exchanger cycle," *Energy Procedia*, vol. 6, pp. 759–768, 2011.

[71] J. Dieckmann, K. Roth, and J. Brodrick, "Dedicated outdoor air systems revisited," *ASHRAE J.*, vol. 49, no. 12, pp. 127–129, 2007.

[72] S. A. Mumma, "Decoupling OA and Space Thermal Control," *IAQ Appl.*, pp. 12–15, 2003.

[73] J. W. Jeong, S. a. Mumma, and W. P. Bahnfleth, "Energy conservation benefits of a dedicated outdoor air system with parallel sensible cooling by ceiling radiant panels," *ASHRAE Trans.*, vol. 109 PART 2, pp. 627–636, 2003.

[74] S. A. Mumma and K. M. Shank, "Achieving dry outside air in an energy-efficient manner," *ASHRAE Trans.*, vol. 107, pp. 553–561, 2001.

[75] C. L. Conroy and S. A. Mumma, "Ceiling radiant cooling panels as a viable distributed parallel sensible cooling technology integrated with dedicated outdoor air systems," in *ASHRAE Transactions*, 2001, vol. 107 PART., pp. 578–585.

[76] X. Hao, G. Zhang, Y. Chen, S. Zou, and D. J. Moschandreas, "A combined system of chilled ceiling, displacement ventilation and desiccant dehumidification," *Build. Environ.*, vol. 42, pp. 3298–3308, 2007.

[77] E. M. Saber, R. Iyengar, M. Mast, F. Meggers, K. W. Tham, and H. Leibundgut, "Thermal comfort and IAQ analysis of a decentralized DOAS system coupled with radiant cooling for the tropics," *Build. Environ.*, vol. 82, pp. 361–370, 2014.

[78] D. Song, T. Kim, S. Song, S. Hwang, and S.-B. Leigh, "Performance evaluation of a radiant floor cooling system integrated with dehumidified ventilation," *Appl. Therm. Eng.*, vol. 28, no. 11–12, pp. 1299–1311, 2008.

[79] D. Stanke, "Single-zone and dedicated-OA systems," *ASHAE J.*, vol. 46, no. 10, pp. 12–21, 2004.

[80] D. B. Crawley *et al.*, "EnergyPlus: Creating a new-generation building energy simulation program," *Energy Build.*, vol. 33, no. 4, pp. 319–331, 2001.

[81] D. B. Crawley, L. K. Lawrie, F. C. Winkelmann, and C. O. Pedersen, "EnergyPlus: New Capabilities in a Whole-Building Energy Simulation Program," *Build. Simul. 2001*, pp. 51–58, 2001.

[82] N. Enteria *et al.*, "Experimental heat and mass transfer of the separated and coupled rotating desiccant wheel and heat wheel," *Exp. Therm. Fluid Sci.*, vol. 34, no. 5, pp. 603–615, 2010.

[83] J. Mathur, V. Garg, and V. Murthy, *INDIAN WEATHER DATA 2017*. ISHRAE, 2017.

[84] I. Nexant, "M & V Guidelines: Measurement and Verification for Federal Energy Projects. Version 3.0," *US Dep. Energy*, no. April, 2008.

LIST OF PUBLICATIONS

1. Prateek Srivastava, Yasin Khan, Jyotirmay Mathur, Mahabir Bhandari, Rana Veer Pratap "Calibrated Simulation Analysis for Integration of Evaporative Cooling and Radiant Cooling System for Different Indian Climatic Zones". **Journal of Building Engineering, 2018**.

2. Yasin Khan, Gaurav Singh, Jyotirmay Mathur, Mahabir Bhandari, Prateek Srivastava, Performance Assessment of Radiant Cooling System Integrated with Desiccant Assisted DOAS with Solar Regeneration. **Applied Thermal Engineering, 2017.**

3. Mahabir Bhandari, Yasin Khan, Prateek Srivastava, Vivek Kumar, Jyotirmay Mathur Development of Heat Transfer Model for Ceiling Radiant Cooling Panel through Combined Experimental and Simulation Study, **ASHRAE Transaction, 2017**.

4. Prateek Srivastava, Yasin Khan, Jyotirmay Mathur, Mahabir Bhandari, Analysis of radiant cooling system integrated with thermal storage and cooling tower for composite climatic conditions, **Building Simulation 2017**, San Francisco, California, USA. August 07-09, 2017.

5. Jyotirmay Mathur, Mahabir Bhandari, Robin Jain, Yasin Khan, Prateek Srivastava**,** Analysis of Radiant Cooling System Configurations Integrated with Cooling Tower for Different Indian Climatic Zones, **ASHRAE Annual Conference,** St. Louis, MO, USA, June 25-29, 2016.

6. Anuj Mathur, Prateek Srivastava, Jyotirmay Mathur, Mahabir Bhandari, Performance evaluation of ceiling radiant cooling system in composite climate, **14th International conference of the International Building Performance Simulation Association**, Hyderabad, India, December 7-9, 2015.

BRIEF BIO-DATA OF AUTHOR

Mr Prateek Srivastava is a Research scholar in Centre for Energy and Environment, Malaviya National Institute of Technology (MNIT), Jaipur. He has received his B.Tech. degree in Mechanical Engineering from Rajasthan Technical University, Kota in 2011. He has received his Master's degree from NIT, Silchar in Thermal Engineering in 2014 and then joined the Ph.D. program in July 2014 under the supervision of Dr Jyotirmay Mathur, (Professor, Centre for Energy and Environment, MNIT, Jaipur) and Dr Mahabir Bhandari (Scientist, Oak Ridge National Laboratory, USA). During his PhD he won Building Energy Efficiency Higher & Advanced Network (BHAVAN) internship sponsored by Indo-U.S. Science and Technology Forum (IUSSTF) and successfully completed six-month internship at Oak Ridge National Laboratory, TN, USA. His research interests are Heating Ventilation Air Conditioning, Building Energy Efficiency, Green Buildings, Energy simulations, CFD. Prateek has published several research papers in national and international conferences and journals.

Appendix I: Simulation Results of Warm & Humid, Composite and Temperate Climatic Conditions of Chapter 4

Warm & Humid climate

This is the most unfavourable climate zone for the radiant cooling system as it has a very high latent load as compared to other climates. Chennai has been selected for this climate zone. The annual energy consumption for the different strategy for Chennai climate has been shown in below Figure 7-1. The annual energy consumption of conventional all-air system for conventional side of the building is 436 MWh. Out of that 101 MWh energy is consumed in pumping the air for meeting the load. In the Strategy-1, where radiant cooling system integrated with cooling coil based DOAS, i.e. sensible load is met by the RCS and providing outdoor air and meeting latent load is done by DOAS. Strategy-1 consumes 376 MWh i.e. 14% energy saving over a conventional system. By changing the air system (Conv case) to RCS (Strategy-1) the fan energy is reduced by 72%. In the Strategy-2; the annual energy consumption is 354 MWh which gives 19% energy saving over a conventional system. In this strategy, the cooling energy delivered by the ERW is almost 182.6 MWh which reduces the electric energy consumption of DOAS chiller by 33.8 MWh. Addition of ERW in Strategy-2 is exchanging heat of outdoor air with return air. ERW is reducing load of the cooling coil which is reducing DOAS chiller energy consumption. Addition of ERW in the air path is additionally increasing pressure drop across the fan; energy consumption of the fan motor is increased to 11.7 MWh. In the Strategy-3 the annual energy consumption is 357 MWh which gives 18% energy saving over a conventional system (Conv case). In this strategy sensible wheel is added after the LT coil and sensible wheel is exchanging heat with the return air. Sensible wheel is reducing load on the cooling coil and increasing the temperature of the supply air entering the building. The sensible wheel reduces the load on DOAS chiller by 20 MWh. However, in this strategy, the radiant side chiller energy and fan energy consumption is increased by 11.9 MWh and 6.2 MWh respectively. Therefore, the energy saving achieved in DOAS chiller is compensated in radiant side chiller and fan energy.

Figure 7-2 shows the comparison of the annual thermal energy of the low-temperature cooling coil in Strategy 1, 2 &3 for the hot and dry climate. Strategy-1 has the total air load on the cooling coil and delivering the cooling energy of 1043 MWh. In Strategy-2 addition of the ERW has reduced the load on the cooling coil and found to

save 17% savings in the thermal energy. In Strategy-3 a sensible wheel is added in the air path along with
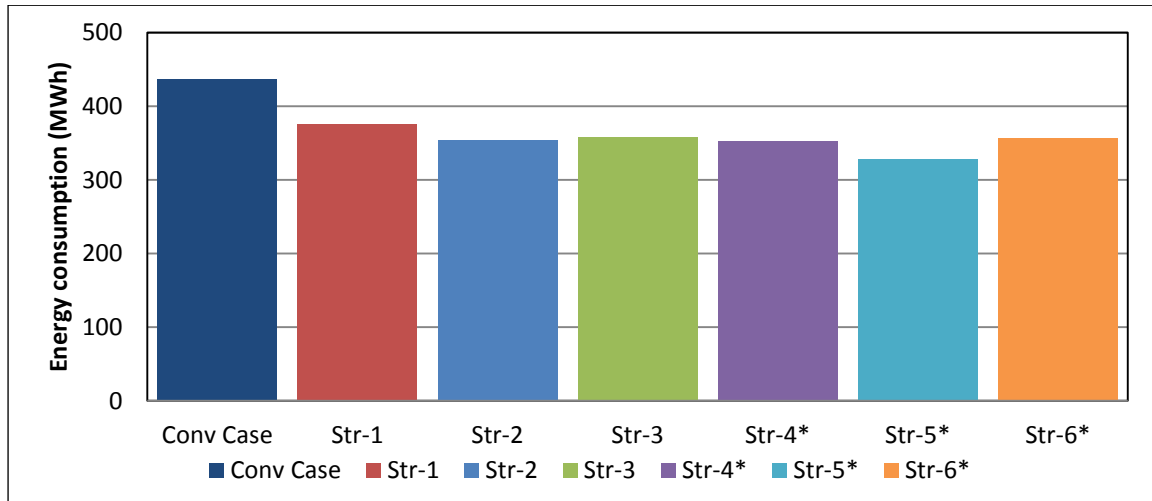

Figure 7-1: Comparison of annual energy consumption for different Strategies coupled with RCS for warn and humid climate zone
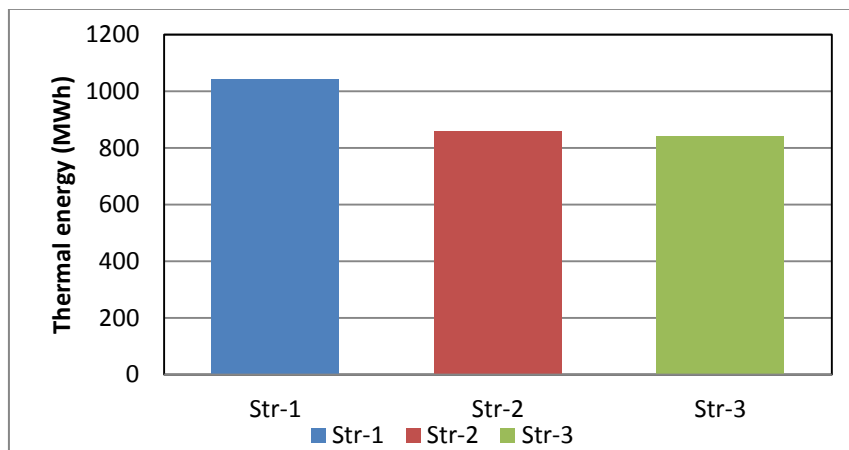

Figure 7-2: Comparison of the annual thermal energy of the low-temperature cooling coil in Strategy 1, 2 &3 for Warm and humid climate
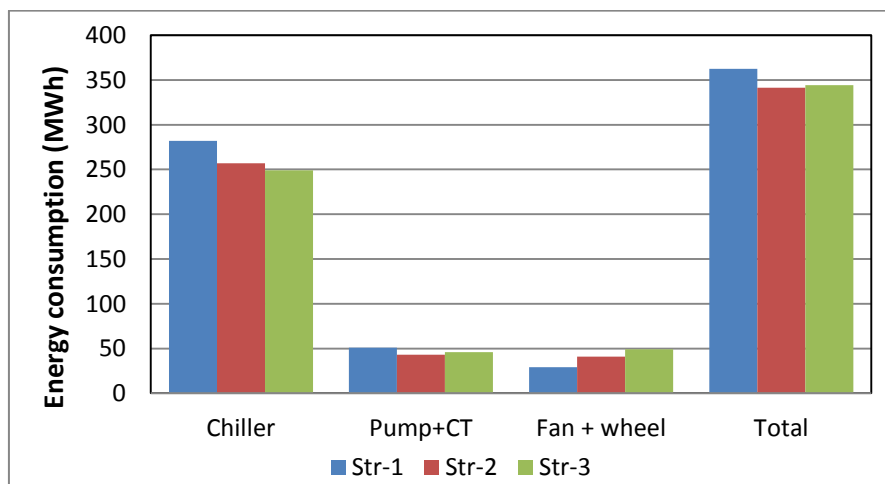

Figure 7-3: Comparison of energy consumption of chiller, pump + cooling tower, fan + wheel & total of the cooling coil based Strategy 1, 2 &3.

ERW and cooling coil, has further reduced the thermal energy to 19%. Strategy-2 is found to be most suitable for cooling coil based strategy Warm and Humid climate. Figure 7-3 shows the comparison of energy consumption of chiller, pump + cooling tower, fan + wheel & total of the cooling coil based Strategy 1, 2 &3.

Now desiccant based strategies i.e. Strategy-4* to Strategy-6* will be discussed for warm and humid climate. DOAS of Strategy-4* comprise of desiccant wheel, HTTP and a HT coil. In the Strategy-4* the annual energy consumption is 353.2 MWh which provide 19% energy saving as compared to the conventional system. RCS is responsible for meeting the sensible load of the radiant side of the building. The energy consumption in the RCS is 142 MWh. DOAS is responsible for providing outdoor air and meeting the latent load. The energy consumption in dehumidification and sensible cooling of supply air is 1.95 MWh and 140 MWh respectively. To avoid attainment of saturation of the desiccant wheel regeneration is required, to regenerate desiccant wheel heating of air is done using HTTP. The energy consumption in regeneration and fan motor is 94.4 MWh and 44.1 MWh respectively, the magnitude of energy consumption in regeneration is comparatively higher as compared to Hot and Dry climate due to high latent load. DOAS of Strategy-5* comprise of desiccant wheel, HTTP, sensible wheel and a HT coil. In the Strategy-5* the annual energy consumption is 327.6 MWh which provide 25% energy saving over a conventional system. The energy consumption in the radiant system is 141 MWh. Addition of sensible wheel is exchanging heat of supply side with the return side as a result it is improving coefficient of performance of the HTTP. In this strategy, the energy consumption in regeneration is reduced by 27.4 MWh. The sensible wheel also provides almost 15 MWh of sensible cooling of supply air. Addition of sensible wheel in the air path has increased the pressure drop, the fan energy is increased by 9 MWh. The energy consumption in sensible cooling of supply air is reduced by 11 MWh. DOAS of Strategy-6* comprise of desiccant wheel, IDEC and a HT coil. In the Strategy-6* the annual energy consumption is 356.3 MWh which is equal to 18% energy saving over a conventional system. The energy consumption in the radiant cooling system is 145 MWh. The energy consumption in sensible cooling of supply air is slightly lower as compared to the Strategy-4. However, the regeneration energy consumption in this strategy is same as Strategy-4*. The energy consumption in IDEC is 12.8 MWh. The energy consumption in the fan is 46.2 MWh due to increased pressure drop in the air path. Based on the analysis of desiccant wheel based strategy it was found in Strategy-5* sensible wheel is performed

better to improve the performance of HTTP as compared to IDEC in Strategy-6*. Strategy-5 is found to be a most suitable strategy in desiccant wheel based strategy for the Warm and Humid climate in desiccant wheel based strategies. Figure 7-4 shows the comparison of the annual thermal energy regeneration and cooling (FC coil and HT coil) in Strategy 4, 5 &6 for the Warm and humid climate. As compared to Strategy-4*, the addition of sensible wheel in Strategy-5* reduces both in terms of thermal energy in cooling and regeneration. In Strategy-6* the thermal energy in sensible cooling of air is reduced to 17% compared to Strategy-4* and the thermal energy for regeneration is same as Strategy-4*. Figure 7-5 shows the comparison of energy consumption of chiller, pump + cooling tower, fan + wheel IDEC, heat pump & total of the desiccant wheel based Strategy 4*, 5* &6*.
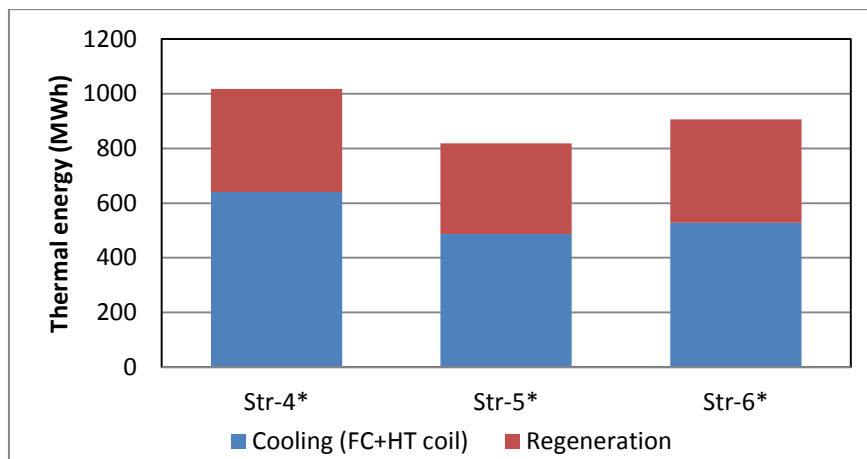

Figure 7-4: Comparison of annual thermal energy in regeneration and cooling (FC coil and HT coil) in Strategy 4*, 5* &6*
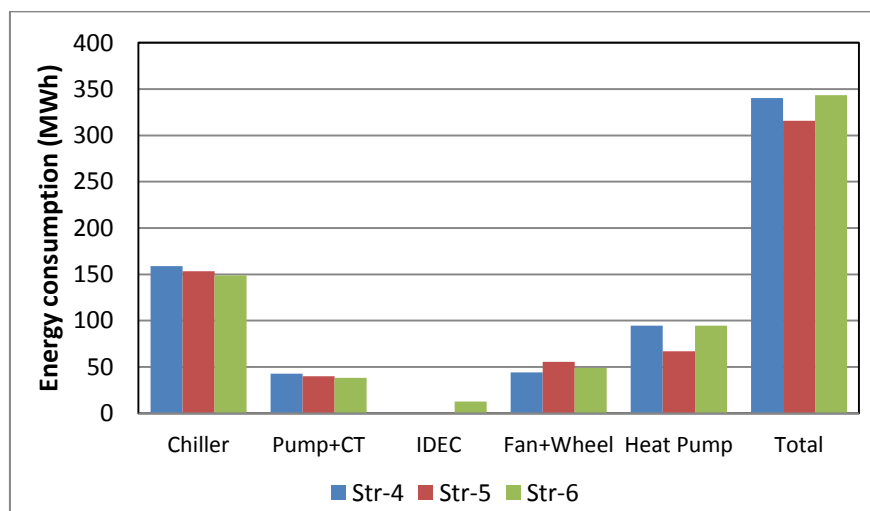

Figure 7-5: Comparison of energy consumption of chiller, pump + cooling tower, fan + wheel IDEC, heat pump & total of the desiccant wheel based Strategy 4*, 5* &6*.

Composite climate

171

Jaipur has been selected for this climate zone. The annual energy consumption for the different strategies for Composite climate has been shown in below Figure 7-6. The energy consumption for conventional air conditioning system in the Conv case is 383 MWh. The total load of the building is met by convection and conduction of air, 116 MWh is consumed by the fan motor. In Strategy-1 radiant cooling system integrated with DOAS was found to consume 292 MWh and providing 24% saving compared to the conventional case. In Strategy-1 the conventional air system is replaced with the RCS, in RCS air is only supplied for providing outdoor air and meeting latent load and around 74.9% fan energy is saved compared to the conventional case. In the Strategy-2 the annual energy consumption is 281 MWh which gives 27% energy saving over a conventional system. In this strategy ERW is added before LT coil, ERW is exchanging energy with the return air and reducing load of the cooling coil. In this strategy, the cooling energy delivered by the ERW is almost 91.2 MWh which reduces the electric energy consumption of DOAS chiller by 23.4 MWh. Addition of ERW in the air path has added higher pressure drop across the fan and fan motor energy is increased to 11.68 MWh compared to Strategy-1. In the Strategy-3 the annual energy consumption is 287 MWh which gives 25% energy saving over a conventional system. The sensible wheel is added in this strategy after the cooling coil. Sensible wheel is exchanging heat with the return air as a result it is reducing load of the cooling coil and also increasing the temperature of the supply air entering the building. The sensible wheel reduces the load on DOAS chiller, saves 13.7 MWh in electric energy consumption. However, in this strategy, the radiant side chiller energy and fan energy consumption is increases by 11.6 MWh and 8.9 MWh respectively. Therefore, the energy saving achieved in DOAS chiller is compensated in radiant side chiller and fan energy.

Figure 7-7 shows the Comparison of the annual thermal energy of the low-temperature cooling coil in Strategy 1, 2 & 3 for the Composite climate. In Strategy-1, the total cooling energy in the supply air was taken care by cooling coil was 719.3 MWh. In Strategy-2, the addition of ERW has reduced the load by 16% and in Strategy-3 the addition of sensible wheel has reduced the load to 16.4% compared to Strategy-1. Based on the result Strategy-2 was found to be a most suitable strategy in cooling coil based strategy in Composite climate. Figure 7-8 shows the comparison of energy consumption of chiller, pump + cooling tower, fan + wheel & total of the cooling coil based Strategy 1, 2 &3.
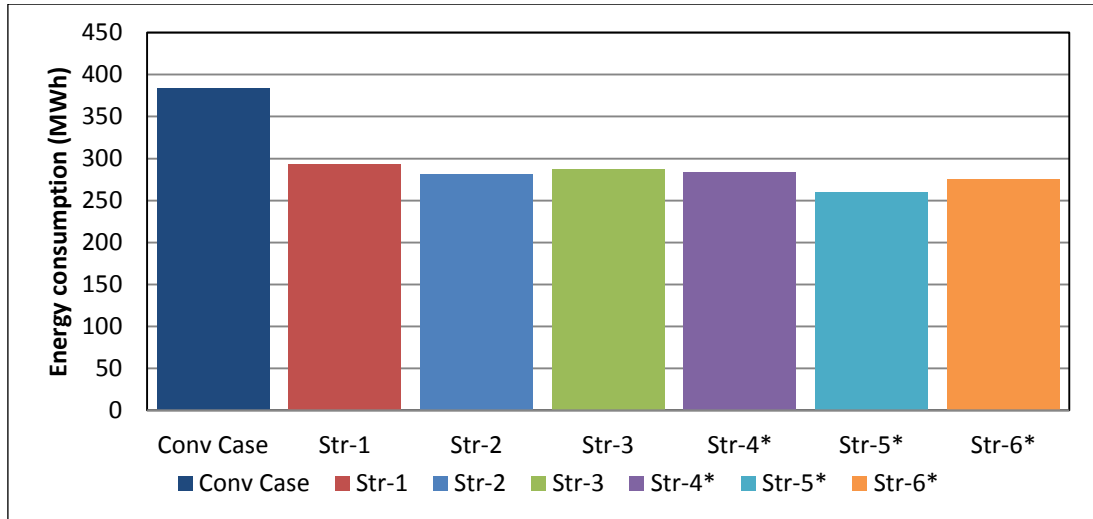
Figure 7-6: Comparison of annual energy consumption for different Strategies coupled with RCS for composite climate zone
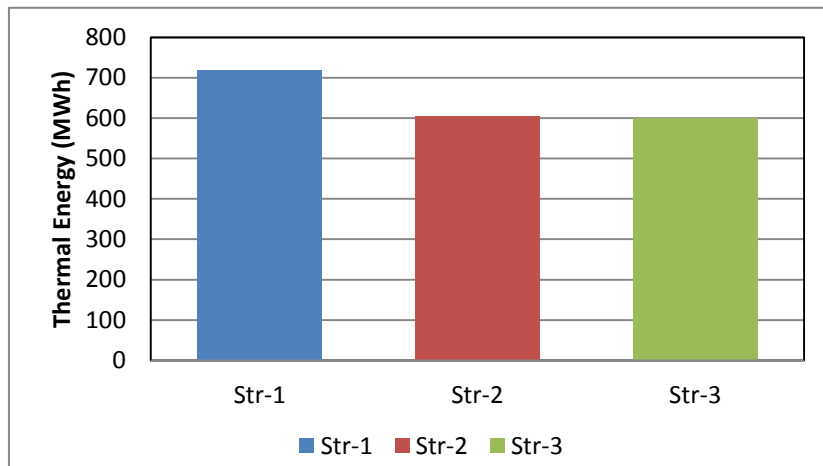

Figure 7-7: Comparison of the annual thermal energy of the low-temperature cooling coil in Strategy 1, 2 &3 for Composite climate
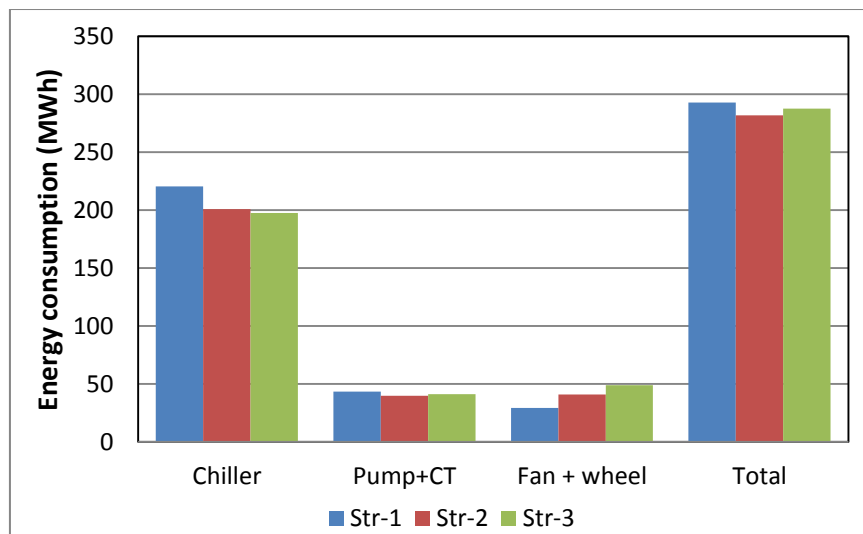

Figure 7-8: Comparison of energy consumption of chiller, pump + cooling tower, fan + wheel & total of the cooling coil based Strategy 1, 2 &3.

Now desiccant based strategies i.e. Strategy-4* to Strategy-6* will be discussed for composite climate. DOAS of Strategy-4* comprise of desiccant wheel, HTTP and a HT coil. In the Strategy-4* the annual energy consumption is 283.7 MWh which provide 24% energy saving as compared to the conventional system. The energy consumption in the radiant system is 119.6 MWh. DOAS is responsible for providing outdoor air and meeting the latent load. The energy consumption in dehumidification and sensible cooling of supply air is 1.9 MWh and 98.4 MWh respectively. The energy consumption in regeneration and fan motor is 50 MWh and 37.5 MWh respectively. DOAS of Strategy-5* comprise of desiccant wheel, HTTP, sensible wheel and a HT coil. In the Strategy-5* the annual energy consumption is 256.3 MWh which provide 31% energy saving over a conventional system. The energy consumption in the radiant system is 120.1 MWh. Addition of sensible wheel is exchanging heat of supply side with the return side as a result it is improving coefficient of performance of the HTTP. In this strategy, the energy consumption in regeneration is decreased by 21 MWh by sensible heating of return air by sensible wheel. The sensible wheel also provide almost 23 MWh sensible cooling of supply air, however because of high-pressure drop the fan energy is increased by 8 MWh compared to Strategy-4*. The energy consumption in dehumidification and sensible cooling of supply air is reduced. In the Strategy-6* annual energy consumption is 275.3 MWh which is equal to 28% energy savings over a conventional system. The energy consumption in the radiant cooling system is 120.3 MWh. The energy consumption in dehumidification and sensible cooling of supply air is lower than Strategy-4*, the addition of IDEC in the supply path has reduced the load on cooling coil and increased pressure drop in the supply path. However, the regeneration energy consumption in this strategy is almost same as Strategy-4. The energy consumption in IDEC is 12.8 MWh. Strategy-5* is found to be most suitable for the Composite climate in desiccant wheel based strategies.

Figure 7-9 shows the comparison of annual thermal energy in regeneration and cooling (FC coil and HT coil) in Strategy 4*, 5* & 6*. In Strategy-4* the total cooling energy in free cooling coil and LT coil is 532 MWh and thermal energy consumed in regeneration is 200MWh. Addition of sensible wheel in Strategy-5* has reduced the cooling load to 17% and regeneration load to 3%. In Strategy-6* addition of IDEC has reduced the cooling load to 14%. Based on the results Strategy-5* was found to be most suitable for desiccant wheel based strategy for composite climate. Figure 7-10 shows the

comparison of energy consumption of chiller, pump + cooling tower, fan + wheel IDEC, heat pump & total of the desiccant wheel based Strategy 4*, 5* &6*.
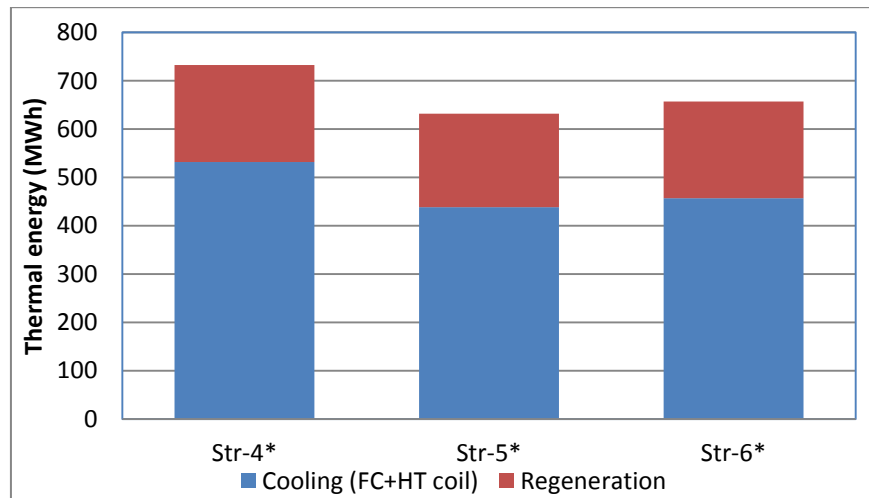

Figure 7-9: Comparison of annual thermal energy in regeneration and cooling (FC coil and HT coil) in Strategy 4*, 5* &6*
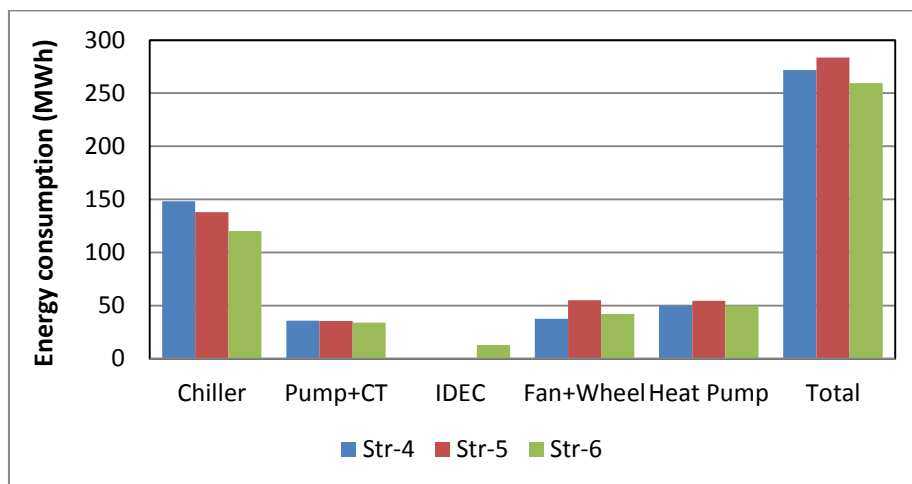

Figure 7-10: Comparison of energy consumption of chiller, pump + cooling tower, fan + wheel IDEC, heat pump & total of the desiccant wheel based Strategy 4*, 5* &6*.

Temperate climate

Bengaluru has been considered for the temperate climatic zone. The annual energy consumption for different strategies for Bengaluru climate has been shown in Figure 7-11. The energy consumption for conventional air conditioning system is 317.8 MWh out of which 103 MWh is consumed by fan motor. In Strategy-1 radiant cooling system integrated with DOAS was found to consume 232 MWh and providing 27% saving compared to conventional case and around 71.7% fan energy is saved compared to conventional case. In the Strategy-2 the annual energy consumption is 241 MWh which gives 24% energy saving over conventional system. In this strategy ERW is added before

the LT coil, ERW is exchanging energy with the return air, ERW is reducing load on the cooling coil. The cooling energy delivered by the ERW is almost 6.9 MWh which reduces the electric energy consumption of DOAS chiller by 2.96 MWh. Due to lower temperature difference between the temperature of outdoor air and the return air ERW is unable to provide much energy savings. Addition of ERW in the air path has increased the pressure drop across the fan, the fan motor energy consumption is increased to 11.6 MWh compared to Strategy-1. Overall addition of ERW has increased the energy consumption of Strategy-2 compared to Strategy-1. In the Strategy-3 the annual energy consumption is 245 MWh which gives 23% energy saving over conventional system. The sensible wheel has reduces the load on DOAS chiller which saves 1 MWh in electric energy consumption. However, in this strategy the radiant side chiller energy and fan energy consumption is increased by 8.92 MWh and 6.27 MWh respectively. Therefore, the energy saving achieved in DOAS chiller is compensated in radiant side chiller and fan energy. In temperate climate addition of ERW in Strategy-2 and addition of ERW and sensible wheel in Strategy-3 has provided penalty on energy saving as in this climate round the year ambient condition are very moderate and magnitude of the temperature difference between the temperature of outdoor air and the return air is small.
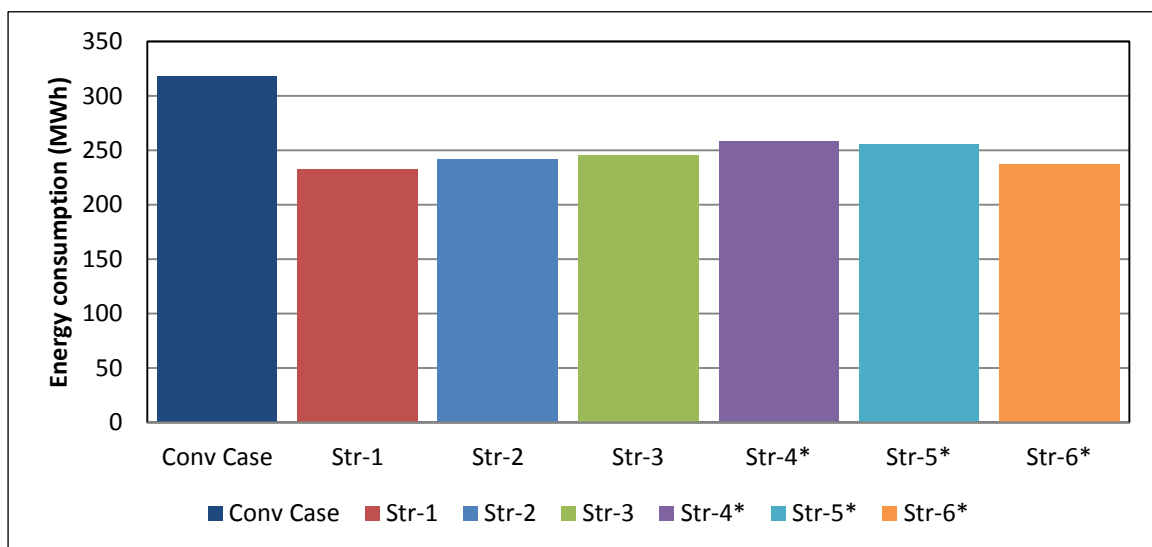

Figure 7-11: Comparison of annual energy consumption for different Strategies coupled with RCS for temperate climate zone.

Figure 7-12 shows the comparison of annual thermal energy of the low temperature cooling coil. In Strategy-1 the total cooling load on the cooling coil is 547.9 MWh. Addition of the ERW has increased the load of the cooling coil by 5% because in most of the period of the year Bengaluru has a lower humidity in the ambient as

compared to room air. In Strategy-3 addition of sensible wheel has does not change the load significantly and is almost same as Strategy-5. Strategy-1 was found to be most suitable in cooling coil based strategy in temperate climate. Figure 7-13 shows the comparison of energy consumption of chiller, pump + cooling tower, fan + wheel & total of the cooling coil based Strategy 1, 2 &3.
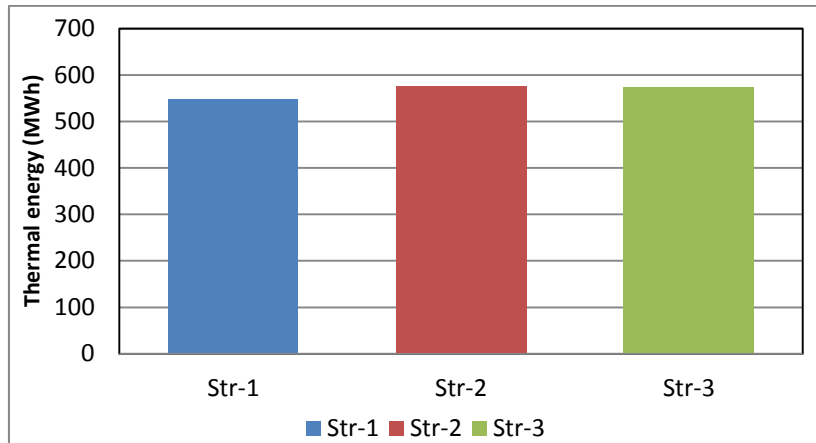

Figure 7-12: Comparison of annual thermal energy of the low temperature cooling coil in Strategy 1, 2 &3
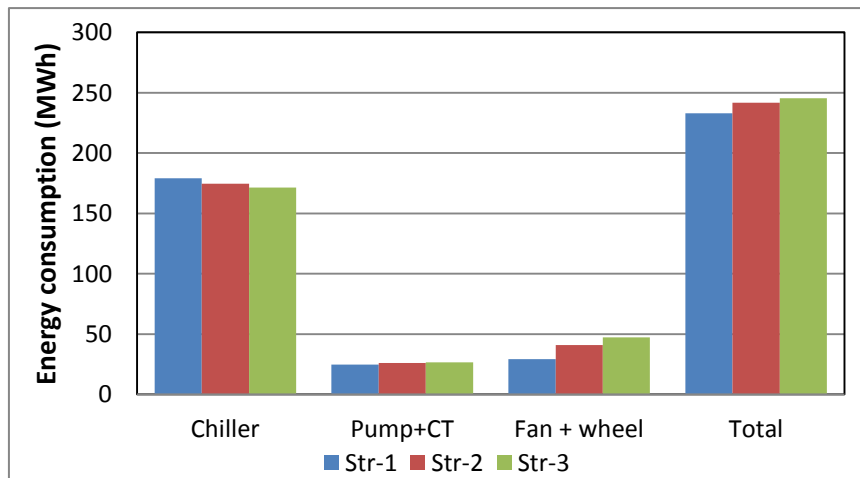

Figure 7-13: Comparison of energy consumption of chiller, pump + cooling tower, fan + wheel & total of the cooling coil based Strategy 1, 2 &3.

Now desiccant based strategies i.e. Strategy-4* to Strategy-6* will be discussed for temperate climate. DOAS of Strategy-4* comprise of desiccant wheel, HTTP and a HT coil. In the Strategy-4* the annual energy consumption is 547.9 MWh which provide 19% energy saving as compared to the conventional system. The energy consumption in radiant system is 106.6 MWh. DOAS is responsible for meeting the latent load of the building. The energy consumption in dehumidification and sensible cooling of supply air is 1.9 MWh and 32.1 MWh respectively. Regeneration of desiccant wheel is done by

heating the air by HTTP to avoid attainment of saturation of the wheel. The energy consumption in regeneration and fan motor is 78.9 MWh and 40.2 MWh respectively. DOAS of Strategy-5* comprise of desiccant wheel, HTTP, sensible wheel and a HT coil. In the Strategy-5* the annual energy consumption is 255.5 MWh which provide 16% energy saving over conventional system. The energy consumption in radiant system is 105 MWh. Addition of sensible wheel is exchanging heat of supply side with the return side as a result it is improving coefficient of performance of the HTTP. In this strategy, the energy consumption in regeneration is reduced by 16 MWh by sensible heating of return air by sensible wheel. Addition of sensible wheel has increased pressure drop in the air path; the fan energy is increases by 15 MWh. The energy consumption in dehumidification and sensible cooling of supply air is increased by 11.4 MWh. DOAS of Strategy-6* comprise of desiccant wheel, HTTP, IDEC and a HT coil. In the Strategy-6* annual energy consumption is 237.3 MWh which is equal to 25% energy saving over conventional system. The energy consumption in radiant cooling system is 101 MWh. The energy consumption in dehumidification and sensible cooling of supply air is 21 MWh. However, the regeneration energy consumption in this strategy is almost same as Strategy-4. The energy consumption in IDEC is 12.8 MWh.
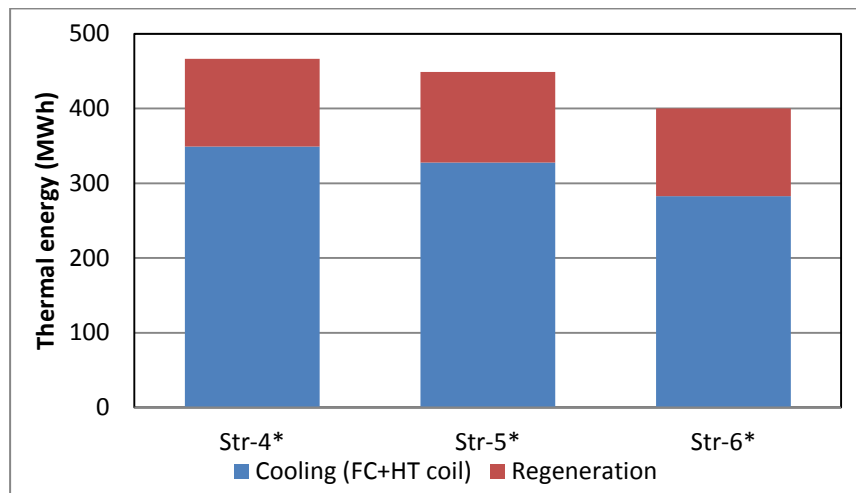

Figure 7-14: Comparison of annual thermal energy in regeneration and cooling (FC coil and HT coil) in Strategy 4*, 5* &6*

Figure 7-9 shows the comparison of the annual thermal energy in regeneration and cooling (FC coil and HT coil) in Strategy 4*, 5* &6*. As compared to Strategy-4*, the addition of sensible wheel in Strategy-5* reduces load in terms of thermal energy in cooling by 6% and has slightly increased the load of regeneration. In Strategy-6* the thermal energy in sensible cooling of air is reduced to 19% compared

to Strategy-4* and the thermal energy for regeneration is same as Strategy-4*. Based on the analysis of desiccant based strategies it is found sensible wheel in Strategy-5* is providing savings in decreasing cooling load in supply side and increasing load in the regeneration side and in case of Strategy-6* IDEC in providing better cooling as compared to sensible wheel in Strategy-5*. Strategy-6* is found to be most suitable for temperate climate.
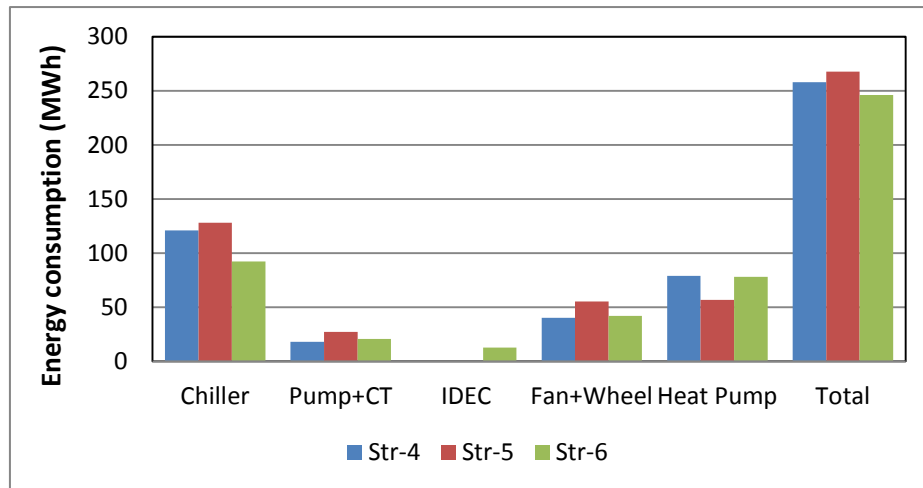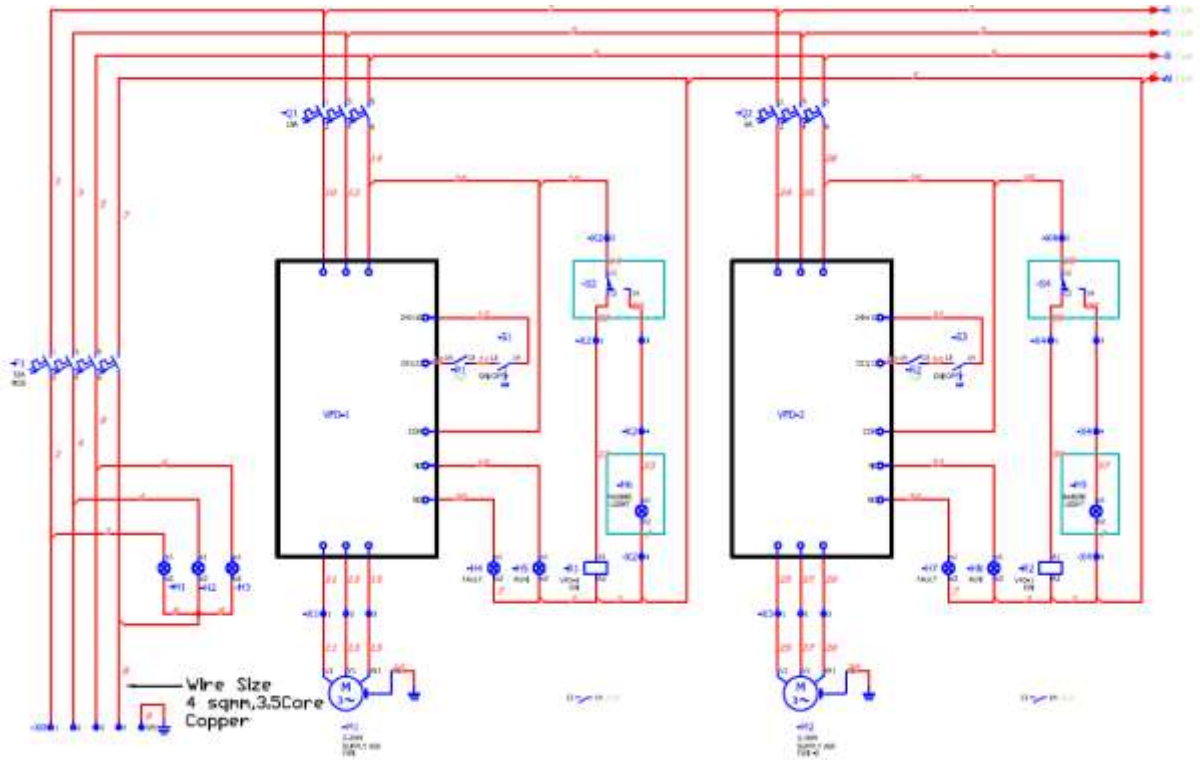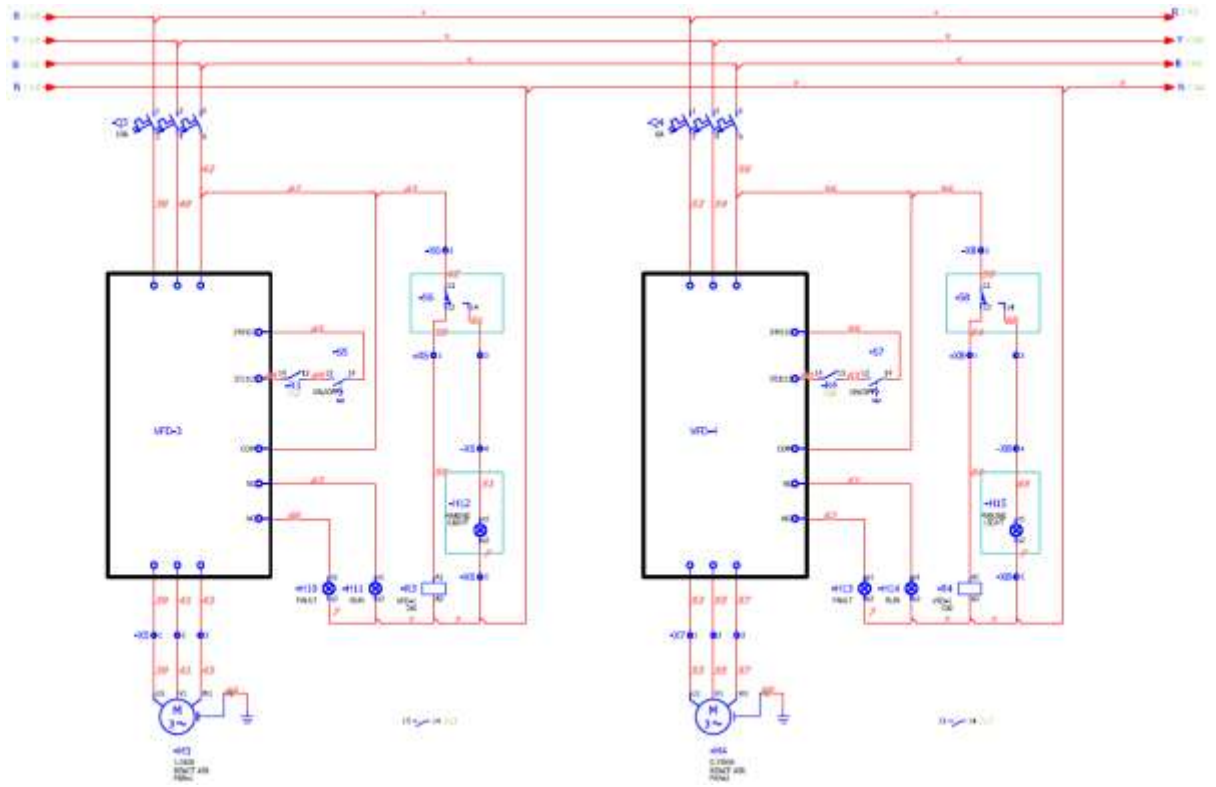

Figure 7-15: Comparison of energy consumption of chiller, pump + cooling tower, fan + wheel IDEC, heat pump & total of the desiccant wheel based Strategy 4*, 5* &6*.
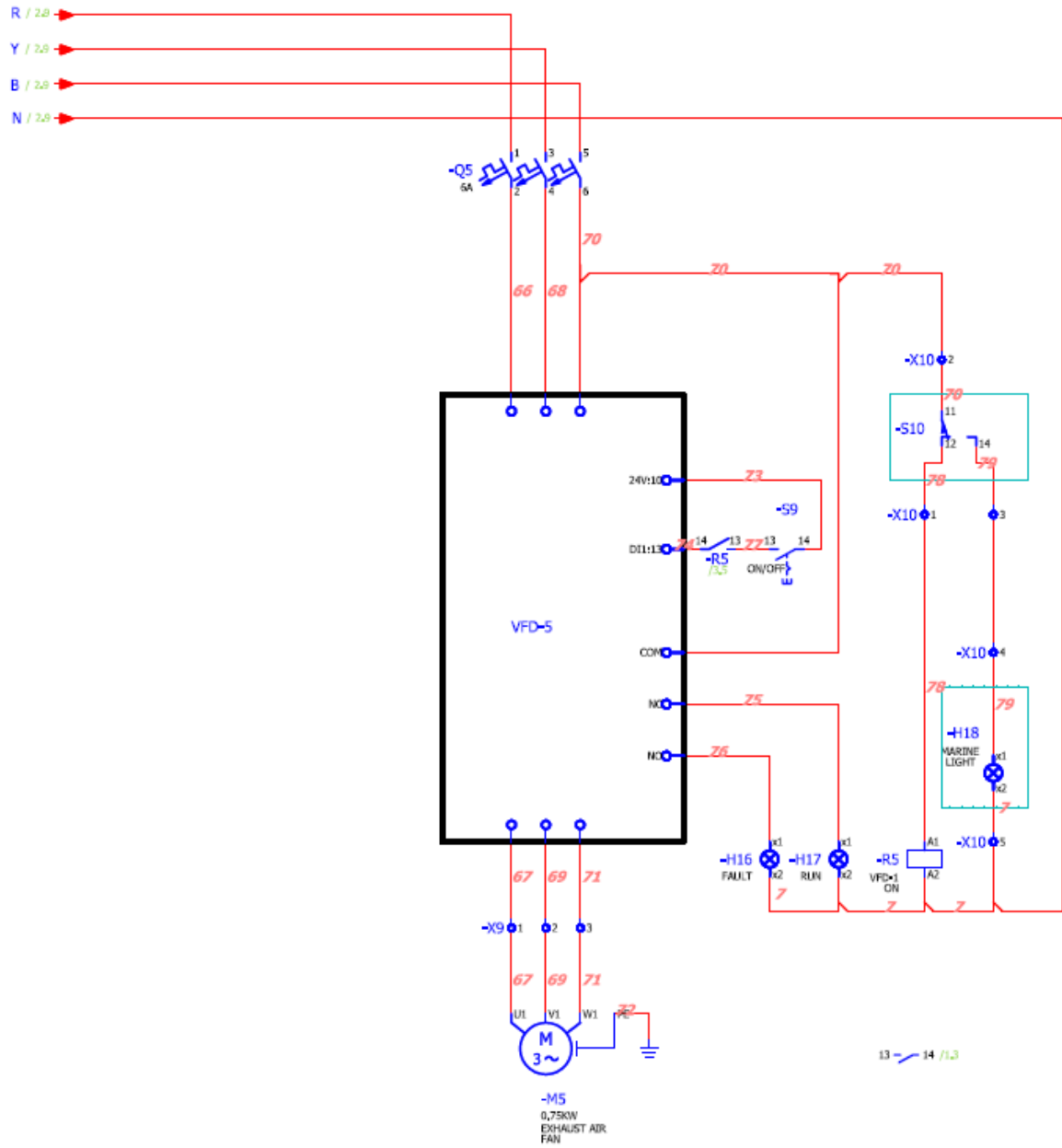
Figure 7-14 shows the comparison of the annual thermal energy in regeneration and cooling (FC coil and HT coil) in Strategy 4*, 5* &6*. As compared to Strategy-4*, the addition of sensible wheel in Strategy-5* reduces load in terms of thermal energy in cooling by 6% and has slightly increased the load of regeneration. In Strategy-6* the thermal energy in sensible cooling of air is reduced to 19% compared to Strategy-4* and the thermal energy for regeneration is same as Strategy-4*. Based on the analysis of desiccant based strategies it is found sensible wheel in Strategy-5* is providing savings in decreasing cooling load in supply side and increasing load in the regeneration side and in case of Strategy-6* IDEC in providing better cooling as compared to sensible wheel in Strategy-5*. Strategy-6* is found to be most suitable for temperate climate. Figure 7-15 shows the comparison of energy consumption of chiller, pump + cooling tower, fan + wheel IDEC, heat pump & total of the desiccant wheel based Strategy 4*, 5* &6*.

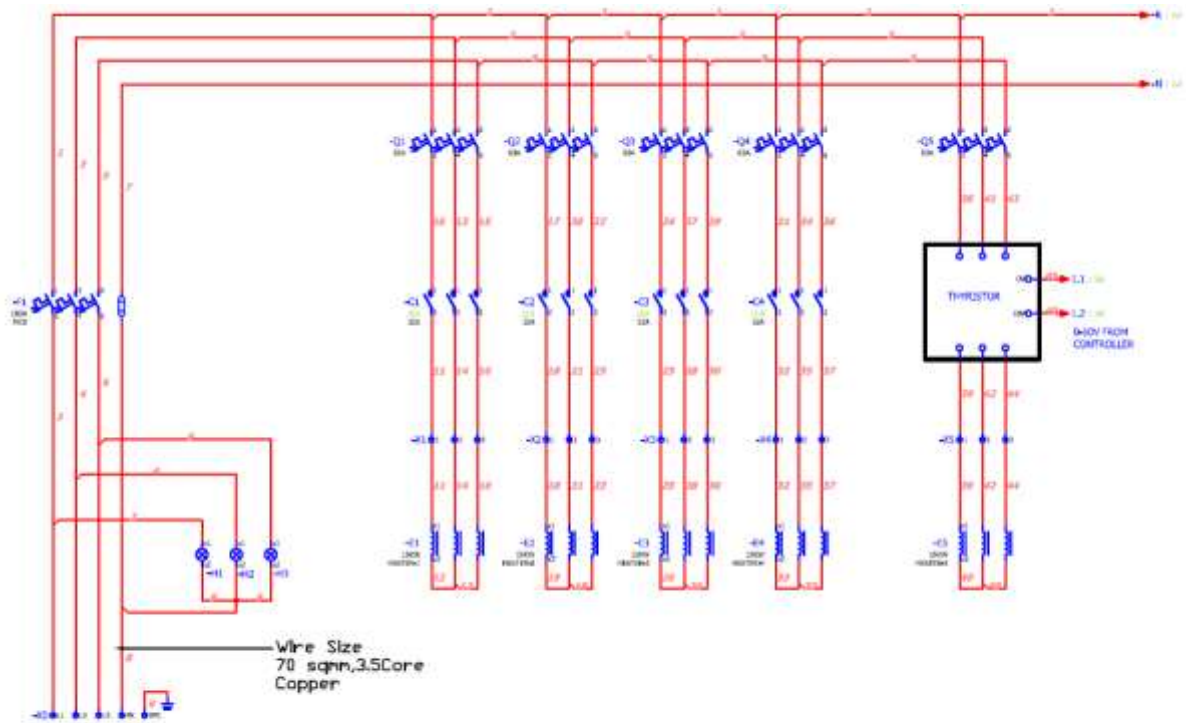**Appendix II: Wiring Diagram and Specification of Experimental Setup of Chapter 5**

Wiring diagram of fans in modular DOAS

R / 2.0
Y / 2.0
B / 2.0
N / 2.0

-Q5
6A

1 3 5
2 4 6

70

66 68

20 20

-X10 2

70

-S10

11

12 14

78

-X10 1 3

24V:10 73

-S9

DI1:13 74 14 13 77 13 14

-R5
/13

ON/OFF

-X10 4

78 79

COM

-H18
MARINE
LIGHT

x1

NC 75

x2

NO 76

VFD-5

67 69 71

-X9 1 2 3

67 69 71

U1 V1 W1 72

-M5
0,75KW
EXHAUST AIR
FAN

-H16
FAULT

x1
x2

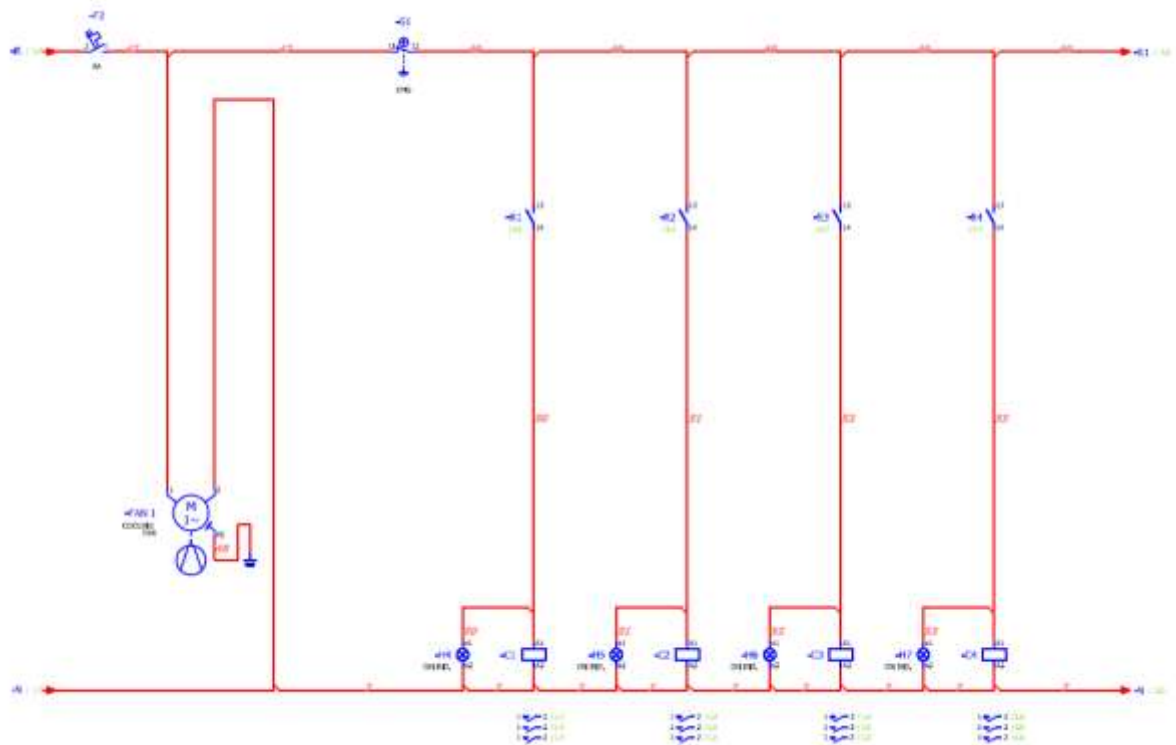-H17
RUN

x1
x2

-R5
VFD-1
ON

A1
A2

-X10 5

7 7 7

13 14 /13

Wiring diagram of the heater in modular DOAS

Wire Size
70 sqmm,3.5Core
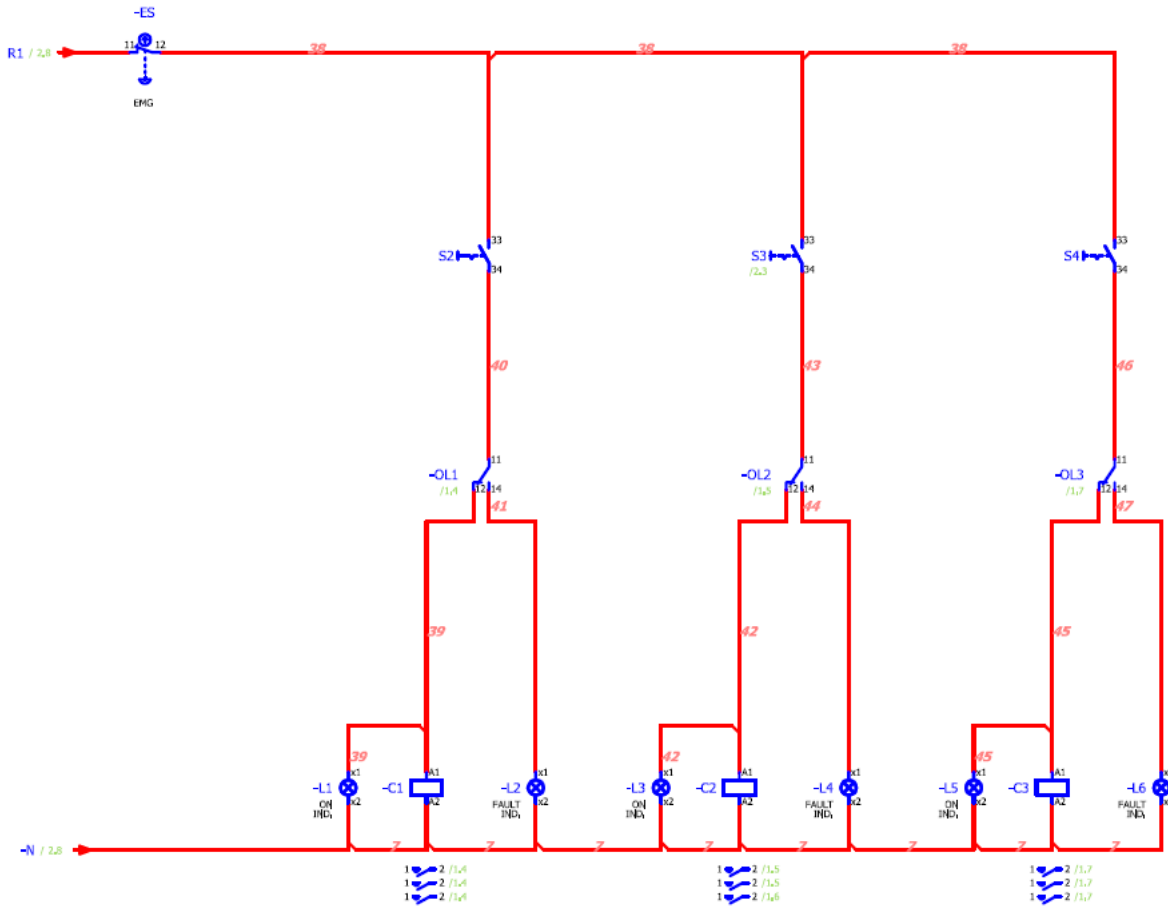Copper

Power Supply
415V/3PH/50HZ
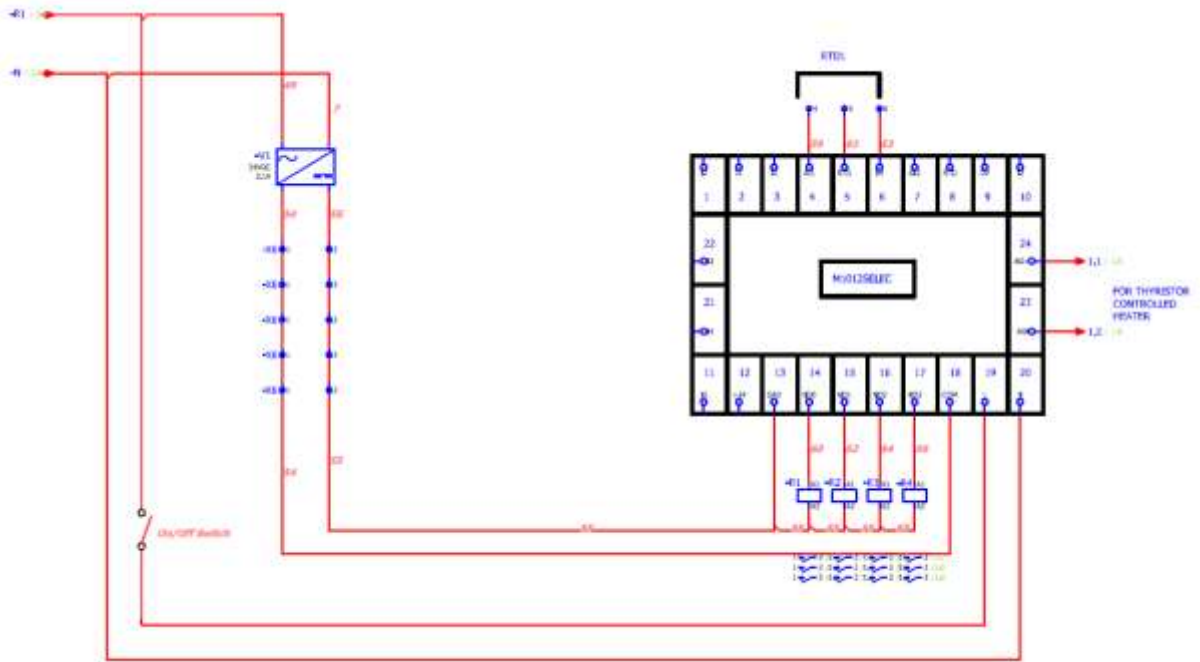
Wiring diagram of the wheels of the modular DOAS

Wire Size
2.5 sqmm,3.5Core
Copper
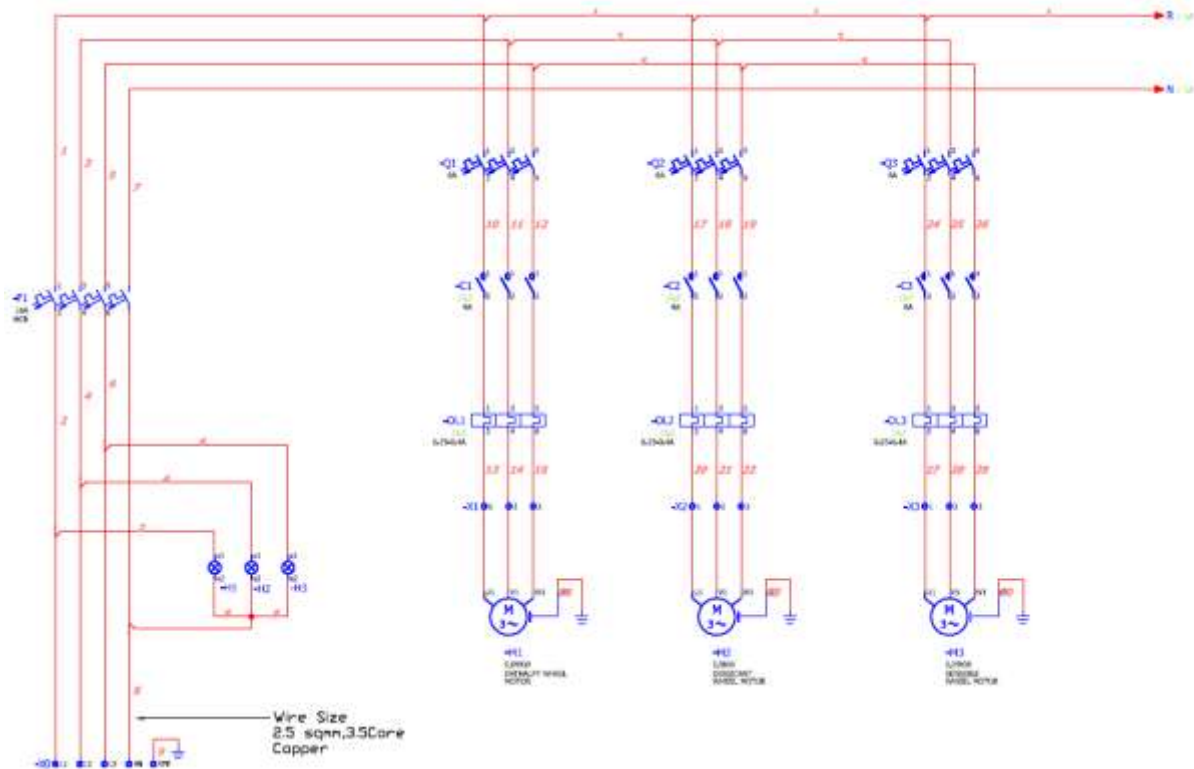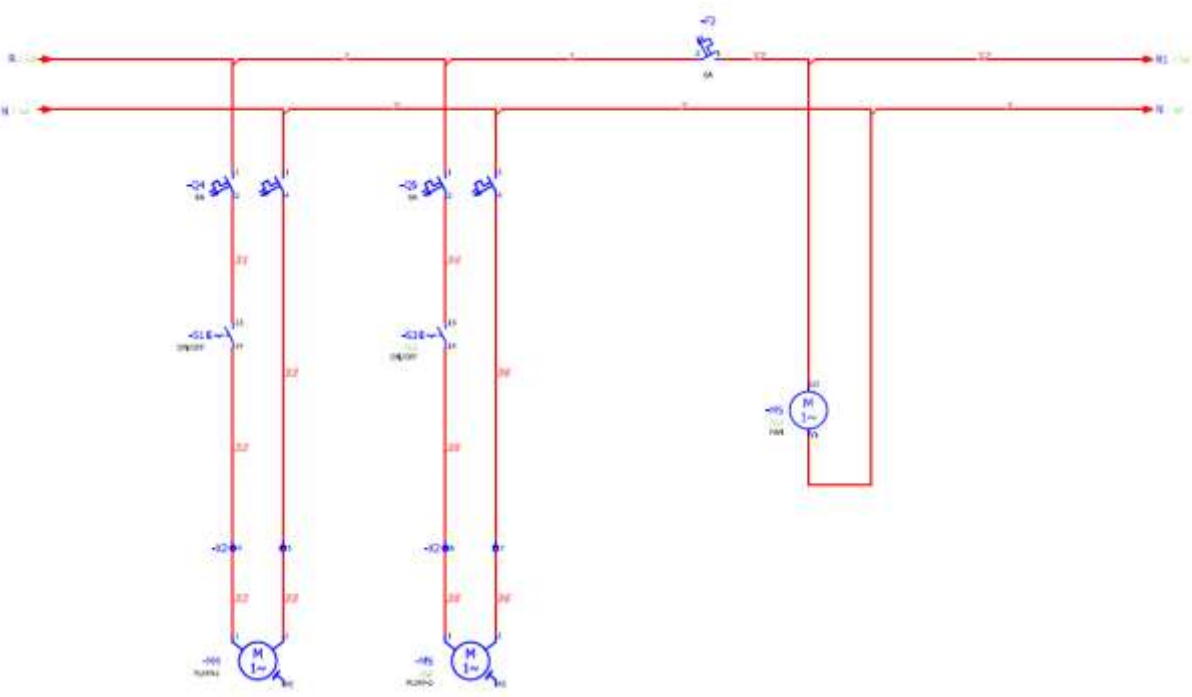
Specification of the Chiller 1: Chiller coupled with AHU of outdoor chamber

Nominal Capacity (TR/kW)		5/17.6
Rated COP (at AHRI condition)		3.3 or above
Nominal dimension	Length (mm)	1240
	Width (mm)	450
	Height (mm)	1370
Net weight/unit (kg)		196
Operating weight (kg)		256
Refrigerant		R-22/ R-407c/R-410a/R-134a
Power supply		400V/ 3 Phase/ 50Hz, AC
Compressor		
Type		Scroll/Centrifugal
Input power (kW)		5.3
Quantity (Nos.)		1
Evaporator		
Type		Plate type heat exchanger
Quantity (Nos.)		1
Construction material		Stainless steel
Fan diameter, quantity (Inch, Nos.)		18´´,2
Fan material		Aluminium, GI
Motor make, type, speed		GE, totally enclosed 900 TPM
Motor input power (each fan) (kW)		0.13
Quantity (Nos.)		2
Chilled water pump		
Type		Centrifugal, Monoblock
Rated flow rate (LPM/USGPM)		45.5/12
Rated head (m)		38
Maximum flow rate (LPM/USGPM)		70/18.5
Maximum pressure head (m)		45
Pump power input (kW)		0.6
Pump maximum input power (W)		1510
Safety device		High pressure switch, low pressure switch, flow switch, antifreeze protection, alarm with buzzer.
Electrical safety		Crankcase heater, overload for pump, circuit breaker for compressor (single phase/ phase reverse protection only for scroll compressor)
Tank capacity (l)		55 or more
Interface		Modbus/backnet interface is required

Specification of the Chiller 2: Chiller coupled with cooling coil of modular DOAS

Nominal Capacity (TR/kW)		10/35
Rated COP (at AHRI condition)		3.3 or above
Nominal dimension	Length (mm)	1410
	Width (mm)	755
	Height (mm)	1275
Net weight/unit (kg)		535
Operating weight (kg)		655
Refrigerant		R-22/ R-407c/R-410a/R-134a
Power supply		400V/ 3 Phase/ 50Hz, AC
Compressor		
Type		Scroll
Input power (kW)		5.3
Quantity (Nos.)		2
Evaporator		
Type		Plate type heat exchanger
Quantity (Nos.)		1 (Dual)
Construction material		Stainless steel
Fan diameter, quantity (Inch, Nos.)		22´´,2
Fan material		Aluminium, GI
Motor make, type, speed		GE, totally enclosed 900 TPM
Motor input power (each fan) (kW)		0.42
Quantity (Nos.)		2
Chilled water pump		
Type		Centrifugal, Monoblock
Rated flow rate (LPM/USGPM)		91/24
Rated head (m)		48
Maximum flow rate (LPM/USGPM)		105/27.7
Maximum pressure head (m)		65
Pump power input (kW)		1.6
Pump maximum input power (W)		1930
Safety device		High-pressure switch, low-pressure switch, flow switch, antifreeze protection, alarm with buzzer.
Electrical safety		Crankcase heater, overload for pump, circuit breaker for compressor (single phase/ phase reverse protection only for scroll compressor)
Tank capacity (l)		120
Interface		Modbus/BACnet interface is required

Specification of the Pump 2: Pump attached with Chiller 2 and cooling coil of modular DOAS

Parameters	Details
Volts	200/240
Frequency	50 Hz
Class	A
RPM	2900
Size	40x40 m
Head	8 m
Capacity (HP/kW)	0.5/0.37
Flow	200 LPM

Specification of AHU for outdoor chamber

Casing Construction of DOAS Units:
Construction: 50 mm thick panel with Fiber Glass insulation (48Kg/m^3) & Thermal Break profile. Material: Frame - Extruded Aluminium Profile. Outer Casing: 0.8mm Pre Plasticized Pre Coated GI Sheet & Inner Casing: 0.8mm Galvanized Steel Sheet.

Air filter section with Damper.

Air filter: Efficiency of 90% down to 10 Microns (G4) with Aerofoil Design- Aluminum Dampers with Class III.

Heater : 20 kW (4 kW x 5 Nos), controls - 4 Nos : Fixed (ON/OFF) + 1 No with Thyristor Control & one RTD Sensor with Temp display

Supply Air Fan : The fan Section is direct driven plug fan AMCA certified fans. The impeller and the fan casing shall be made of hot galvanized sheet steel. The impeller is statically and dynamically balanced. Make: Nicotra

Fan Motor: Fan motor 415 volts, 50 cycles, 3φ phase squirrel cage, totally enclosed fan cooled with IP – 55 protections. Belt – drive arrangement. Belts are of oil resistant type. Both fan motors are having an efficiency class of EFF-1. Motor kW: 1.5 kW with VFD

Humidifier : Humidifier capacities of 4 to 8.0 kgs/hr capacity with Modulating controller

Make: Rapid cool**, Type**: Horizontal, Construction: Tank made from 1.5mm S.S Sheet (304L), welded construction, Top Openable with S.S Bolts,

Controls: Level Switch for Low Level, Filter assembly, Motorized Valve with Timer for auto flushing, Mist outlet fan.

COOLING COIL SECTION –Low Temperature cooling coil

Cooling coil section is chilled water type provided with 6 RD cooling coil. Coil is capable of providing desired dew point. Coil is AHRI Certified. Coil shall be mounted in powder coated holding racks Water coil supply and return connection shall be extended to the unit exterior. Cooling coil shall be mounted on a insulated SS drain pan.

Specification of AHU for indoor chamber

Casing Construction of DOAS Units:
Construction: 50 mm thick panel with Fiber Glass insulation (48Kg/m3) & Thermal Break profile.
Material: Frame - Extruded aluminium Profile. Outer Casing: 0.8mm Pre Plasticized Pre Coated GI Sheet & Inner Casing: 0.8mm Galvanized Steel Sheet.

Air filter section with Damper.

Air filter : Efficiency of 90% down to 10 Microns (G4) with Aerofoil Design- Aluminum Dampers with Class III.

Heater : 10 kW (2 kW x 5 Nos) ,Controls - 4 Nos : Fixed (ON/OFF) + 1 No with Thyristor Control & one RTD Sensor with Temp display

Supply Air Fan : The fan is direct driven plug fan AMCA certified fans. The impeller and the fan casing are made of hot galvanized sheet steel. The impeller is statically and dynamically balanced. Make: Nicotra

Fan Motor: Fan motor shall be energy efficient and suitable for 415 volts, 50 cycles, 3 φ phase squirrel cage, totally enclosed fan cooled with IP – 55 protections. Belt – drive arrangement, belts is of oil resistant type. Both fan motors is having efficiency class of EFF-1. Motor kW: 0.75 kW with VFD

Humidifier : Humidifier capacities of 0.5 to 4.0 kgs/hr capacity with Modulating controller, **Type** : Horizontal, **Construction** : Tank made from 1.5mm S.S Sheet (304L), welded construction, Top Openable with S.S Bolts ,**Controls** : Level Switch for Low level, filter assembly, motorized Valve with Timer for auto flushing, Mist outlet fan. **Control Panel** : 16 Gauge CRC sheet Panel duly epoxy painted, Power Supply (SMPS), M.C.B, Relay card, Cooling fan Connectors, On/Off Switch with Light, Indication Light for drain valve, Humidity Off, Supply On and Low Level.

Appendix III: Measurement Plots & Range of Measurement of Experimental Data of Chapter 5

Appendix III provides graphical plot and range of measurement of measured data of modular DOAS experiments of Chapter 5. Figure 7-11 to Figure 7-14 are showing the conditions of the outdoor chamber in DOAS experiments of different climatic conditions.
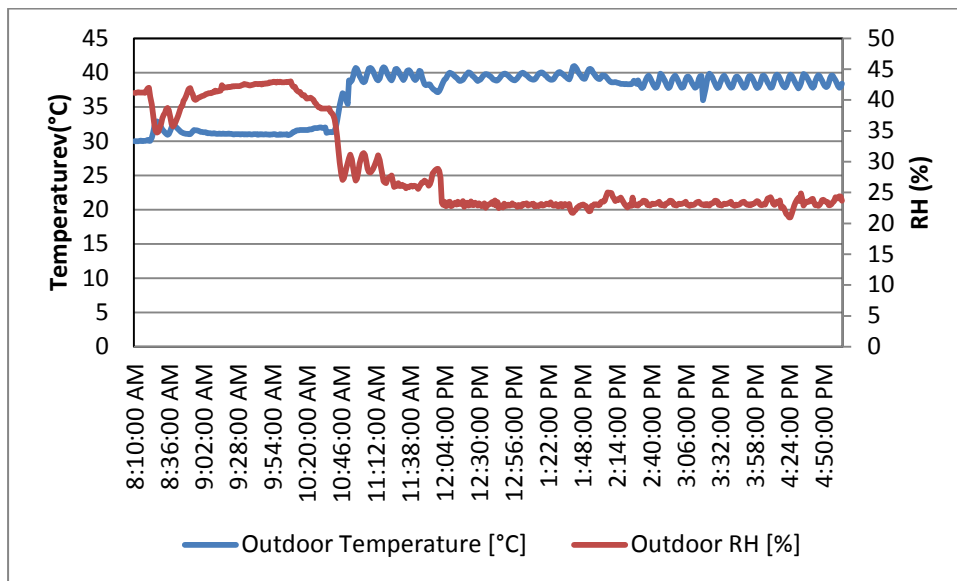

Figure 7-16: Temperature and RH achieved in the outdoor chamber for DOAS experiment for Hot and Dry climate
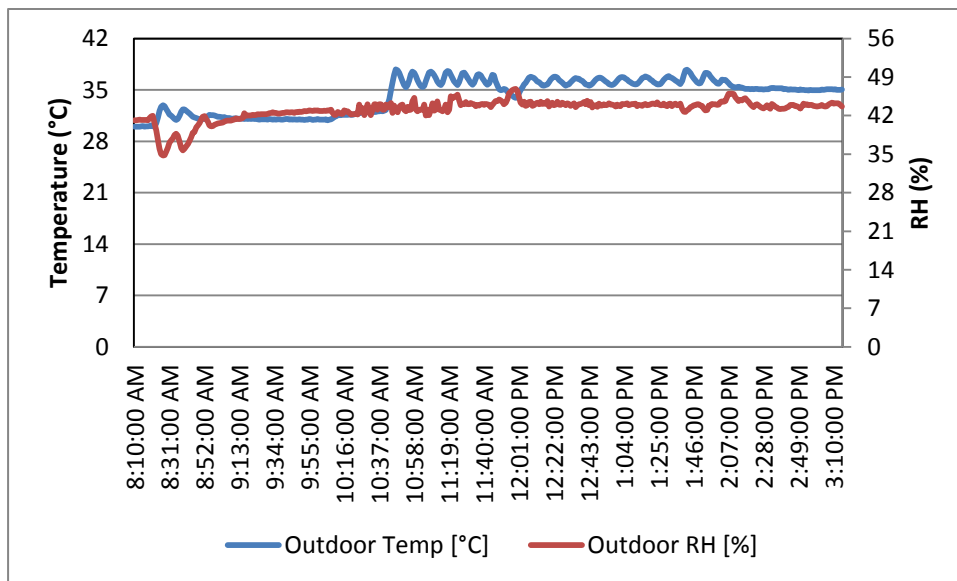

Figure 7-17: Temperature and RH achieved in the outdoor chamber for DOAS experiment for warm and humid
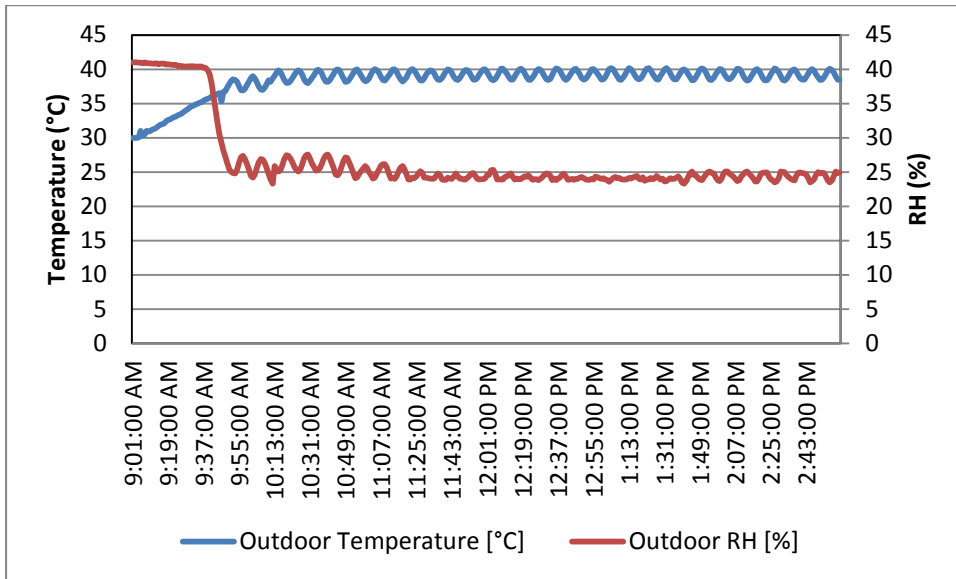
Figure 7-18: Temperature and RH achieved in the outdoor chamber for DOAS experiment in composite climate
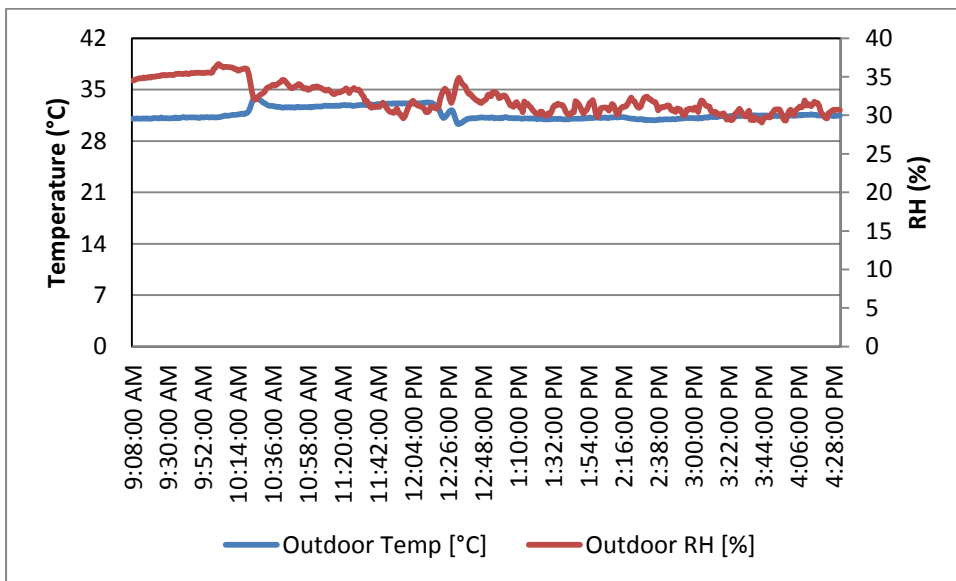

Figure 7-19: Temperature and RH achieved in the outdoor chamber for DOAS experiment of temperate climate

Detailed measurement values of the experiments conducted for modular DOAS (Chapter five) are provided below. Table 7-1 to Table 7-4 provides minimum, maximum and mean values of measured data along different points in the most efficient DOAS strategies for different climatic conditions. Figure 7-15,

Hot and dry climate

Table 7-1: Psychrometric values of Strategy-2 for hot and dry climate.

State Point	T (°C)	w (g/kg)

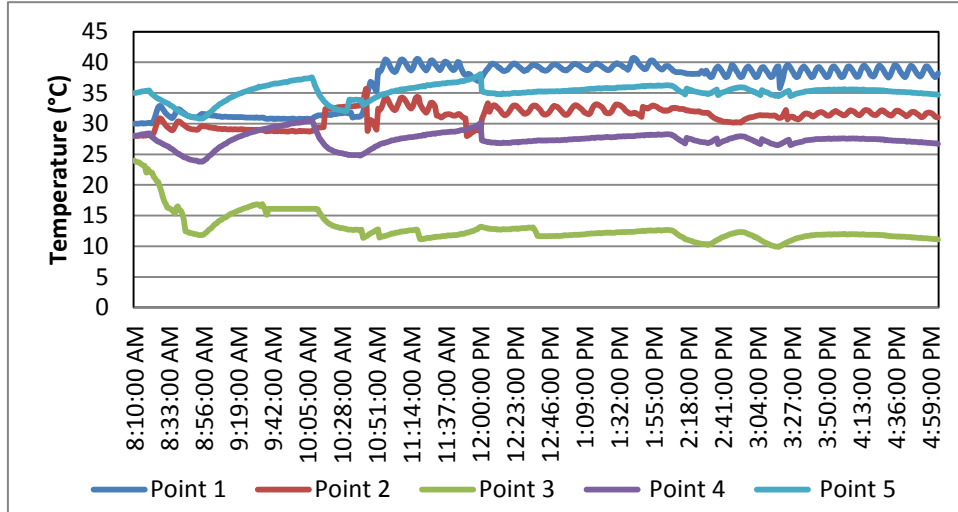| 1 | (Min: 38.4), (Max: 40.7), (Mean: 39.2) | (Min: 10.1), (Max: 10.7), (Mean: 10.5) |
2	(Min: 31.1), (Max: 33.4), (Mean: 32.3)	(Min: 9.4), (Max: 10), (Mean: 9.8)
3	(Min: 11.6), (Max: 13.1), (Mean: 12.3)	(Min: 6.8), (Max: 7.5), (Mean: 7.2)
4	(Min: 26.8), (Max: 28.3), (Mean: 27.5)	(Min: 8.9), (Max: 9.6), (Mean: 9.3)
5	(Min: 34.8), (Max: 36.3), (Mean: 35.5)	(Min: 9.6), (Max: 10.2), (Mean: 9.9)

Figure 7-20: Graphical representation of temperature plot of measured data of Strategy-2 for hot and dry climate

Table 7-2: Psychrometric values of Strategy-5 for hot and dry climate

| State Point	T (°C)	w (g/kg)
1	(Min: 38.3), (Max: 40.4), (Mean: 39.9)	(Min: 10.1), (Max: 10.8), (Mean: 10.5)
2	(Min: 38.1), (Max: 50.3), (Mean: 49.3)	(Min: 7.3), (Max:8.2), (Mean: 7.8)
3	(Min: 33.2), (Max: 35.6), (Mean: 34.3)	(Min: 7.4), (Max: 8.3), (Mean: 7.8)
4	(Min: 18.6), (Max: 19.9), (Mean: 19.4)	(Min: 7.3), (Max: 8.2), (Mean: 7.7)
5	(Min: 26.6), (Max: 28.5), (Mean: 27.2)	(Min: 8.6), (Max: 9.3), (Mean: 9.1)
6	(Min: 41.6), (Max: 42.9), (Mean: 42.3)	(Min: 8.8), (Max: 9.5), (Mean: 9.3)
7	(Min: 53.6), (Max: 54.3), (Mean: 54)	(Min: 8.8), (Max: 9.5), (Mean: 9.2)
8	(Min: 44), (Max: 44.9), (Mean: 44.7)	(Min: 12.3), (Max: 12.9), (Mean: 12.6)
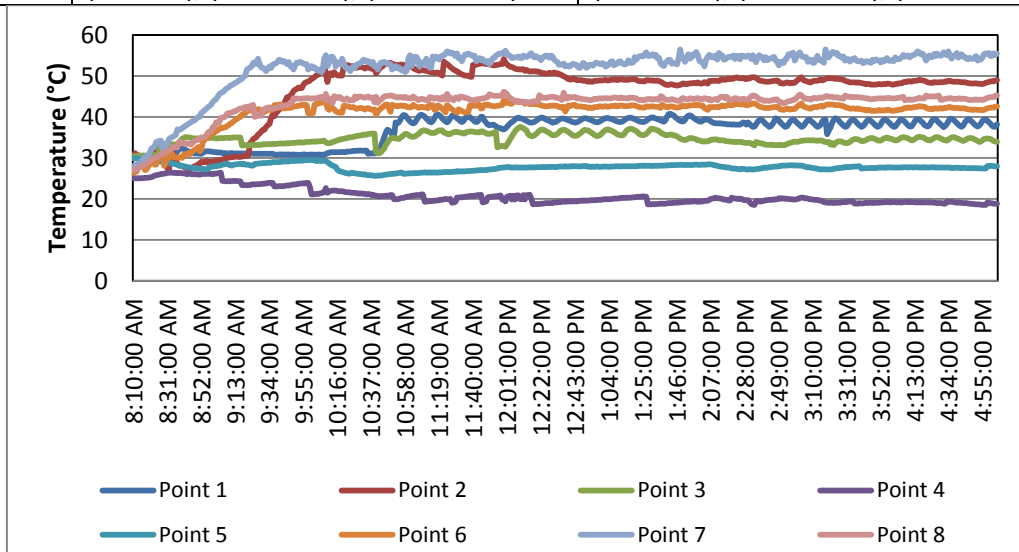
Figure 7-21: Graphical representation of temperature plot of measured data of Strategy-5 for hot and dry climate
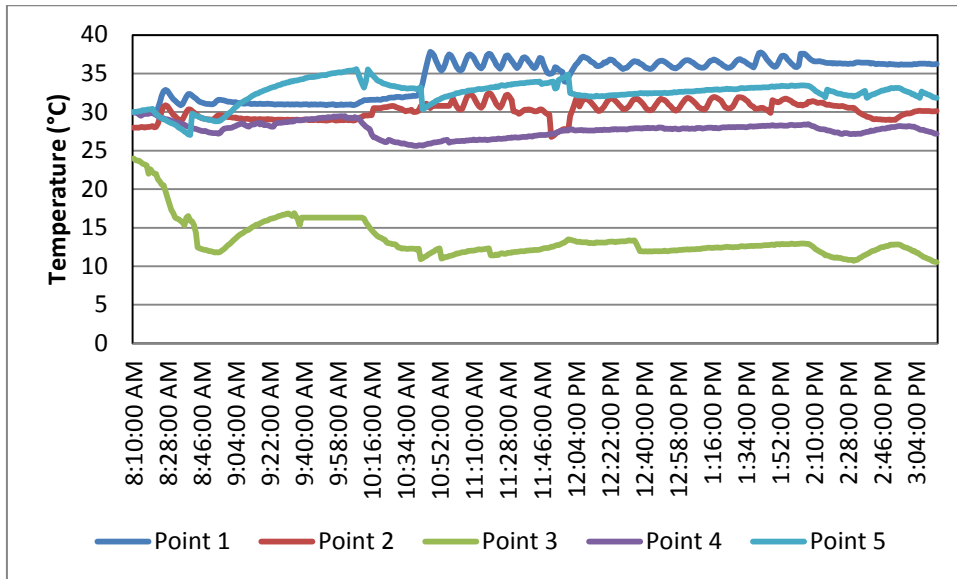
Warm and humid climate

Figure 7-22: Graphical representation of temperature plot of measured data of Strategy-2 for warm and humid climate

Table 7-3: Psychrometric values of Strategy-2 for warm and humid climate

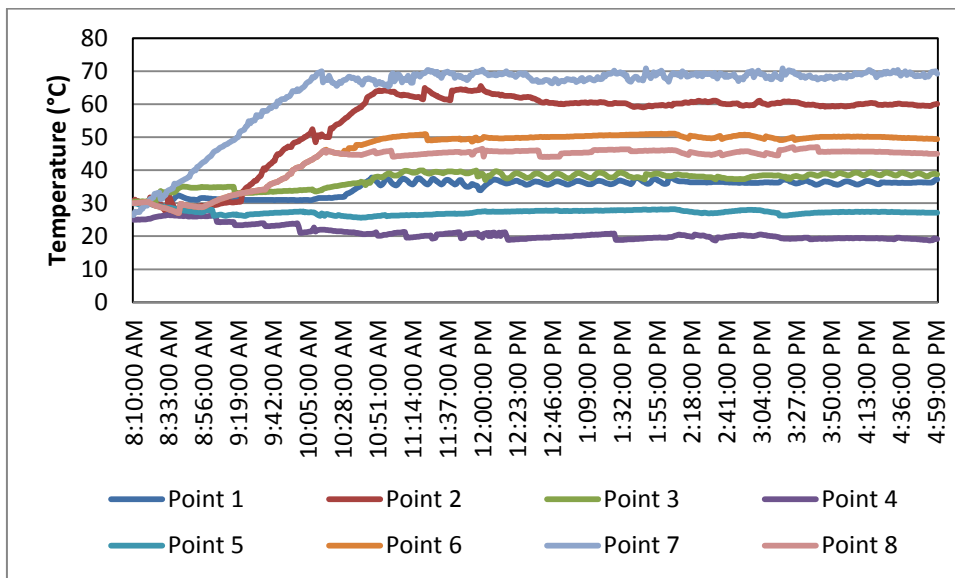| State Point	T (ºC)	w (g/kg)
1	(Min: 35.6), (Max: 37.7), (Mean: 36.3)	(Min: 16.3), (Max: 16.9), (Mean:16.7)
2	(Min: 29.9), (Max: 31.9), (Mean: 30.9)	(Min: 11.5), (Max: 12.2), (Mean: 11.9)
3	(Min: 11.9), (Max: 13.6), (Mean: 12.6)	(Min: 6.9), (Max: 7.5), (Mean: 7.2)
4	(Min: 27.6), (Max: 28.4), (Mean: 27.9)	(Min: 9.1), (Max: 9.6), (Mean: 9.4)
5	(Min: 32.1), (Max: 33.5), (Mean: 32.77)	(Min: 13.9), (Max: 14.4), (Mean: 14.1)

Figure 7-23: Graphical representation of temperature plot of measured data of Strategy-5 for warm and humid climate

Table 7-4: Psychrometric values of Strategy-5 for warm and humid climate

State Point	T (ºC)	w (g/kg)

| 1	(Min: 35.6), (Max: 36.4), (Mean: 36.1)	(Min: 10.1), (Max: 10.8), (Mean: 16.6)
2	(Min: 60.1), (Max: 61.4), (Mean: 61)	(Min: 7.4), (Max:8.3), (Mean: 7.96)
3	(Min: 37.9), (Max: 38.4), (Mean: 38.3)	(Min: 7.4), (Max: 8.2), (Mean: 7.9)
4	(Min: 19.2), (Max: 20.1), (Mean: 19.7)	(Min: 7.3), (Max: 8.2), (Mean: 7.7)
5	(Min: 26..6), (Max: 28.3), (Mean: 27.2)	(Min: 8.6), (Max: 9.4), (Mean: 9.1)
6	(Min: 49.3), (Max: 49.9), (Mean: 49.8)	(Min: 9.4), (Max: 10.1), (Mean: 9.8)
7	(Min: 67.3), (Max: 68.4), (Mean: 68)	(Min: 9.3), (Max: 10), (Mean: 9.8)
8	(Min: 44.9), (Max: 45.5), (Mean: 45.2)	(Min: 17.9), (Max: 18.6), (Mean: 18.1)

Composite climate
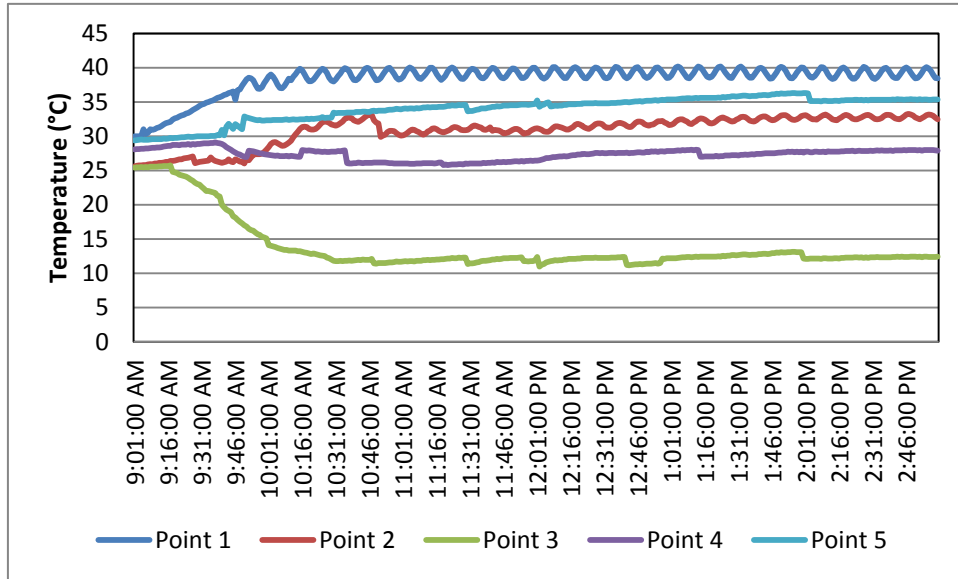
Figure 7-24: Graphical representation of temperature plot of measured data of Strategy-2 for composite climate

Table 7-5: Psychrometric values of Strategy-2 for composite climate

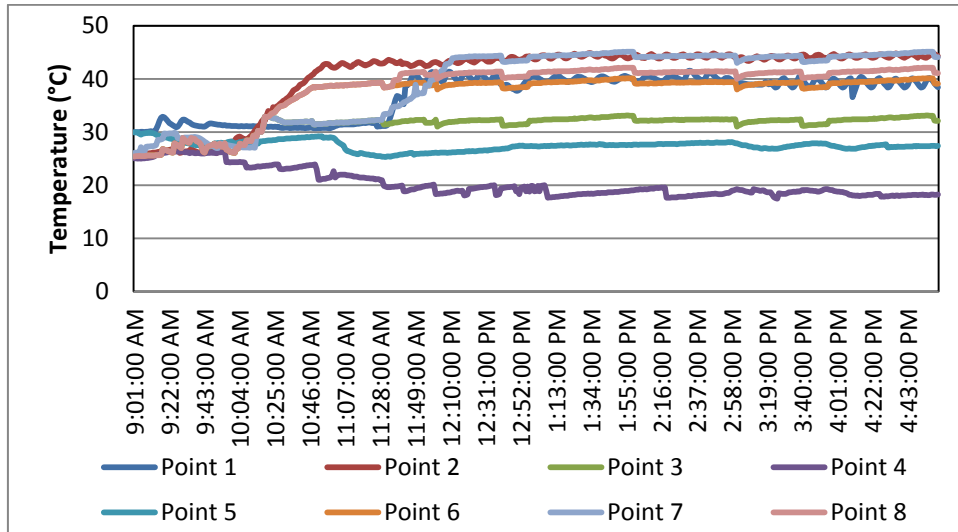| State Point	T (°C)	w (g/kg)
1	(Min: 38.8), (Max: 40.2), (Mean: 39.3)	(Min: 10), (Max: 10.5), (Mean: 10.2)
2	(Min: 31.3), (Max: 33.2), (Mean: 32.4)	(Min: 10.1), (Max: 10.8), (Mean: 10.4)
3	(Min: 11.2), (Max: 13.1), (Mean: 12.3)	(Min: 6.9), (Max: 7.5), (Mean: 7.2)
4	(Min: 27), (Max: 228), (Mean: 27.6)	(Min: 9.1), (Max: 9.7), (Mean: 9.5)
5	(Min: 34.9), (Max: 36.3), (Mean: 35.5)	(Min: 10.1), (Max: 10.5), (Mean: 10.3)

Figure 7-25: Graphical representation of temperature plot of measured data of Strategy -5 for composite climate

Table 7-6: Psychrometric values of Strategy -5

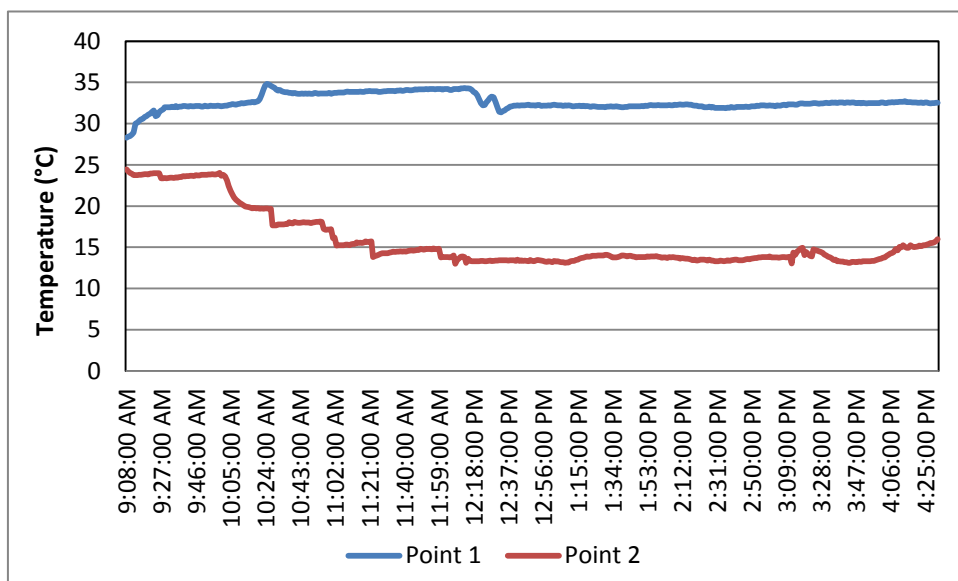| State Point	T (°C)	w (g/kg)
1	(Min: 39.7), (Max: 40.4), (Mean: 40.1)	(Min: 9.8), (Max: 10.4), (Mean: 10.1)
2	(Min: 43.8), (Max: 44.3), (Mean: 44)	(Min: 7), (Max:7.6), (Mean: 7.3)
3	(Min: 32), (Max: 32.6), (Mean:32.4)	(Min: 6.9), (Max: 7.5), (Mean: 7.2)
4	(Min: 18), (Max: 18.5), (Mean: 18.2)	(Min: 6.9), (Max: 7.6), (Mean: 7.2)
5	(Min: 26.6), (Max: 27.4), (Mean:27.2)	(Min: 8.5), (Max: 9.2), (Mean: 8.9)
6	(Min: 38.6), (Max: 39.6), (Mean: 39.2)	(Min: 8.7), (Max: 9.4), (Mean:9)
7	(Min: 44), (Max: 44.8), (Mean: 44.4)	(Min: 8.7), (Max: 9.4), (Mean:9)
8	(Min: 40.8), (Max: 41.6), (Mean: 41.2)	(Min: 9.6), (Max: 10.1), (Mean:9.9)

Temperate climate

Figure 7-26: Graphical representation of temperature plot of measured data of Strategy -2 for temperate climate

195

Table 7-7: Psychrometric values of Strategy-1 for temperate climate

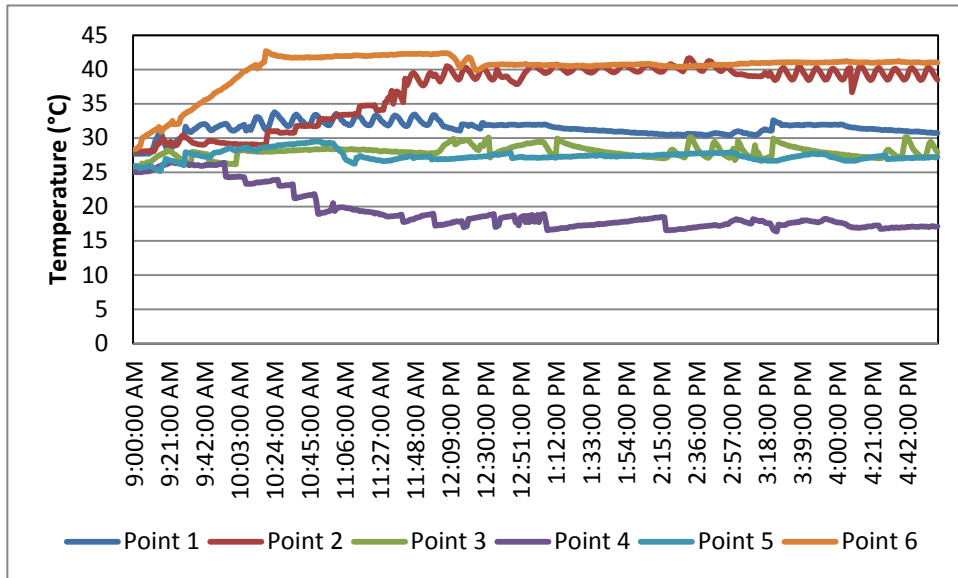| State Point	T (°C)	w (g/kg)
1	(Min: 31.9), (Max: 32.3), (Mean: 32.1)	(Min: 9), (Max: 9.6), (Mean: 9.3)
2	(Min: 13.1), (Max: 14.1), (Mean: 13.6)	(Min: 6.8), (Max: 7.6), (Mean: 7.2)

Figure 7-27: Graphical representation of temperature of measured data of Strategy-5 for temperate climate

Table 7-8: Psychrometric values of Strategy-6 for temperate climate

State Point	T (°C)	w (g/kg)
1	(Min: 31.8), (Max: 32.4), (Mean: 32.2)	(Min: 8.3), (Max: 8.8), (Mean: 8.6)
2	(Min: 39.5), (Max: 40.2), (Mean: 39.8)	(Min: 7), (Max:7.6), (Mean: 7.4)
3	(Min: 27.8), (Max: 28.4), (Mean: 28)	(Min: 7.1), (Max: 7.6), (Mean: 7.4)
4	(Min: 17), (Max: 17.5), (Mean: 17.3)	(Min: 6.9), (Max: 7.6), (Mean: 7.3)
5	(Min: 26.8), (Max: 27.5), (Mean: 27.1)	(Min: 8.9), (Max: 9.2), (Mean: 9.1)
6	(Min: 40.9), (Max: 41.5), (Mean: 41.1)	(Min: 10.6), (Max: 11.1), (Mean: 10.9)